Title
Biomass-derived polymers and copolymers incorporating monolignols and their derivatives

Author
UPTON, BRIANNA M.

Publication Date
2016

UNIVERSITY OF CALIFORNIA

Los Angeles

Biomass-derived polymers and copolymers incorporating monolignols and their derivatives

A dissertation submitted in partial satisfaction of the
requirements for the degree Doctor of Philosophy
in Chemistry

by

Brianna Marie Upton

2016

ABSTRACT OF THE DISSERTATION

Biomass-derived polymers and copolymers incorporating monolignols and their derivatives

by

Brianna Marie Upton

Doctor of Philosophy in Chemistry

University of California, Los Angeles, 2016

Professor Andrea M. Kasko, Co-Chair

Professor Heather D. Maynard, Co-Chair

Due to the importance of developing more sustainable commodity materials, this dissertation focuses on the synthesis and characterizarion of a series of polymers and copolymers from monolignols and other biomass components. The polymers described within were designed to feature a modular synthesis and were persued due to their structural similarities to commodity materials. Chapter 2 focuses on the synthetic development, thermal properties, and hydrolytic degradation of a series of monolignols-based poly(ester-amides) via interfacial polymerization with a monolignol-based ester dimer and aliphatic or aromatic diamines. These polymers were found to have differing thermal and degradation properties depending on the length (aliphatic) or structural (aromatic versus aliphatic) characteristics of the diamine utilized. Chapter 3 focuses on the development of the analogous monolignol-based poly(ether-amide) systems. These poly(ether-amide)s were synthesized used a monolignol-based ether dimer and aliphatic or aromatic diamines. As seen previously, the identity of the diamine linker played a role in the observed physical characteristics of the resulting polymers. Finally, Chapter 4 will focus on the development of a series of polymers from monolignols and citraconic anhydride as biologically-derived analogues to petroleum-based polystyrene-co-maleic anhydride and their use in polymer blends with commodity polymers. The monomers were polymerized using BF_3Et_2O as an initiator in cationic polymerization and the structure and physical properties of the resulting oligomers were then thoroughly studied. The oligomers were then used and studied in polymer blends with polystyrene and poly(lactic-acid). In summary, this dissertation focuses on the synthesis and study of several classes of polymeric materials generated directly from biomass components as chemical sources, with a focus on modularity and the tunability of observed properties.

The dissertation of Brianna Marie Upton is approved.

Richard B. Kaner

Tatiana Segura

Heather D. Maynard, Committee Co-chair

Andrea M. Kasko, Committee Co-chair

University of California, Los Angeles

2016

To Michael,

My life, my love, my everything.

Without your never-ending support

this would not have been possible.

And to my Mom and Dad,

Thank you for always believing in me and

raising me to see the infinite value

in chasing my dreams, despite

obstacles I may face.

TABLE OF CONTENTS

LIST OF FIGURES

CHAPTER 1

CHAPTER 2

CHAPTER 3

CHAPTER 4

LIST OF TABLES

CHAPTER 1

CHAPTER 2

CHAPTER 3

CHAPTER 4

LIST OF SCHEMES

CHAPTER 2

CHAPTER 3

CHAPTER 4

ACKNOWLEDGEMENTS

This dissertation would not have been possible without the help and support of many people I have gotten to know through my time at UCLA and Iowa State. While it may seem like a lonely road at times, I truly could not have gotten where I am today without the help and guidance of many people who believed in me.

First, I would like to thank my advisor Dr. Andrea Kasko for her unwavering support of me and my research for the last three years. When I walked into her office, I was unsure if she would even consider allowing me to work for her, but she was willing to take a chance on me as a student. I feel incredibly blessed to have gotten to know and work with her as an advisor, mentor, and friend. Andrea has taught me to become both a better scientist and person, and I only hope that I have lived up to a fraction of the scientist she believed I could be on the first day we met. I would like to thank Dr. Heather Maynard for her willingness to serve as my committee co-chair, as well as her encouragement and advice throughout my time at UCLA. I would also like to thank my other committee members Dr. Ric Kaner, Dr. Tatiana Segura, and Dr. Jeffery Zinc for your thoughtful guidance, time, and support throughout this process.

To the members of the Kasko Lab: Darice, Ken, Fafa, Walter, Sammy, Sam, Stephanie, Shadi, Patrick, Yu, and Elli – your kindness, laughter, and friendship were what got me through some of the not-so-fun days. You all took me into our lab family with open arms and I will be forever thankful for that. I especially want to thank Ken for being a spectacular first hood mate and tying my shoes, Darice for all of her hugs and perfectly timed advice, Fafa for her endless chemistry knowledge, and Walter for all of the SEAS runs. Shadi – my twin – I don’t know what I will do without you next year. Thank you for always making sure I had eaten something that day, supporting my Diet Coke addiction, and sitting through the many times I couldn't hold the tears back anymore. Your never-ending laughter and optimism always brought a smile to my face and I loved every second we got to work together.

To Aaron and the members of the Sadow Lab: KaKing, James, Steven, David, Kuntal, Andy, Stephanie, Rick, and Megan – you not only sparked my interest in synthetic chemistry but your patience, dedication, and passion groomed me into the chemist I am today. Under the guidance of Aaron and KaKing, I learned how to dream bigger and work harder than I knew was possible. Working in the Sadow lab was the first time I really understood the power of synthetic chemistry and with all of your support I developed a passion for organic and organometallic synthesis.

To Mrs. Beghun – you are the first person who ever introduced chemistry to me over ten years ago and without you I never would have even started down this path. Thank you for being a brilliant educator who pushed me and lit the spark for what has become my life, future, and passion.

To my parents: Dean and Nancy – thank you for raising me to think independently and know the value of my own voice. You both have been such an inspiration to me throughout my whole life, always encouraging me to continually work harder and never give anything less than my best effort at all times. While we may not have always kept in touch, I know you both were with me through it all. To my sisters: Cory, Katie, and Jessica – thank you for all of the late night phone chats and goofy times we shared together when reunited. While we all have now spread out across the continent, we are still connected always. To my Grandparents: Dean and Mary – thank you for giving me my very first science kit and all of the trips to the Science Center. You both always encouraged my curiosity, even when that meant making a baking soda-vinegar volcano in your kitchen (and cleaning up the mess that went along with it!).

To Hannah – you never stopped believing in me even when I did and was pretty much convinced this was never going to happen. Your never-ending optimism and kindness was a bright light throughout all of the darkest of times. So blessed to have such a wonderful friend and person in my life.

And finally to Michael – you have been my rock throughout all of this. While I knew this wouldn't be easy, I never thought it would be this hard to navigate the way at times. And regardless of what you had going on in your school or professional life, you were always there to help me no matter if that meant making dinner or running to make copies at 1 am. From deciding to move to Los Angeles, to getting married, to navigating a long-distance relationship between LA and DC, its been a crazy ride and I can't think of anyone I would rather share this journey with. All my love, always.

VITA

2007-2011	Iowa State President's Award of Competitive Excellence
2008-2011	Undergraduate Research Assistant in Professor Aaron D. Sadow's Laboratory
2009	H.F. Plagens' Undergraduate Research Stipend
2011	Bachelor of Science in Chemistry at Iowa State University
2011-2013	Graduate Student Researcher in Professor Paula L. Diaconescu's Laboratory
2011- 2015	Teaching Assistant at University of California, Los Angeles
2012	Master of Science in Chemistry at University of California, Los Angeles
2012	Hansen-Dow Excellence in Teaching Award
2013-2016	Graduate Student Researcher in Professor Andrea M. Kasko's Laboratory
2014	Department of Chemistry and Biochemistry Graduate Research Fellowship
2015	Teaching Assistant Consultant for UCLA Office of Instructional Development
2015-2016	Dissertation Year Fellowship

PUBLICATIONS AND PRESENTATIONS

Messina, M.S.; Axtell, J.C.; Wang, Y.; Chong, P.; Wixtrom, A.I.; Kirlikovali, K.O.; Upton, B.M.; Hunter, B.M.; Shafaat, O.S.; Khan, S.I.; Winkler, J.R.; Gray, H.B.; Alexandrova, A.N.; Maynard, H.D.; Spokoyny, A.M. “Visible-Light-Induced Olefin Activation Using 3D Aromatic Boron-Rich Cluster Photooxidants” *J. Am. Chem. Soc.* **2016** DOI: 10.1021/jacs.6b03568

Upton B. M. and Kasko, A.M. “Strategies for the Conversion of Lignin to High-Value Polymeric Materials: Review and Perspective” *Chem. Rev.* **2016**, *116*, 2275-2306

Upton, B. M.; Gipson, R.; Duhovic, S.; Lydon, B.; Matsumoto, N.; Maynard, H.; Diaconescu, P. “Synthesis of ferrocene-functionalized monomers for biodegradable polymer formation”. *Inorg. Chem. Front.* **2014**, *1*, 271-277

Yan, K.; Upton, B. M.; Zhu, J.; Ellern, A.; Sadow, A.D. “Nucleophilicity of Neutral versus Cationic Magnesium Silyl Compounds” *Organometallics*, **2013**, *32*, 6834-6843

Yan, K; Schoendorff, G.; Upton, B. M.; Ellern, A.; Windus, T.; Sadow, A. D. “Intermolecular β-Hydrogen Abstraction in Ytterbium, Calcium, and Potassium Tris(dimethylsilyl)methyl Compounds” *Organometallics*, **2013**, *32*, 1300–1316

Huang, W.; Upton, B. M.; Khan, S.; Diaconescu, P. “Synthesis and Characterization of Paramagnetic Lanthanide Benzyl Complexes” *Organometallics,* **2013**, *32*, 1379–1386

Yan, K.; Upton, B. M.; Ellern, A.; Sadow, A. D. "Lewis Acid Mediated α-Hydride Abstraction Reactions of Divalent $M(C(SiHMe_2)_3)_2THF_2$ (M = Ca, Yb)." *J. Am. Chem. Soc.*, **2009**, *131*, 15110-15111

“Biomass-derived polymers incorporating monolignols” Oral presentation selected for *Excellence in Graduate Polymer Research Symposium* at 251st National Meeting of the American Chemical Society. March 2016 in San Diego, CA.

“Monolignol-based polymeric materials from biomass” Poster presentation for Polymat-2015 Conference. October 2015 in Huatulco, Mexico.

“Polymeric Materials from Biomass” Poster presentation at 249th National Meeting of the American Chemical Society. March 2015 in Denver, CO.

Chapter 1: Introduction to lignin-based polymeric materials

Adapted with permission from Upton, B.M. and Kasko, A.M. *Chem. Rev.*, **2016**, *116* (4) 2275-2306. Copyright 2016 American Chemical Society.

1.1 Introduction

Increasing steadily since the 1940s[1], the majority of commodity plastics and materials are derived from petroleum-based chemicals, illustrating the strong dependence on products derived from non-renewable energy sources. Global demand for polyethylene, for example, is expected to reach 99.6 million metric tons in 2018[2]. In response to the awareness of limited petroleum resources, an increased focus has been placed on identifying renewable feedstocks to replace current materials. The US Department of Agriculture and US Department of Energy have set a goal to increase the percentage of commodity chemicals and materials made from bio-based materials from 5% in 2005 to 25% in 2030[3]. As the most accessible renewable form of carbon (in comparison to CO_2)[4], lignocellulosic biomass (defined as organic matter available on a renewable basis[5]) has been acknowledged as the most logical carbon-based feedstock for a variety of materials such as biofuels and chemicals[6].

Lignocellulosic biomass has three main components: cellulose, hemicellulose and lignin. Cellulose comprises 30 – 50% of biomass, depending on the plant species, and is a polymer of glucose. A smaller portion, 20-35%, is hemicellulose, which is a heteropolymer containing primarily xylose. Lignin accounts for the remaining 15-30% of biomass and is a cross-linked, aromatic-based heteropolymer responsible for water transport and structural integrity in plants. Lignin is an amorphous polymer containing three phenylpropanolic monomers (monolignols) linked by carbon-carbon and ether bonds. As the second most abundant natural polymer and accounting for approximately 30% of organic carbon in the biosphere[7], lignin is the only scalable renewable feedstock consisting of aromatic monomers[8] and is highly underutilized. Only an estimated 2% of the 50 million tons of lignin isolated from pulping processes in 2010 was used for specialty products while the rest was burned as a low-value fuel[9]. This underutilization sparks the desire to develop not only processes to isolate lignin from biomass more efficiently, but also to engineer lignin-based products of increased commercial value. The scope of this introduction will focus on methods developed to synthesize polymers derived from lignin, monolignols, and lignin-derived chemicals.

1.2 Lignin

1.2.1 Lignification and structure

Lignin is composed of three different cinnamyl alcohol monomers: *p*-coumaryl alcohol, coniferyl alcohol and sinapyl alcohol (**Figure 1.1**). The ratios of each monomer differ based on plant species. Grasses typically contain all three monomers while softwood (coniferous tree-based) lignins contain mainly coniferyl alcohol and hardwood (deciduous tree-based) lignins contain both coniferyl and sinapyl alcohol[10]. With differing monomer content, bonds formed during polymerization also differ as coniferous wood contains more carbon-carbon bonds than deciduous wood[11]. The diversity in both monomer content and chemical bonds makes the determination of the exact chemical structure of each isolated lignin extremely difficult.

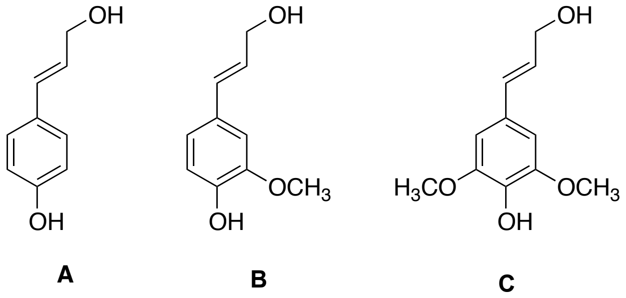

Figure 1.1 Three standard monolignol monomers. **A**=*p*-coumaryl alcohol; **B**=coniferyl alcohol; **C**=sinapyl alcohol

Lignin is polymerized *in vivo* via an enzyme-mediated dehydrogenation polymerization (ligninfication) resulting in a cross-linked amorphous material with both ether and carbon-carbon bonds (**Figure 1.2**)[12]. Deposited in the cell wall during cell differentiation, lignin is necessary for both the structural integrity of each cell as well as the stiffness of the entire plant[13-14]. The hydrophobicity of lignin allows for the transport of water and other nutrients, as well as offering protection from invading pathogens and insects[15-16]. In general, most lignin linkages are formed by oligomer-oligomer or oligomer-monomer couplings while fewer are formed from monomer-monomer coupling reactions[17].

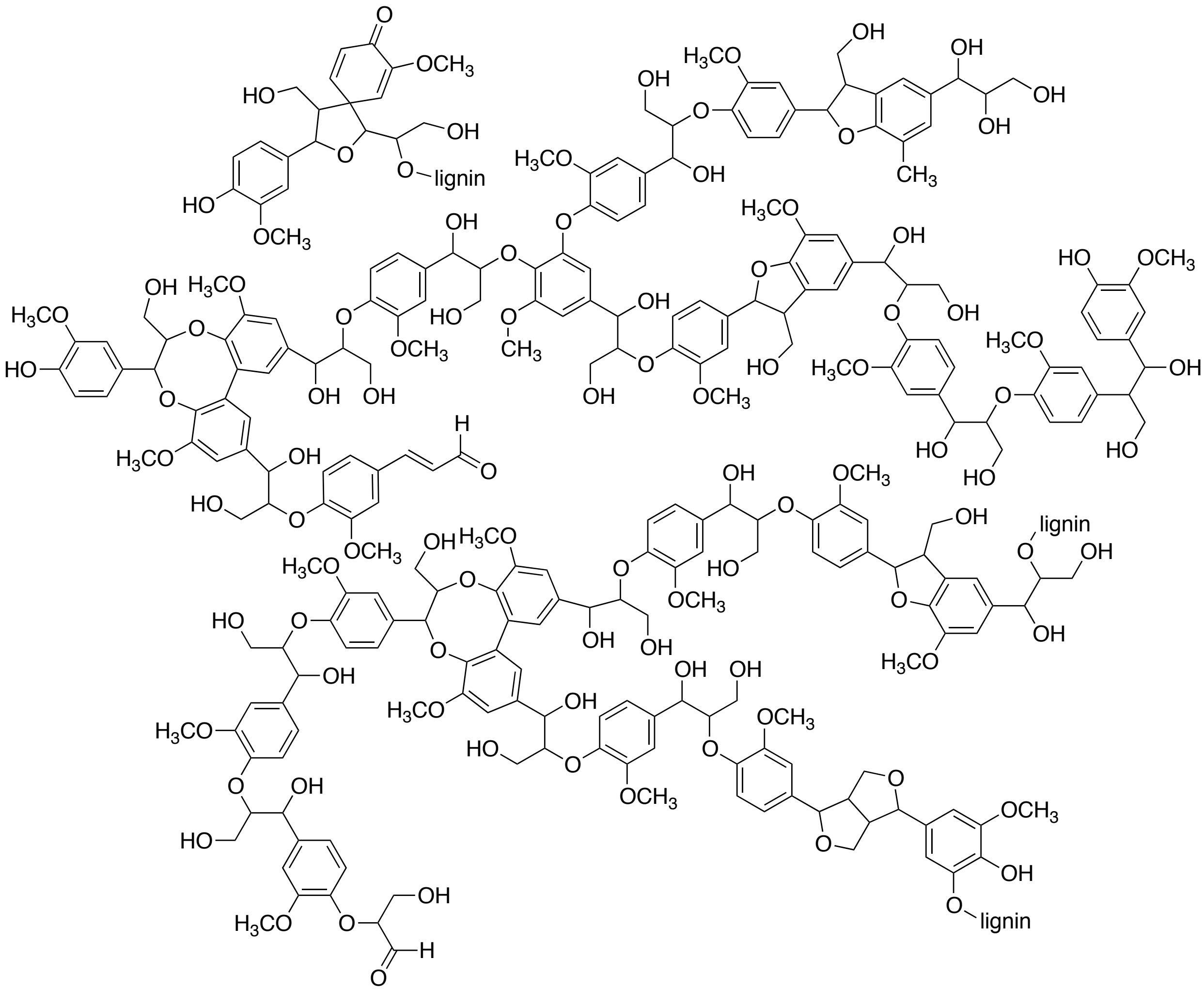

Figure 1.2 Structural motifs of softwood lignin. Reproduced with permission from ref. 12. Copyright 1980 Springer.

The most common linkage, a β-O-4 ether linkage, typically accounts for 50% of bonds formed during the polymerization reaction[18-19] and is the key target of most degradation studies. Other major linkages include β-5, β-1, β- β, 5-5 and 4-*O*-5, which are significantly more complicated to degrade and often become increasingly difficult to degrade during traditional processing methods because of significant radical and carbon-carbon bond formation (**Figure 1.3**). The structures of several different lignins have been explored through many spectroscopic techniques and chemical methods, however due to the promiscuous nature of the polymerization, it is doubtful that the full structure of any lignin will ever be fully elucidated.

1.2.2 Isolation and depolymerization of lignin from biomass

As with all sourced materials, both industrial and lab-scaled processes for isolating

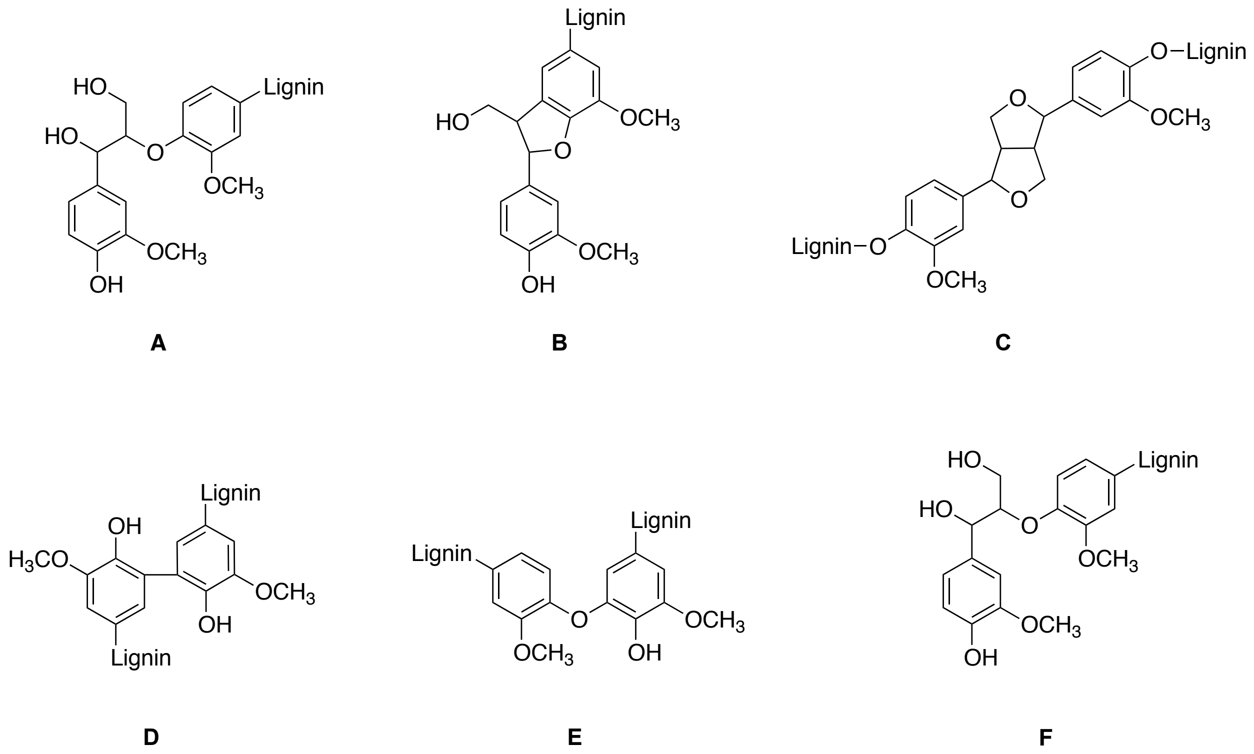

Figure 1.3 Six common linkages found in lignin: **A**=β-O-4, **B**=β-5, **C**=β-β', **D**=5-5', **E**=4-O-5, **F**=β-1'

lignins from lignocellulosic biomass have been developed. All isolation methods have the same goal, chemical degradation of the polymeric lignin structure until the resulting fragments become soluble in the pulping media. Depending on the method employed, the properties of the resulting isolated lignin differ. Key factors in the success of each process include: the pH of the entire system, the ability of the solvent and/or solute to participate in lignin fragmentation, ability of the solvent and/or solute to prevent lignin recondensation and ability of the solvent to dissolve lignin fragments[20]. Currently, there are four industrial processes used to isolate pure lignin that can be divided into two categories based on if the resulting product contains sulfur (**Table 1.1**). Lignins isolated from the sulfite and kraft processes contain sulfur while lignins isolated from the soda and organosolv process do not[21]. In addition to functionalization either with or without sulfur, the resulting products also differ in levels of purity, structure of the resulting fragments, and molecular weight of the isolated degraded lignin. Lignins isolated by any of these methods are generally referred to as technical lignins.

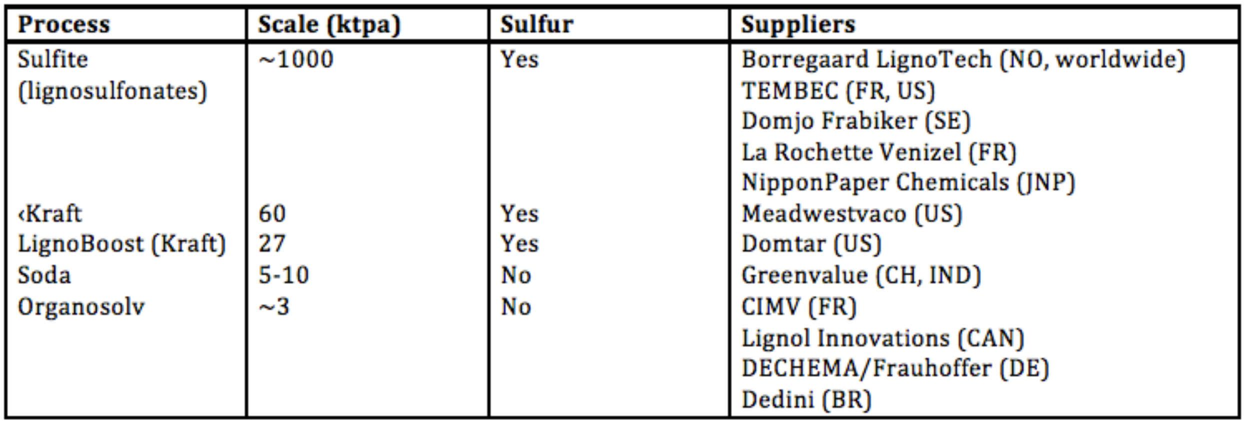

Process	Scale (ktpa)	Sulfur	Suppliers
Sulfite (lignosulfonates)	~1000	Yes	Borregaard LignoTech (NO, worldwide) TEMBEC (FR, US) Domjo Frabiker (SE) La Rochette Venizel (FR) NipponPaper Chemicals (JNP)
‹Kraft	60	Yes	Meadwestvaco (US)
LignoBoost (Kraft)	27	Yes	Domtar (US)
Soda	5-10	No	Greenvalue (CH, IND)
Organosolv	~3	No	CIMV (FR) Lignol Innovations (CAN) DECHEMA/Frauhoffer (DE) Dedini (BR)

Table 1.1 Commercial lignin production. Reproduced with permission from ref. 21. Under Creative Commons License BY 3.0.

The sulfite process is the most commonly used, producing approximately 1,000 metric tons per year. Sulfite pulping is a process which uses a heated aqueous solution of a sulphite or bisulfite salt with countercations such as sodium, ammonium, magnesium or calcium[22]. Depending on the identity of the cation and its solubility in aqueous solutions, the resulting pH of the solution varies between 1 and 13.5, and can be a criterion for choice of both cation and anion. The defining reaction in delignification by the sulfite process is the sulphonation of the lignin aliphatic chain, which occurs in different locations depending on the pH of the pulping solution. After reacting, the resulting lignosulfonate is now water-soluble and can be dissolved in the aqueous pulping liquor along with hemicellulose. To isolate lignin from this aqueous mixture, other techniques such as precipitation, ultrafiltration, chemical destruction of sugars, or alcohol fermentation of sugars followed by distillation of fermentation product must be used.

The soda process is typically reserved for non-wood based biomass sources, e.g. sugar cane or flax. During this process, the fiber is added to an aqueous solution of sodium hydroxide and is heated to approximately 160 ^{o}C. Lignin depolymerization primarily occurs with cleavage of α and β ether bonds resulting in the generation of free phenolic groups. The resulting lignin fragments are now water-soluble and can easily be isolated from the pulping liquor via precipitation once the solution is acidified. Lignin isolated in this method has a greater purity than that obtained by the sulfite process, but is much lower in molecular weight.

The kraft process also generates sulfated lignin and its products are rarely used in chemical or material production, but rather are burned as energy for pulping mills. In this process, the feedstock is added to a mixture of sodium hydroxide and sodium sulfide and heated between 150-180 ^{o}C. Lignin is depolymerized primarily in the same mechanism as the soda process, cleavage of α and β ether bonds once again resulting in increased solubility of the fragments. With the presence of hydrosulfide anions, a small portion of the resulting lignin is sulfated, but the majority of the remaining lignin is sulfate-free allowing isolation of the lignin through acidification and precipitation. Isolation of lignin from this process has been enhanced through LignoBoost™ technology[23]. This process utilizes CO_2 as an acid for precipitation and a double slurry and washing process with H_2SO_4 to maximize the quantity and purity of lignin isolated from the black liquor. This process has recently been commercialized and introduced to the market, producing 27,000 metric tons of kraft lignin in 2013.

The organosolv process has emerged more recently as an industrial scale method for lignin isolation. This method utilizes an aqueous-organic solvent mixture, such as ethanol, acetone, methanol or organic acids (acetic or formic acid), heated to isolate individual streams of hemicellulose, cellulose, and lignin[24]. This acidic method is advantageous because it allows isolation of all three components found in biomass simultaneously. It is also seen as environmentally friendly as this method lacks the sulfur, high temperatures, and high pressures required by the methods discussed above. While the organosolv process has yet to lead the market in production, it is possible that this method will replace kraft lignin over time, as it is capable of yielding each biomass component in relatively high purity. The recovery of materials (e.g. solvent) has not been optimized for the organosolv process, making this approach relatively high cost compared to other methods. In addition to the four methods discussed in detail above, there are several mechanoprocesses (ball-milling, milling with a catalyst) and other processes (steam explosion[25], pyrolysis, and processing with ionic liquids[26]) utilized in the lab or in pilot plant reactors that have yet to reach the marketplace, and therefore are outside the scope of this introduction and will not be discussed in detail.

1.2.3 Chemical and physical properties

As described previously, variation of monolignol content in plant sources yields diversity in both the physical and chemical properties of the resulting lignin materials. Depending on the oligomeric or monomeric linkages formed, the varying functional groups present may include: carboxylic, methoxy, aliphatic and phenolic hydroxyls, and carbonyl groups[27]. The broad range of chemical functionalities in lignin offer a significant potential for chemical modification. In order to be optimally used as a raw material for modification, identification and quantification of reactive groups is crucial. The following sections will address the solution-phase and solid-state characterization methods used to measure, identify and quantify the chemical and physical properties of lignin.

1.2.3.1 Solution-phase characterization

Solution-phase spectroscopic characterization (such as ^{1}H and ^{13}C NMR or UV spectroscopy) of lignin has been primarily used to determine hydroxyl[28] and monolignol content. Lignin, in its naturally occurring form, has been largely difficult to study as its high degrees of crosslinking lead to insolubility in common solvents. Thus, most techniques require that lignin be degraded into smaller units for solution-phase study. In contrast to other natural polymers that are easily degraded enzymatically or through hydrolysis, lignin contains robust carbon-carbon and diphenyl ether bonds making it difficult to degrade. The only readily accessible mode of lignin degradation is cleavage of

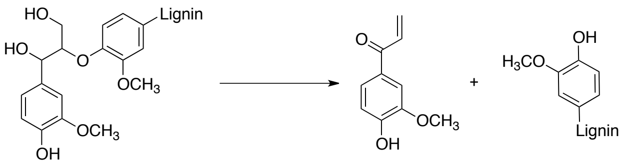

Figure 1.4 Oxidative cleavage of β-O-4 linkage

the β-O-4 ether linkage (**Figure 1.4**), which is commonly utilized in most chemical degradation methods such as acidolysis, thioacidolysis, Derivatization Followed by Reductive Cleavage (DFRC)[29], and Tosylation-Iodination-Zinc (TIZ) treatment[30]. Spectroscopic methods utilized include UV (Ultraviolet), FTIR (Fourier Transform Infrared), ^{1}H NMR, ^{13}C NMR, 2D NMR, and ESR (Electron Spin Resonance) spectroscopy.

1.2.3.2. Solid State Characterization

The study of physical properties through solid-state characterization is more facile (in terms of sample preparation) but yields significant variance in results depending on the method used to isolate the lignin from its source, water content, thermal history and lignin molecular weight. Solid-state characterization of lignin has included[31] FTIR Spectroscopy, UV Microscopy, Interference Microscopy, Electron Microscopy, Cross Polarization/Magic Angle Spinning (CP/MAS) NMR Spectroscopy, Raman Spectroscopy, Gas Chromatography-Mass Spectrometry (GC-MS), Thermogravimetry (TG), Differential Thermal Analysis (DTA), and Differential Scanning Calorimetry (DSC). While all of the above methods provide important and diverse information, many of these techniques require both specialized equipment and training. With these limiting factors, we will focus on thermal characterization techniques (TG, DSC and DTA) as these are the most facile, accessible, and directly informative techniques regarding the physical properties of lignin and their potential use in commercialize materials.

Methods for determining the glass transition temperature (T_g) of lignin (an important and accessible physical property) can give different results depending on a number of factors, making reported characteristic temperatures quite imprecise or very narrowly applicable. As an amorphous polymer, only T_g and decomposition temperature

(T_d) are applicable (not melting or crystallization temperature) to lignin. Nevertheless, the glass transition temperature for amorphous polymers varies drastically with thermal history, isolation methods, water content, crosslink density, and molecular weight[32]. Not only do these variables affect the consistency of measurements from a single method but also causes large variation in T_g measured with different methods. For example, utilizing infrared spectrometry to determine molecular motion, Hatakeyma[33] et al. measured the T_g of Björkman lignin to be 97-117 ^oC. In a later publication using differential scanning calorimetry (DSC), Hatakeyma[34] et al. measured T_g to be between 92-142 ^oC. The large difference in the two methods as well as the broad range given demonstrates not only the importance of sample handling and preparation but also the method used. To account for these differences, the T_g of lignin is typically reported to occur between 70 – 170 ^oC, depending on the structure and molecular weight of the fragments[35]. This range is obviously quite large and difficult to use when comparing the properties of lignin to other materials with more well defined thermal transitions.

Similar inconsistencies can also be seen in the measurement of decomposition temperature (T_d) with thermogravimetry. Chauvette et al.[36] showed lignin could be clearly identified from the other components of wood samples through its characteristic decomposition between 360 - 480 ^oC. In addition to simply identifying lignin, the coupling of thermogravimetry with mass spectrometry (TG-MS) has been well established as a technique for studying both lignin decomposition and its decomposition products. Faix et al. studied the decomposition products of high molecular weight lignins (e.g. monolignols) via direct pyrolysis-gas chromatography-mass spectrometry (Py-GC-MS) as a method to determine the monomeric content of selected lignins[37]. Later, Faix et al.[38] focused on lower molecular weight decomposition products, utilizing thermogravimetry-mass spectrometry (TG-MS) to identify decomposition products and their direct relationship to differences seen in decomposition temperature of lignin from different sources (e.g. that bamboo undergoes higher mass loss at lower temperatures than spruce or beech lignin samples). Similarily, Domburg et al.[39] measured the thermal degradation of lignins isolated from different techniques, demonstrating that the source of lignin matters (deciduous versus coniferous), as does the technique of isolation from the source. Thermal decomposition was shown to begin as low as 160 ^{o}C for dimethylsulfoxide lignin or as high as 350 ^{o}C for alkali-methylated lignin. While no single technique can completely characterize the physical properties of lignin samples, the combination of several techniques has been successful in probing the industrial applicability of lignin. In general, the thermal stability and amorphous characteristics of lignin indicate that it may have potential in commercial applications.

1.2.4 Chemical products of lignin depolymerization

As previously mentioned, lignin is highly under utilized as a feedstock for polymeric materials and chemicals as it is commonly burned as a fuel source for pulping plants (**Figure 1.5**). Previous sections discussed methods used in the chemical degradation of lignin to yield a soluble and isolable product from biomass, known generally as technical lignin. In contrast, this section will be devoted to degradation methods and chemical processes necessary to convert technical lignin isolated by other methods into useful (chemical) products. There has been increased interest recently to develop upgrading processes to harness the aromaticity of lignin, yielding aromatic chemical products without the use of petroleum-based feedstocks. The three most desirable aromatic starting

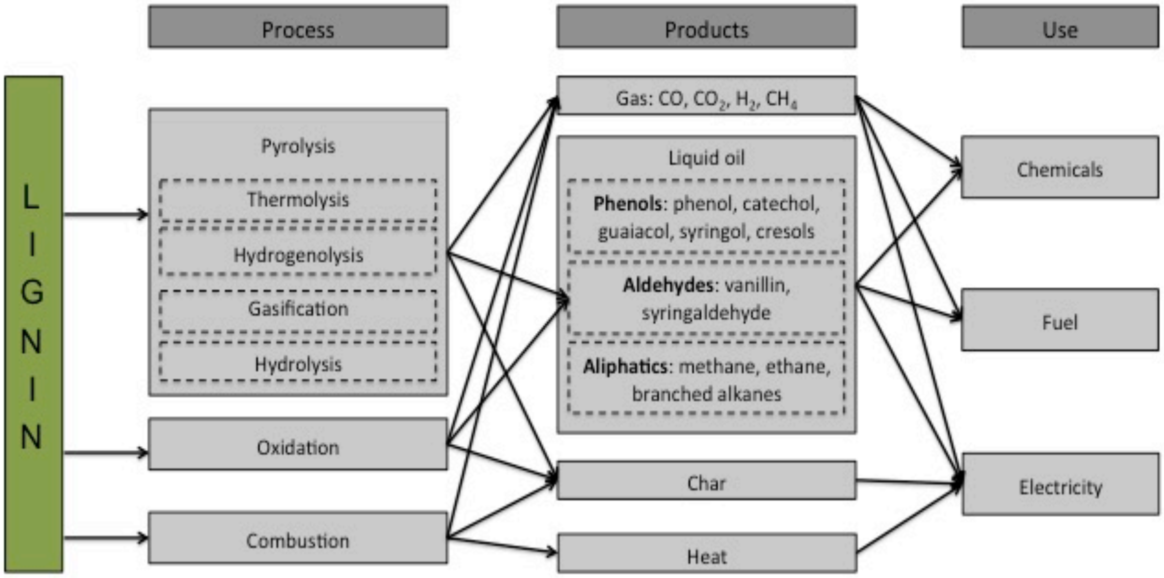

Figure 1.5 Major thermochemical lignin conversion processes. Reproduced with permission from ref. 44. Copyright 2010 John Wiley and Sons.

materials are benzene, toluene and xylene, which were produced from petroleum in 2011 at a global production volume of 36, 10 and 35 Mt/year, respectively[40]. These three aromatic starting materials serve as the building blocks for a multitude of other chemicals. While it would be ideal to harness these products from lignin rather than petroleum, this would require that aromatic monomers be isolated from polymeric lignin and that those monomers be completely deoxygenated. While chemical processes for these required conversions exist, they have yet to be applied to this particular system and on a commercial scale due to cost and efficiency. The chemical products obtained from lignin still typically possess some oxygenation, including products such as phenol or vanillin. In addition, the harsh conditions required for pulping generates a cascade of radicals during the cleavage of the more labile lignin linkages which can lead to the formation of more stable carbon-carbon bonds[41]. The presence of these new stable biphenyl structures increases the difficulty of upgrading lignin into chemical products. Not only must the bonds in lignin be broken but the method must also prevent repolymerization of the generated radical fragments. Several reviews[6,42-44] and perspectives[21,45] have been recently published on the valorization of lignin, so only methods used to upgrade lignins to chemicals will be discussed in the following sections. With this in mind, there are two major thermochemical routes used to isolate useful chemical products from lignin: hydrogenolysis and oxidation[44].

1.2.4.1 Hydrogenolysis

Hydrogenolysis is pyrolysis (the heating of organic substances in the absence of air resulting in smaller fragments while minimizing combustion to carbon dioxide) in the presence of hydrogen. This process is also referred to as hydrogenation. Hydroforming and hydrocracking have been very successful in petroleum processing, thus suggesting potential success for hydrogenation in lignin processing. By adding solvents and/or catalysts to these reactions, the hydrogenation process can be accelerated and yield of the desired products can be manipulated. The hydrogen source acts as a radical scavenger, capping and thus quenching radicals formed during the depolymerization process. Lignin is typically hydrogenated between 300 to 600 ^{o}C either under hydrogen gas or in a hydrogen-donating solvent such as formic acid. Additionally, other catalysts and solvent mixtures are still being explored to increase the relative efficiency and industrially favorable conditions of this process. The first commercial system utilizing the hydrogenation of lignin was the production of phenols via the Noguchi Process in Japan in 1952[46]. This method utilized a desulfontated lignin source, generated in a two-step treatment process, and a sulfated metal catalyst to generate approximately 44% monophenol products (phenol, *o*-cresol, *p*-cresol, *p*-ethylcresol, and *p*-propylcresol). The catalyst was iron (II) sulfide with at least one sulfide cocatalyst of copper, silver, tin, cobalt, chromium, nickel, zinc or molybdenum added[47]. The success of this process on the pilot scale attracted the interest of US-based Crown-Zellerbach in 1961[46]. Despite attempts to improve the method, they were unable to develop an approach to synthesize aromatics that was competitive with the low-cost of production from coal or petroleum. Furthermore, Crown-Zellerbach was unable to isolate monophenolic products in yields higher than 21% (compared to 44% reported by the Noguchi Institute) and the products isolated were more diverse and difficult to separate than indicated by the Noguchi Institute. The two-step lignin desulfonation and de-ashing process also added substantial cost to the process, with each pound of lignin costing about three cents to prepare for hydrogenation[46] in comparison to the petroleum-based feedstock, crude oil, which cost less than 0.6 cents per pound[48] (in 1961 from OPEC and defining the density of crude oil as 816-850 kg/m^3). A series of optimization experiments were attempted to both lower the cost and increase the yield of these reactions, however no conditions were found that would either significantly lower the cost to match the market value of monophenolic products or improve the hydrogenation yield of monophenols. Goheen speculated that the yield of monophenols from lignin waste would have to be 50% greater to become a profitable method. With these difficulties and financial barriers, the commercial production of aromatic compounds from the depolymerization of lignin was discontinued.

Bench-top scaled catalytic hydrogenations utilizing expensive noble-metal catalysts on organic supports (e.g. metals on carbon) such as Ru/C, Pd/C or Pt/C are prevalent in the literature[49]. Non-sulfided catalysts are known to have lower reactivity in lignin hydrogenation[50] and the addition of sulfur either via sulfide catalysts or carbon disulfide is known to improve lignin depolymerization[51]. Less common are first-row transition metals capable of this transformation. Recently, the Hartwig Group developed a nickel-catalyzed system that selectively cleaves aromatic C-O bonds under relatively mild conditions (80-120 °C, 1 bar H_2)[52]. This system offers great industrial potential with the relatively low cost of nickel in addition to industrially favorable conditions and the cleavage of one of lignin's most robust bonds. In addition to single metal systems, bimetallic systems such as FeMo[53], TiNi[54], NiRu, NiRh, and NiPd[55] have been explored as well as NiO and MoO[56] zeolite (aluminosilicates, $SiO_2 \bullet Al_2O_3$) supported systems. However, few methods have become commercially scaled processes due to high cost, poor yields, or severe conditions required.

In addition to metal-catalyzed hydrogenations, there are also reports using hydrogen-donating solvents. Solvent mixtures, such as phenol-water[57], or super-critical solvents such as methanol or water[58] have been used as alternative methods of lignin degradation. While generally low yielding, these methods offer increased success as they allow degradation without the formation of char, allowing mostly chemical products to be isolated. The most successful approach to date used a combination of metal-based catalysis in super-critical solvents. The Hensen group utilized a $CuMgAlO_x$ catalyst in super critical ethanol to generate 23 wt% of (mostly) aromatic monomers from lignin[59], which is high given the potential for over-hydrogenation. In addition, almost half of the aromatic monomers isolated were deoxygenated, simultaneously preventing repolymerization and allowing for more end-use applications. Ionic liquids have also served as alternate solvents for hydrogenation. Ionic liquids are broadly defined as ionic compounds (salts) with a melting point less than 100 °C and relatively low viscosity[60]. Binder et al. evaluated the conversion of lignin model compounds in 1-ethyl-3-methylimidizolium chloride and triflate

([EMIM]Cl and [EMIM]OTf) with a series of metal, Lewis acid, and Brønsted acid catalysts in reducing conditions[61]. By modifying the catalyst, they were able to isolate several different aromatic compounds, including guaiacol, 4-propylguaiacol, and isoeugenol, in relatively high yields.

In general, hydrogenation or hydrogenolysis is useful for lignin processing but can be difficult to control, often yielding non-aromatic monomers and thus limiting the advantages of using lignin as a feedstock.

1.2.4.2. Oxidation

Oxidation is another technique utilized to isolate aromatic products from lignin. The products generated from this process typically possess increased complexity and functionalization, in comparison to products from hydrogenation. Industrially, lignin is most commonly oxidized with nitrobenzene, hydrogen peroxide, or metal oxides[44]. Other methods involve utilizing both an oxidant (typically gaseous O_2) and a catalyst. While a catalyst is not required for the oxidative degradation of lignin with O_2, reactions without a catalyst are less selective, frequently cause over oxidation, and feature a significantly reduced level of conversion to desired products[62-64]. As the oxidation of lignin is decreased without adding a catalyst and industrial methods have not seen recent modification, we will instead focus on new catalytic oxidative methods found in the literature. The catalytic oxidation of lignin can be divided into two categories (depending on the state or origin of the catalyst): heterogeneous and homogeneous. With ease of catalyst recovery, heterogeneous catalysts are usually preferred industrially and have proven to be advantageous in lignin oxidation[65].

Heterogeneous catalysts are most commonly metal or surface supported metal catalysts, as they must be in a different physical state by definition. While there are examples that use Noble metals such as Pt, Pd and Re, lignin oxidation catalysts are more commonly derived from first-row (or less precious) transition metals such as Ti, Ni and Cu. TiO_2[66] and TiO_2-supported Pt[67] or Fe oxidatively degrade lignin when exposed to UV-light. Ni supported on MgO in supercritical water has been utilized to create gaseous (H_2, CO_2, CH_4) products from lignin in relatively high yields, but has little use in chemical upgrading[68]. Crestini and coworkers studied an immobilized CH_3ReO_3 catalyst in acetic acid with H_2O_2 for the oxidation of both lignin and lignin model compounds[69]. Moderate yields were achieved when starting with model compounds (**Figure 1.6**) but less than one percent of each oxidation product was isolated when the starting material was lignin. While these are all interesting applications of heterogeneous catalysis to lignin, there is not yet a catalyst capable of producing oxidative chemical products from lignin in high yield with relatively low cost.

Homogeneous oxidation catalysts include both metal-based and organic compounds. Divalent transition metal salts such as $Co(OAc)_2$, $Mn(OAc)_2$ and $Zn(OAc)_2$ in the presence of an oxidant (O_2 or air) in acidic conditions give moderate yields of oxidation

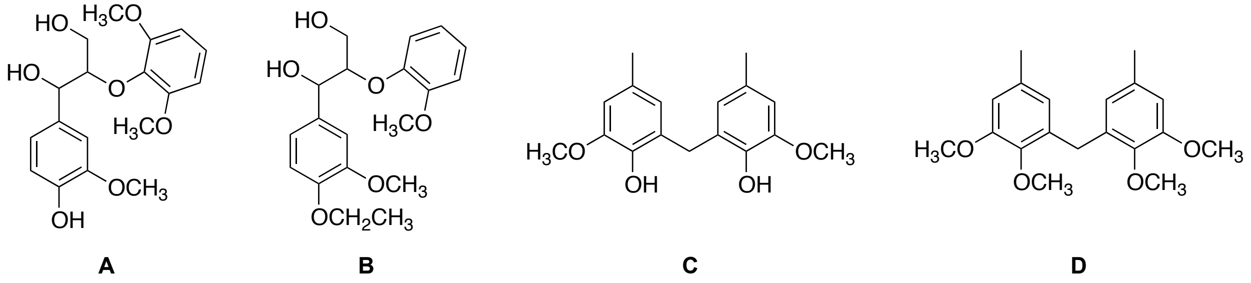

Figure 1.6 Model lignin compounds used by Crestini et al. (ref. 69) **A**=1-(4-hydroxy-3-methoxyphenyl)-2-(2,6-dimethoxyphenoxy)-3-hydroxypropanol; **B**=1-(4-ethoxy-3-methoxyphenyl)-2-(2-methoxyphenoxy)propane-1,3-diol; **C**=2,2'-methylenebis(6-methoxy-4-methylphenol); **D**=1,1'-methylenebis(2,3-dimethoxy-5-methylbenzene)

products such as benzaldehydes from model compounds[70] but low yields from technical lignin[71]. The most successful metal salt for the conversion of lignin to oxidation products is $Cu(OH)_2$, but isolated product mixtures have yields between 20.9 and 38.1%, and thus the reaction yield is still too low to be commercially relevant[72]. In a biomimetic approach, transition metal metalloporphyrin catalysts utilizing Fe, Co or Mn were synthesized as analogues to peroxidases found in fungi capable of oxidative degradation of lignin. Despite their likeness to existing enzymes, these catalysts show no improvement in the yield of oxidation products with model compounds[73,74] and exhibit no measurable reactivity with technical lignins[75]. As a simplified analogue to porphyrins, Schiff-base Cobalt(salen) [salen= N,N'-bis(salicylidene)ethylenediamine] complexes have been identified as effective oxidants for the conversion of model lignin phenolic compounds to the corresponding benzoquinones in moderate yields[76]. Drago et al. also reported the successful oxidation of lignin using Co(salen) complexes[77], but did not quantify or characterize the resulting products. Despite lack of reactivity with lignin, homogenous organometallic oxidation catalysts offer promise as effective oxidation catalysts with their relative ease of synthesis, stability and generally high reactivity with model compounds.

Alternative catalytic systems have focused on the use of ionic liquids to control the degree of oxidative degradation as well as increase lignin solubility[78-79]. Stark et al. screened a series of ionic liquids and metal catalysts to ensure optimal oxygen solvation and prevent over oxidation[80]. Through a rapid screening protocol, they found $Mn(NO_3)_2$ (2% catalyst loading) in 1-ethyl-3-methylimidazolium-trifluoromethansulfonate ($[EMIM][CF_3SO_3]$) gives the highest conversion (63%) to monomeric products such as vanillin, syringaldehyde, syringol, and 2,6-dimethyoxylbenzoquinone. Zakzeski et al.

utilized a similar approach by studying the oxidation of lignin with $CoCl_2$ and O_2 in a series of ionic liquids[81]. They determined that the identity of the anion in the ionic liquid most significantly impacted the overall yield of monomeric products. Later studies showed that the anion plays a critical role by stabilization of intermediates and therefore strongly controls the overall reaction yield[82]. Liu et al. synthesized a series of ionic liquids capable of mediating both the oxidation of lignin and separation of formed products in a batch reactor[83]. With 1,3-dimethylimidazolium dimethylphosphate ([MIMM][Me_2PO_4]) as the ionic liquid and $CuSO_4$ as the oxidation catalyst, they were able to prevent over oxidation while isolating up to 29.9% of monomeric products.

Moving towards wholly metallic systems, polyoxometallates (POMs) (metal-oxygen clusters) have also been explored as lignin oxidation catalysts in the presence of oxygen. POMs have potential as lignin oxidation catalysts as they are known to suppress radical oxygen reactions and exhibit a lower oxidation potential in comparison to lignin[84]. Heterometallic POMs of La and Mn[85] or Co[86] have been somewhat successful, but the isolated yield of products is significantly less than methods discussed previously. von Rohr and coworkers studied the catalytic potential of a commercially available molybdenum-based POM ($H_3PMo_{12}O_{40}$), as its redox potential was high enough to oxidize lignin but also low enough to be reoxidized (regenerated) by molecular oxygen[41]. Despite these benefits, this catalyst failed to convert lignin into oxidation products in a reasonable yield. In contrast to the purely chemical methods mentioned previously, Zhu et al. recently published a method to electrochemically and chemically oxidize lignin in a cylindrical electrochemical cell[87] with an outer RuO_2-IrO_2/Ti mesh anode and an inner porous felt graphite cathode. They were able to oxidatively degrade up to 59.2% of the lignin sample into aromatic monomers both on the anode surface as well as chemically by the H_2O_2 generated in solution using this system. While its is clear there are many possible approaches to the oxidative degradation of lignin into useful commercial products, no method has yet to be high yielding, industrially relevant or low-cost. With the development of better catalysts in the future, it is reasonable to believe that lignin could be used as a feedstock for oxidized aromatic products.

1.2.4.3 Other degradation techniques

While hydrogenation and oxidation are the two most common techniques used to degrade lignin, there are many examples in the literature of other degradation techniques. One of these non-pyrolysis based techniques is acidolysis, or the acid catalyzed hydrolysis of bonds found in lignin. Similar to the acidic conditions utilized to isolate technical lignins from biomass, this method is typically used to degrade the β-*O*-4 linkage. Jia et al. utilized metal chlorides ($AlCl_3$, $CuCl_2$, and $FeCl_2$) and lignin model compounds to generate a series of aromatic products[88]. With yields of the desired product, guaiacol, as high as 49%, they hypothesized that the degradation method was an acid-catalyzed hydrolysis of the β-*O*-4 linkage. Jia et al. later utilized an alternative system with an acidic ionic liquid, 1-*H*-3-methylimidazolium chloride ([HIMM]Cl), to undergo the same acid-catalyzed hydrolysis of model compounds, with yields of guaiacol up to 57%[89]. Cox et al. applied [HIMM]Cl to the depolymerization of lignin[90]. They did not quantify their yields of aromatic products, but rather studied the effects of temperature and presence of water on the rate of degradation. A later study by Cox et al. investigated the effects of the anion on relative acidity and conversion to monomeric products, finding that hydrogen bond basicity and size of the anion is more critical to higher conversion that the relativity acidity of the ionic liquid[91].

Rahimi et al. utilized a formic acid and sodium formate system to degrade oxidated lignin to aromatic monomers[92]. Through study of the mechanism, they determined it was a redox-neutral process that did not consume the formic acid but rather utilized it to generate a reactive species for hydrolysis of ether linkages. This method was able to convert more than 52% of lignin to aromatic compounds that could be characterized. Deepa and Dhepe used a series of solid acids for the catalytic depolymerization of lignin, which offered extremely high yields of aromatic monomers in comparison to other methods[93]. Zeolites composed of silicon and aluminum oxide (Si:Al = 15) were the most effective catalysts with a conversion of 60%. Deepa and Dhepe later compared the effectiveness of solid acid catalysts on six different types of technical lignin[94]. Once again zeolites of silicon and aluminum oxide (Si:Al = 15) were the highest yielding catalysts with a 30% yield of aromatic monomers for Organosolv lignin and almost 60% yield for the other five types of lignin.

1.2.4.4 Chemical Products

A study performed in 2004 through a collaboration between the Pacific Northwest National Laboratory and the National Renewable Energy Laboratory identified twelve “building block” chemicals for biorefineries to isolate that are not only easy to synthesize but also compatible with existing petroleum processing methods[5] (**Figure 1.7**). While these goals are noteworthy, all of the products identified are synthesized from sugars found in lignocellulosic biomass rather than from lignin. More specifically, many chemical products in the current literature are labeled as lignin-based or lignin-derived while few actually are. As of 2007, only three products are commercially produced from lignin: vanillin, dimethyl sulfide and dimethyl sulfoxide[95]. Vanillin is commercially isolated

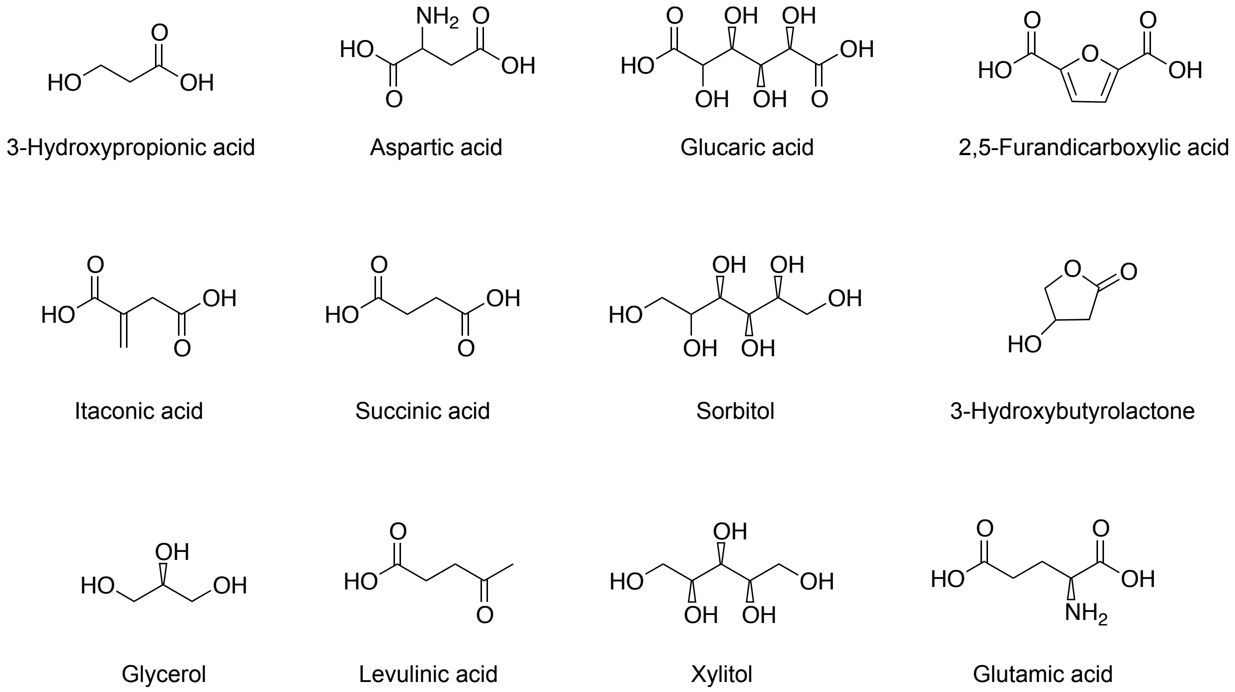

Figure 1.7 Twelve "building block" chemicals identified by PNNL and NREL as the most promising chemicals from sugars in lignocellulosic biomass. Reproduced with permission from ref. 5 Copyright 2006 NRC Research Press.

through the oxidation of lignin in alkaline conditions. Dimethyl sulfide is isolated from the reaction of kraft lignin with molten sulfur in basic conditions, where two methyl groups are transferred from lignin to sulfur[96]. Isolated dimethyl sulfide can then be oxidized with nitrogen dioxide to produce dimethyl sulfoxide. As dimethyl sulfide and dimethyl sulfoxide have no potential as a

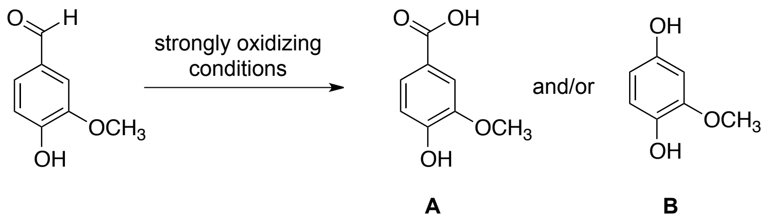

Figure 1.8a Formation of vanillic acid (A) and/or methoxyhydroquinone (B) under strongly oxidizing conditions

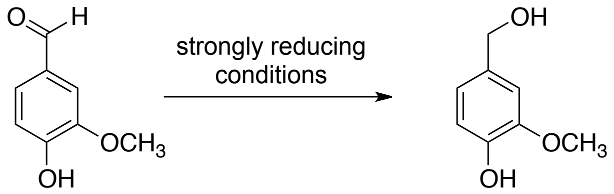

Figure 1.8b Formation of vanillic alcohol under strongly reducing conditions.

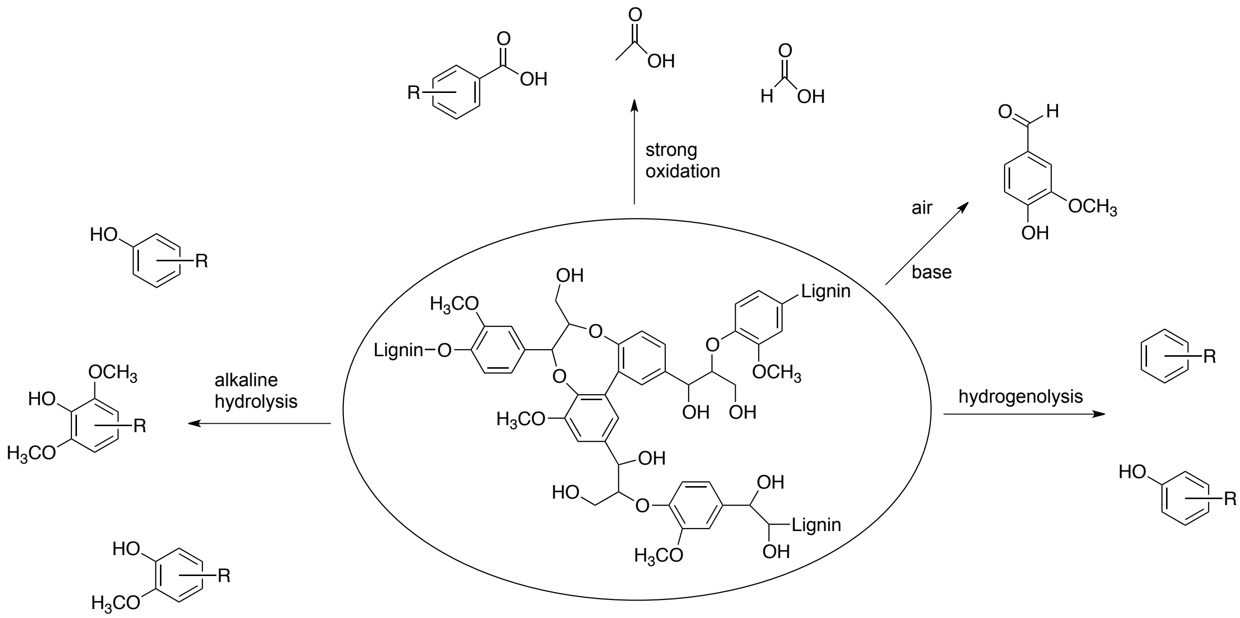

Figure 1.9 Previous commercial lignin transformations. Reproduced with permission from ref. 95 Published by Pacific Northwest National Laboratory, 2007.

monomers, only products from vanillin or vanillin derivatives will be discussed in sections regarding lignin-derived chemicals. Relevant vanillin derivatives are those that could be reasonably isolated under pulping conditions. In strongly oxidizing conditions, vanillin may be oxidized to vanillic acid or to methoxyhydroquinone via decarboxylation (**Figure 1.8a**)[97]. While in strongly reducing conditions, vanillin can be reduced to vanillic alcohol (**Figure 1.8b**). Previously, processes of lignin valorization[95] included the production of phenols by alkaline hydrolysis, dimethyl sulfoxide by oxidation of sulfated lignin, organic acids (benzoic, toluic, methoxybenzoic, acetic and formic) by oxidation, and phenols and aromatic hydrocarbons by the Nogichi or Crown-Zellerbach processes (**Figure 1.9**). Since petroleum-based methods to synthesize these chemicals cost significantly less, lignin-based methods (at least short-sightedly) are unnecessary. In contrast, based on the rate of production and consumption for these aromatic or aromatic-based products, an affordable alternative feedstock could supplement or replace current petroleum-based methods. With the development of more cost-effective and efficient hydrogenation or oxidation systems, more products may be isolated and the development of these processes could aid in the reduction of fossil fuel consumption. For the scope of this introduction, materials will only be considered lignin-based if they are actually sourced from lignin (e.g. organosolv lignin or sulfated lignin) or from a reaction using a lignin-sourced chemical.

1.3 Lignin and monolignol-derived polymers

1.3.1 Lignin as a macromonomer

The degradation of lignin to phenolic products or monolignols is an energy intensive process, which is one of the reasons lignin currently has more value as a fuel than as a feedstock. Methods that could utilize lignin as a source to synthesize new materials without any additional degradation would not only be useful but also energetically and environmentally favorable. Lignin has a widely varying structure depending on the source of the material and the process used to isolate it from the wood pulp. Despite these differences, all isolated lignins contain both phenolic and aliphatic hydroxyl groups. Once the proportions of these components have been adequately characterized[98], these functionalities can be used as linkers to create lignin-based macromonomers. Lignin has been used as a macromonomer for the synthesis of polyurethanes, polyesters, epoxide resins and phenolic resins.

1.3.1.1 Polyurethanes

Polyurethanes are synthesized from the polyaddition reaction of diisocyanates (or polyisocyanates) and polyols with terminal hydroxyl groups, forming polyurethane (carbamate) groups in the polymer backbone[99]. These polymers have a wide variety of applications and physical properties depending on the materials used and method of

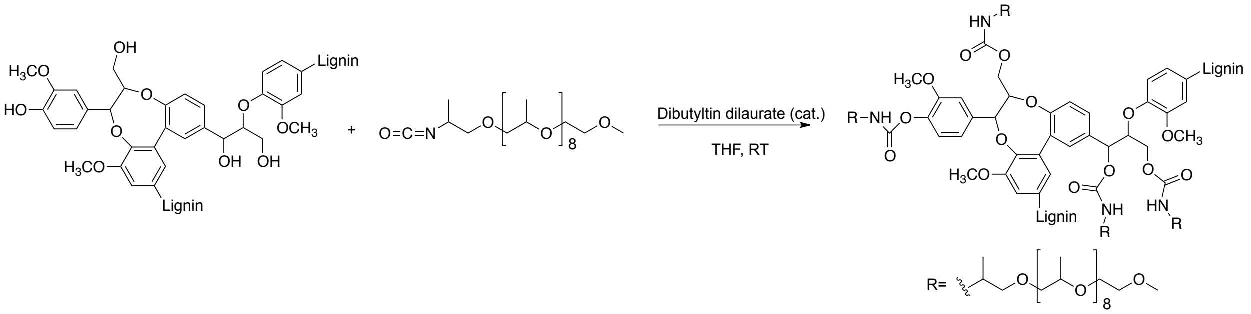

Figure 1.10 Polyurethane synthesis from organosolv lignin and an isocyanate-terminated polypropylene oxide macromonomer catalyzed by dibutyltin dilaurate from Gandini et al. (ref. 103)

---

synthesis. As lignin contains a large number of phenolic and aliphatic hydroxyl functionalities, it is able to replace the macropolyol component of polyurethanes quite easily[100]. In addition, biomass-based polyurethanes are more biodegradable than those derived from petroleum-based polyols[101-102]. Gandini et al. showed that both aliphatic and phenolic hydroxyl components of lignin reacted with an aliphatic isocyanate to form urethanes (**Figure 1.10**)[103]. When repeating the polymerizations with a macrodiisocyante, the flexibility of their diisocyanate over-compensated for the stiffness of the lignin and upon condensation resulted in a series of gel-like products with low T_g. As the ratio of isocyanate to hydroxyl groups was increased from 0.2 to 0.8 the T_g dropped from 44 ^{o}C to -15 ^{o}C[103]. Bonini and coworkers completed a similar study using steam-exploded lignin and 4,4'-methylenebis(phenylisocyanate) as a potential wood adhesive[104]. These materials cross-link at moderate temperatures (72 ^{o}C), suggesting potential as a stable adhesive. Duong et al. generated a high molecular weight polyurethane by controlling both the reaction temperature and length of reaction time[105]. Using Kraft lignin, molecular weights up to 912,000 g/mol were achieved in only three hours[105]. Hatakeyama combined each of four different types of technical lignin (kraft, alcoholysis, ligonsulfonate, and solvolysis lignin) with polyethylene glycol (PEG) or polypropylene glycol (PPG) and reacted the resulting mixture with diphenylmethane diisocyanate[106]. Regardless of the type of lignin used, Hatakeyma determined that lignin content is more influential on resulting material properties than any other factors such as the molecular weight of the polyols (PEG or PPG) or the ratio of isocyanate to hydroxyl groups. Similarly, Thring et al. combined lignin from the Alcell (an organosolv) process with PEG and reacted this mixture with polymeric methyl-diisocyante to generate polyurethane films that were then tensile tested[107-108]. They determined that both the ratio of hydroxyl to isocyanate functionalities and the amount of lignin used in the polyurethane strongly affected tensile properties[107]. Pohjanlehto and coworkers synthesized a sugar-based polyol, xylaric acid, and reacted it with lignin and PEG to generate a series of polyurethanes (**Figure 1.11**)[109]. Increasing lignin content in the product had little effect on T_g or Young's modulus, but the thermal stability improved slightly, suggesting the lignin acted to stabilize the final product. Pursuing materials with increased stiffness, Xue prepared a series of lignin-based rigid polyurethane foams using as much as 39.17 wt% lignin[110]. These biofoams featured increased thermal conductivity because of larger cell size and lower density than traditional

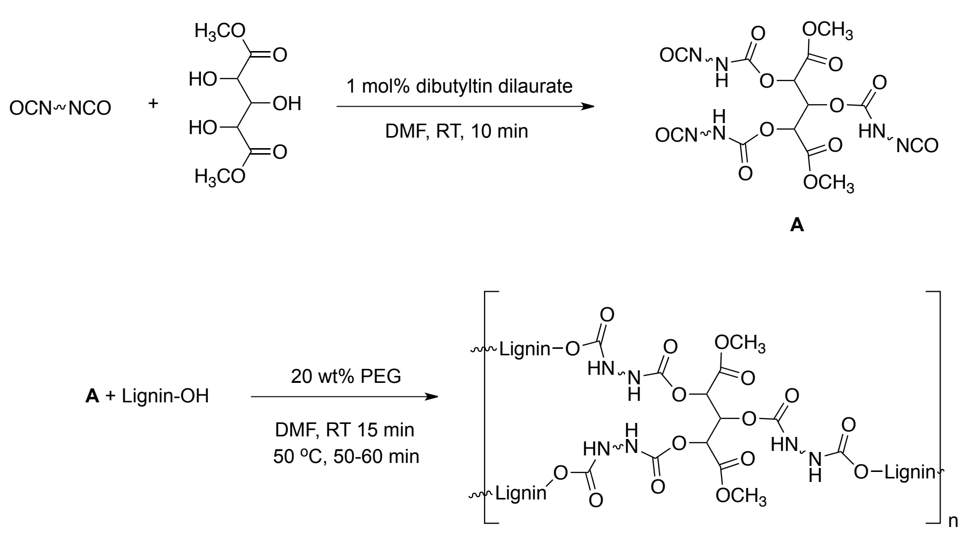

Figure 1.11 Lignin-based polyurethane synthesis from a xylaric acid-based triisocyanate macromonomer and Protobind™ lignin. OCN~NCO=methylene diphenyl diisocyanate. Reproduced with permission from ref. 109. Copyright 2013 John Wiley and Sons.

polyurethanes. In contrast to rigid polyurethane foams, flexible polyurethanes incorporate both soft (stretchable) and hard (cross-linked) blocks. Cinelli synthesized flexible polyurethane foams from kraft lignin utilizing lignin to form the hard blocks and a chain extender, such as castor oil, as the soft blocks once polymerized[111]. The addition of the chain extenders lowered the T_g of the polyurethane significantly, making the foams flexible. In contrast to the more typical applications of lignin incorporation, Yiamsawas et al. recently reported the synthesis of lignin-polyurethane nanocontainers by inverse miniemulsion[112]. A suspension of the sodium lignosulfonic acid in water was mixed with a surfactant (polyglycerol polyricinolate) prior to reaction with toluene diisocyanate. This method created hollow, cross-linked lignin-polyurethane nanocontainers of diameters between 311 to 390 nm (in water) capable of containing water-soluble cargo. They were shown to be stable in aqueous solution for weeks and readily degraded over 24 hours using natural enzymes. While these results demonstrate proof-of-concept for the incorporation of lignin, many properties must be fine-tuned before lignin-based polyurethanes are available as a commodity material. Additionally, batch-to-batch variation in lignin will lead to batch-to-batch variation in these systems.

1.3.1.2 Polyesters

Polyesters are polymeric materials containing ester linkages that can be synthesized in three different ways: polyesterification of dicarboxylic acids with diols or dihalides, self-polyesterification reactions of hydroxycarboxylic acids, and the ring-opening polymerization reactions of lactones and cyclic esters[113]. The use of lignin as a macromonomer for polyester synthesis typically limits polymerization reactions to

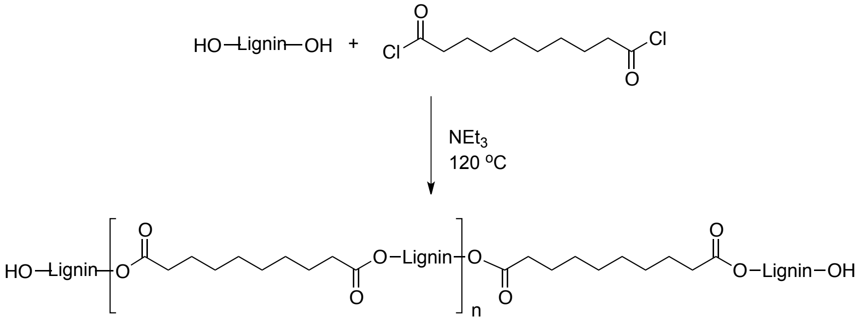

Figure 1.12 Polyesters synthesized via the condensation of Kraft lignin with sebaccoyl chloride. Reproduced with permission from ref. 115. Copyright 2009 Taylor & Francis.

condensation reactions, but some examples of ring-opening reactions of lactones have also been reported.

Guo and Gandini synthesized a series of cross-linked polyesters using polyethylene glycol, dicarboxylic acid chlorides, and lignin[114]. While the incorporation of lignin causes some solubility issues, increasing lignin content from 0 to 35% resulted in a modest increase in T_g (-60 °C to -50 °C, respectively). In a similar system, Binh et al. combined kraft lignin and sebacoyl chloride under basic conditions to generate polyesters via condensation (**Figure 1.12**)[115]. The resulting polyester had a T_g of 70 °C and molecular weights of 39,000 g/mol were reached. Moreover, this polymer was shown to be capable of melt processing between 120 – 140 °C without changes in color or the formation of an odor, suggesting potential commercial use[115]. Bonini et al. reacted steam-explosion lignin with dodecandioyl dichloride to generate a series of polymers with low molecular weights of M_n between 1,915 and 6,382 g/mol[104]. Other properties of the resulting materials were not characterized, but Bonini suggested they could potentially be used in the formation of coatings. Gandini and coworkers determined how modifying linker stiffness affected T_g of the resulting material[103]. Using a flexible linker, sebacoyl chloride, they were able to obtain materials with T_g as low as -60 °C. When using a stiff aromatic linker, they were able to obtain materials with T_g as high as 150 °C. Gandini also tested the effects of incorporating as much

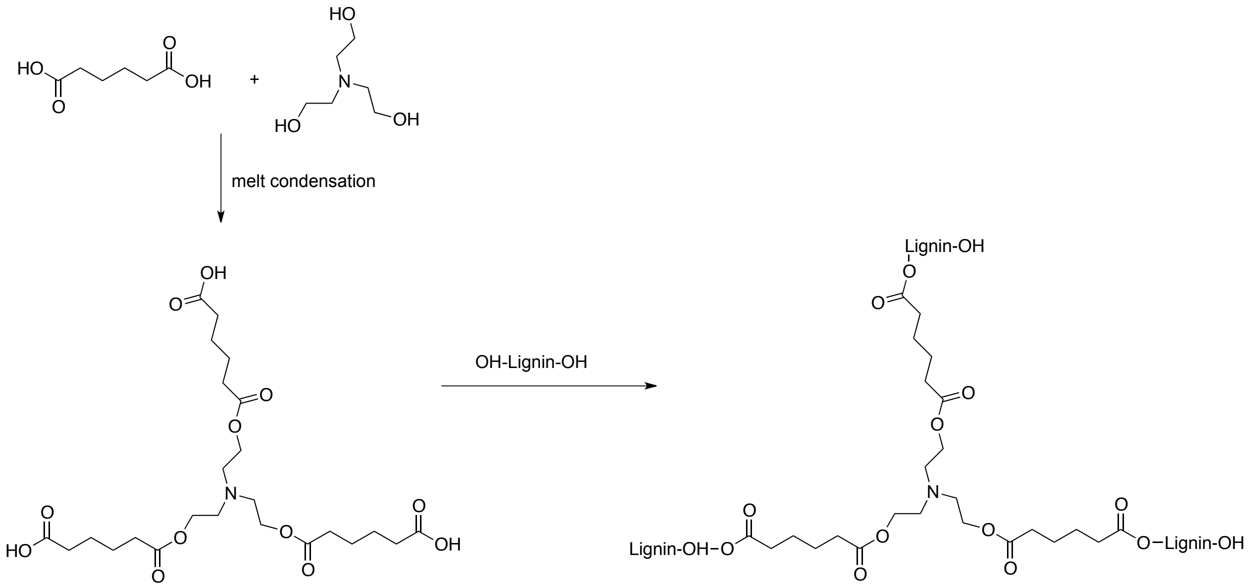

Figure 1.13 Lignin-based polyester synthesis via melt condensation of Protobind™ lignin with 1,1,1-triethanolamine and adipic acid-based tricarboxylic acid macromonomer. Reproduced with permission from ref. 117. Copyright 2011 Elsevier.

as 65% polyethylene glycol into the polymerization reactions and found those products incorporating more lignin had significantly better thermal stability[103]. Using carboxylic acid functionalized lignin and ε-caprolactone, Matsushita et al. created polyesters via condensation of poly ε-caprolactone with the functionalized lignin surface[116]. The resulting polymer had a higher melting temperature and increased loss and storage modulus in comparison to poly ε-caprolactone. Sivasankarapillai created a highly branched polymer network through the condensation of lignin with a tri-branched carboxylic acid monomer. The triacid monomer was synthesized via the condensation of adipic acid with 1,1,1-triethanolamine prior to the condensation reaction with lignin (**Figure 1.13**)[117]. Polyesters isolated from this process were flexible and tough and these properties were easily varied with the ratio of lignin used.

1.3.1.3 Epoxide resins

Epoxide resins are a type of thermoset polymer, which are composed of monomers containing at least one epoxide group. With highly tunable properties, these resins are typically used in coatings, adhesives, composites and electronic materials. The epoxide groups can be homopolymerized using anionic or cationic polymerization, or they can be copolymerized with comonomers (also known as hardeners) such as polyfunctional amines, acids, anhydrides, alcohols, thiols and phenols[118]. Selection of the epoxide and the curing agent(s) greatly impacts the chemical, mechanical and physical properties of the resulting product. While lignin itself contains no epoxides naturally, the same macromonomer phenolic structure utilized in the synthesis of polyurethanes and polyesters can also be used in the synthesis of epoxide resins as a hardener/ cross-linking agent. Epoxide resin reactions with lignin components are typically either catalyzed with a small amount of an amine or an amine is added quantitatively to the reaction as an additional cross-linker.

A water-soluble variation was synthesized by Nonaka et al. through the mixing of an alkaline solution of Kraft lignin with polyethylene glycol diglycidyl ether[119]. The glass transition temperature was easily adjusted through the addition of alternate crosslinkers (e.g. bisphenol A). Feldman et al. also tested a series of epoxy resins with lignin (up to 40 wt%) and other hardeners incorporated[120-122]. Incorporation of lignin was shown to improve adhesive strength in tension thus adding lignin could lower the production cost of materials requiring strong adhesion[120]. Additionally, the identity of the hardener did not impact the physical properties of the adhesive as much as the quantity of lignin incorporated, implying the least expensive material could be chosen to lower production cost[122]. Engelmann and Ganster combined a low molecular weight lignin fraction (M_n=1,300 g/mol) with 1,3-glycerol diglycidyl ether to generate a series of solvent-free resins with lignin content as high as 50 wt%[123]. The higher wt% lignin-based resins exhibited greater thermal stability than those made with pyrogallol with T_g up to 66 °C. In general, lignin imparts thermal stability to the resulting resin but cannot act as the sole cross-linker in the system; another cross-linking agent must be added to obtain desirable properties.

1.3.1.4 Phenolic resins

Analogous to epoxide resins, phenolic resins are thermosets created via the acid or base-catalyzed step growth polymerization of phenols and aldehydes. The ratio of phenol to aldehyde controls the degree of crosslinking in the final product and determines if a crosslinker must be added to harden the resin. The most common phenolic resins are produced from phenol and formaldehyde and are typically used as adhesives. Bakelite, a phenolic resin synthesized from phenol and formaldehyde, was the first completely synthetic polymer developed and commercialized,[124] demonstrating the widespread use of

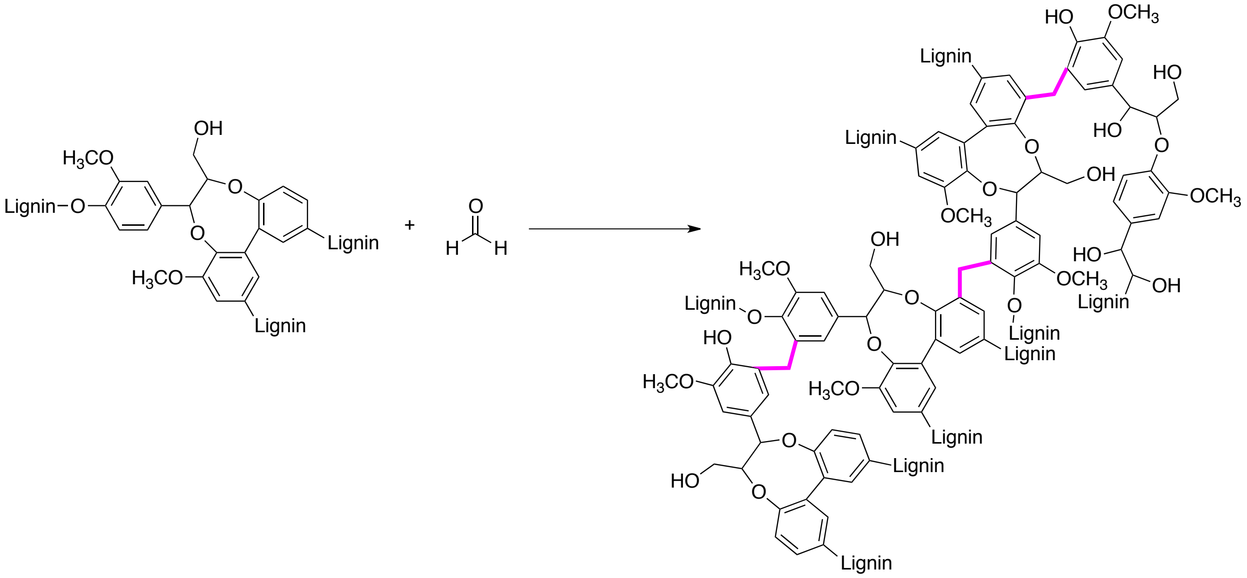

Figure 1.14 General scheme of phenol-formaldehyde resins formed with lignin instead of phenols. New methylene crosslinks from condensation with formaldehyde are shown in magenta.

these resins. For lignin-based phenolic resins, the phenol-rich structure of lignin lends itself quite readily to replace phenol in traditional synthesis protocols (**Figure 1.14**). While no resins using only lignin exist to our knowledge, there have been several attempts to incorporate lignin into phenol-formaldehyde resins by replacing a portion of the phenol used with lignin. Cure rate, viscosity and the mechanical properties of the resin are important in determining the appropriate application. Peng and Riedi studied the rheology of a series of resins that incorporated between 0 and 40% ammonium lignosulfonate with phenol and formaldehyde, determining that the cure rate of the resins decreased with increased lignin content[125]. Further exploring this concept, Alonso et al. studied the gelation and vitrification of lignin-phenol-formaldehyde resins[126]. In these isoconversional experiments, they found the resin with lignin incorporated had a slightly lower activation energy than the standard phenolic resin, which results in a slightly lower the degree of curing at the gel point (irreversible point at which viscous liquid becomes an elastic gel). Vázques et al. incorporated lignin into a phenolic resin used as an adhesive for plywood[127]. Lignin was dissolved in phenol and reacted with paraformaldehyde to yield an adhesive that incorporated approximately 20 wt % lignin into the final material. While this adhesive took longer to cure than traditional phenol-formaldehyde resins, the resulting plywood boards exhibited equal strength to boards prepared using traditional methods. Danielson and Simonson also prepared lignin-phenol-formaldehyde resins as adhesives for plywood and evaluated their potential industrial use[128-129]. Once again, resins with different percentages of lignin incorporated were prepared (between 0 and 80 wt % lignin). Boards adhered with phenolic resins containing 20 and 60% lignin possessed shear strength at the joint equivalent or superior to that of standard phenol-formaldehyde resins. At 80%

incorporation, the adhesive strength was significantly diminished due to the brittle nature of lignin. Danielson et al. found that the incorporation of 50% lignin was ideal to maintain storage stability, resin viscosity and bonding ability most similar to phenol-formaldehyde resins[128]. Sarkar and Adhikari obtained similar results when they studied the effects of lignin content on both wood-wood and metal-metal adhesion[130]. They found that adding 50 wt% lignin decreased the adhesive strength for wood-wood joints to 78% of maximum compared to a non-lignin phenol-formaldehyde adhesive, and 86% for metal-metal (Al-Al) joints. As observed by other groups, lowering lignin content improved joint adhesion but increasing lignin content provided higher thermal stability.

1.3.2 Functionalized lignin as a macromonomer

Lignin is often functionalized to generate new active sites and aid in the synthesis of new macromolecular materials, which allows lignin to be incorporated into new materials. While lignin has many functionalities (e.g. hydroxyl or phenol), these potentially active sites are often concealed or sterically hindered by the high-cross link density of lignin. Functionalization can improve issues related to the chemical structure of lignin by decreasing brittleness, increasing solubility in organic solvents, improving processability and improving reactivity. This section will highlight polymeric materials synthesized from lignin that has been chemically modified to either add reactive groups not present in native lignin or enhance functional groups available on the native lignin scaffold that are critical to the development of the respective polymeric material. Polymers with modified lignins as macromonomers include polyurethanes, epoxide resins, and phenolic resins. Modified lignins have also served as macromonomers in the development of both hydrogels and vinyl-based graft copolymers.

1.3.2.1 Polyurethanes

Chung et al. took one of the simplest functionalization approaches by demethylating lignin methoxy groups with Lewis acid catalysts to generate 28% more hydroxyl groups on average[131]. The demethylated lignin was then reacted with toluene-2,4-diisocyante to generate polyurethanes with significantly increased cross-link density. Recently, Laurichesse et al. functionalized hydroxyl groups in lignin with oleic acid via esterification

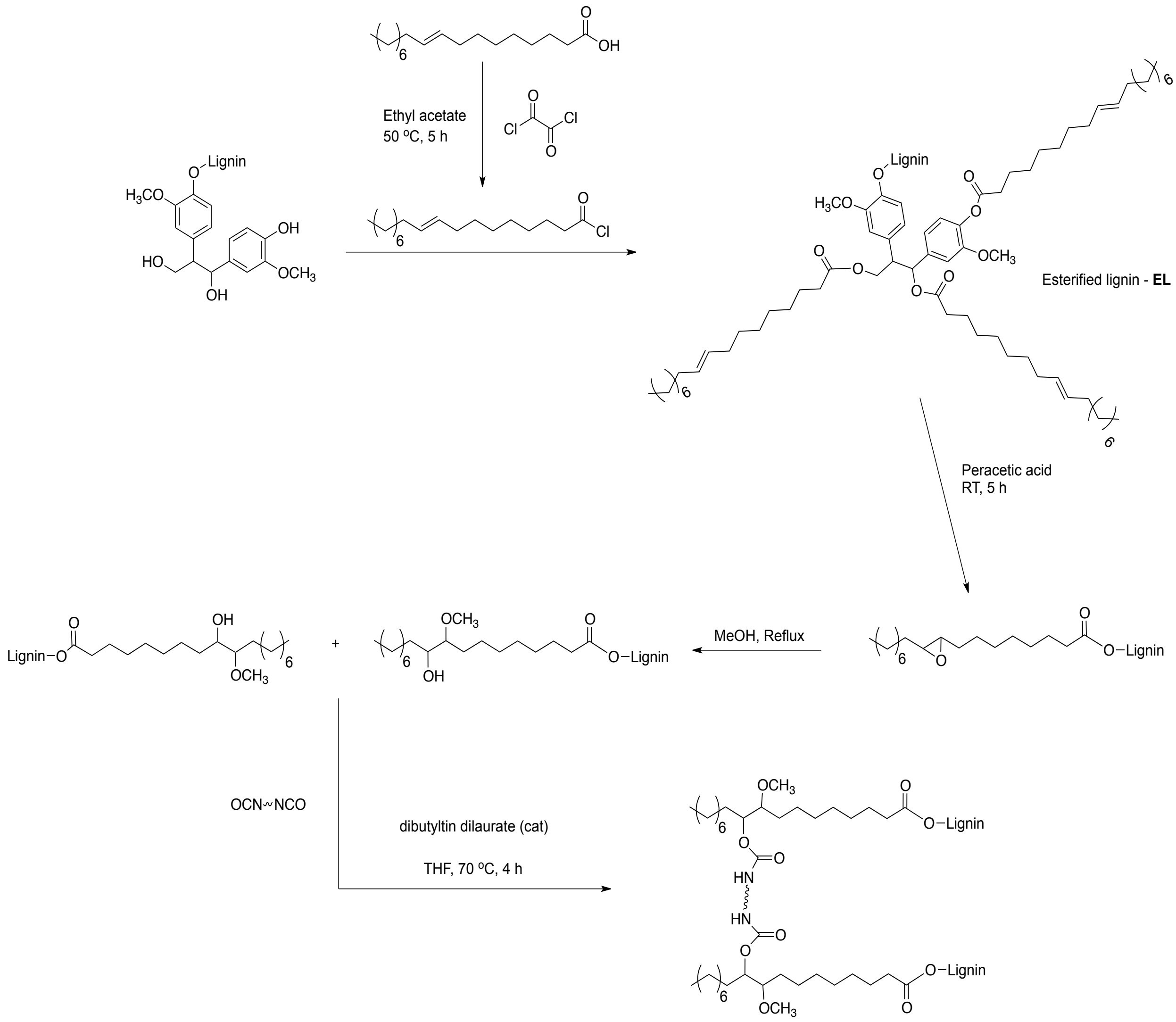

Figure 1.15 Synthesis of polyurethanes from lignin-oleic acid based polyols (LOAP). OCN~NCO are polypropylene oxide diisocyanates of molecular weights of 425, 1000 and 2000 g/mol, respectively. Reproduced with permission from ref. 132. Copyright 2014 Royal Society of Chemistry.

to generate an esterified lignin[132]. They then utilized the fatty acid double bond to form an epoxide and subsequently ring-opened it to generate a new lignin-oleic acid based polyol (**Figure 1.15**). Upon reaction with polyisocyanates, T_g was shown to decrease both with an increased length of the polyisocyanates and also with increased ratios of isocyanate to hydroxyl groups (NCO:OH)[132]. Nadji et al. developed a series of rigid polyurethane foams with insulating and physical properties similar to those derived from petroleum-based products[133]. In this functionalization method, propylene oxide was reacted with the hydroxyl functionalities on lignin to extend access to these reactive groups out of the cross-linked and sterically hindered lignin network. This technique was also used by Cateto et al. in a series of rigid polyurethane foams from four different oxypropylated lignins as co-polyols[102]. The biodegradability of polyurethanes with only lignin-based polyols was shown to be higher than those with an additional (non-lignin) polyol incorporated. Hatakeyma and coworkers utilized the hydroxyl functionalities of lignin to initiate the ring-opening polymerization of ε-caprolactone to extend hydroxyl functionalities beyond the lignin network[134]. This caprolactone-capped lignin was then reacted with diphenylmethane diisocyanate to form polyurethanes. The length of the polycaprolactone cap was shown to have little effect on T_g at $DP \geq 5$, but prior to reaching this plateau, T_g dropped from -28 °C with two caprolactone units to -50 °C with five caprolactone units[134]. Liu found that the functionalization of lignin with amines via a Mannich condensation with formaldehyde increased the water solubility, reactivity with isocyanates and long-term stability of the polyurethane product[135]. Zhu et al. developed a lignin-based, flame-retardant polyurethane foam via the synthesis of a lignin-based phosphate melamine compound in three steps[136]. The resulting polyurethane showed increased compression strength, thermal stability, char residue formation, and self-extinguishment. Many of the lignin-based polyurethanes mentioned exhibited superior physical properties compared to more traditional petroleum-based materials, but with the difficulty associated in the complete characterization of lignin prior to functionalization, these materials will require additional study and development before entering the market.

1.3.2.2 Epoxide resins

While lignin itself contains no epoxides naturally, lignin-based epoxide resins are usually synthesized in one of two ways: a) epoxide groups can be added to the lignin molecular structure or b) the macromonomer phenolic structure can be enhanced to improve incorporation into epoxide-based resins. As mentioned in Section 1.3.1.3, amines are typically utilized in lignin-based epoxide resin reactions either as a catalyst or quantitatively as an additional cross-linker. Epoxide groups are added to lignin in several ways with the simplest method being the functionalization of phenolic hydroxyl groups through a reaction with epichlorohydrin in basic conditions (**Figure 1.16**). This method was initially published by Mikhailov[137] and Mihailo[138] but featured little characterization of the resulting products. Later, this method was patented by D'Alelio et al., but once again featured minimal characterization of the polymeric materials synthesized[139]. Subsequently, El Mansouri et al. characterized the resulting products and found that the quantity of incorporation of lignin in the samples improved both thermal

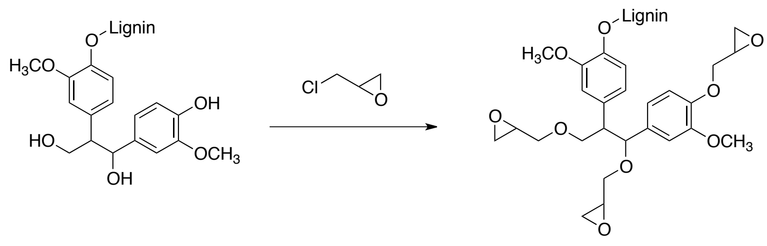

Figure 1.16 Epoxide functionalization via a condensation reaction between lignin and epichlorohydrin.

stability and epoxy index[140]. Okabe and Kagawa have also determined the importance of the molecular weight of the lignin used in polymerization[141]. When the weight average molecular weight (M_w) was less than 300 g/mol, stabilizing effects with lignin incorporation were not observed, but if the M_w was larger than 10,000 g/mol the resulting epoxy compound was no longer soluble in organic solvents for processing.

To improve the degree of epoxide functionalization with epichlorohydrin, lignin is typically pre-functionalized to increase the number of hydroxyl units present. The most common method in literature is the incorporation of additional phenolic moieties. Simionescu et al. described the synthesis of epoxides from lignosulfonates and studied their degradation[142-143]. Directly reacting iron or ammonium lignosulfonate with phenols created a phenolated product, which was then epoxidized with epichlorohydrin. In this process, two different resins were generated, one that was partially water-soluble and one that was insoluble in water, but neither were characterized significantly beyond ensuring epoxidation of the material[144]. Tai et al. increased the number of phenolic units present in native lignin using phenol, bisphenol A or acetone, before reacting with epichlorohydrin[145-147]. This pre-functionalization reaction led to higher levels of epoxidation and when cross-linked with triethylene tetramine, the resulting product exhibited good waterproof adhesion after curing.

Other possible methods to increase reactivity of native phenolic groups towards functionalization with epichlorohydrin include adding an “extender” to allow the reactive hydroxyl groups to reach outside the tightly cross-linked lignin network. Hofmann and Glasser compared a series of lignins where the hydroxyl functionality was chain extended via either propoxylation with propylene oxide or ethoxylation with ethylene oxide prior to epoxidation[148-149]. Increased lignin content significantly impacted both the curing and glass transition temperatures with increased degrees of crosslinking. Additionally, the chemical kinetics of the curing reaction were not affected by the incorporation of lignin[150].

In contrast to its epoxide-functionalized variation, lignin can also be functionalized with other reactive groups for incorporation in epoxide resins as a cross-linking agent. Hirose et al. dissolved lignin in ethylene glycol and reacted the product with succinic anhydride to generate a mixture of both a lignin-based carboxylic acid derivative and an ethylene glycol-based polyacid as products[151]. These products were then reacted with ethylene glycol diglycidyl ether to generate resins. By varying the ratio of epoxides to carboxylic acid, they were able to manipulate T_g. Additionally, all resins showed good thermal stability[152]. Ismail et al. utilized a similar system, adding glycerol to the reaction and generating a second polyacid *in situ*[153]. Once again, increased lignin content leads to a higher T_g with increased cross-linking. The same effect was also seen when the concentration of glycerol was increased. Despite an increased chain length, this was postulated to occur with the higher concentration of hydroxyl groups present, therefore increasing the degree of interchain hydrogen bonding in the resulting resin. Lignin has also been functionalized with amines via a Mannich condensation reaction to yield a cross-linker that was reacted with the diglycidyl ether of bisphenol A (**Figure 1.17**)[154]. Mendis et al. demonstrated that

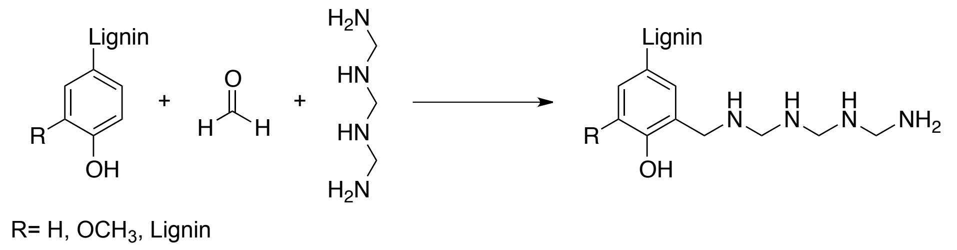

Figure 1.17 Mannich condensation of lignin with *N,N'*-hexamethylenediamine. Reproduced with permission from ref. 154. Copyright 2015 John Wiley and Sons.

this method of functionalization increased the dispersion of lignin in an epoxy matrix, resulting in materials with properties more similar to that of traditional epoxy resins.

1.3.2.3 Phenolic Resins

While unmodified lignin is considered an effective replacement for phenol in phenolic resins, lignin can be hydroxymethylated (methylolated) or phenolated to increase reactivity (rate of incorporation), producing materials with properties more analogous to traditional phenolic resins. Peng and Riedi compared the rheology of hydroxymethylated and non-hydroxymethylated lignin-phenol-formaldehyde resins[125]. While the reactivity of the hydroxymethylated lignin was higher that of the non-hydroxymethylated, the cure rate of the resulting resin was lowered as the functionalized lignin acted as a diluent in the system. Conversely, at the gel point for all temperatures measured, the hydroxymethylated lignin had a much higher degree of curing than phenol-formaldehyde resins. Benar et al. tested the maximum level of incorporation of hydroxymethylated lignin into lignin-phenol-formaldehyde resins without significant loss of desired properties (e.g. viscosity, strength, thermal stability, crosslinking temperature)[155]. They determined that up to 50% hydroxymethylated lignin could be incorporated, to yield products with viscosities appropriate for use as particleboard adhesives. A more recent study by Alonso et al. suggests that only up to 35 % hydroxymethylated lignin can be incorporated while maintaining properties (e.g. viscosity, gelation time) similar to a commercial phenol-formaldehyde resin[156]. The difference in the value may originate from their methods of characterization, as they only compare it to one commercial product rather than investigating ranges of acceptable values. Vaquez et al. compared the effects of lignin modification by hydroxymethylation or phenolation on lignin-phenol-formaldehyde resins[157]. Gelation times of these resins were between 11.0 and 24.7 minutes, which were similar to gelation times of commercial phenol-formaldehyde resins. In testing, all boards prepared with either resin met European standards. The lignin-added resin offered better spreadability and prevented blowouts during processing, suggesting an advantage to using lignin-added resins. In this case, no significant differences in resulting material properties were seen between resins prepared with phenolated or hydroxymethylated lignins.

1.3.2.4 Hydrogels

While not a unique polymer structure or type of polymer, hydrogels serve unique functions and thus several examples will be identified separately here. Hydrogels are water-swollen, cross-linked, three-dimensional polymer networks synthesized from the reaction of one or more monomers[158]. Hydrogels are hydrophilic but do not dissolve in water, and instead maintain their three-dimensional shape. Hydrogels can be either biologically derived (natural polymers) or synthetic and have many potential applications such as protein or drug delivery systems, scaffolds for tissue engineering, or absorbents. Hydrogels often incorporate a large amount of water, with Q_v (volume swelling ratio= swollen gel volume/dry gel volume) ranging from 1-100 or more, depending on the relative hydrophilicty of the polymeric repeat units.

Many of the hydrogels developed using lignin have low water swelling capacities with $g_{H2O}/g_{gel} < 10$ (gram of water/grams of dry gel) [159]. While this is logical given the hydrophobic nature of lignin, several research groups have been able to either increase this swelling ratio or develop a novel use for the material. Passauer et al. synthesized a series of lignin-based hydrogels with oxidatively activated lignin (pre-reaction with hydrogen peroxide in an alkaline solution) and polyethylene glycol diglycidyl ether[159-161]. These hydrogels featured swelling ratios up to $g_{H2O}/g_{gel} = 75$. With this increased water content, Passauer postulated that they would be useful as soil additives for water and nutrient retention. Feng et al. recently reported the synthesis of a hydrogel from acrylamide and acetic acid functionalized lignin, using ethylene glycol dimethyacrylate as a cross-linker[150]. This hydrogel was designed for use as a polymeric flocculent.[162] While functionalized lignin has been utilized in flocculation, to our knowledge, this is the only known example of lignin incorporation into a hydrogel for use in flocculation, as alkali lignin is typically considered a contaminant in aqueous waste streams of pulping mills. The adsorption of dye in the hydrogels was shown to increase with increasing lignin content, up to 29.65 mg of methylene blue per gram of hydrogel[150]. While not a hydrogel, but instead an organogel, Cunha et al. prepared a series of lignin-based polymer networks that were shown to swell in toluene[163]. They functionalized lignin with methyl methacrylate and then copolymerized the functionalized lignin macromonomer with additional methyl methacrylate. The swelling ratio was shown to decrease with increasing lignin content as the network became denser.

1.3.2.5 Vinyl-based Graft Copolymers

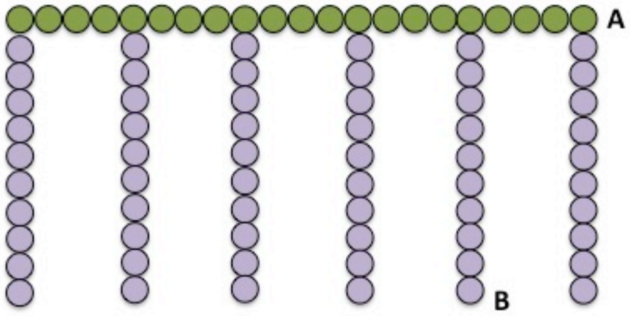

Figure 1.18 General scheme of A-graft-B copolymer where the green circles denote monomer A and the purple circles denote monomer B.

Graft copolymers describe a type of copolymer architecture where chains of one polymer (B) are attached at points on the other polymer (A) (**Figure 1.18**)[164]. This co-polymer can be described as A-*graft*-B or A-*g*-B. Graft co-polymers are used to improve the mechanical properties of composites, reduce frictional force between two dissimilar surfaces and reduce the flammability of materials[164]. Copolymerization of lignins with vinyl comonomers has provided insight into lignin reactivity in addition to generating novel graft-co-polymers. In work by Chen et al., calcium lignosulfonate that had been activated through ozonolysis was used as the polymer backbone and grafted with styrene[165]. This co-polymerization was a heterogeneous system with a Fenton initiator (ferrous chloride and hydrogen peroxide) in methanol, which allowed higher degrees of incorporation into the lignin network. The grafting efficiency of styrene co-polymerization plateaued at 18%, regardless of initiator concentration. Acrylic-based graft copolymers with lignin were also synthesized. Chen and Kokta prepared a series of copolymers from calcium lignosulfonate and either methyl methacrylate, methyl acrylate or methylacrylic acid where each polymerization was initiated with a Fenton initiator[166]. They found the degree of polymerization was highly influenced by the reaction solvent as well as the ratio of hydrogen peroxide to monomer used. Grafting efficiency was maximized at 60% using methyl acrylate or methylacrylic acid, while methyl methacrylate was much less efficient at 32% because of lower propagating radical reactivity. Li et al. also utilized a Fenton initiator, in this case to graft styrene onto dealkaline lignin[167]. With optimization of the system they were able to achieve a grafting yield of 59.5% as well as a grafting efficiency of 53.7% for lignin. Liu and coworkers grafted methyl methacrylate onto lignin activated with calcium chloride and hydrogen peroxide[168]. The resulting copolymers had very low grafting yields (around 8.58%) but the products showed both enhanced thermal stability and increased hydrophobicity. Cunha et al. demonstrated that lower grafting yields of methyl methacrylate with lignin can be expected when using a radical initiator due to side

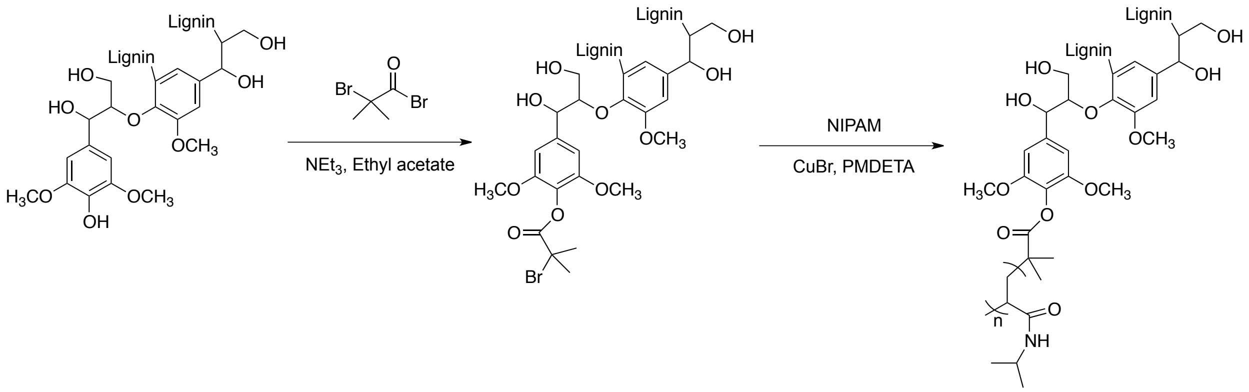

Figure 1.19 Scheme for the synthesis of lignin-g-(poly)NIPAM copolymers via ATRP.
NIPAM=*N*-Isopropylacrylamide
PMEDTA= N,N,N'N",N"-pentamethylenediethylenetriamine
Reproduced with permission from ref. 173. Copyright 2010 American Chemical Society.

reactions with phenolic hydroxyl groups[169]. A more recent study from Ye et al. suggests that phenolic hydroxyl groups do not always inhibit polymerization, but rather are the active site for grafting chain growth[170]. While they were unable to provide compelling evidence that this is the mechanism of the grafting reaction, their data shows that the phenolic hydroxyl content is proportional to both monomer conversion and grafting yield suggesting there is some correlation between phenolic hydroxyl content and the radical polymerization reaction. Moreover phenols are known chain transfer agents, such as the chain transfer constant for 4-methoxyphenol is on the order of 10^{-4} for methyl methacrylate[171] and methyl acrylate[172] depending on the reaction conditions. Investigating controlled polymerization methods, Kim and Kadla utilized atom transfer radical polymerization (ATRP) to synthesize a thermoresponsive graft lignin copolymer reducing bimolecular chain termination and the limited grafting yields seen with free radical polymerization[173]. Kraft lignin was functionalized with 2-bromoisobutyryl ester to create a macroinitiator for ATRP and then was grafted with *N*-isopropylacrylamide (NIPAM) under mild ATRP conditions (**Figure 1.19**). The polymerization reactions were well controlled resulting in polymers with PDI as low as 1.09 and grafting chains up to DP=43. These copolymers also exhibited a lower critical solution temperature (LCST) at 32 °C, which is identical to that of poly(NIPAM), indicating the incorporation of lignin has no impact on the thermal properties of the poly(NIPAM) chains. A similar approach utilizing ATRP was employed by Hillburg et al. to generate lignin graft co-polymers with styrene and methyl methacrylate[174]. Lignin was functionalized with 2-bromoisobutyryl ester to generate a macroinitiator before ATRP with either styrene or methyl methacrylate, which generated well-defined polymer structures featuring a lignin core surrounded by the copolymer matrix (**Figure 1.20**). The resulting copolymers also had improved thermal stability and toughness compared to the corresponding homopolymers. Yu et al. saw similar results in a

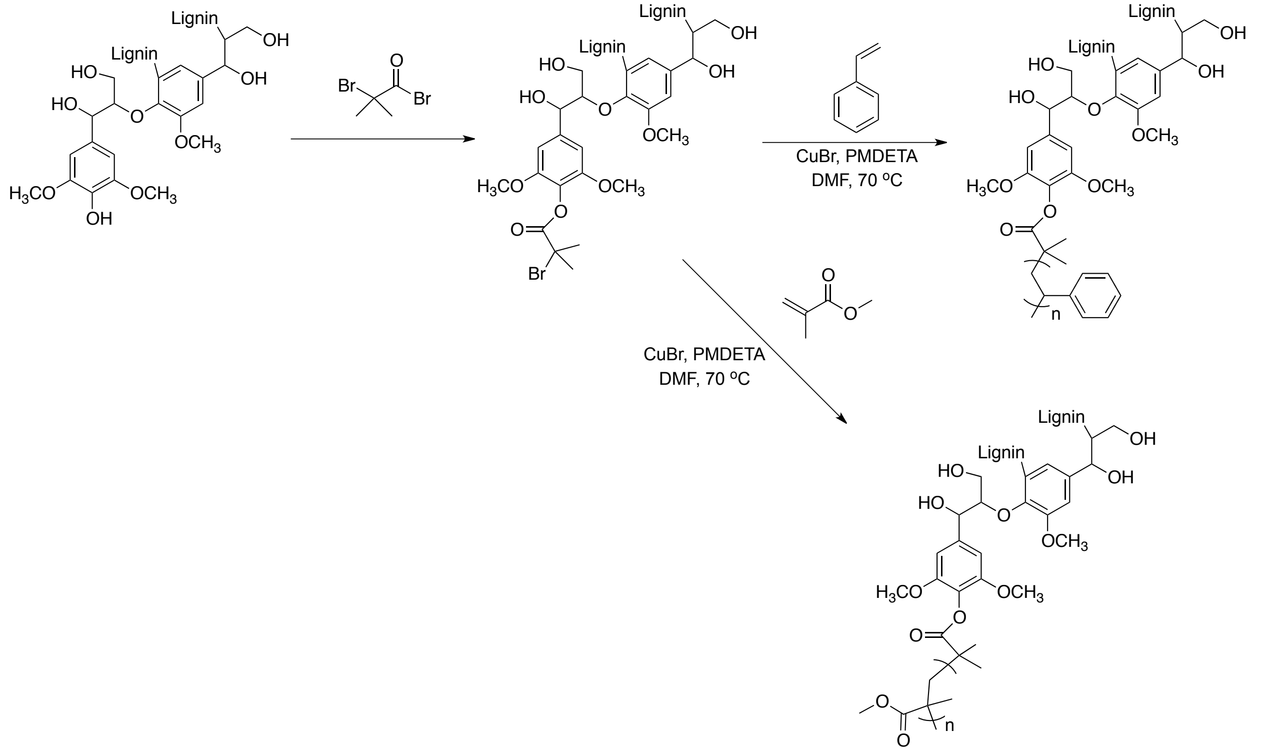

Figure 1.20 Synthetic scheme for the synthesis of lignin-g-poly(styrene) and lignin-g-poly(methyl methacrylate) via ATRP. Reproduced with permission from ref. 174. Copyright 2014 Elsevier.

series of lignin-grafted copolymers from methyl methacrylate and butyl acrylate. The grafted chains were random polymers of methyl methacrylate and butyl acrylate. By controlling the ratio of the monomers, they were able to control the T_g of the resulting material. These materials were also shown to have strong absorption in the UV spectrum, offering potential in coatings applications. Chung et al. synthesized a lignin-lactide copolymer by grafting lactide onto acylated lignin catalyzed by 1,5,7-triazabicylo[4.4.0]dec-5-ene (TBD)[175]. The resulting copolymers were found to have an increased T_g as well as enhanced UV absorption when used as dispersion modifiers in polylactide-based materials.

1.3.3 Monolignols as monomers

There are three monolignols found in plants: *p*-coumaryl alcohol, coniferyl alcohol and sinapyl alcohol (Figure 1.1). Monolignols are functionalized phenols that can be utilized in aromatic or phenol-based polymer systems, as seen with lignins. While there are only three monolignols, there are several analogous compounds also included in this section. Though the exact biosynthetic pathway has yet to be fully elucidated, monolignols are generally believed to be synthesized *in planta* through a pathway beginning with the deamination of phenylalanine to cinnamic acid[7]. Then, depending on the target monolignol, the species may undergo a series of hydroxylation and methylation reactions prior to reduction of the side-chain carboxylic acid to an alcohol (**Figure 1.21**). With this in mind, this section will include not only monolignols as monomers in polymer synthesis but also the corresponding precursor carboxylic acids: cinnamic acid, *p*-coumaric acid (also commonly referred to in literature as 4-hydroxycinnamic acid), ferulic acid and sinapic acid. Because fewer polymeric materials have been produced from these monomers, both

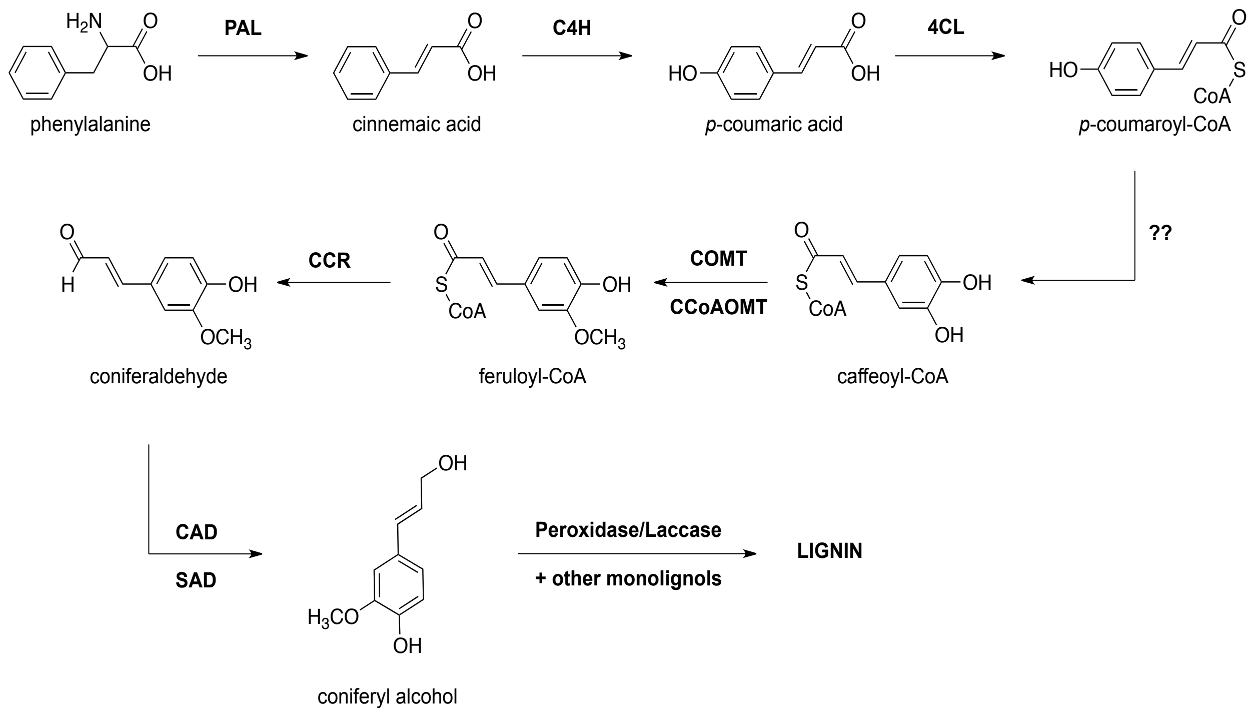

Figure 1.21 One proposed biosynthetic pathway for the monolignol coniferyl alcohol[5]. CoA=Coenzyme A PAL= phenylalanine ammonia-lyase; C4H= cinnamate 4-hydroxylase; 4CL= Coenzyme A ligase; ?? = Unknown step; COMT= caffeic acid-*O*-methyltransferase ; CCoAOMT= caffeoyl-CoA *O*-methyltransferase; CCR= cinnamoyl CoA reductase ; CAD= cinnamyl alcohol dehydrogenase ; SAD= sinapyl alcohol dehydrogenase. Reproduced with permission from ref. 7. Copyright 2003 Annual Reviews.

unmodified and functionalized monolignols and carboxylic acids will be included in the same section.

1.3.3.1 Polyurethanes

As mentioned previously, polyurethanes are synthesized via the reaction of polyols with diisocyanates. While monolignols are unable to act as either component without modification or dimerization, they offer the potential to be incorporated into these polymeric structures. Oulame et al. synthesized a ferulic acid-based dimer by coupling ferulic acid with either aliphatic diols of different lengths or isosorbide[176]. The resulting diol was then polymerized with either 1,4-tolulene diisocyanate or 1,6-hexamethylene diisocyanate to yield a series of polyurethanes (**Figure 1.22**). These polyurethanes could

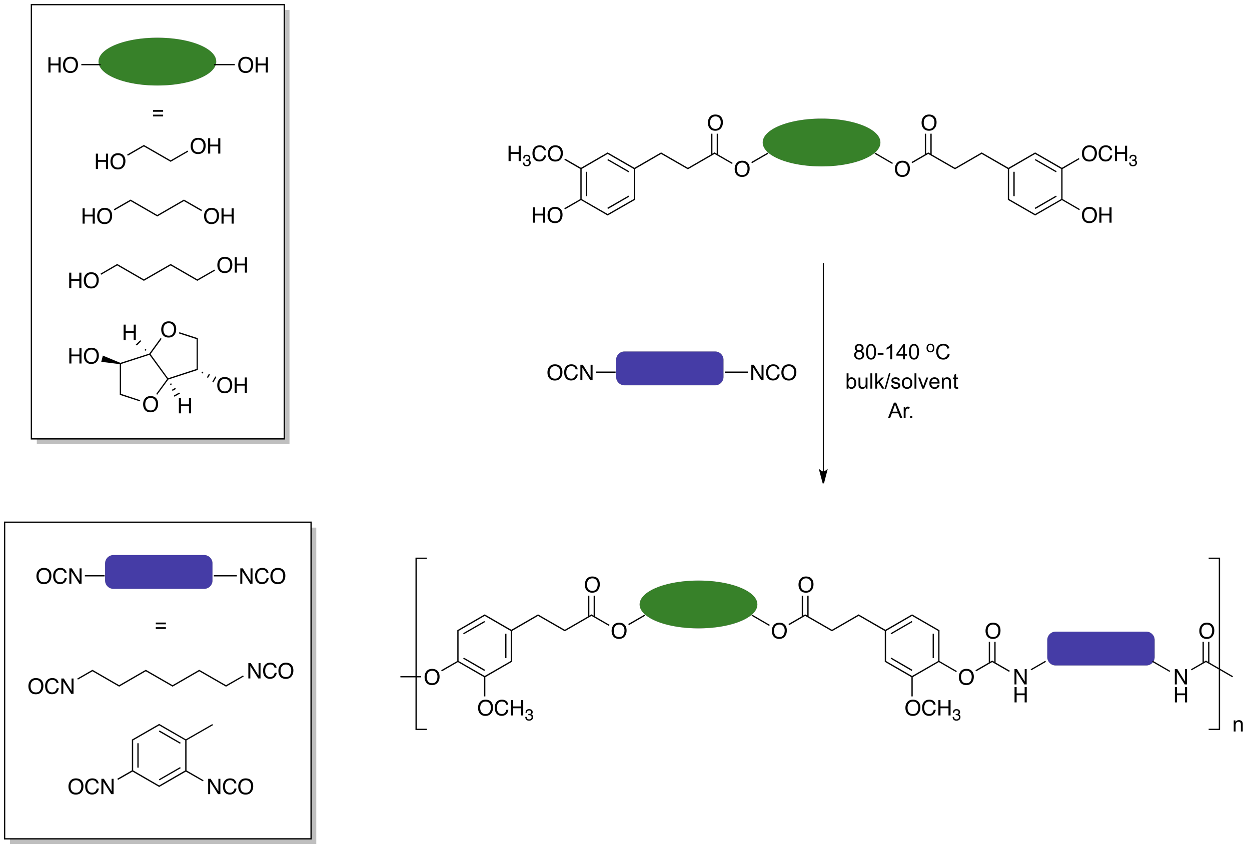

Figure 1.22 Synthetic scheme for the synthesis of eight poly(ester-urethane)s from ferulic acid-based diols. Reproduced with permission from ref. 176. Copyright 2015 Elsevier.

be synthesized in solvent or solvent-free conditions and exhibited high thermal stability and varying T_g (depending on the linkers used). While the products were generally low in molecular weight, they serve as a proof of concept for synthesis of polyurethane materials from monolignols or their analogues/precursors. More recently, Chen et al. synthesized polyurethanes from a dimeric cresol-based monomer[177]. After the dimerization, cresol was first functionalized with epichlorohydrin to generate a bisepoxide which was then reacted with CO_2 to yield the corresponding bis(cyclic carbonate) monomer. This bifunctional monomer was then reacted with either hexamethylene diamine or isophorondiamine to yield polyurethanes with high thermal stability.

1.3.3.2 Polyesters

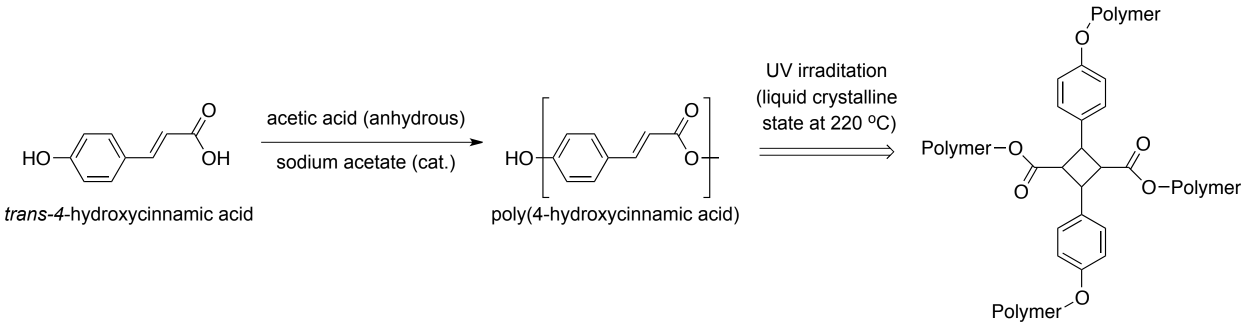

Figure 1.23 Proposed 2+2 cycloaddition of poly(4-hydroxycinnamic acid) in the liquid crystalline state at 220 °C. Reproduced with permission from ref. 178. Copyright 2004 John Wiley and Sons.

As mentioned previously, polyesters are most typically formed by condensation reactions (although other methods are known). The incorporation of monolignols and their corresponding carboxylic acid precursors into polyesters should be relatively facile, given their hydroxyl-rich functionality. Nevertheless, there are few examples of polyester formation solely from unmodified monolignols, as the high aromatic content in the resultant polymer results in brittle materials similar to natural lignins. Kaneko et al. synthesized a bio-based polymer from *p*-coumaric acid via melt condensation with acetic acid and sodium acetate as the first example of a liquid-crystalline polymer from a single natural monomer (**Figure 1.23**). The resulting polymer underwent a photoinitiated 2+2 cycloaddition in the liquid-crystalline state and was shown to have good cell compatibility[178]. Kaneko later created a biodegradeable hyperbranched copolymer from the polymerization of *p*-coumaric acid and 3,4-dihydroxycinnamic acid[179]. The resulting materials had high enough T_g for processing (115 °C < T_g < 169 °C), photoreactivity in the liquid-crystalline state, and readily decomposed via hydrolysis. Spiliopoulos and Mikroyannidis copolymerized *p*-coumaric acid with *p*-hydroxybenzaldehyde using thionyl chloride in basic conditions[180]. While the copolymers were amorphous, once crosslinked, the resulting polyesters exhibited a significant increase in T_g. Matsusaki and coworkers copolymerized *p*-coumaric acid with lactic acid in both solvent and solvent-free conditions[181]. While significantly less *p*-coumaric acid was incorporated into the copolymer than lactic acid, the resulting copolymers were shown to have photoreactivity, high solubility in organic solvents and biodegradability. Jin et al. developed a degradable terpolymer featuring *p*-coumaric acid, glycolic acid and *p*-hydroxybenzoic acid[182]. In this reaction, *p*-coumaric acid acted as a promoter to increase the copolymerization of the other two monomers. The resulting products possessed good thermal stability (T_g=82 °C) and mechanical strength. They were also shown to degrade by hydrolysis, with a 70% decrease in their viscosity over 200 hours of stirring in a pH 7 buffer.

Examples using a modified monolignol or precursor are much more abundant in the literature, as modification allows for monomers with improved thermal stability (aromatic content). Introducing other functionalities reduces the brittleness of the resulting polyester materials. Kimura et al. synthesized 4-acetoxycinnamic acid by reacting *p*-coumaric acid with acetic anhydride[183]. Kimura then synthesized poly(*p*-oxycinnamoyl) microspheres through the condensation of 4-acetoxycinnamic acid in liquid paraffin[184]. Changing the solvent could control the diameter of the microspheres and the resulting materials

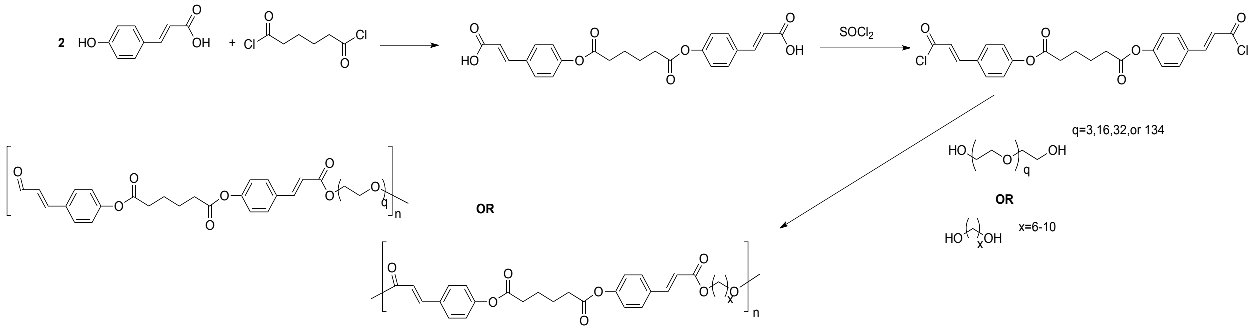

Figure 1.24 Synthetic scheme for 4-hydroxycinnamic acid dimer-based polyester from either polyethylene glycol or short chain diols. Reproduced with permission from ref. 188. Copyright 2003 John Wiley and Sons.

exhibited good thermal stability. Thi and coworkers reported the synthesis of a macromonomer through the coupling of 3,4-diacetoxycinnamoyl chloride with short-chain poly(L-lactic acid)[185]. This macromonomer was polymerized with sodium acetate in solvent-free conditions resulting in a branched, polydisperse, high-molecular weight polyester[186]. The thermal and mechanical properties of the polymer were superior to those seen in poly(L-lactic acid) and the rate of degradation increased with the incorporation of the acetylated coumaric acid. Photocuring provided control over degradation. Sapich et al. synthesized a dichloride dicarboxylic acid by first joining *p*-coumaric acid with brominated diols with chain lengths between six and twelve carbons, and subsequently chlorinating with thionyl chloride[187]. The dichloride was condensed with methylhydroquinone and isosorbide to generate a series of polymers with unique optical properties that could be set using photocuring. Nagata and Hizakae synthesized a macromonomer by capping both hydroxyl functionalities of *p*-coumaric acid with adipoyl dichloride to create a new dichloride macromonomer (**Figure 1.24**)[188]. This macromonomer was condensed with hexane-1,6-diol resulting in new high-molecular weight co-polyesters. These polymers underwent rapid enzymatic degradation unless crosslinked via photodimerization of the double bond (**Figure 1.25**). At high-molecular weights the crosslinked polymers swell in water. Nagata expanded the repertoire of biodegradable polymeric materials created by using the same adipoyl dichloride capped *p*-coumaric acid macromonomer, by condensing it with short chain poly-ε-caprolactone diols[189]. The resulting high-molecular weight polyesters were photocured without a photosensitizer to create biodegradable, elastic materials with improved thermal properties. Kreye et al. created a monomer from ferulic acid in three steps by esterification with methanol to methyl ferulate, hydrogenation of the

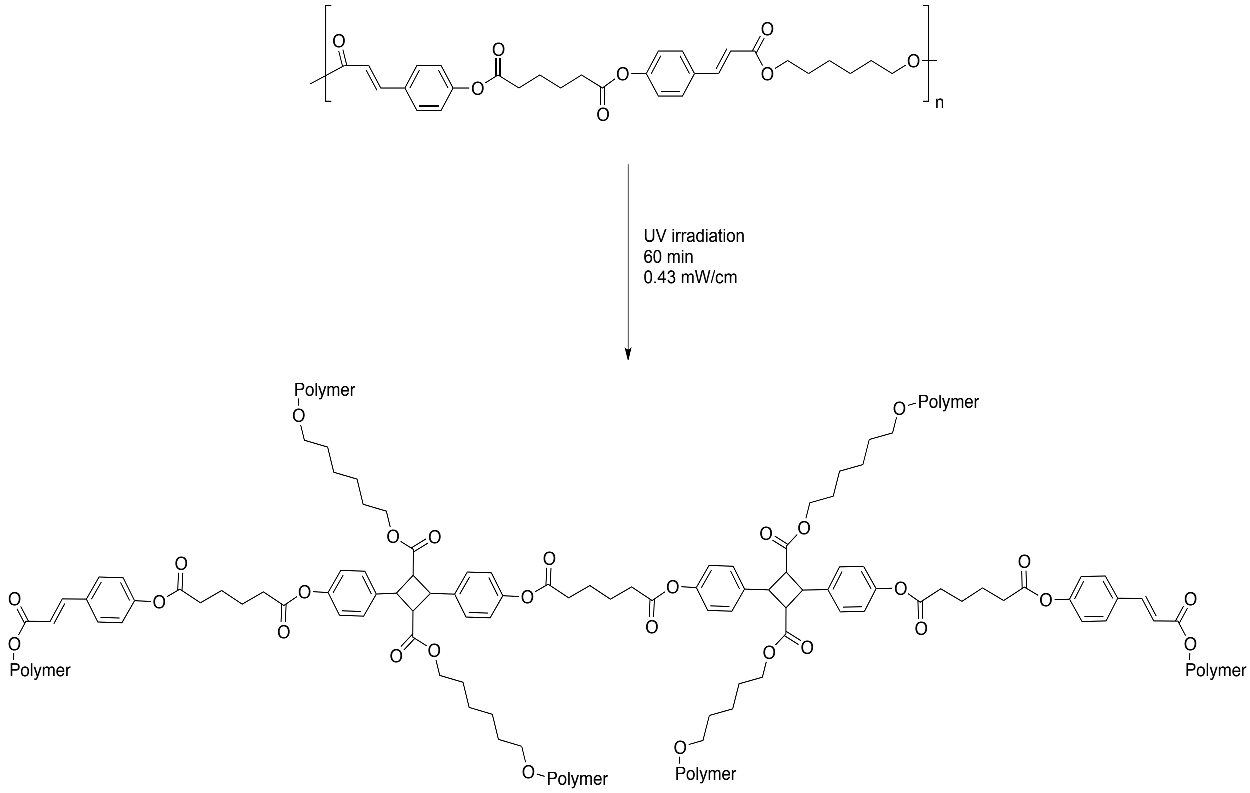

Figure 1.25 Example of 2+2 cycloaddition of 4-hydroxycinnamic acid dimer-based polyesters via UV irradiation from Nagata et al. (ref. 188).

conjugated double bond, and hydroxyethylation with ethylene carbonate[190]. This methyl ester derivative of ferulic acid was then co-polymerized with rapeseed-oil-derived oleic and erucic acid monomers to generate a series of polyesters. More recently, Ouimet et al. synthesized a *p*-coumaric acid dimer macromonomer through the reaction of two equivalents of *p*-coumaric acid with adipoyl chloride[191]. The resulting diacid was polymerized in solution with triphosgene, resulting in a polyester that could be decomposed into *p*-coumaric acid and adiapic acid in a controlled fashion. As *p*-coumaric acid has shown antioxidant activity but has a short half-life *in vivo*, this method could allow for therapeutic levels to be maintained in the body. Ouimet also prepared an analogous series of diacids with ferulic acid, showing similar degradation and antioxidant properties[192]. Ouimet suggested that the release of both ferulic and *p*-coumaryl acid could be controlled based upon the length of linker used in the macromonomer diacid. Pion et al. utilized a similar linking technique with ferulic acid and either 1,4-butanediol or isosorbide as a linker to create a macromonomer diol[193]. They then copolymerized this diol with diacyl chlorides of differing lengths to control the thermal properties of the resulting material. The polymers exhibited high thermal stability and properties similar to those of commercial materials such as polyethylene terephthalate, but the polymerization was not well controlled as seen in the high PDI and M_w values.

1.3.3.3 Epoxide resins

As mentioned previously, the observable properties of epoxide resins are based upon the selection of both the epoxide and curing agent(s). The molecular structure of these components and their correlating rigidity are crucial in the development of useful resins. Resins fabricated with compounds containing more rigid structures such as

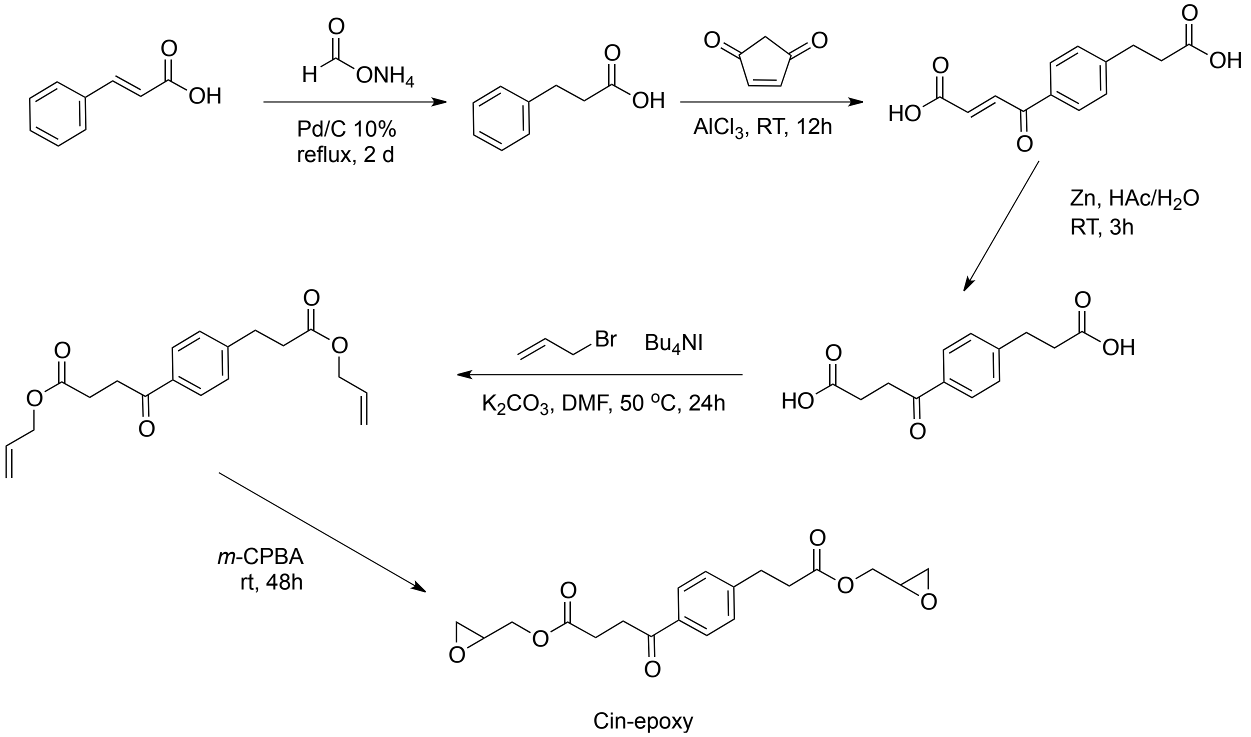

Figure 1.26 Synthesis of cinnamic acid-dervied epoxy (Cin-epoxy). Reproduced with permission from ref. 194. Copyright 2014 Royal Society of Chemistry.

aromatic rings are much more thermally stable and desirable than more flexible compounds such as aliphatic chains. While lignin has been employed in many formulations of epoxide resins, its limited solubility is often an issue in the development or processing of new materials. Monolignols or the precursor carboxylic acids contain the same ideal aromatic structure without the solubility issues observed when using lignin as a macromonomer. Xin et al. modified cinnamic acid through two synthetic steps (allylation then epoxidation) to generate a bifunctional epoxy monomer[194]. This epoxy monomer was then cured with maleic anhydride derivatives as cross-linkers to generate a series of resins (**Figure 1.26**). The curing properties of the resins were similar to that of petroleum-based resins. Kim created a crosslinked epoxy resin by reacting cinnamic acid with a series of epoxy resins[195]. The functionalized epoxy resins were then photocured to result in a product with enhanced thermal stability and improved optical properties. Zhao et al. recently synthesized an epoxide resin by functionalizing 2-methoxy-4-propylphenol (a methoxylphenol product isolated from the degradation of lignin) with epichlorohydrin to create an epoxide monomer which was then cured with diethylenetriamine and octadecylamine modified nano-montmorillonite (a nanoclay)[196]. The resulting epoxide resin exhibited high thermal stability, which increased with higher nanoclay loadings, and good mechanical strength. Fache et al. also recently synthesized epoxide resins from a mixture of aromatic monomers produced from the degradation of lignin to vanillin[197]. The mixtures (soft or hardwood) containing vanillin, syringealdehyde, p-hydroxybenzaldehyde, vanillic acid, syringic acid, acetovanillone, and aceteosyringone were first subjected to a Dakin oxidation to generate diphenolic compounds. The resulting compounds were then functionalized with epichlorohydrin to yield the corresponding epoxides. Fache et al. next cross-linked the soft and hardwood mixtures (separately) of epoxide products with isophorone diamine to generate epoxide resins. These resins were shown to have high thermal stability and exhibited fire retardation properties.

1.3.3.4 Phenolic resins

Both monolignols and the precursor carboxylic acids feature phenolic hydroxyl functionalities, making them suitable to replace phenols in phenolic resins. Polybenzoxazines are a specific type of phenolic-cure resin typically synthesized by the condensation of phenol and an amine in the presence of formaldehyde to generate a six-membered heterocyclic ring[198]. Under curing conditions, this heterocycle is thermally ring-opened resulting in a polybenzoxazine. Depending on the substitution of the amine or phenol, both curing temperature and resulting polymer physical properties can be controlled. Comí et al. synthesized a series of benzoxazines from coumaric and ferulic acid through the condensation of the carboxylic acid with aniline and formaldehyde[199]. The curing temperature required for these monomers was higher than a temperature at which they were thermally stable, resulting in decomposition rather than polymerization. Boron trifluoride was added as a ring-opening catalyst (3%) to lower the curing temperature allowing the formation of several polymeric products (**Figure 1.27**). These products were

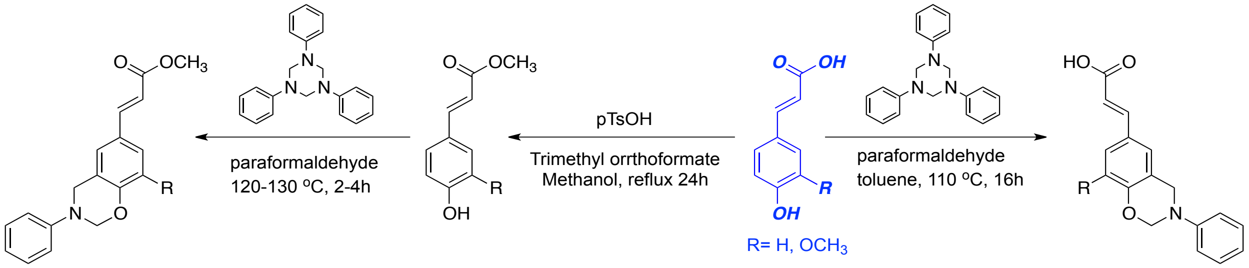

Figure 1.27 Synthesis of *p*-coumaric acid and ferlulic acid-based benzoxazines. Benzoaxines were synthesized from both the acids and their corresponding methyl esters. Reproduced with permission from ref. 199. Copyright 2013 John Wiley and Sons.

shown to be thermally stable and comparable to petroleum-derived products.

1.3.3.5 Polyamides

Polyamides are a class of polymers featuring an amide linkage in the polymer backbone. These materials are typically formed through the condensation of a diacid monomer with a diamine monomer or self-condensation of an amino acid. Many well-known commercial materials such as Kevlar, Nomex and Nylon feature this type of polymeric linkage. As neither monolignols nor precursor carboxylic acids have the required bifunctionality to form polyamide linkages, only modified monomers have been used in the synthesis of polyamides. Castillo and coworkers synthesized polyamides from the polymerization of hexamethylenediamine with a ferulic acid dimer[200]. The ferulic acid dimer was synthesized by the UV-catalyzed 2+2 cycloaddition of acetylated ferulic acid to generate a diacid species, which was then polymerized with a diamine (**Figure 1.28**). While reactivity with the diamine was low due to competing side reactions, the resulting polymers exhibited increased thermal stability and antioxidant activity. Noel et al. synthesized a series of amide monomers by coupling ferulic acid with amino acids[201]. The macromonomer synthesized with L-serine was unable to be polymerized because of an elimination pathway, but when L-tyrosine ethyl ester was used instead a series of polymers

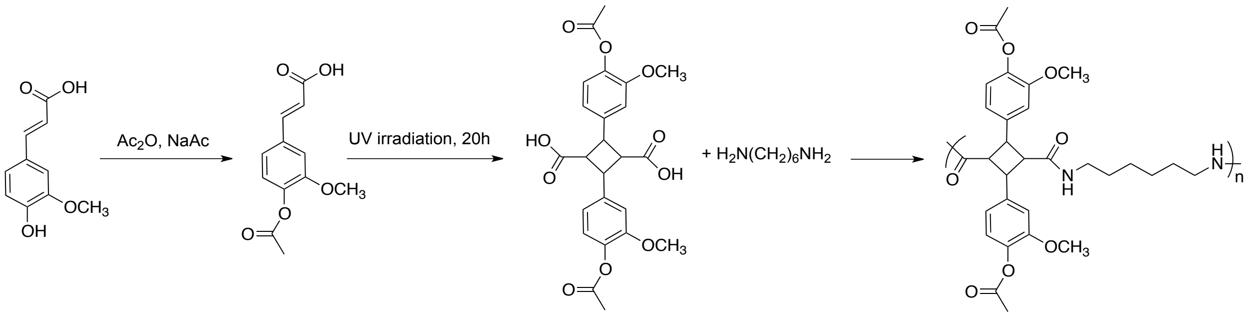

Figure 1.28 Synthesis of poly(amide) from photo-dimerized ferulic acid. Reproduced with permission from ref. 200. Copyright 2004 Taylor & Francis.

was obtained. The polymerization was shown to proceed in a well-controlled fashion and improved the observed thermal and fluorescence properties. Both regioregular and regiorandom polymers could be synthesized. More extensive characterization showed the observed fluorescence could be shifted depending on the regiochemistry of the polymer[202]. The polymer was stable in both neutral and acidic conditions, suggesting possible use in long-term bioengineering applications where fluorescence is necessary.

1.3.3.6 Vinyl-based polymers

As a parallel to previous sections focused on vinyl-based graft copolymers in lignin-bases constructs, this section will focus on vinyl groups or copolymers with vinyl functionalities in combination with monolignols or their carboxylic acid precursors. Kreye et al. synthesized a diene derivative from ferulic acid in two steps by first reducing the double bond in ferulic acid and followed by the condensation of both hydroxyl groups with allyl bromide[203]. The resulting diene was then polymerized in a controlled fashion via acyclic diene metathesis (ADMET) using a series of ruthenium catalysts. Homopolymerization of the ferulic acid-based diene led to polymers with low molecular weights, thus copolymers with diene-functionalized fatty acids were obtained. These copolymers had improved thermal properties, compared to the homopolymers, but were

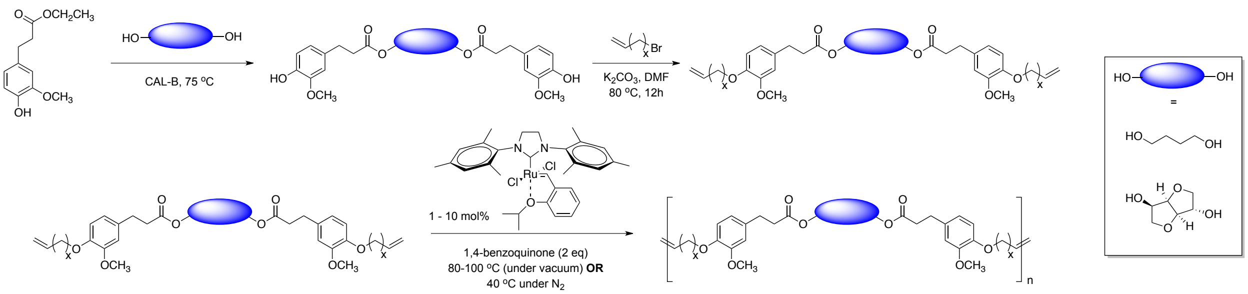

Figure 1.29 Synthesis and ADMET polymerization of ferulic acid-based vinyl dimer. Reproduced with permission from ref. 204. Copyright 2015 Elsevier.

still low in molecular weight. Barbara et al. took a similar approach and synthesized a ferulic acid-based diene monomer in two steps by first creating a ferulic acid dimer with several diols as linkers, then functionalizing the resulting diols with allyl bromide[204]. The resulting monomers were polymerized via ADMET with a ruthenium catalyst, this time resulting in higher molecular weight polymers (**Figure 1.29**). The increased polymeric activity lead to higher molecular weight polymers featuring increased thermal stability and tunable T_g by changing the length of the linker used in the synthesis of the diene. Iemma et al. took a more direct approach and copolymerized ferulic acid with methacrylic acid (MAA)[205]. While the exact polymeric structure was unable to be elucidated they speculate that both the "styrene-like" double bond and phenolic radical could be incorporated into the resulting polymer. The copolymer had high antifungal and antioxidant properties, suggesting possible use in biological applications.

1.4. Polymers from lignin-derived chemicals

As discussed in Section 1.2.4.3, the number of lignin-derived chemicals is actually quite small with the relatively high cost of production in comparison to petroleum-derived chemicals. While a host of aromatic chemical products were previously synthesized from lignin, only vanillin is currently produced from lignin on a commercial scale. With this in mind, only vanillin and vanillin-derivatives will be discussed as feedstocks for monomer and polymer synthesis. Chemicals as scaffolds for monomer and polymer synthesis discussed in this section will be vanillin, vanillic acid, and vanillic alcohol.

1.4.1 Vanillin

Vanillin is a phenolic aldehyde commonly used as a flavoring compound in food, beverage and pharmaceutical products. While vanillin can be extracted from natural sources, synthetic vanillin from lignin or guaiacol is more commonly available. With its functionalities and large-scale availability, vanillin is an ideal scaffold for monomer synthesis. Amarasekara et al. prepared polyvanillin through the reductive coupling of divanillin in an electrochemical cell[206]. Divanillin is a vanillin dimer synthesized through either metal-based or enzymatic methods. The resulting polyvanillin had poor solubility in most organic solvents but high thermal stability at modest molecular weights (M_n=11,784). Chauhan synthesized a vanillin-based condensation terpolymer by polymerizing vanillin oxime, 4-hydroxyacetophenone and formaldehyde[207]. Vanillin oxime was prepared by reacting vanillin with hydroxylamine hydrochloride under basic conditions. The resulting terpolymer had high thermal stability and antimicrobial activity. Holmberg et al. synthesized a series of block copolymers via reversible addition-fragmentation chain transfer (RAFT) with vanillin methacrylate and laurel methacrylate[208]. Vanillin methacrylate was synthesized by reacting vanillin with methacrylic anhydride. A homopolymer of vanillin methacrylate was synthesized and used as a macro-chain transfer agent in block copolymer synthesis with laurel methacrylate (**Figure 1.30**). Not only did these block copolymers have excellent thermal properties (T_g above 100 °C and T_d greater than 300 °C), they were also shown to self-assemble into nanospheres. Modifying the comonomers and ratios used lead to block copolymers with different thermal properties

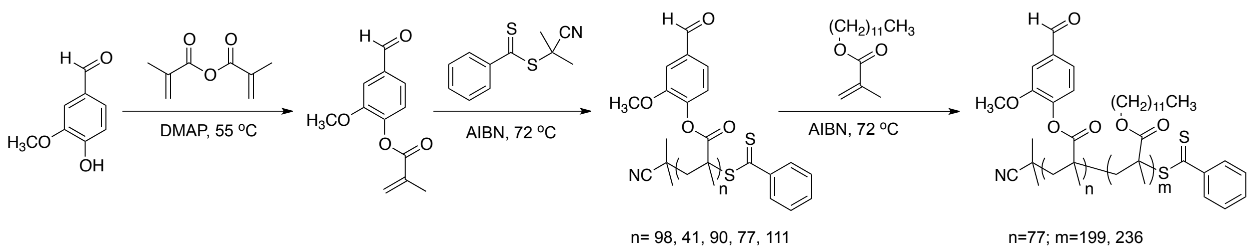

Figure 1.30 Synthesis and RAFT polymerization of vanillin and fatty acid-based copolymer. Reproduced with permission from ref. 208. Copyright 2014 American Chemical Society.

and morphologies. Stanzione and coworkers condensed vanillin methacrylate (synthesized in the same method as above) with glycerol dimethyacrylate to form a vinyl ester resin[209]. The resulting resin was a low viscosity resin at room temperature, requiring curing with Trigonox 239 (a hydroperoxide) to form a hard, transparent polymer. The resin had a broad T_g and high thermal stability, similar to that of commercial vinyl ester resins. Renbutsu et al. utilized vanillin methacrylate derivatives, functionalized either with glycidyl methacrylate or methacrylic acid, to modify chitosan by conjugating the chitosan amine to the aldehyde of the functionalized vanillin[210]. The resulting material was photocrosslinked using Irgacure 1000 as a photoinitiator, resulting in biocompatible, natural hydrogels. Rao and Samui synthesized a series of vanillin-based polyester epoxides that exhibited photoactive liquid crystalline behavior[211-212]. Diols were synthesized by the dimerization of vanillin with either acetone or cyclohexanone linkers. The diols were then epoxidized by reacting with epichlorohydrin under basic conditions. The resulting epoxides were copolymerized with either terephthalic or trimesic acid resulting in linear or branched architecture, respectively (**Figure 1.31**)[211]. Sini and coworkers synthesized a benzoxazine monomer from the condensation of vanillin and furfurylamine with formaldehyde[213]. The thermal initiated ring-opening of the benzoxazine monomer was estimated to occur between 170 and 190 ^{o}C. The presence of the formyl group yielded additional crosslinking at higher temperatures, leading to increased char yield, thermal stability and T_g. Pemba et al. synthesized a series of cyclic and spriocyclic polyacetal ethers from vanillin[214]. The synthesis of these polymers is complicated, beginning with the synthesis of a vanillin dimer linked with dibromoethane. This dimer was then condensed with either pentaerythiritol or di(trimethylolpropane) to yield the corresponding

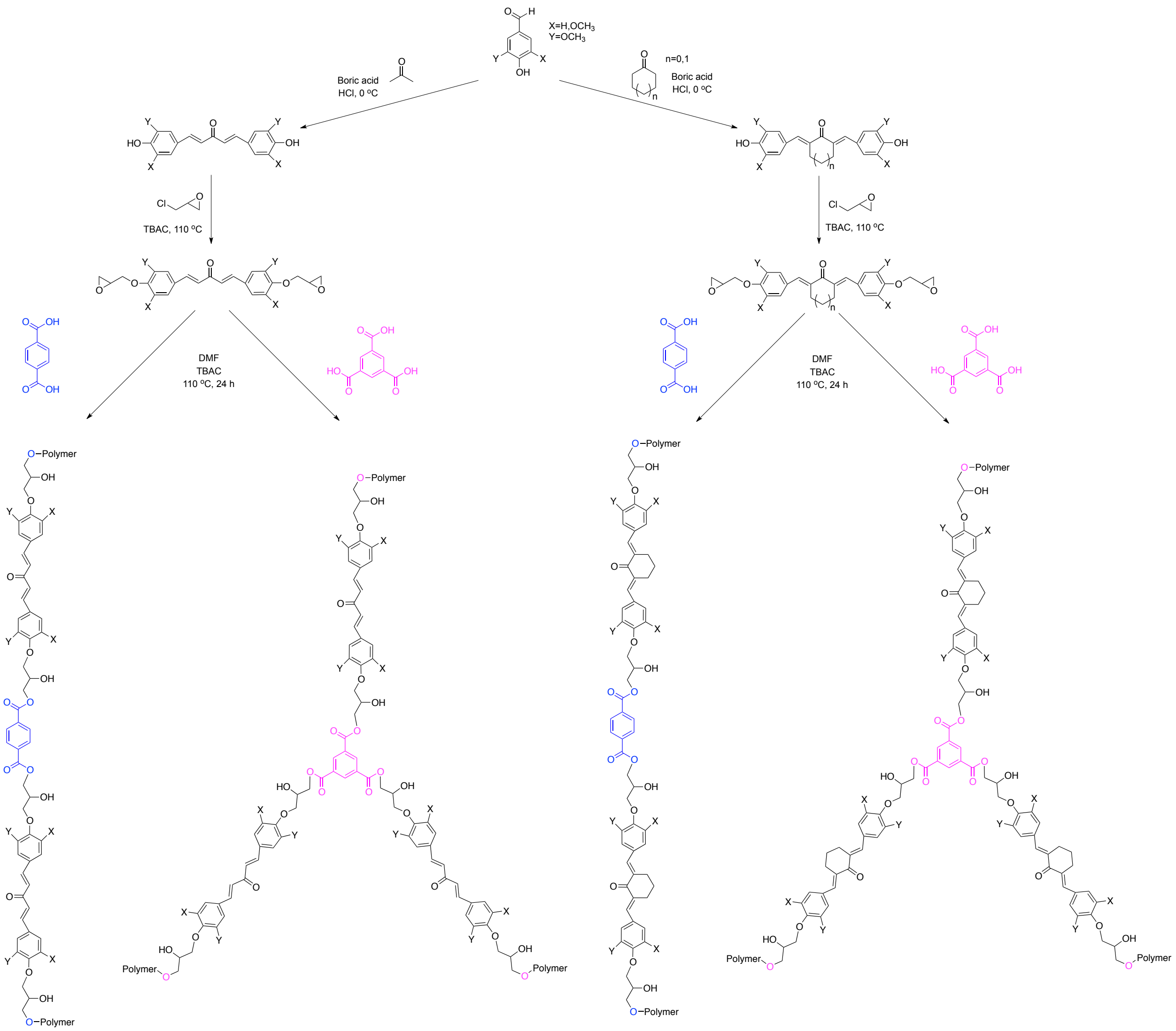

Figure 1.31 Synthesis of branched and hyperbranched vanillin and 4-hydroxy-3,5-dimethoxybenzaldehyde epoxide dimers. Reproduced with permission from ref. 211. Copyright 2008 John Wiley and Sons.

spriocyclic polyacetal ether or cyclic polyacetal ether, respectively. The resulting polymers featured relatively high T_g, and are susceptible to acid-catalyzed acetal hydrolysis, making them potentially useful replacements for commodity plastics. Mialon et al. synthesized a biorenewable polyethylene terephthalate mimic from acetylated vanillin[215]. Vanillin was acetylated with acetic anhydride to yield acetylferulic acid, which was then hydrogenated to remove the styrenic double bond before condensation polymerization catalyzed by zinc

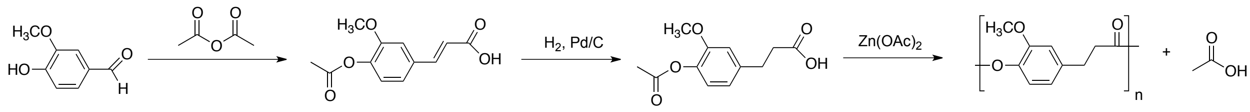

Figure 1.32 Synthesis of vanillin-based PET mimic poly(dihydroferluic acid). Reproduced with permission from ref. 215. Copyright 2010 Royal Society of Chemistry.

acetate to poly(dihydroferulic acid) (**Figure 1.32**). The resulting thermal properties (T_g and T_m) of the polymeric material are close to that of polyethylene terephthalate making it a potential biobased mimic of the well-known petroleum based chemical.

1.4.2 Vanillic Acid

Vanillic acid is formed through the oxidation of vanillin to the corresponding carboxylic acid. This is easily achieved either in oxidative lignin processing (harsh reaction conditions) or in a one-step reaction from vanillin. Mialon et al. synthesized several hydroxyl-acid monomers from vanillic acid through functionalization with chloroalkanols such as 2-chloroethanol or 3-chloropropan-1-ol (**Figure 1.33**)[216]. By decreasing the length of the alkane spacer, they were able to obtain higher molecular weight polyesters with higher T_g and T_m but with slightly lowered thermal stability (**Table 1.2**). Despite this, all polyesters generated exhibited relative thermal stability (in comparison to other materials) and the simplistic monomer functionalization could allow for the rapid synthesis of a diverse set of monomers and polymers with tunable properties. Based on similar structural motifs between terephthalic acid and vanillic acid, Pang et al. created two analogous

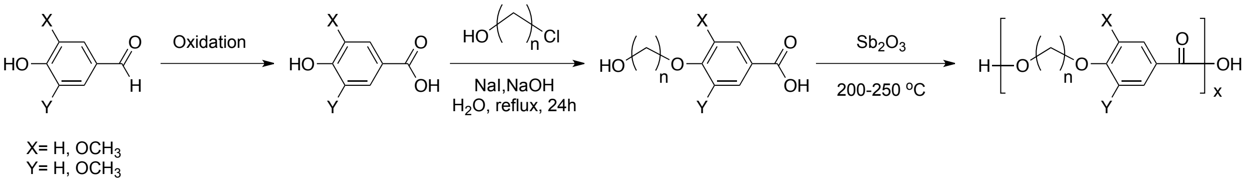

Figure 1.33 Synthesis of polyalkylene 4-hydroxybenzoates, polyalkylene vanillates, and polyalkylene syringates from lignin-based aldehydes. Reproduced with permission from ref. 216. Copyright 2011 John Wiley and Sons.

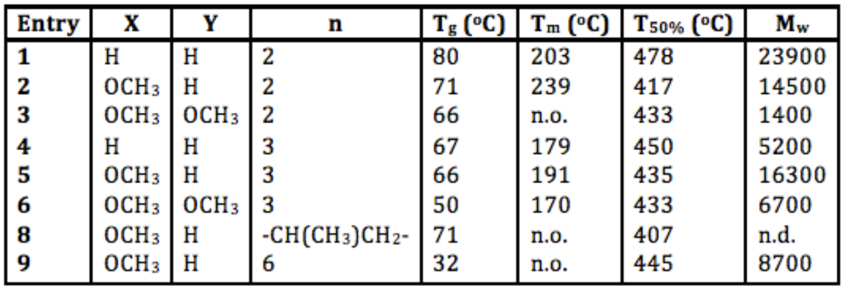

Entry	X	Y	n	T_g (°C)	T_m (°C)	$T_{50\%}$ (°C)	M_w
1	H	H	2	80	203	478	23900
2	OCH_3	H	2	71	239	417	14500
3	OCH_3	OCH_3	2	66	n.o.	433	1400
4	H	H	3	67	179	450	5200
5	OCH_3	H	3	66	191	435	16300
6	OCH_3	OCH_3	3	50	170	433	6700
8	OCH_3	H	$-CH(CH_3)CH_2-$	71	n.o.	407	n.d.
9	OCH_3	H	6	32	n.o.	445	8700

Table 1.2 Thermal and physical properties of polyalkylenes featuring different length spacers from lignin-based aldehydes. Reproduced with permission from ref. 216. Copyright 2011 John Wiley and Sons.

dicarboxylic acid monomers either through the dimerization of vanillic acid with 1,4-dibromobutane or the condensation of vanillic acid with chloroacetic acid[217]. Both monomers were copolymerized with aliphatic diols of differing lengths ($[CH_2]_x$ = 2,3,4, or 10) resulting in a series of thermoplastic poly(ester-ether)s. The copolymers were amorphous, had a random microstructure, and exhibited good thermal stability. The mechanical properties improved with decreasing the length of the aliphatic diol, suggesting potential use as a commodity material. Pang et al. synthesized two other monomers from the corresponding methyl ester, methyl vanillate, using the same methods specified previously yielding either dimeric or monomeric vanillic acid diesters[218]. These diester vanillic acid monomers were copolymerized with a series of diol or ester-alcohol terminated aliphalic monomers synthesized from 10-undecanoic acid and thiolene addition. The resulting copolyesters were semicrystalline or amorphous (depending on the comonomers used), had moderate molecular weights and good thermal stability (**Table 1.3**). The tensile properties of the materials were shown to improve with the addition of vanillic acid into the copolymeric structure.

Aouf and coworkers synthesized a series of vanillic acid based epoxide monomers in

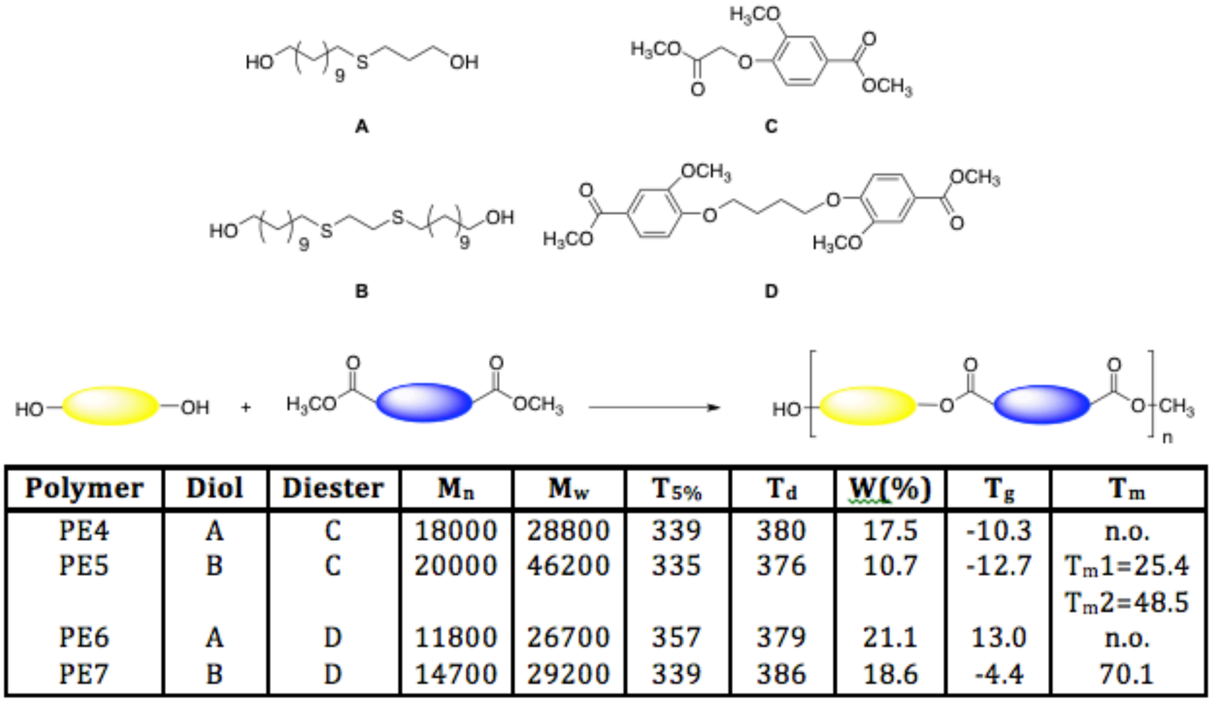

Polymer	Diol	Diester	M_n	M_w	$T_{5\%}$	T_d	W(%)	T_g	T_m
PE4	A	C	18000	28800	339	380	17.5	-10.3	n.o.
PE5	B	C	20000	46200	335	376	10.7	-12.7	T_m1=25.4 T_m2=48.5
PE6	A	D	11800	26700	357	379	21.1	13.0	n.o.
PE7	B	D	14700	29200	339	386	18.6	-4.4	70.1

Table 1.3 Thermal and physical properties of polyesters synthesized from vanillic acid and aliphatic diols of differing lengths. Reproduced with permission from ref. 218. Copyright 2014 Royal Society of Chemistry.

two steps, beginning with the allylation of vanillic acid with allyl bromide and then epoxidation of the allylated compound with *m*-chloroperoxybenzoic acid[219]. A dimeric epoxide monomer was also synthesized via an additional synthetic step prior to the allylation. Vanillic acid was dimerized with 1,5-dibromopentane to yield a diol that was then functionalized with allyl bromide and epoxidized with *m*-chloroperoxybenzoic acid. This method allowed for the development of a series of epoxide prepolymers from vanillic acid without the use of epichlorohydrin or bisphenol A. Fache and coworkers took a more comprehensive approach by synthesizing six different monomers from vanillic acid (**Figure 1.34**)[97]. They first synthesized two different monomers by functionalizing vanillic acid with either epichlorohydrin to generate an epoxide monomer or with allyl bromide to generate an allylated monomer. The allylated monomer was then functionalized with three

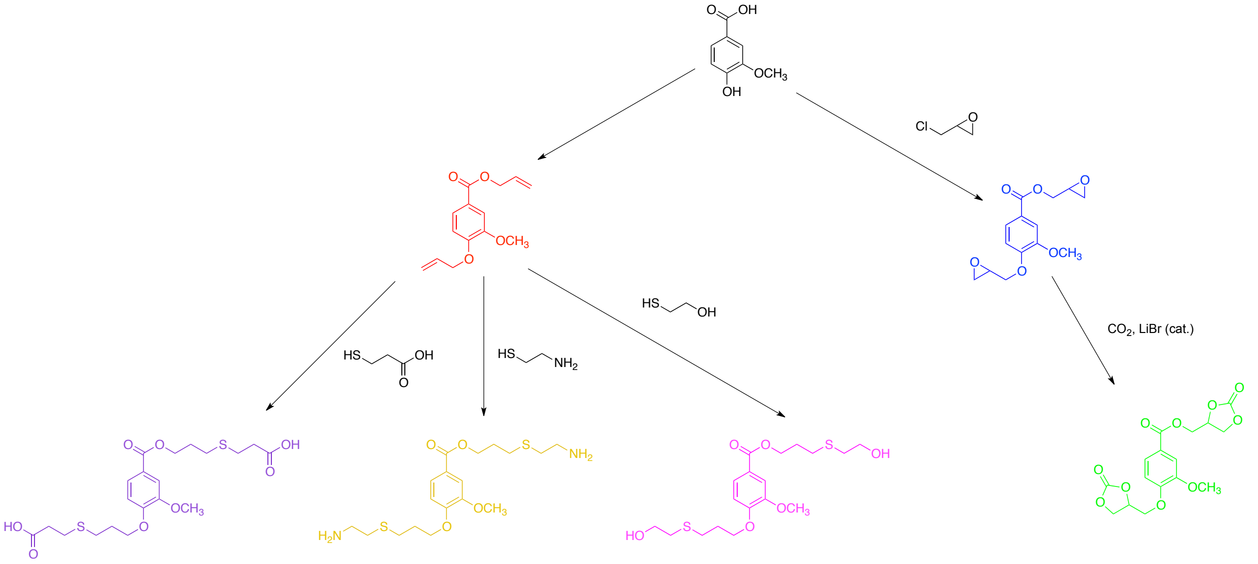

Figure 1.34 Synthetic scheme for six different monomers from vanillic acid. Reproduced with permission from ref. 97. Copyright 2014 Royal Society of Chemistry.

different aliphatic thiols via thiol-ene addition to generate a diol, diamine or dicarboxylic acid monomer. The epoxide functionalities on the epoxide monomer were converted to cyclic carbonates by CO_2 insertion (catalyzed by LiBr) into the oxirane rings. This multifaceted approach led to the synthesis of a wide range of vanillic acid based monomers in minimal synthetic steps making this an ideal method for the rapid development of novel materials.

1.4.3 Vanillic Alcohol

Vanillic or vanillin alcohol is a disubstituted benzyl alcohol formed via reduction of the aldehyde functionality in lignin to an alcohol. This product is easily obtained either in reductive lignin processing or via a one-step chemical reduction and is commercially available. Firdaus and Meier synthesized an allylated vanillic alcohol monomer through the reaction of vanillic alcohol with 11-bromo-1-undecene[220]. They then utilized this monomer as a platform species for the creation of other monomers and polymers. Firdaus synthesized two different diene monomers by transesterification to create either an allyl

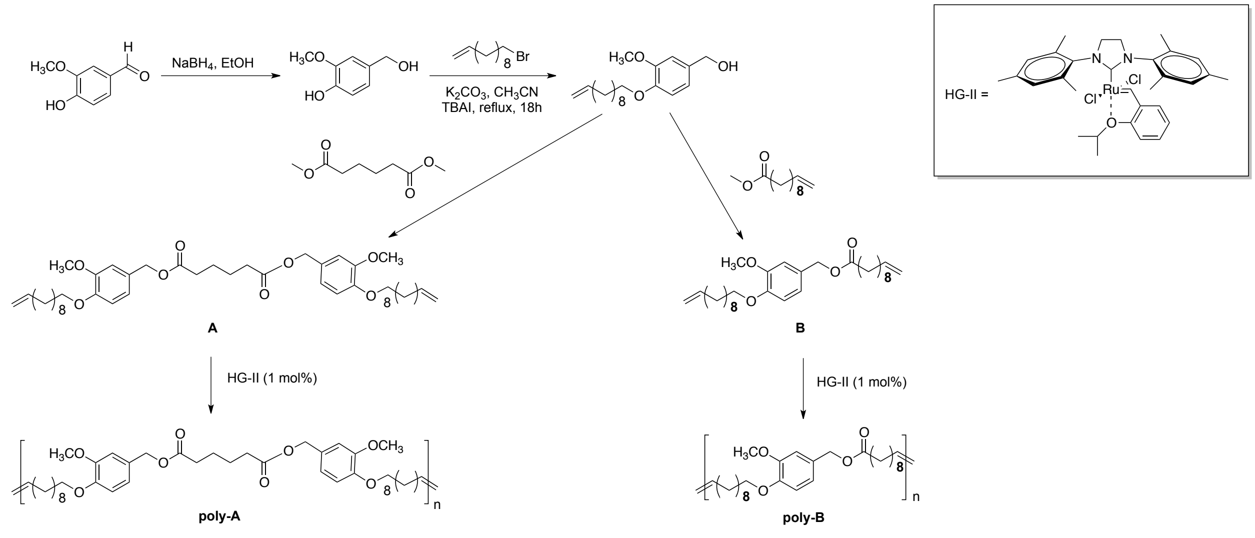

Figure 1.35 Synthesis of vanillic alcohol-based dienes via ADMET. Reproduced with permission from ref. 220. Copyright 2013 Elsevier.

vanillic alcohol dimer with dimethyl adipate or a monomer with methyl 10-undecenoate (**Figure 1.35**). These two monomers were then either polymerized in a controlled fashion via ADMET with a ruthenium catalyst or via radical initiated thiol-ene polymerization with dithiols. The thiol-ene polymerizations had relatively low conversion and low T_g and T_m. While the ADMET polymerizations featured a higher degree of polymerization, the resulting products were amorphous and had low T_g. Fache et al. utilized the same synthetic routes discussed in Section 1.4.2 to synthesize six unique monomers from vanillic alcohol[97]. This platform-based approach allowed for the synthesis of a series of vanillic alcohol-based monomers without significant modifications to the synthetic pathway.

1.5 Lignin-based composites

Lignin has many properties ideal for use in polymers such as high thermal stability, biodegradability, antioxidant and antimicrobial behavior, and relative abundance. However, as an amorphous polymer with diverse properties and structures depending on both the identity of the plant source and method of isolation, using unmodified lignin as a macromonomer for controlled polymer synthesis is difficult. With these difficulties in mind, lignin has received the most attention as a component of lignin-based composites. Composites are materials with two or more chemically and physically different phases that are separated by an interface, meaning each component retains its own identity but the resulting combined material has bulk properties that differ from the individual components[221]. Lignin features many desired properties, as mentioned above, rendering it an increasingly common choice to reinforce composites. Several reviews or book chapters[222-227] discussing the use of lignin in polymer composites or blends have been recently published. Additionally, this introduction focuses only on the polymerization of monolignols and lignin derivatives and thus composites and blends will not be discussed in detail.

1.6 Perspective

The field of lignin-based polymeric materials and composites has seen great growth in the past ten years, although the field still has room to grow. To develop bio-based polymeric materials to replace those from petroleum-based sources will require significant progress in several different areas. Methods to isolate more useful lignin-based chemical products, such as benzene, toluene or xylenes, must be developed. In addition, methods to chemically functionalize lignin to synthetically useful products without the use of expensive reagents or complicated synthetic routes must be identified. While lignin model compounds have been used to elucidate the potential reactivity of lignin, more structurally relevant systems such as those prepared by Lancefield and Westwood[228] should be utilized to study new depolymerization and upgrading techniques. By investigating the most structurally relevant and well-defined materials, newly developed techniques are more likely applicable to naturally occurring lignin. Polymerization systems and reactions should be designed to allow for "high-throughput type screening" to easily modify polymeric materials towards commercially relevant targets. The combination of these developments will allow not only for the synthesis of polymeric materials capable of competing with commodity commercial polymeric materials but also allow for the development of more sustainable synthetic practices.

1.7 Dissertation Overview

Towards the aforementioned goals, this dissertation is focused on the development of a series of monolignol-based polymers and copolymers. While the specifics of each system will be discussed in greater detail in the following chapters, in general, the systems were designed to be easily modified and sourceable from lignin or other biomass components. Chapter 2 focuses on the synthetic development, thermal properties, and degradation (hydrolysis) of a series of monolignols-based poly(ester-amides) via interfacial polymerization with a monolignol-based acid chloride dimer and aliphatic or aromatic diamines. These polymers were found to have differing thermal and degradation properties depending on the length (aliphatic) or structural (aromatic versus aliphatic) characteristics of the diamine utilized. Chapter 3 focuses on the development of the analogous monolignol-based poly(ether-amide) system. As seen previously, the identity of the diamine linker played a role in the observed physical characteristics of the resulting polymers. Finally, Chapter 4 will focus on the development of a series of copolymers from monolignols and citraconic anhydride as biologically-derived analogues to petroleum-based polystyrene-co-maleic anhydride and their use in polymer blends with commodity polymers. The monomers were polymerized using either BF_3Et_2O, as an initiator for cationic polymerization, or AIBN, as an initiator for radical polymerization. The structure and physical properties of the resulting oligomers were thoroughly studied. The oligomers were then used in polymer blends with polystyrene and poly(lactic-acid). In summary, this dissertation focused on the synthesis and study of several classes of polymeric materials generated from monolignols with a focus on tunability and direct translation from lignin, monolignols, or biomass as a chemical source to useful polymeric materials with varying properties.

1.8 References

(1) Sun, N.; Rodriguez, H.; Rahman, M.; Rogers, R. D. Where are ionic liquid strategies most suited in the pursuit of chemicals and energy from lignocellulosic biomass? *Chem. Commun.* **2011**, *47*, 1405-1421.

(2) 2014 "World Polyethylene", Freedonia Group

(3) Perlack, R. D.; Wright, L. L.; Turhollow, A. F.; Graham, R. L.; Stokes, B. J.; Erbach, D. C. 2005 "Biomass as a Feedstock for a Bioenergy and Bioproducts Industry: The technical feasibility of a billion-ton annual supply", US Department of Energy

(4) Lanzafame, P.; Gabriele, C.; Perathoner, S. Catalysis for biomass and CO_2 use through solar energy: opening new scenarios for a sustainable and low-carbon chemical production. *Chem. Soc. Rev.* **2014**, *43*, 7562-7580.

(5) Lucia, L. A.; Argyropoulos, D. S.; Adamopoulos, L.; Gaspar, A. R. Chemicals and energy from biomass. *Can. J. Chem.* **2006**, *84*, 960-970.

(6) Luterbacher, J. S.; Alonso, D. M.; Dumesic, J. A. Targeted chemical upgrading of lignocellulosic biomass to platform molecules. *Green Chem.* **2014**, *16*, 4816-4838.

(7) Boerjan, W.; Ralph, J.; Baucher, M. Lignin Biosynthesis. *Annu. Rev. Plant Biol.* **2003**, *54*, 519-546.

(8) Tuck, C. O.; Perez, E.; Horvath, I. T.; Sheldon, R. A.; Poliakoff, M. Valorization of Biomass: Deriving more value from waste. *Science* **2012**, *337*, 695-699.

(9) Stewart, D. Lignin as a base material for materials applications: Chemistry, applications and economics. *Ind. Crops Prod.* **2008**, *27*, 202-207.

(10) Dorrestijn, E.; Laarhoven, L. J. J.; Arends, I. W. C. E.; Mulder, P. The occurance and reactivity of phenoxyl linkages in lignin and low rank coal. *J. Anal. Appl. Pyrolysis* **2000**, *54*, 153-192.

(11) Nguyen, T.; Zavarin, E.; Barral, E. M., II Thermal Analysis of Lignocellulosic Materials. Part I. Unmodified Materials. *J. Macromol. Sci., Rev. Macromol. Chem. Phys.* **1981**, *20*, 1-65.

(12) Sakakibara, A. A structural model of softwood lignin. *Wood Sci. Technol.* **1980**, *14*, 89-100.

(13) Chabannes, M.; Ruel, K.; Yoshinaga, A.; Chabbert, B.; Jauneau, A. In situ analysis of lignins in transgenic tobacco reveals a differential impact of individual transformations on the spacial patterns of lignin deposition at the cellular and subcellular levels. *Plant J.* **2001**, *28*, 271-282.

(14) Jones, L.; Ennos, A. R.; Turner, S. R. Cloning and characterization of irregular xylem4 (irx4): a severely lignin-deficient mutant of Arabidosis. *Plant J.* **2001**, *26*, 205-216.

(15) Sarkanen, K. V.; Ludwig, C. H. *Lignins: Occurence, Formation, Structure and Reactions*; Wiley-Interscience: New York 1971; p 19-38.

(16) Vermerris, W.; Sherman, D. M.; McIntyre, L. M. Phenotypic plasticity in cell walls of maize brown midrib mutants is limited by lignin composition. *J. Exp. Bot.* **2010**, *61*, 2479-2490.

(17) Ralph, J.; Lundquist, K.; Brunow, G.; Lu, F.; Kim, H.; Schatz, P.; Marita, J. M.; Hatfield, R. D.; Ralph, S. A.; Christensen, J. H.et al. Lignins: Natural polymers from oxidative coupling of 4-hydroxyphenylpropanoids. *Phytochem. Rev.* **2004**, *3*, 29-60.

(18) Whetten, R.; Sederoff, R. Lignin Biosynthesis. *Plant Cell* **1995**, *7*, 1001-1013.

(19) Boudet, A. M.; Lapierre, C.; Grima-Pettenati, J. Biochemistry and molecular biology of lignification. *New Phytol.* **1995**, *129*, 203-236.

(20) McDonough, T. J. The chemistry of organosolv delignininification. *Tappi* **1993**, *76*, 186-193.

(21) Strassberger, Z.; Tanase, S.; Rothenberg, G. The pros and cons of lignin valorisation in an integrated biorefinery. *RSC Adv.* **2014**, *4*, 25310-25318.

(22) Lora, J. Industrial Commercial Lignins: Sources, Properties and Applications In *Monomers, Polymers and Composites from Renewable Resources*; Belgacem, M. N., Gandini, A., Eds.; Elsevier, 2008. p 225-241.

(23) Oehman, F.; Theliander, H.; Tomani, P.; Axegard, P. WO 2009104995, 2008; *Chem. Abstr.* **2009**,*151*, 268770.

(24) Kumar, P.; Barrett, D. M.; Delwiche, M. J.; Stroeve, P. Methods for Pretreatment of Lignocellulosic Biomass for Efficient Hydrolysis and Biofuel Production. *Ind. Eng. Chem. Res.* **2009**, *48*, 3713-3729.

(25) Avellar, B. K.; Glasser, W. G. Steam-assisted biomass fractionation. I. Process considerations and economic evalutation. *Biomass Bioenergy* **1998**, *14*, 205-218.

(26) Brandt, A.; Gräsvik, J.; Hallett, J. P.; Welton, T. Deconstruction of lignoncellulosic biomass with ionic liquids. *Green Chem.* **2103**, *15*, 550-583.

(27) Adler, E. Lignin Chemistry - Past, Present and Future. *Wood Sci. Technol.* **1977**, *11*, 169-218.

(28) Faix, O.; Argyropoulos, D. S.; Robert, D.; Neirinck, V. Determination of hydroxyl groups in lignins. Evaluation of 1H-, 13C-, 31P-NMR, FTIR and wet chemical methods. *Holzforschung* **1994**, *48*, 387-394.

(29) Lu, F.; Ralph, J. DFRC Method for Lignin Analysis. 1. New method for β-Aryl Ether Cleavage: Lignin Model Studies. *J. Agric. Food Chem.* **1997**, *45*, 4655-4660.

(30) Katahira, R.; Ujihara, M.; Nakatsubo, F. A Novel Selective Cleavage Method for β-O-4 Substructure in Lignins Named TIZ Method. I. Degredation of Guaiacyl and Syringyl Models. *J. Wood Chem. Technol.* **2003**, *23*, 71-87.

(31) Faix, O.; Fukazawa, K.; Donaldson, L. A.; Saka, S.; Leary, G. J.; Newman, R. H.; Atalla, R. H.; Agarwal, U. P.; Bond, J. S.; Meier, D.et al. *Methods in Lignin Chemistry* Springer-Verlag: Berlin, 1992; p 83-214.

(32) Wunderlich, B.; Bodily, D. M.; Kaplan, M. H. Theory and Measurements of the Glass-Transformation Interval of Polystyrene. *J. Appl. Phys.* **1964**, *35*, 95 - 102.

(33) Hatakeyama, H.; Nakano, J.; Hatano, A.; Migita, N. Variation of Infrared Spectra with Temperature for Lignin and Lignin Model Compounds. *Tappi* **1969**, *52*, 1724-1728.

(34) Hatakeyama, H.; Kubota, K.; Nakano, J. Thermal analysis of lignin by differential scanning calorimetry. *Cellul. Chem. Technol.* **1972**, *6*, 521-529.

(35) Belgacem, M. N.; Gandini, A. Lignins as Components of Macromolecular Materials In *Monomers, Polymers and Composites from Renewable Resources*; Belgacem, M. N., Gandini, A., Eds.; Elsevier. p 243-271.

(36) Chauvette, G.; Heitz, M.; Rubio, M.; Khorami, J.; Chornet, E.; Menard, H. TG/DTG as a rapid method for the characterization of solid residues derived from liquefaction of lignocelluloses. *Thermochim. Acta* **1985**, *84*, 1-5.

(37) Faix, O.; Meier, D.; Grobe, I. Studies on isolated lignins and lignins in woody materials by pyrolysis-gas chromatography-mass spectrometry and off-line pyrolysis-gas chromatography with flame ionization detection. *J. Anal. Appl. Pyrolysis* **1987**, *11*, 403-416.

(38) Faix, O.; Jakab, E.; Szekely, T. Study on low mass thermal degredation products of milled wood lignins by thermogravimetry-mass spectrometry. *Wood Sci. Technol.* **1988**, *22*, 323-334.

(39) Domburg, G. E.; Sergeeva, V. N.; Kalninish, A. I. International Conference on Thermal Analysis, Davos, Switzerland, 1971; p 327-340.

(40) Cherubini, F.; Stromman, A. H. Principles of Biorefining In *Biofuels- Alternative Feedstocks and Conversion Processes*; Pandey, A., Larroche, C., Ricke, S. C., Dussap, C.-G., Gnansounou, E., Eds.; Academic Press: Amsterdam, 2011. p 3-23.

(41) Voitl, T.; Rudolf von Rohr, P. Oxidation of Lignin Using Aqueous Polyoxometalates in the Presence of Alcohols. *ChemSusChem* **2008**, *1*, 763-769.

(42) Zakzeski, J.; Bruijnincx, P. C. A.; Jongerius, A. L.; Weckhuysen, B. M. The Catalytic Valorization of Lignin for the Production of Renewable Chemicals. *Chem. Rev.* **2010**, *110*, 3552-3599.

(43) Lange, H.; Decina, S.; Crestini, C. Oxidative upgrade of lignin - Recent routes reviewed. *Eur. Polym. J.* **2013**, *49*, 1151-1173.

(44) Pandey, M. P.; Kim, C. S. Lignin Depolymerization and Conversion: A Review of Thermochemical Methods. *Chem. Eng. Technol.* **2011**, *34*, 29-41.

(45) Ragaukas, A. J.; Beckham, G. T.; Biddy, M. J.; Chandra, R.; Chen, F.; Davis, M. F.; Davison, B. H.; Dixon, R. A.; Gilna, P.; Keller, M.et al. Lignin Valorization: Improving Lignin Processing in the Biorefinery. *Science* **2014**, *344*, 709-719.

(46) Goheen, D. W. Hydrogenation of Lignin by the Noguchi Process In *Lignin Structure and Reactions*; Marton, J., Ed.; American Chemical Society, 1966; Vol. 59. p 205-225.

(47) Oshima, M.; Maeda, Y.; Kashima, K. US Patent 3105095, 1963; *Chem. Abstr.* **1963**,*59*, 69871.

(48) 2015 "Average Prices for OPEC crude oil from 1960 to 2015 (in U.S. dollars per barrel)", Statistica

(49) Yan, N.; Zhao, C.; Dyson, P. J.; Wang, C.; Liu, L.-T.; Kou, Y. Selective Degradation of Wood Lignin over Nobel-Metal Catalysts in a Two-Step Process. *ChemSusChem* **2008**, *1*, 626-629.

(50) Faix, O.; Meier, D. Utilization and analysis of lignins: 1st European Workshop on Lignocellulosics and Pulp (EWLP), Hamburg-Bergedorf, Germany, 1990; p 198-203.

(51) Brendenberg, J. B.; Huuska, M.; Toropainen, P. Hydrogenation of differently substituted methoxyphenols. *J. Catal.* **1989**, *120*, 401-408.

(52) Sergeev, A. G.; Hartwig, J. F. Selective, Nickel-Catalyzed Hydrogenolysis of Aryl Ethers. *Science* **2011**, *332*, 439- 443.

(53) Rensel, D. J.; Rouvimov, S.; Gin, M. E.; Hicks, J. C. Highly selctive bimetallic FeMoP catalysts for C-O bond clevage of aryl ethers. *J. Catal.* **2013**, *305*, 256-263.

(54) Molinari, V.; Giordano, C.; Antonietti, M.; Eposito, D. Titanium Nitride-Nickel Nanocomposite as Heterogeneous Catalyst for the Hyrogenolysis of aryl ethers. *J. Am. Chem. Soc.* **2014**, *136*, 1758-1761.

(55) Zhang, J.; Teo, J.; Chen, X.; Asakura, H.; Tanaka, T.; Teramura, K.; Yan, N. A series of NiM (M=Ru, Rh, Pd) Bimetallic Catalysts for Effective Lignin Hydrogenolysis in Water. *ACS Catal.* **2014**, *4*, 1574-1583.

(56) Meier, D.; Ante, R.; Faix, O. Catalystic Hydropyrolysis of Lignin: Influence of Reaction Conditions on the Formation and Composition of Liquid Products. *Bioresour. Technol.* **1992**, *40*, 171-177.

(57) Okuda, K.; Umetsu, M.; Takami, S.; Adschiri, T. Disassembly of lignin and chemical recovery - rapid depolymerization of lignin without char formation in water-phenol mixtures. *Fuel Process. Technol.* **2004**, *85*, 803-813.

(58) Yokoyama, C.; Nishi, K.; Nakajima, A.; Seino, K. Thermolysis of Organosolv Lignin in Supercritical Water and Supercritical Methanol. *Sekiyu Gakkaishi* **1998**, *41*, 243-250.

(59) Huang, X.; Koranyi, T. I.; Boot, M. D.; Hensen, E. J. M. Catalytic Depolymerization of Lignin in Supercrtical Ethanol. *ChemSusChem* **2014**, *7*, 2276-2288.

(60) Wasserscheid, P.; Keim, W. Ionic Liquids - New "Solutions" for Transition Metal Catalysis. *Angew. Chem. Int. Ed.* **2000**, *39*, 3772-3789.

(61) Binder, J. B.; Gray, M. J.; White, J. F.; Zhang, Z. C.; Holladay, J. E. Reactions of lignin model compounds in ionic liquids. *Biomass Bioenergy* **2009**, *33*, 1122-1130.

(62) Tarabanko, V. E.; Koropatchinskaya, N. V.; Kudryashev, A. V.; Kuznetsov, B. N. Influence of lignin origin on the efficiency of the catalytic oxidation of lignin into vanillin and syringaldehyde. *Russ. Chem. Bull.* **1995**, *44*, 367-371.

(63) Villar, J. C.; Caperos, A.; Garcia-Ochoa, F. Oxidation of hardwood kraft-lignin to phenolic derivatives with oxygen as oxidant. *Wood Sci. Technol.* **2001**, *35*, 245-255.

(64) Rodrigues, P. C.; Borges da Silva, E. A.; Rodriguez, A. E. Insights into Oxidative Conversion of Lignin to High-Added-Value Phenolic Aldehydes. *Ind. Eng. Chem. Res.* **2011**, *50*, 741-748.

(65) Das, L.; Kolar, P.; Sharma-Shivappa, R. Heterogeneous catalytic oxidation of lignin into value-added chemicals. *Biofuels* **2012**, *3*, 155-166.

(66) Portjanskaja, E.; Stepanova, K.; Klauson, D.; Preis, S. The influence of titanium dioxide modifications on photocatalytic oxidation of lignin and humic acids. *Catal. Today* **2009**, *144*, 26-30.

(67) Ma, Y.-S.; Chnag, C.-N.; Chaing, Y.-P.; Sung, H.-F.; Chao, A. C. Photocatalytic degredation of lignin using Pt/TiO_2 as the catalyst. *Chemosphere* **2008**, *71*, 998-1004.

(68) Furusawa, T.; Sato, T.; Saito, M.; Ishiyama, Y.; Sato, M.; Itoh, N.; Suzuki, N. The evaluation of the stability of Ni/MgO catalysts for the gasificiation of lignin in supercritical water. *Appl. Catal., A* **2007**, *327*, 300-310.

(69) Crestini, C.; Caponi, M. C.; Argyropoulos, D. S.; Saladino, R. Immobilized methyltrioxo rhenium (MTO)/H_2O_2 systems for the oxidation of lignin and lignin model compounds. . *Bioorg. Med. Chem.* **2006**, *14*, 5292-5302.

(70) DiCosmio, R.; Szabo, H. C. Oxidation of lignin model compounds using single-electron-transfer catalysts. *J. Org. Chem.* **1988**, *53*, 1673-1679.

(71) Partenheimer, W. The Aerobic Oxidative Cleavage of Lignin to Produce Hydroxyaromatic Benzaldehydes and Carboxylic Acids via Metal/Bromide Catalysts in Acetic Acid/Water Mixtures. *Adv. Synth. Catal.* **2009**, *351*, 456-466.

(72) Pepper, J. M.; Casselman, B. W.; Karapally, J. C. Lignin Oxidation: Preferential use of cupric oxide. *Can. J. Chem.* **1967**, *45*, 3009-3012.

(73) Zhu, W.; Ford, W. T. Oxidation of lignin model compounds in water with dioxygen and hydrogen peroxide catalysed by metallophthalocyanines. *J. Mol. Catal.* **1993**, *78*, 367-378.

(74) Cui, F.; Dolphin, D. Metallophthalocyanines as possible lignin peroxidase models. *Bioorg. Med. Chem.* **1995**, *3*, 471-477.

(75) Paszczynski, A.; Crawford, R. L.; Blanchette, R. A. Delignification of Wood Chips and Pulps Using Natural and Synthetic Porphyrins: Models of Fungal Decay. *Appl. Environ. Microbiol.* **1988**, *54*, 62-68.

(76) Bozell, J. J.; Hames, B. R.; Dimmel, D. R. Cobalt-Schiff Base Complex Catalyzed Oxidation of Para-substituted Phenolics. Preparation of Benzoquinones. *J. Org. Chem.* **1995**, *60*, 2398-2404.

(77) Drago, R. S.; Corden, B. B.; Barnes, C. W. Novel Cobalt(II)-Catalyzed Oxidative Cleavage of a Carbon-Carbon Double Bond. *J. Am. Chem. Soc.* **1986**, *108*, 2453-2454.

(78) Wang, H.; Block, L. E.; Rogers, R. D. Catalytic Conversion of Biomass in Ionic Liquids In *Catalysis in Ionic Liquids: From Catalyst Synthesis to Application*; Royal Society of Chemistry, 2014. p 1-19.

(79) Chatel, G.; Rogers, R. D. Review: Oxidation of Lignin Using Ionic Liquids - An Innovative Strategy To Produce Renewable Chemicals. *ACS Sustainable Chem. Eng.* **2014**, *2*, 322-339.

(80) Stärk, K.; Taccardi, N.; Bösmann, A.; Wasserscheid, P. Oxidative Depolymerization of Lignin in Ionic Liquids. *ChemSusChem* **2010**, *3*, 719-723.

(81) Zakzeski, J.; Jongerius, A. L.; Weckhuysen, B. M. Transtion metal catalyzed oxidation of Acell lignin, soda lignin, and lignin model compounds in ionic liquids. *Green Chem.* **2010**, *12*, 1225-1236.

(82) Zakzeski, J.; Bruijnincx, P. C. A.; Weckhuysen, B. M. In situ spectroscopic investigation of the cobalt-catalyzed oxidation of lignin model compounds in ionic liquids. *Green Chem.* **2011**, *13*, 671-680.

(83) Liu, S.; Shi, Z.; Li, L.; Yu, S.; Xie, C.; Song, Z. Process of lignin oxidation in an ionic liquid coupled with seperation. *RSC Adv.* **2013**, *3*, 5789-5793.

(84) Gaspar, A. R.; Gamelas, J. A. F.; Evtuguin, D. V.; Neto, C. P. Alternatives for lignocellulosic pulp delignification using polyoxometalates and oxygen: A review. *Green Chem.* **2007**, *9*, 717-730.

(85) Deng, H.; Lin, L.; Sun, Y.; Pang, C.; Zhaung, J.; Pingkai, O.; Li, Z.; Liu, S. Perovskite-type Oxide $LaMnO_3$: An Efficient and Recyclable Hererogeneous Catalyst for the Wet Aerobic Oxidation of Lignin to Aromatic Aldehydes. *Catal. Lett.* **2008**, *126*, 106-111.

(86) Deng, H.; Lin, L.; Sun, Y.; Pang, C.; Zhuang, J.; Ouyang, P.; Li, J.; Liu, S. Activity and Stabilty of Perovskite-Typer Oxide $LaCoO_3$ Catalyst in Lignin Catalytic Wet Oxidation to Aromatic Aldehydes Process. *Energy Fuels* **2009**, *23*, 19-24.

(87) Zhu, H.; Wang, L.; Chen, Y.; Li, G.; Li, H.; Tang, Y.; Wan, P. Electrochemical depolymerization of lignin into renewable aromatic compounds in a non-diaphragm electrolytic cell. *RSC Adv.* **2014**, *4*, 29917-29924.

(88) Jia, S.; Cox, B. J.; Guo, X.; Zhang, Z. C.; Ekerdt, J. G. Hydrolytic clevage of B-O-4 Ether Bonds of Lignin Model Compounds in an Ionic Liquid with Metal Chlorides. *Ind. Eng. Chem. Res.* **2011**, *50*, 849-855.

(89) Jia, S.; Cox, B. J.; Guo, X.; Zhang, Z. C.; Ekerdt, J. G. Cleaving the B-O-4 Bonds of Lignin Model Compounds in an Acidic Ionic Liquid, 1-H-3-Methylimidazolium Chloride: An Optional Strategy for the Degradation of Lignin. *ChemSusChem* **2010**, *3*, 1078-1084.

(90) Cox, B. J.; Ekerdt, J. G. Depolymerization of oak wood lignin under mild conditions using the acidic ionic liquid 1-H-3-methylimidazolium chloride as both solvent and catalyst. *Bioresour. Technol.* **2012**, *118*, 584-588.

(91) Cox, B. J.; Jia, S.; Zhang, Z. C.; Ekerdt, J. G. Catalytic degredation of lignin model compounds in acidic imidazolium based ionic liquids: Hammett acidity and anion effects. *Polym. Degrad. Stab.* **2011**, *96*, 426-431.

(92) Rahimi, A.; Ulbrich, A.; Coon, J. J.; Stahl, S. S. Formic-acid-induced depolymerization of oxidized lignin to aromatics. *Nature* **2014**, *515*, 249-252.

(93) Deepa, A. K.; Dhepe, P. L. Solid Acid catalyzed depolymerization of lignin into value added aromatic monomers. *RSC Adv.* **2014**, *4*, 12625-12629.

(94) Deepa, A. K.; Dhepe, P. L. Lignin Depolymerization into Aromatic Monomers over Solid Acid Catalysts. *ACS Catal.* **2015**, *5*, 365-379.

(95) Holladay, J. E.; White, J. F.; Bozell, J. J.; Johnson, D. 2007 “Top Value-Added Chemicals from Biomass- Volume II—Results of Screening for Potential Candidates from

Biorefinery Lignin" PNNL-16983, Pacific Northwest National Laboratory, Richland, WA.

(96) Laurichesse, S.; Avérous, L. Chemical modification of lignins: Towards biobased polymers. *Prog. Polym. Sci.* **2014**, *39*, 1266-1290.

(97) Fache, M.; Darroman, E.; Besse, V.; Auvergne, R.; Caillol, S.; Boutevin, B. Vanillin, a promising biobased building-block for monomer synthesis. *Green Chem.* **2014**, *16*, 1987-1998.

(98) Cateto, C. A.; Barrerio, M. F.; Rodriguez, A. E.; Brochier-Salon, M. C.; Thielemans, W.; Belgacem, M. N. Lignins as Macromonomers for Polyurathane Synthesis: A Comparative Study on Hydroxy Group Determination. *J. Appl. Polym. Sci.* **2008**, *109*, 3008-3017.

(99) Engels, H.-W.; Pirkl, H.-G.; Albers, R.; Albach, R. W.; Krause, J.; Hoffman, A.; Casselmann, H.; Dormish, J. Polyurethanes: Versatile Material and Sustainable Problem Solvers for Today's Challenges. *Angew. Chem. Int. Ed.* **2013**, *52*, 9422-9441.

(100) Zhang, Q.; Zhang, G.; Xu, J.; Gao, C.; Wu, Y. Recent Advances in Lignin-Derived Polyurethane Polymers. *Reviews on Advanced Materials Science* **2015**, *40*, 146-154.

(101) Hu, S.; Luo, X.; Li, Y. Polyols and Polyurethanes from the liquifaction of Lignocellulosic Biomass. *ChemSusChem* **2014**, *7*, 66-72.

(102) Cateto, C. A.; Barrerio, M. F.; Ottati, C.; Lopretti, M.; Rodriguez, A. E.; Belgacem, M. N. Lignin-based rigid polyurethane foams with improved biodegredation. *J. Cell. Plast.* **2014**, *50*, 81-95.

(103) Gandini, A.; Belgacem, M. N.; Guo, Z.-X.; Montanari, S. Lignins as Macromonomers for Polyesters and Polyurethanes In *Chemical Modification, Properties and Usage of Lignin*; Hu, T. Q., Ed.; Kluwer Academic/Plenum: New York, NY, 2002. p 57-80.

(104) Bonini, C.; D'Auria, M.; Emanuele, L.; Ferri, R.; Pucciariello, R.; Sabia, A. R. Polyurethanes and Polyesters from Lignin. *J. Appl. Polym. Sci.* **2005**, *98*, 1451-1456.

(105) Duong, L. D.; Nam, G.-Y.; Oh, J.-S.; Park, I.-K.; Luong, N. D.; Yoon, H.-K.; Lee, S.-H.; Lee, Y.; Yun, J.-H.; Lee, C.-G.et al. High Molecular-Weight Thermoplastic Polymerization of Kraft Lignin Macromers with Diisocyante. *Bioresources* **2014**, *9*, 2359-2371.

(106) Hatakeyama, H. Polyurethanes containin Lignin In *Chemical Modification, Properties and Usage of Lignin*; Hu, T. Q., Ed.; Kluwer Academic/Plenum: New York, NY, 2002. p 41-56.

(107) Thring, R. W.; Vanderlaan, M. N.; Griffin, S. L. Polyurethanes from Alcell lignin. *Biomass Bioenergy* **1997**, *13*, 125-132.

(108) Vanderlaan, M. N.; Thring, R. W. Polyurethanes from Alcell lignin fractions obtained by seqential solvent extraction. *Biomass Bioenergy* **1998**, *14*, 525-531.

(109) Pohjanlehto, H.; Setäkä, H. M.; Kiely, D. E.; McDonald, A. G. Lignin-xylaric acid-polyurethane-based polymer network systems: Preparation and characterization. *J. Appl. Polym. Sci.* **2014**, 10.1002/app.39714.

(110) Xue, B.-L.; Wen, J.-L.; Sun, R.-C. Lignin-based Rigid Polyurethane Foam Reinforced with Pulp Fiber: Synthesis and Characterization. *ACS Sustainable Chem. Eng.* **2014**, *2*, 1474-1480.

(111) Cinelli, P.; Anguillesi, I.; Lazzeri, A. Green synthesis of flexible polyurethane foams from liquefied lignin. *Eur. Polym. J.* **2013**, *49*, 1174-1184.

(112) Yiamsawas, D.; Baier, G.; Thines, E.; Landfester, K.; Wurm, F. R. Biodegradable lignin nanocontainers. *RSC Adv.* **2014**, *4*, 11661-11663.

(113) Braun, E.; Levin, B. C. Polyesters: A Review of the Literature on Products of Combustion and Toxicity. *Fire Mater.* **1986**, *10*, 107-123.

(114) Guo, Z.-X.; Gandini, A. Polyesters from lignin. 2. The copolyesterification of Kraft lignin and polyethylene glycols with dicarboxylic acid chlorides. *Eur. Polym. J.* **1991**, *27*, 1177-1180.

(115) Binh, N. T. T.; Luong, N. D.; Kim, D. O.; Lee, S. H.; Kim, B. J.; Lee, Y. S.; Nam, J.-D. Synthesis of Lignin-Based Thermoplastic Copolyester Using Kraft Lignin as a Macromonomer. *Compos. Interfaces* **2009**, *16*, 923-935.

(116) Matsushita, Y.; Inomata, T.; Takagi, Y.; Hasegawa, T.; Fukushima, K. Conversion of sulfuric acid lignin generated during bioethanol production from lignocellulosic materials into polyesters with ε-caprolactone. *J. Wood Sci.* **2011**, *57*, 214-218.

(117) Sivasankarapillai, G.; McDonald, A. G. Synthesis and properties of lignin-highly branched poly(ester-amine) polymeric systems. *Biomass Bioenergy* **2011**, *35*, 919-931.

(118) Aurvergne, R.; Caillol, S.; David, G.; Boutevin, B.; Pascault, J.-P. Biobased Thermosetting Epoxy: Present and Future. *Chem. Rev.* **2014**, *114*, 1082- 1115.

(119) Nonaka, Y.; Tomita, B.; Hatano, Y. Synthesis of Lignin/Epoxy Resins in Aqueous Systems and their properties. *Holzforschung* **1997**, *51*, 183-187.

(120) Feldman, D.; Banu, D.; Khoury, M. Epoxy-Lignin Polyblends. III. Thermal Properties and Infrared Analysis. *J. Appl. Polym. Sci.* **1989**, *37*, 877-887.

(121) Feldman, D.; Banu, D.; Natansohn, A.; Wang, J. Structure-Properties Relations of Thermally Cured Epoxy-Lingin Polyblends. *J. Appl. Polym. Sci.* **1991**, *42*, 1537-1550.

(122) Wang, J.; Banu, D.; Feidman, D. Epoxy-lignin polyblends: effects of various components on adhesive properties. *J. Adhes. Sci. Technol.* **1992**, *6*, 587-598.

(123) Engelmann, G.; Ganster, J. Bio-based epoxy resins with low molecular weight kraft lignin and pyrogallol. *Holzforschung* **2014**, *68*, 435-446.

(124) Pilato, L. *Phenolic Resins: A Century of Progress*; Springer: New Jersey, 2010; p 1-5.

(125) Peng, W.; Riedi, B. The chemorheology of phenol-formaldehyde thermoset resin and mixtures of the resin with lignin fillers. *Polymer* **1994**, *35*, 1280-1286.

(126) Alonso, M. V.; Oliet, M.; Garcia, J.; Rodriguez, F.; Echeverria, J. Gelation and isoconversional kinetic analysis of lignin-phenol-formaldehyde resol resins cure. *Chem. Eng. J.* **2006**, *122*, 159-166.

(127) Vasquez, G.; Antorrena, G.; Gonzales, J.; Mayor, J. Lignin-phenol-formaldehyde adhesives for exterior grade plywoods. *Bioresour. Technol.* **1995**, *51*, 187-192.

(128) Danielson, B.; Simonson, R. Kraft Lignin in phenol-formaldehyde resin. Part 1. Partial replacement of phenol by kraft lignin in phenol-formaldehyde adhesives for plywood. *J. Adhes. Sci. Technol.* **1998**, *12*, 923-939.

(129) Danielson, B.; Simonson, R. Kraft lignin in phenol-formaldehyde resin. Part 2. Evalutation of an industrial trial. *J. Adhes. Sci. Technol.* **1998**, *12*, 941-946.

(130) Sarkar, S.; Adhikari, B. Lignin-modified phenolic resin: synthesis optimization, adhesive strength and thermal stability. *J. Adhes. Sci. Technol.* **2000**, *14*, 1179-1193.

(131) Chung, H.; Washburn, N. R. Improved Lignin Polyurethane Properties with Lewis Acid Treatment. *ACS Appl. Mater. Interfaces* **2012**, *4*, 2840-2846.

(132) Laurichesse, S.; Huillet, C.; Avérous, L. Original polyols based on organosolv lignin and fatty acids: new bio-based building blocks for segmented polyurethane synthesis. *Green Chem.* **2014**, *16*, 3958-3970.

(133) Nadji, H.; Bruzzese, C.; Belgacem, M. N.; Benaboura, A.; Gandini, A. Oxypropylation of Lignins and Preparation of Rigid Polyurethane Foams from the Ensuing Polyols. *Macromol. Mater. Eng.* **2005**, *290*, 1009-1016.

(134) Hatakeyama, T.; Izuta, Y.; Hirose, S.; Hatakeyama, H. Phase transitions of lignin-based polycaprolactones and their polyurethane derivatives. *Polymer* **2002**, *43*, 1177-1182.

(135) Liu, J.; Liu, H.-F.; Deng, L.; Liao, B.; Guo, Q.-X. Improving aging resistance and mechanical properties of waterborne polyurethanes modified by lignin amines. *J. Appl. Polym. Sci.* **2013**, *130*, 1736-1742.

(136) Zhu, H.; Peng, Z.; Chen, Y.; Li, G.; Wang, L.; Tang, Y.; Pang, R.; Khan, Z. U. H.; Wang, P. Preparation and characterization of flame retardant polyurethane foams containing phosphorous-nitrogen functionalized lignin. *RSC Adv.* **2014**, *4*, 55271-55279.

(137) Mikhailov, M.; Budevska, K. Preparation of epoxy resins from lignin. *Izv. Inst. Obshta Neorg. Khim. Org. Khim., Bulg. Akad Nauk.* **1962**, *9*, 187-196.

(138) Mihailo, M.; Budevska, C. Epoxy resins from lignin. *Dokl. Bulg. Akad. Nauk.* **1962**, *15*, 155-158.

(139) D'Alelio, G. F. US Patent 3984363, 1976; *Chem. Abstr.* **1975**,*83*, 195567.

(140) El Mansouri, N.-E.; Yuan, Q.; Huang, F. Synthesis and Characterization of Kraft Lignin Based Epoxy Resins. *Bioresources* **2011**, *6*, 2492-2503.

(141) Okabe, Y.; Kagawa, H. US Patent 8232365, 2010; *Chem. Abstr.* **2010**,*153*, 118103.

(142) Simionescu, C. I.; Rusan, V.; Turta, K. I.; Bobcova, S. A.; Macoveanu, M. M.; Cazacu, G.; Stoleriu, A. Synthesis and Characterization of some iron-lignosulfonate-based lignin-epoxy resins. *Cellul. Chem. Technol.* **1993**, *27*, 627-644.

(143) Simionescu, C. I.; Vasile, C.; Macoveanu, M.; Cazacu, G.; Loanid, A. Behaviour of epoxy, lignin-epoxy resins and their mixtures during their soil burial. *Cellul. Chem. Technol.* **1994**, *28*, 517-539.

(144) Zhao, B.; Chen, G.; Liu, Y.; Hu, K.; Wu, R. Synthesis of lignin-based epoxy resin and its characterization. *J. Mater. Sci. Lett.* **2001**, *20*, 859-862.

(145) Tai, S.; Nakano, J.; Migita, N. Studies on Utilization of Lignin. V. Adhesive from Lignin Epoxide. *Mokuzai Gakkaishi* **1967**, *13*, 257-262.

(146) Tai, S.; Nakano, J.; Migita, N. Studies on Utilization of Lignin. VI. Activation of Thiolignin with Phenol. *Mokuzai Gakkaishi* **1986**, *14*, 40-45.

(147) Tai, S.; Nagata, M.; Nakano, J.; Migita, N. Studies on Utilization of Lignin. IV. Epoxidation of Thiolignin. *Mokuzai Gakkaishi* **1967**, *13*, 102-107.

(148) Hofmann, K.; Glasser, W. G. Enginerring Plastics from Lignin. 22. Cure of Lignin Based Epoxy Resins. *J. Adhes.* **1993**, *40*, 229-241.

(149) Hofmann, K.; Glasser, W. G. Engineering plastics from lignin. 23. Network formation of lignin-based epoxy resins. *Macromol. Chem. Phys.* **1994**, *195*, 65-80.

(150) Feng, Q.; Li, J.; Cheng, H.; Chen, F.; Xie, Y. Synthesis and Characterization of Porous Hydrogel Based on Lignin and Polyacrylamide. *Bioresources* **2014**, *9*, 4369-4381.

(151) Hirose, S.; Hatakeyama, T.; Hatakeyama, H. Synthesis and Thermal Properties of Epoxy Resins from Ester-Carboxylic Acid Derivatives of Alcoholysis Lignin. *Macromol. Symp.* **2003**, *197*, 157-169.

(152) Hirose, S.; Hatakeyama, T.; Hatakeyama, H. Glass transition and thermal decomposition of epoxy resins from the carboxylic acid system consisting of ester-carboxylic acid derivatives of alcoholysis lignin and ethylene glycol with various di carboxylic acids. *Thermochim. Acta* **2005**, *431*, 76-80.

(153) Ismail, T. N. M. T.; Hassan, H. A.; Hirose, S.; Taguchi, Y.; Hatakeyama, T.; Hatakeyama, H. Synthesis and thermal properties of ester-type crosslinked epoxy resins derived from lignosulfonate and glycerol. *Polym. Int.* **2010**, *59*, 181-186.

(154) Mendis, G. P.; Hua, I.; Youngblood, J. P.; Howarter, J. A. Enhanced Dispersion of Lignin in Epoxy Compounds Through Hydration and Mannich Functionalization. *J. Appl. Polym. Sci.* **2015**, 10.1002/app.41263.

(155) Benar, P.; Goncalves, A. T.; Mandelli, D.; Schuchardt, U. Eucalyptus organosolv lignins: study of the hydroxymethylation and use in resols. *Bioresour. Technol.* **1999**, *68*, 11-16.

(156) Alonso, M. V.; Oliet, M.; Rodriguez, F.; Astarloa, G.; Echeverria, J. M. Use of a Methylolated Softwood Ammonium Lignosulfonate As Partial Substitute of Phenol in Resol Resins Manufacture. *J. Appl. Polym. Sci.* **2004**, *94*, 643-650.

(157) Vasquez, G.; Gonzales, J.; Freire, S.; Antorrena, G. Effect of chemical modification of lignin on the gluebond performance of lignin-phenolic resins. *Bioresour. Technol.* **1997**, *60*, 191-198.

(158) Vermonden, T.; Censi, R.; Hennink, W. E. Hydrogels for Protien Delivery. *Chem. Rev.* **2012**, *112*, 2853-2888.

(159) Passauer, L. Highly Swellable Lignin Hydrogels: Novel Materials with Interesting Properties In *Functional Materials from Renewable Sources*; Liebner, F., Rosenau, T., Eds.; American Chemical Society, 2012; Vol. 1107. p 211-228.

(160) Passauer, L.; Fischer, K.; Liebner, F. Preparation and physical characterization of strongly swellable oligo(oxyethylene) lignin hydrogels. *Holzforschung* **2011**, *65*, 309-317.

(161) Passauer, L.; Fischer, K.; Liebner, F. Activation of Pine Kraft Lignin by Fenton-type oxidation for cross-linking with oligo(oxyethylene) diglycidyl ether. *Holzforschung* **2011**, *65*, 319-326.

(162) Lee, C. S.; Robinson, J.; Chong, M. F. A review on application of flocculants in wastewater treatment. *Process Saf. Environ. Prot.* **2014**, *92*, 489-508.

(163) Cunha, C. D.; Deffieux, A.; Fontanille, M. Synthesis and Polymerization of Lignin-Based Macromonomers. III. Radical Copolymerization of Lignin-Based Macromonomers with methyl methacrylate. *J. Appl. Polym. Sci.* **1993**, *48*, 819-831.

(164) Jenkins, D. W.; Hudson, S. M. Reivew of Vinyl Graft Copolymerization Featuring Recent Advances toward Controlled Radical-Based Reactions and illustrated with Chitin/Chitosan Trunk Polymers. *Chem. Rev.* **2001**, *101*, 3245-3273.

(165) Chen, R.; Kokta, B. V.; Valade, J. L. Graft Copolymerization of Lignosulfonate and Styrene. *J. Appl. Polym. Sci.* **1979**, *24*, 1609-1618.

(166) Chen, R.; Kokta, B. V. Graft Copolymerization of Lignosulfonate with Methacrylic Acid and Acrylate Monomers In *Graft Copolymerization of Lignocellulosic Fibers*; Hon, D. N.-S., Ed.; American Chemical Society, 1982. p 285-299.

(167) Li, H.; Zhang, Q.; Gao, P.; Wang, L. Preparation and characterization of graft copolymer from dealkaline lignin and styrene. *J. Appl. Polym. Sci.* **2015**, 10.1002/app.41900.

(168) Liu, X.; Xu, Y.; Yu, J.; Li, S.; Wang, J.; Wang, C.; Chu, F. Integration of lignin and acrylic monomers towards grafted copolymers by free radical polyerization. *Int. J. Biol. Macromol.* **2014**, *67*, 483-489.

(169) Cunha, C. D.; Deffieux, A.; Fontanille, M. Synthesis and polymerization of lignin macromonomers. II. Effects of lignin fragments on methyl methacrylate radical polymerization. *J. Appl. Polym. Sci.* **1992**, *44*, 1205-1215.

(170) Ye, D. Z.; Jiang, L.; Ma, C.; Zhang, M.-h.; Zhang, X. The graft polymers from different species of lignin and acrylic acid: Synthesis and mechanism study. *Int. J. Biol. Macromol.* **2014**, *63*, 43-48.

(171) Barton, S. C.; Bird, R. A.; Russell, K. E. The Effect of Phenols and Aromatic Thiols on the Polymerization of Methyl Methacrylate. *Can. J. Chem.* **1963**, *41*, 2737-2741.

(172) Bagdasar'ian, K. S.; Sinitsina, Z. A. Polymerization Inhibition by Aromatic Compounds. *J. Polym. Sci., Part A: Polym. Chem.* **1961**, *52*, 31-38.

(173) Kim, Y. S.; Kadla, J. F. Preparation of a Thermoresponsive Lignin-based Biomaterial through Atom Transfer Radical Polymerization. *Biomacromolecules* **2010**, *11*, 981-988.

(174) Hillburg, S. L.; Elder, A. N.; Chung, H.; Ferebee, R. L.; Bockstaller, M. R.; Washburn, N. R. A universal route towards thermoplastic lignin composites with improved mechanical properties. *Polymer* **2014**, *55*, 995-1003.

(175) Chung, Y.-L.; Olsson, J. V.; Li, R. J.; Frank, C. W.; Waymouth, R. M.; Billington, S. L.; Sattely, E. A renrewable Lignin-Lactide Copolymer and application in biobased composites. *ACS Sustainable Chem. Eng.* **2013**, *1*, 1231-1238.

(176) Oulame, M. Z.; Pion, F.; Allauddin, S.; Raju, K. V. S. N.; Ducrot, P.-H.; Allais, F. Renewable alternating aliphatic-aromatic poly(ester-urethane)s prepared from ferulic acid and bio-based diols. *Eur. Polym. J.* **2015**, *63*, 186-193.

(177) Chen, Q.; Gao, K.; Peng, C.; Xie, H.; Zhao, Z. K.; Bao, M. Preparation of lignin/glycerol-based bis(cyclic carbonate) for the synthesis of polyurethanes. *Green Chem.* **2015** 4546-4551.

(178) Kaneko, T.; Matsusaki, M.; Hang, T. T.; Akashi, M. Thermotropic Liquid-Crystalline Polymer Dervived from Natural Cinnamoyl Biomonomers. *Macromol. Rapid Commun.* **2004**, *25*, 673-677.

(179) Kaneko, T.; Thi, T. H.; Shi, D. J.; Akashi, M. Environmentally degradable, high-performance thermoplastics from phenolic phytomonomers. *Nat. Mater.* **2006**, *5*, 966-970.

(180) Spiliopoulos, I. K.; Mikroyannidis, J. A. Unsaturated Polyamides and Polyesters Prepared from 1,4-Bis-(2-carboxyvinyl)benzene and 4-Hydroxycinnamic acid. *J. Polym. Sci., Part A: Polym. Chem.* **1996**, *34*, 2799-2807.

(181) Matsusaki, M.; Kishida, A.; Stainton, N.; Ansell, C. W. G.; Akashi, M. Synthesis and Characterization of Novel Biodegradable Polymers Composed of Hydroxycinnamic Acid and D,L-Lactic Acid. *J. Appl. Polym. Sci.* **2001**, *82*, 2357-2364.

(182) Jin, X.; Carfagna, C.; Nicolais, L.; Lanzetta, R. Synthesis, Characterization, and in vitro Degradation of a Novel Thermotropic Ternary Copolyester based on p-

Hydroxybenzoic Acid, Glycolic Acid and p-Hydroxycinnamic Acid. *Macromolecules* **1995**, *28*, 4785-4794.

(183) Krigbaum, W. R.; Ishikawa, T.; Wantanabe, J.; Toriumi, H.; Kubota, K. Thermotropic homopolyesters. III. Preparation and properties of polymers based on 4'-hydroxyphenyl-4-hydroxycinnamate. *J. Polym. Sci., Part B: Polym. Phys.* **1983**, *21*, 1851-1872.

(184) Kimura, K.; Inoue, H.; Kohama, S.-i.; Yamashita, Y.; Sakaguchi, Y. Self-Organizing Polycondensation of (E)-4-Acetoxycinnamic Acid for Preparation of Poly(p-oxycinnamoyl) Microspheres. *Macromolecules* **2003**, *36*, 7721-7729.

(185) Thi, T. H.; Matsusaki, M.; Akashi, M. Thermally stable and photoreactive polylactides by the terminal conjucation of bio-based caffeic acid. *Chem. Commun.* **2008**, *33*, 3918-3920.

(186) Thi, T. H.; Matsusaki, M.; Akashi, M. Development of Photoreactive Degradable Branched Polyesters with High Thermal and Mechanical Properties. *Biomacromolecules* **2009**, *10*, 766-772.

(187) Sapich, B.; Stumpe, J.; Krawinkel, T.; Kricheldorf, H. R. New Polymer Syntheses. 95. Photosetting Cholesteric Polyesters Derived from 4-Hydroxycinnamic Acid and Isosorbide. *Macromolecules* **1998**, *31*, 1016-1023.

(188) Nagata, M.; Hizakae, S. Synthesis and characterization of photocrosslinkable biodegradeable polymers derived from 4-hydroxycinnamic acid. *Macromol. Biosci.* **2003**, *3*, 412-419.

(189) Nagata, M.; Sato, Y. Biodegradable elastic photocured polyesters based on adipic acid, 4-hydroxycinnamic acid, and poly(e-caprolactone) diols. *Polymer* **2004**, *45*, 87-93.

(190) Kreye, O.; Oelmann, S.; Meier, M. A. R. Renewable Aromatic-Aliphatic Copolyesters Derived from Rapeseed. *Macromol. Chem. Phys.* **2013**, *214*, 1452-1464.

(191) Ouimet, M. A.; Stebbins, N. D.; Uhrich, K. E. Biodegradable Coumaric Acid-Based Poly(anhydride-ester): Synthesis and Subsequent Controlled Release. *Macromol. Rapid Commun.* **2013**, *34*, 1231-1236.

(192) Ouimet, M. A.; Griffin, J.; Carbone-Howell, A. L.; Wu, W.-H.; Stebbins, N. D.; Di, R.; Uhrich, K. E. Biodegradable Ferulic Acid-Containing Poly(anhydride-ester): Degradation Products with Controlled Release and Sustained Antioxidant Activity. *Biomacromolecules* **2013**, *14*, 854-861.

(193) Pion, F.; Ducrot, P.-H.; Allais, F. Renewable Alternating Aliphatic-Aromatic Copolyesters derived from Biobased Ferluic Acid, Diols and Diacids: Sustainable Polymers with Tunable Thermal Properties. *Macromol. Chem. Phys.* **2014**, *215*, 431-439.

(194) Xin, J.; Zhang, P.; Huang, K.; Zhang, J. Study of green epoxy resins dervied from renewable cinnamic acid and dipentene: sythesis, curing and properties. *RSC Adv.* **2014**, *4*, 8525-8532.

(195) Kim, W. G. Photocure Properties of High Heat-Resistant Photoreactive Polymers with Cinnamate Groups. *J. Appl. Polym. Sci.* **2008**, *107*, 3615-3624.

(196) Zhao, S.; Abu-Omar, M. M. Biobased Epoxy Nanocomposites Derived from Lignin-Based Monomers. *Biomacromolecules* **2015**, *16*, 2025-2031.

(197) Fache, M.; Boutevin, B.; Caillol, S. Epoxy thermosets from model mixtures of the lignin-to-vanillin process. *Green Chem.* **2015**, 10.1039/C5GC01070E.

(198) Ghosh, N. N.; Kiskan, B.; Yagci, Y. Polybenzoxazines - New high performance thermosetting resins: Synthesis and properties. *Prog. Polym. Sci.* **2007**, *32*, 1344-1391.

(199) Comí, M.; Lligadas, G.; Ronda, J. C.; Galià, M.; Cádiz, V. Renewable benzoxazine monomers from "lignin-like" naturally occurring phenolic derivatives. *J. Polym. Sci., Part A: Polym. Chem.* **2013**, *51*, 4894-4903.

(200) Castillo, E. A.; Miura, H.; Hasegawa, M.; Ogawa, T. Synthesis of novel polyamides starting from ferulic acid dimer derivative. *Des. Monomers Polym.* **2004**, *7*, 711-725.

(201) Noel, A.; Borguet, Y. P.; Raymond, J. E.; Wooley, K. L. Poly(carbonate-amide)s derived from Bio-Based Resources: Poly(ferulic acid-co-tyrosine). *Macromolecules* **2014**, *47*, 2974-2983.

(202) Noel, A.; Borguet, Y. P.; Raymond, J. E.; Wooley, K. L. Poly(ferulic acid-co-tyrosine): Effect of the Regiochemistry on the Photophysical and Physical Properties en Route to Biomedical Applications. *Macromolecules* **2014**, *47*, 7109-7117.

(203) Kreye, O.; Toth, T.; Meier, M. A. R. Copolymers derived from rapeseed derivatives via ADMET and thiol-ene addition. *Eur. Polym. J.* **2011**, *47*, 1804-1816.

(204) Barbara, I.; Flourat, A. L.; Allais, F. Renewable polymers dervied from ferulic acid and biobased diols via ADMET. *Eur. Polym. J.* **2015**, *62*, 236-243.

(205) Lemma, F.; Puoci, F.; Curico, M.; Parisi, O. I.; Cirillo, G.; Spizzirri, U. G.; Picci, N. Ferulic Acid as a Comonomer in the Synthesis of a Novel Polymeric Chain with Biological Properties. *J. Appl. Polym. Sci.* **2010**, *115*, 784-789.

(206) Amarasekara, A. S.; Wiredu, B.; Razzaq, A. Vanillin based polymers: I. An electrochemical route to polyvanillin. *Green Chem.* **2012**, *14*, 2395-2397.

(207) Chauhan, N. P. S. Preparation and characterization of bio-based terpolymer derived from vanillin oxime, formaldehdye, and p-hydroxyacetophenone. *Des. Monomers Polym.* **2014**, *17*, 176-185.

(208) Holmberg, A. L.; Stanzione, J. F. I.; Wool, R. P.; Epps, T. H. I. A Facile Method for Generating Designer Block Copolymers from Functionalized Lignin Model Compounds. *ACS Sustainable Chem. Eng.* **2014**, *2*, 569-573.

(209) Stanzione, J. F. I.; Sadler, J. M.; La Scala, J. J.; Reno, K. H.; Wool, R. P. Vanillin-based resin for use in composite applications. *Green Chem.* **2012**, *14*, 2346-2352.

(210) Renbutsu, E.; Hirose, M.; Omura, Y.; Nakatsubo, F.; Okamura, Y.; Okamoto, Y.; Saimoto, H.; Shigemasa, Y.; Minami, S. Preparation and Biocompatability of Novel UV-Curable Chitosan Derivatives. *Biomacromolecules* **2005**, *6*, 2385-2388.

(211) Rao, V. S.; Samui, A. B. Molecular Engineering of Photoactive Liquid Crystalline Polyester Epoxies Containing Benzylidene Moiety. *J. Polym. Sci., Part A: Polym. Chem.* **2008**, *46*, 7637-7655.

(212) Rao, V. S.; Samui, A. B. Structure-Property Relationship of Photoactive Liquid Crystalline Polyethers containing Benzylidene Moiety. *J. Polym. Sci., Part A: Polym. Chem.* **2009**, *47*, 2143-2155.

(213) Sini, N. K.; Bijwe, J.; Varma, I. K. Renewable Benzoxazine Monomer from Vanillin: Synthesis, Characterization, and Studies on Curing Behavior. *J. Polym. Sci., Part A: Polym. Chem.* **2014**, *52*, 7-11.

(214) Pemba, A. G.; Rostagno, M.; Lee, T. A.; Miller, S. A. Cyclic and spirocyclic polyacetal ethers from lignin-based aromatics. *Polym. Chem.* **2014**, *5*, 3214-3221.

(215) Mialon, L.; Pemba, A. G.; Miller, S. A. Biorenewable polyethylene terephthalate mimics derived from lignin and acetic acid. *Green Chem.* **2010**, *12*, 1704-1706.

(216) Mialon, L.; Vanderhenst, R.; Pemba, A. G.; Miller, S. A. Polyalkylenehydroxybenzoates (PAHBs): Biorenewable Aromatic/Aliphatic Polyesters from Lignin. *Macromol. Rapid Commun.* **2011**, *32*, 1386-1392.

(217) Pang, C.; Zhang, J.; Zhang, Q.; Wu, G.; Wang, Y.; Ma, J. Novel vanillic acid-based poly(ether-ester)s: from synthesis to properties. *Polym. Chem.* **2015**, *6*, 797-804.

(218) Pang, C.; Zhang, J.; Wu, G.; Wang, Y.; Gao, H.; Ma, J. Renewable polyesters derived from 10-undecenoic acid vanillic acid with versatile properties. *Polym. Chem.* **2014**, *5*, 2843-2853.

(219) Aouf, C.; Lecomte, J.; Villeneuve, P.; Dubreucq, E.; Fulcrand, H. Chemo-enzymatic functionalization of gallic and vanillic acids: synthesis of bio-based epoxy resins prepolymers. *Green Chem.* **2012**, *14*, 2328-2336.

(220) Firdaus, M.; Meier, M. A. R. Renewable co-polymers derived from vanillin and fatty acid derivatives. *Eur. Polym. J.* **2013**, *49*, 156-166.

(221) Jose, J. P.; Joesph, K. Advances in Polymer Composites: Macro- and Microcomposites - State of the Art, New Challenges, and Opportunities In *Polymer Composites: Volume I*; Thomas, S., Joseph, K., Malhotra, S. K., Goda, K., Sadasivan, S. M., Eds.; Wiley-VCH Verlag GmbH & Co., 2012. p 1-16.

(222) Thakur, V. K.; Thakur, M. K.; Raghavan, P.; Kessler, M. R. Progress in Green Polmyer Composites from Lignin for Multifunctional Applications: A Review. *ACS Sustainable Chem. Eng.* **2014**, *2*, 1072-1092.

(223) Ten, E.; Vermerris, W. Recent Developments in polymers derived from industrial lignin. *J. Appl. Polym. Sci.* **2015**, 10.1002/app.42069.

(224) Sen, S.; Patil, S.; Argyropoulos, D. S. Thermal properties of lignin in copolymers, blends, and composites: a review. *Green Chem.* **2015**, 10.1039/C5GC01066G.

(225) Thielemans, W.; Can, E.; Morye, S. S.; Wool, R. P. Novel Applications of Lignin in Composite Materials. *J. Appl. Polym. Sci.* **2002**, *83*, 323-331.

(226) Feldman, D. Lignin and Its Polyblends In *Chemical Modification, Properties, and Usage of Lignin*; Hu, T. Q., Ed.; Kluwer Academic/Plenium Publishers: New York, N.Y., 2002. p 81-99.

(227) Hatakeyama, H.; Hatakeyama, T. Lignin Structure, Properties, and Applications. *Adv. Polym. Sci* **2010**, *232*, 1-63.

(228) Lancefield, C. S.; Westwood, N. J. The synthesis and analysis of advance lignin model polymers. *Green Chem.* **2015**, 10.1039/C5GC01334H.

Chapter 2: Biodegradable aromatic-aliphatic poly(ester-amides) from monolignol-based ester dimers

2.1 Introduction

Due to declining petroleum reserves, the utilization of alternative and renewable feedstocks for chemical and materials synthesis have recently garnered increased attention. More specifically, researchers have identified the targeted upgrading of biomass to commodity chemical or material products as a critical goal to offset an increasing dependence on petroleum worldwide[1]. Because of its abundance and accessibility, lignocellulosic biomass has been the key focus of environmentally-friendly alternatives to petroleum feedstocks[2].

Lignocellulosic biomass features three components: cellulose, hemicellulose, and lignin. Lignin is an amorphous, aromatic polymer formed in the cell wall of plants via the oxidative radical polymerization of *p*-hydroxycinnamyl alcohol monomers, known as monolignols. Comprising 15-30% of biomass, lignin is the second most abundant natural polymer. Unlike the other components of lignocellulosic biomass (cellulose or hemicellulose), lignin has yet to find a commodity industrial application. Approximately 70 million tons of lignin is isolated from the pulp and paper industry annually, but less than 2% is used as a high-value product. The rest is simply burned as a low-value fuel[3]. In addition to its low cost and abundance, lignin also has other useful physical properties such as high thermal stability, high carbon content, and structural rigidity[4,5,6]. However along with its strengths, lignin displays undesirable properties such as brittleness, incompatibility with other polymers, and a highly-varying polymeric structure, making its incorporation into high performance materials challenging. While lignin itself features an ill-defined polymeric structure, lignin monomers (monolignols) are well-defined, aromatic small molecules that offer great potential as scaffolds for monomer and polymer synthesis[7].

Aromatic units are typically introduced to polymers to improve the thermal and mechanical properties of the resulting material, as seen in the difference in thermo-mechanical properties of aliphatic and aromatic polyesters. Aliphatic polyesters are typically amorphous, have a low softening point, and readily degrade in both acidic or basic conditions[8]. Conversely, aromatic polyesters are known for their structural rigidity, thermal stability, and lack of biodegradation, as exemplified by polyethylene terephlatate (PET)[9]. Similar effects can also be seen in polyamides, where wholly aromatic polyamides, such as Nomex and Kevlar, feature high strength and thermal stability in comparison to aliphatic analogues, such as Nylon 6.

Poly(ester-amide)s (PEAs) are polymers which contain both an ester and amide linkage in their backbone. These materials are interesting as they commonly exhibit a mixture of properties of both polyesters and polyamides[10]. Polyesters readily degrade through hydrolysis of their ester linkage, generally feature better solubility in organic solvents, and are typically more flexible. Polyamides are thermally and mechanically robust due to hydrogen bonding between the amide linkages of individual polymer chains. Polyamides are also generally considered non-degradable, due to the slow rate of amide hydrolysis[11]. With the combination of these properties, poly(ester-amide)s are typically sought for applications that require good thermo-mechanical properties, as well as biocompatibility and biodegradation, such as biomedical applications or high-performance polymers with reduced environmental impact[12]. Poly(ester-amide)s are typically synthesized either by the polycondensation of bis-functionalized monomers[13] or by the ring-opening polymerization of depsipeptides[14,15]. While a multitude of PEAs from petroleum-based feedstocks have been synthesized and characterized, there are few examples of poly(ester-amide)s from alternative, bio-based feedstocks. Development of these materials is a critical goal to mitigate petroleum dependence. Lebarbé et al. developed a series of poly(ester-amide)s from caster oil, via the base-catalyzed condensation of C20 dimethyl esters and diols (all from methyl 10-undecenoate)[16]. The resulting polymers featured high thermal stability, with T_{d5}>330 °C, and semi-crystallinity. Zuo generated a series of poly (ester-amide)s from alanine-functionalized oleic acid and azelaoyl dichloride[17]. By altering the ratios of the monomers, they were able to raise or lower the T_g of the materials by increasing or decreasing, respectively, the percentage of amide bonds present. Triki and coworkers described the synthesis of a series of PEAs from a bis-functional furan monomer, hexamethylenediamine, and 1,2-ethanediol[18]. The glass transition temperature of these materials was similarly shown to increase with increasing amide content, but the synthesis of these materials featured several side reactions. End-group etherification and the formation of non-reactive end groups inhibited poly(ester-amide) formation while amide-amine crosslinking lead to the formation of poorly-defined crosslinked materials. Pinilla et al. reported the synthesis of poly(ester-amide)s from a linear carbohydrate derivative of D-xylitol and commercial aromatic diacid halides[19]. Wang et al. recently reported the synthesis of a series of linear PEAs from bio-based chemicals that featured controllable degradation based on monomer feedstock ratios[20]. However, to the best of our knowledge, aromatic-aliphatic poly(ester-amide)s from bio-based feedstocks have yet to be developed.

With this in mind, we synthesized a series of twenty-one poly(ester-amide)s from monolignol-based ester dimers to study the effects of diamine linker identity and methoxy-substitution on the thermal properties and degradation of the resulting polymers. The addition of methoxy side groups should increase the hydrophilicity and therefore the increase degradation of the poly(ester-amide)s, while increased aromatic content or aliphatic chain length should increase the hydrophobicity and reduce the extent of hydrolysis. Five aliphatic and two aromatic diamine linkers were chosen for polymer synthesis, as well as three monolignol-based carboxylic acid ester dimers. Ethylene diamine, 1,4-butanediol, hexamethylenediamine, 1,8-diaminooctane, and 1,10-diaminodecane were chosen as aliphatic linkers due to their availability from biological feedstocks. The production of ethylene diamine, 1,4-butanediol, and hexamethylenediamine has been reported from C5 and C6 plant sugars[21] while 1,8-diaminooctane[22] and 1,10-diaminodecane[23] have been produced from castor oil. While neither aromatic diamine used is commercially available from biological sources yet, other small functionalized aromatics such as catechol and styrene[21] have been successfully sourced from lignin, providing encouragement that these chemicals could eventually also be biologically sourced. Additionally, these monomers were chosen so that a modular approach could be used to generate a series of polymers with tunable properties. With these starting materials in hand, a series of poly(ester-amide)s were synthesized via interfacial polymerization. The resulting family of bio-based polymers was then studied for the effects of each structural variation on thermal stability, glass transition temperature (T_g), melting temperature (T_m), and decomposition in both neutral and acidic conditions.

2.2 Results and Discussion

Dimer synthesis. Petroleum-based polymers are the majority of commodity polymeric materials currently on the market, despite the decline of petroleum reserves.

While some bio-based polymers, such as polylactide (PLA), polyhydroxyalkanoates (PHA), and thermoplastic starch, have been developed and are produced commercially[24], there are only a few examples of well-defined, scalable, aromatic-aliphatic polymers from plant-based sources[25–27]. To add to this new class of aromatic-aliphatic materials, we sought to utilize monolignols as a scaffold for polymer synthesis. In particular, we were interested in developing a series of poly(ester-amide)s due to their thermo-mechanical stability and degradability, which could increase their potential as a replacement for current commodity materials. Three monolignol-based carboxylic acid ester dimers were generated in three steps from the precursor aldehyde (Scheme 2.1). Two dimers, starting from either 4-hydroxybenzaldehyde[28] or vanillin[29], had been previously reported by Ouimet et al., however we were unable to replicate the reported one-pot synthesis of **2a** and **2b** from Meldrum's acid in high yield. Instead, we isolated tert-butyl malonate, as reported by Smith et al.[30], prior to the Doebner-modified Knoevenagel condensation to form **2a**, **2b**, and **2c**. While this condensation reaction was generally low yielding, the increasing degrees of methoxy-substitution increased the yield significantly. Additionally, previous reports required significant excess of the malonate (as high as 2.5 equivalents) for the Knoevenagel

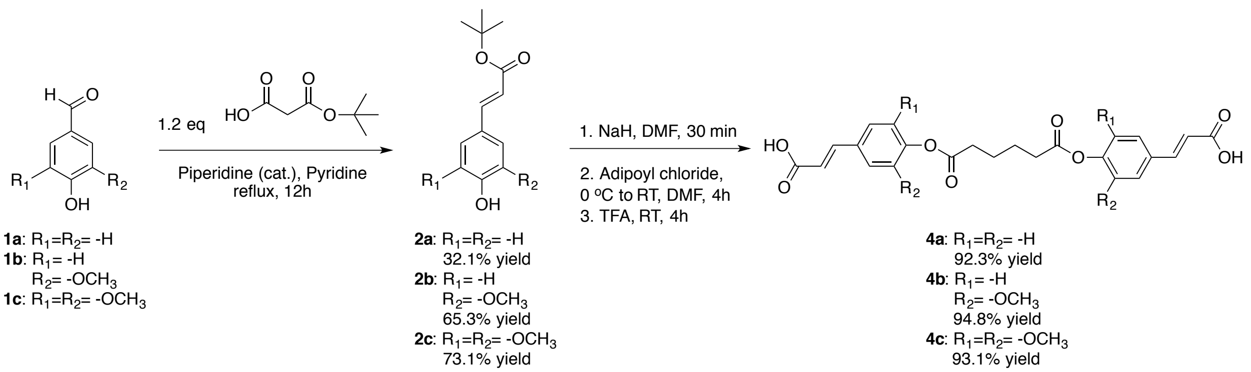

Scheme 2.1: Synthesis of monolignol-based carboxylic acid ester dimers from precursor aldehydes in three steps via Knoevenagel condensation, dimerization with adipoyl chloride, and deprotection with trifluroroacetic acid

condensation, but we obtained similar yields when lowering the quantity of tert-butyl malonate to 1.2 equivalents. After isolation of each cinnamaic tert-butyl ester monomer, the sodium salt of each monomer was generated *in situ* and then dimerized via a salt metathesis reaction with adipoyl chloride to afford protected dimers **3a**, **3b**, and **3c**. The dimers were then deprotected, in near quantitative yield, with trifluroroacetic acid (TFA) to yield the dicarboxylic acid monomers **4a**, **4b**, and **4c**. The reaction time for this deprotection had to be closely monitored and optimized, as the ester dimer could also be cleaved under the deprotection conditions.

Poly(ester-amide) synthesis. Inspired by work by Kwolek and Morgan[31], we sought to generate a series of aromatic-aliphatic poly(ester-amide)s from monolignol-based acid chloride ester dimers via interfacial polymerization. Interfacial polymerization is a useful polymerization technique as it is usually done under mild reaction conditions, only requires short polymerization times, is less influenced by impurities, and does not require a strict adherence to stoichiometry[32]. The largest limitation to this polymerization method is the possibility of acid chloride hydrolysis, which will limit polymerization and decrease both the molecular weight and yield of any polymer generated. However, due to the hydrophobicity of our aromatic monolignol-based acid chloride ester dimer, we believed the hydrolysis side-reaction would be minimal and not greatly affect the polymerization reaction. We first attempted to draw a single fiber from the interface, similar to the *Nylon Rope Trick*[31], but the poly(ester-amide)s formed proved to be too brittle to permit this. Additionally, allowing the poly(ester-amide) to form as a film at the interface led to low conversion and low molecular weight polymers. During polymerization, the poly(ester-amide)s rapidly precipitated from solution, limiting their ability to react and generate high molecular weight polymers[33]. To

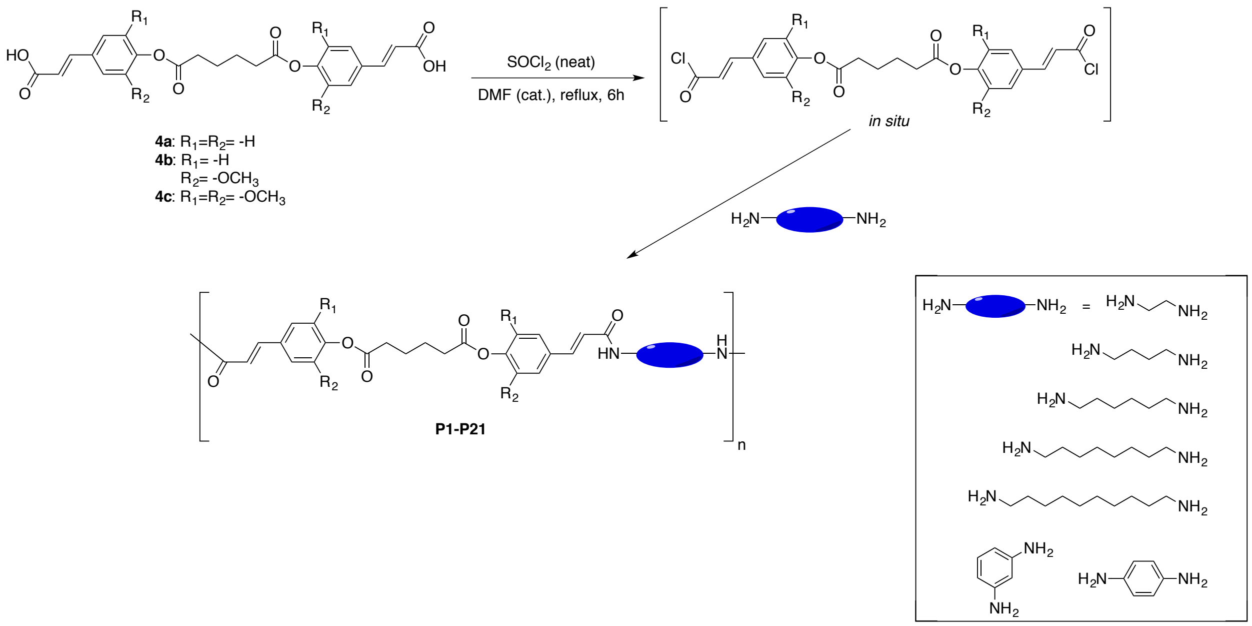

Scheme 2.2: Interfacial polymerization of poly(ester-amide)s via monolignol-based diacid chloride monomers and seven different diamines

eliminate solubility and brittleness issues, the solution was rapidly stirred during the interfacial polymerization reaction to maximize surface area and eliminate mechanical dependence on polymer formation.

Interfacial polymerization was conducted with the desired aliphatic or aromatic diamine and desired monolignol-based diacid chloride ester dimer (Scheme 2.2). The diacid chloride dimer was generated *in situ*, via refluxing in thionyl chloride for six hours. After the reaction time was complete, volatiles were removed under reduced pressure and the diacid chloride ester dimer was used without further purification or characterization. The diacid chloride ester dimer was dissolved in distilled methylene chloride and added to a rapidly stirring, dilute sodium hydroxide solution containing the diamine. Poly(ester-amide)s were isolated as pale yellow powders from the biphasic solution. The resulting polymers were insoluble in standard organic solvents (i.e. acetone, diethyl ether, tetrahydrofuran) and only sparingly soluble in *N,N*-dimethylformamide (DMF), as seen in Table 2.1. For P1, P5, P9, P11, P12, P16, and P20, more than 50% of the polymer sample was insoluble in DMF after 24 hours, with some polymers featuring insolubility as high as 76.3% (P20). The other polymers in the series were slightly more soluble, mostly between 50 and 35% insoluble after 24 hours. This insolubility affected the ability to perform standard solution phase characterization and limited characterization to solid-phase techniques. Formation of amide linkages was confirmed by IR spectroscopy, with the shift of the carboxylic acid C=O stretch to lower wavenumbers (1665-1650 cm^{-1}) with amide bond formation and the appearance of N-H bending (1540-1550 cm^{-1}), as seen in Figure 2.1 (and Figures S7 –S8). As expected, the C=O (1765-1750 cm^{-1}) and C-O stretches (1030-1025 cm^{-1} and 980-975 cm^{-1}) from the dimer ester bonds remain largely unchanged between the dimer starting material and final polymeric product, confirming the dimer remains intact throughout the polymerization procedure.

Table 2.1 Insolubility of poly(ester-amide)s in DMF after 24h[a]

	Polymer	Wt% insoluble[a]
p-coumaryl	P1	62.3
	P2	32.0
	P3	38.5
	P4	47.5
	P5	52.5
	P6	23.3
	P7	46.6
ferulyl	P8	49.7
	P9	67.4
	P10	18.5
	P11	74.3
	P12	57.3
	P13	25.4
	P14	26.7
sinapyl	P15	27.2
	P16	64.8
	P17	45.8
	P18	39.2
	P19	45.2
	P20	76.3
	P21	40.8

[a] 1.0 mL of 10 mM LiBr in DMF was added to weighed polymer samples (10 mg) and allowed to sit at room temperature for 24 h. Solvent was decanted and the residual solid was dried in a vacuum oven overnight. Solid was weighed to determine wt% insoluble.

Molecular weight characterization. As mentioned previously, the series of poly(ester-amide)s were insoluble in common organic solvents and only sparingly soluble in DMF (Table 2.1), hindering the characterization of the resulting materials. While poly(ester-amide)s are generally considered more soluble than polyamides, they are also known to be largely insoluble in common organic solvents[34], depending on the polymeric structure. Due to the amount of polymeric material not soluble in DMF, we speculate that the poly(ester-amide)s produced could be of even higher molecular weight than those reported below. In general, the poly(ester-amide)s generated in this work were of moderate molecular weight (by GPC) and, as expected due to the polymerization method, featured moderate dispersity. As seen in Table 2, the number-average molecular weight (M_n) and weight-average molecular weight (M_w) of each polymer in the series varies greatly depending on the identity of both the monolignol-based ester dimer and the diamine linker. While the majority of the polymers generated were of moderate molecular weight, several polymers featured molecular weights lower than what would be typically expected utilizing interfacial polymerization. With the lack of any methoxy-substituents, *p*-coumaryl derivatives either precipitate more quickly from solution, generating polymers of lower molecular weight, or the isolate polymers feature drastically reduced solubility in DMF. Both scenarios would drastically lower the molecular weight observed by GPC. Polymers

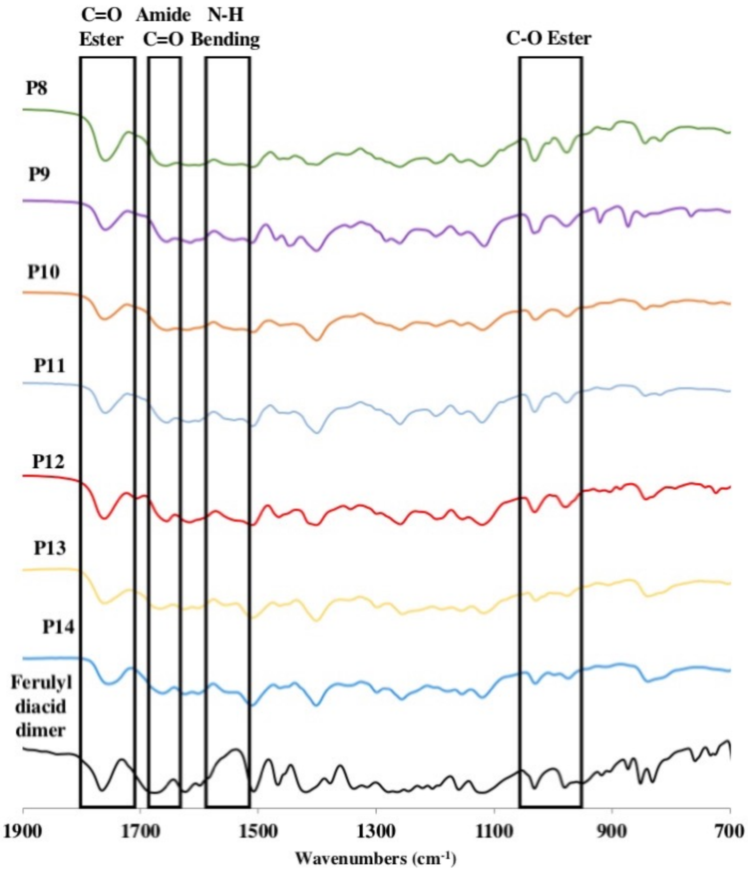

Figure 2.1: Fingerprint region of IR spectra of ferulic-acid based poly(ester-amide)s (P8-P14) in comparison to ferulic-acid dimer

Table 2.2 Molecular weight characterization of poly(ester-amide)s by gel permeation chromatography

Polymer	Dimer	Diamine	M_n[a]	M_w[a]	Đ[b]
P1	*p*-Coumaryl	Ethylene diamine	8,580	16,490	1.92
P2		1,4-diaminobutane	4,050	9,320	2.32
P3		Hexamethylenediamine	7,830	12,660	1.62
P4		1,8-diaminooctane	9,500	11,730	1.24
P5		1,10-diaminodecane	9,190	11,410	1.24
P6		*m*-phenylenediamine	18,770	54,540	2.90
P7		*p*-phenylenediamine	7,560	29,850	3.95
P8	Ferulyl	Ethylene diamine	11,300	16,910	1.50
P9		1,4-diaminobutane	16,710	28,430	1.70
P10		Hexamethylenediamine	16,280	29,440	1.81
P11		1,8-diaminooctane	8,552	9,562	1.12
P12		1,10-diaminodecane	9,280	15,020	1.62
P13		*m*-phenylenediamine	13,720	58,230	4.24
P14		*p*-phenylenediamine	11,880	24,561	2.07
P15	Sinapyl	Ethylene diamine	18,450	36,700	1.99
P16		1,4-diaminobutane	13,110	19,170	1.46
P17		Hexamethylenediamine	27,470	65,780	2.39
P18		1,8-diaminooctane	17,010	31,420	1.84
P19		1,10-diaminodecane	5,130	9,750	1.90
P20		*m*-phenylenediamine	8,170	25,460	3.12
P21		*p*-phenylenediamine	4,780	22,260	4.66

[a]Determined by GPC, 10 mM LiBr in DMF, 40 °C, 1.0 mL/min; [b]$Đ=M_w/M_n$

synthesized from 1,8-diaminooctane or 1,10-diaminodecane, regardless of the identity of the monolignol-based ester dimer, were typically of lower molecular weight, due to the reduced solubility of long aliphatic diamines in the basic aqueous solution. Reducing the amount of soluble diamine present in solution to react during polymerization likely reduced the molecular weight of the polymer generated.

Thermal properties. The thermal stability of the poly(ester-amide)s were examined using thermogravimetic analysis (TGA). Samples were heated from 30 to 800 °C at 10 °C/min under nitrogen (Figure S15-17). All polymers featured good thermal stability, with the onset of decomposition (T_{d5}) typically between 220 and 260 °C (Table 2.3). The high degree of thermal stability makes these materials likely candidates for melt processing. Most

Table 2.3 Thermal characterization of poly(ester-amide)s by DSC and TGA

	Polymer	T_g(°C)^{a}	T_m(°C)^{a}	T_{d5}(°C)^{b,c}	T_{d10}(°C)^{b,d}	T_{d25}(°C)^{b,e}
p-coumaryl	P1	94.5	-	255.4	297.8	371.9
	P2	88.5	-	251.2	307.1	369.5
	P3	84.5	-	264.2	314.4	410.3
	P4	90.3	-	294.1	324.8	394.6
	P5	83.4	-	260.2	302.1	357.6
	P6	79.3	-	233.3	300.0	358.3
	P7	91.4	-	252.5	321.6	364.5
ferulyl	P8	103.3	-	266.9	286.6	340.3
	P9	92.3	-	255.8	287.9	343.9
	P10	91.7	-	249.5	298.3	353.8
	P11	92.7	-	253.9	283.0	330.8
	P12	89.8	-	255.4	297.8	371.9
	P13	119.7	-	231.2	290.1	356.0
	P14	125.9	-	240.1	273.4	332.9
sinapyl	P15	95.9	-	235.6	272.9	322.7
	P16	71.3	-	246.9	285.1	378.6
	P17	-	63.6	256.3	277.4	340.9
	P18	84.3	127.9	252.1	291.8	376.9
	P19	-	141.9	222.4	279.5	396.1
	P20	91.3	-	221.8	254.6	385.8
	P21	67.8	-	203.0	220.1	303.8

[a]Determined by differential scanning calorimetry (DSC), scanned -10 to 200 °C at 10 °C/min; [b] Determined by TGA, heated from 25 °C to 800 °C at 10 °C/min; [c] T_{d5} = temperature at 5% mass loss; [d] T_{d10} = temperature at 10% mass loss; [e]T_{d25} = temperature at 25% mass loss

commercial thermoplastics are processed between 100 and 250 °C, depending on their melting temperature[35]. While thermogravimetric analysis cannot identify the melting point of each polymer, the overall thermal stability of these materials is a key aspect to consider when selecting a processing method.

Amorphous aliphatic polymers typically exhibit lower glass transition temperatures in comparison to aromatic amorphous polymers, due to high chain flexibility. Furthermore, the addition of bulky side groups to both aliphatic and aromatic amorphous polymers commonly increases the glass transition temperature, due to reduced chain flexiblity. As the poly(ester-amide)s in this system feature both aromatic and aliphatic components as well as varying degrees of methoxy substitution, T_g should increase with increasing aromatic content and substitution due to reduced backbone flexibilty. While methoxy groups are hardly considered bulky substituents, this addition could affect the observed thermal properties of the poly(ester-amide)s. As shown in Table 3, the majority of this series of polymers is amorphous in nature, exhibiting T_g between 64.7 and 138.2 ^{o}C. Glass transition temperature should also decrease as the length of the aliphatic chain increases, due to increased flexability of the polymer backbone. While the majority of the polymers follow this trend, there are several notable exceptions (Figure 2.2). Poly(ester-amide)s containing 1,8-diaminooctane (P4, P11) exhibit increased glass transition temperatures. The eight carbon aliphatic spacer offers flexibility and optimal spacing between the amide and ester linkages to allow for increased intermolecular and intramolecular interactions between the chains. A similar effect was seen by Wang et al. in their synthesis of aromatic-aliphatic poly(ester-amide)s containing different length polyethylene glycol (PEG) spacers[36]. The polymers showed increasing T_g as the length of PEG spacer increased, due to decreased molecular mobility with increased interactions. The addition of an aromatic linker, instead of an aliphatic linker, had varied effects on the glass transition temperature. P6, P7, P20, and P21 feature glass transition temperatures comperable to their aliphatic analgoues. High glass transition temperatures associated with aromatic polyamides arise from interchain hydrogen bonding, which can be facilitated by π-π interactions. With these poly(ester-amide)s, the increased

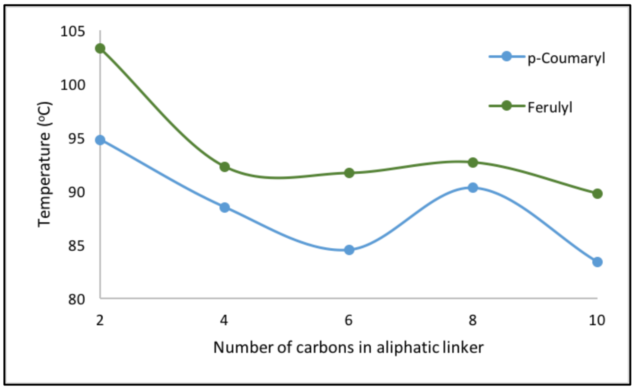

Figure 2.2: Glass transition temperature as a function of aliphatic linker length

aromatic content provides structural rigidity, but does not have strong π-π interactions, limiting the formation of strong hydrogen bonding interactions. This can be seen even more directly in the effect of aromatic substitution on glass transition temperature. For example, P6, which is synthesized with *m*-phenylenediamine, has a T_g 12.1 °C lower than P7, which is synthesized with *p*-phenylenediamine. The meta-substitution prevents the formation of additional π-π interactions and thus interchain interactions, lowering the observed glass transition temperature.

While the degree of methoxy-substitution has little effect on the glass transition temperature, it affects the crystallinity of several poly(ester-amide)s. P17 and P19 exhibit only a single melting temperature (T_m) and no observable glass transition temperature, while P18 exhibits both a T_m and a T_g. The dimethoxy-substitution of the sinapyl-acid based ester dimer in addition to the increased length of the aliphatic linkers allowed for the formation of a crystalline phase upon cooling from the first heating cycle in DSC. While the insolubility of the poly(ester-amide)s would render solution-phase processing difficult, the observed melting temperatures and high thermal stability should allow for heat processing with minimal decomposition. While only P17, P18, and P19 have clearly defined melting temperatures, the other polymers in this series could be expected to have a similar melting points for melt processing. The glass transition temperatures for the majority of the polymers are similar to commodity aromatic polymers, such as polyethylene terephthalate (T_g=70 ^{o}C)[37] or polystyrene (T_g=100 ^{o}C)[38], rendering these materials potentially suitable replacements for commodity materials.

Degradation of poly(ester-amide)s. While aliphatic poly(ester-amide)s are typically capable of degradation under a variety of enzymatic and non-enzymatic conditions, wholly aromatic poly(ester-amide)s are generally considered less degradable than aliphatic analogues[39]. Due to the aromatic-aliphatic structure of our system, we were interesting in studying the degradation of our polymers in both neutral and acidic conditions. Additionally, varying the degree of methoxy substituents should affect the hydrophilicity and therefore the hydrolysis of each respective polymer. Due to the large number of polymers in this study, P15 to P21 (sinapyl acid-based) were compared to determine the role of diamine linker identity in degradation, while P1, P8, and P15 were compared to determine the role of degree of methoxy-substitution in degradation. As mentioned previously, all polymer samples feature moderate dispersity due to the non-controlled, bulk polymerization method utilized and therefore contain both higher and lower molecular weight fractions. Polymer samples were stirred in either pH 5.00 sodium acetate buffer or pH 7.04 water for 30 days, at a concentration of 10 mg/mL. 0.1 mL aliquots of each suspension were taken on day 7, 14, and 30, diluted to a concentration of 1 mg/mL with DMF before analysis by GPC. Due to the low signal intensity in each aliquot, traces were smoothed and normalized for comparison to non-decomposed polymers. As seen in Figure 2.3 (and Figures S18 to S27), all samples did undergo decomposition at both pH 5 and 7, however some large molecular weight fractions remained even after 30 days and increased degradation was observed in the pH 7 solution.

Increasing the length of aliphatic linker decreased the amount of degradation in both solutions. This can be seen in the comparison of P15 (Figure 2.3a and 2.3b), synthesized with ethylene diamine, to P17 (Figure 2.3c and 2.3d), synthesized with hexamethylenediamine. The increased length of the aliphatic linker increases the hydrophobicity of the polymer, thus

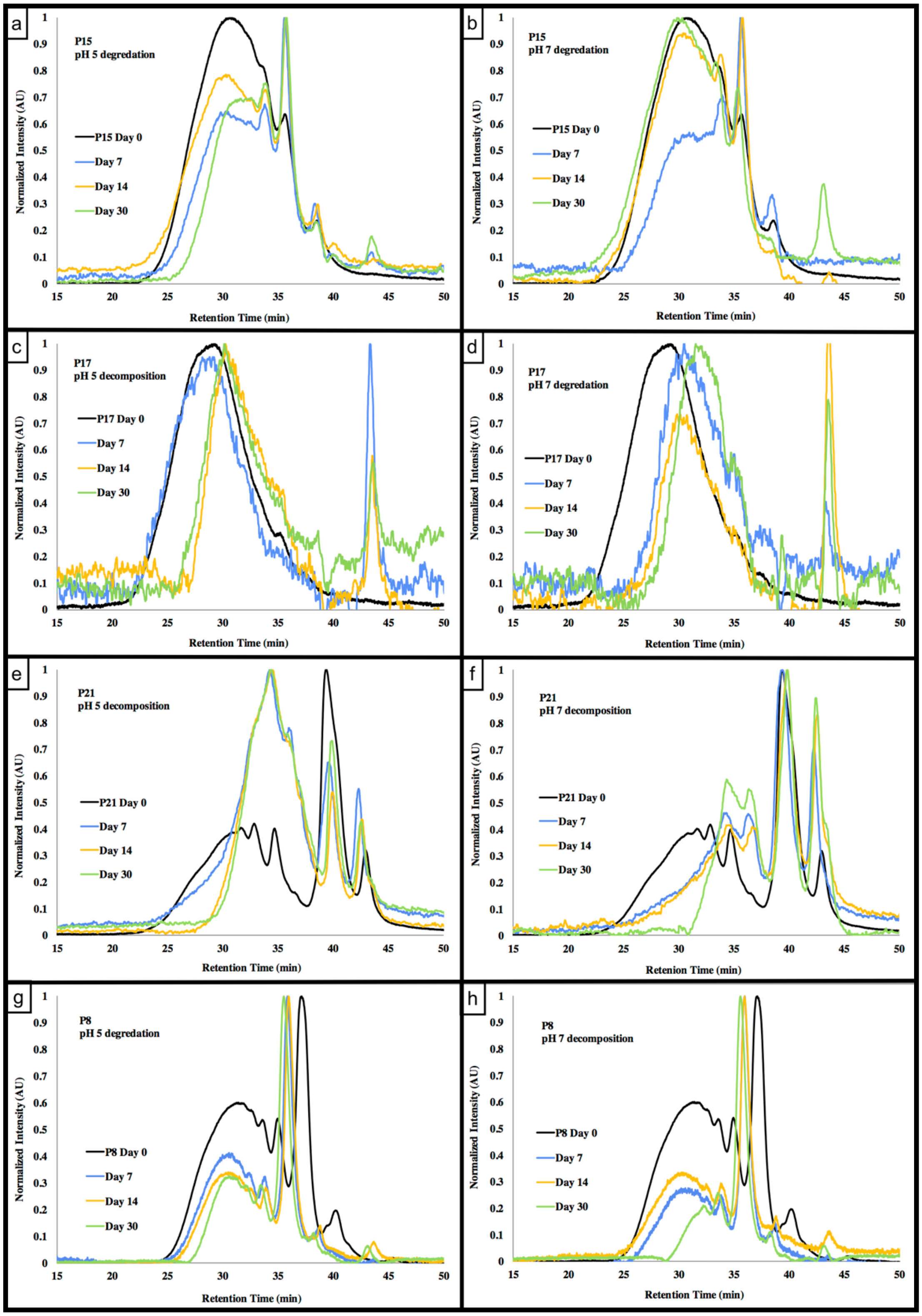

Figure2.3: Stacked GPC traces of poly(ester-amide) degradation a) P15 pH 5 solution; b) P15 pH 7 solution; c) P17 pH 5 solution; d) P17 pH 7 solution; e) P21 pH 5 solution; f) P21 pH 7 solution; g) P8 pH 5 solution; h) P8 pH 7 solution

reducing its ability to undergo hydrolysis. The use of an aromatic diamine linker also shows increased resistance to hydrolysis for higher molecular weight fractions. As seen in Figure 2.3e, the amount of lower molecular weight polymer in solution decreases relative to the higher molecular weight polymer, suggesting that the lower molecular weight fractions are more soluble and thus more readily undergo hydrolysis while the larger molecular weight polymers remain intact.

The degree of methoxy substitution affects solubility and thus the degree of hydrolysis. The ferulic acid (P8; Figure 2.3g and 2.3h) and *p*-coumaryl analogues (P1; Figure S26 and S27) featured minimal hydrolysis, in comparison to sinapyl-based polymers, even after 30 days in both acidic and neutral solutions. Overall, the degradation of the poly(ester-amide)s was moderate, suggesting that these materials would be appropriate for single use applications requiring good thermal properties and biodegradation. Other bio-based materials, such as poly(lactic acid), undergo hydrolysis too rapidly for widespread commercial use, which would not be a limitation of this system. If an increased rate of hydrolysis was desired, the aliphatic ester linkage could be replaced with an ethylene glycol linker to increase hydrophilicity and the rate of degradation, as seen in work by Ouimet et al.[40]

2.3 Conclusions

In this work, we have described the synthesis and characterization of a series of aromatic-aliphatic poly(ester-amide)s from monolignol-based ester dimers. The interfacial condensation polymerization of diamines and monolignol-based carboxylic acid ester dimers yielded a series of twenty-one polymers with varying molecular weights and dispersity. By selecting this method of polymerization and readily interchangeable structural components, we were able to rapidly generate a full series of polymers with tunable properties in a high-throughput manner. Further tuning of this system could yield additional materials with different properties. Moreover, this system is unique as it contains two unreacted double bonds per monolignol-based dimer, allowing it to be further modified, such as the addition of hydrophilic or hydrophobic groups, used as a backbone for graft-co-polymers, or cross-linked into a polymer network. Further research in our group will focus on the development of new applications and functionalization of this poly(ester-amide) system.

2.4 Experimental Section

Materials. 4-hydroxybenzaldehyde (98%, TCI America), vanillin (99%, Alfa Aesar), 3,5-dimethoxy-4-hydroxybenzaldehyde (98%, Acros), malonic acid (99%, Alfa Aesar), tert-butanol (99%, Alfa Aesar), acetic anhydride (99.5%, Fisher), acetone (ACS Grade, Fisher), sulfuric acid (conc., ACS Grade, Fisher), adiopyl chloride (99%, Acros), piperidine (99%, Spectrum), trifluoroacetic acid (99.5%, Fisher) 1,4-diaminobutane (98+%, Alfa Aesar), 1,8-diaminooctane (98%, Acros), 1,10-diaminodecane (97%, Acros), *p*-phenylenediamine (99+%, Acros), *m*-phenylenediamine (99+%, Acros), sodium hydroxide (ACS Grade, Fisher), and N,N-dimethylformamide (HPLC grade, Alfa Aesar) were purchased and used as received. Pyridine (99%, Fisher) was distilled over KOH prior to use. Dichloromethane (ACS Grade, Fisher) was distilled over calcium hydride prior to use. Hexamethylene diamine (99.5%, Acros) was sublimed under reduced pressure prior to use. Ethylenediamine (98%, Acros) was distilled prior to use to remove discoloration. Meldrum's acid[41] and tert-butyl malonate[30] were synthesized according to published procedures. Silica gel 60 (230-400 mesh, Fisher) was used for column chromatography. Thin layer chromatography (TLC) was conducted with silica gel 60–F245 plates and visualized with a handheld UV lamp. NMR solvents d_6-DMSO, $CDCl_3$, and C_6D_6 were obtained from Cambridge Isotope Laboratories and used as received.

^{1}H, ^{13}C, and FTIR Spectroscopy. ^{1}H NMR spectra were recorded on Bruker AV-300 or Bruker DRX-500 spectrometers at room temperature in d_6-DMSO, $CDCl_3$, or C_6D_6. Chemical shifts are reported with respect to internal solvent, 2.50 ppm (d_6-DMSO), 7.26 ($CDCl_3$) or 7.16 (C_6D_6) for ^{1}H NMR spectra. ^{13}C NMR spectra were recorded on a Bruker AV-500 spectrometer with a dual cryoprobe (^{13}C, ^{1}H). Chemical shifts are reported with respect to internal solvent, 39.52 ppm (d_6-DMSO), 77.16 ppm ($CDCl_3$), or 128.06 (C_6D_6) for ^{13}C NMR spectra. Infrared absorption spectra were collected using a Jasco 4210-FT/IR spectrometer from 4000 to 400 cm^{-1} from KBr pellets. All samples were dried at 100 °C in a vacuum oven overnight (at least 12 h) prior to characterization.

Molecular Weight Characterization. Molecular weight (M_n and M_w) and dispersity ($Đ$=M_w/M_n) were determined using gel permeation chromatography (GPC). Samples were dissolved in 10 mM LiBr in *N,N*-dimethylformamide (DMF) at a concentration of 2−5 mg/mL and were passed through a 0.20 µm PTFE filter before injection. GPC for all polymers was conducted on a Jasco system equipped with a refractive index detector, a UV detector, a Waters Styragel guard column, and four Waters HR Styragel 5 µm columns (100-5K, 500-30K, 50-100K, 5-600 K) using 10 mM LiBr in *N,N*-dimethylformamide (DMF) at 40 °C and a flow rate of 1.0 mL/min. Calibration was performed using nine near-monodisperse polystyrene standards (M_n=1,250 to 549,000 Da) from Jordi Laboratories and chromatograms were analyzed using ChromNAV chromatography software. For the degradation studies, due to the low sample concentration in each aliquot, raw GPC traces were smoothed using a median filter (n=15) and normalized in Microsoft Excel.

Thermal Characterization. All samples were dried at 100 °C in a vacuum oven overnight (at least 12 h) prior to all thermal characterization. Thermogravimetric analysis (TGA) was conducted on a Perkin Elmer Pyris Diamond TG/DTA Thermogravimetric/Differential Thermal Analyzer. The TGA instrument was operated under an argon atmosphere, using platinum crucibles. Samples (6-12 mg) were heated from 25 to 800 °C at a rate of 10 °C/min and held at 800 °C for five minutes. Pyris Manager was used to analyze the data. Decomposition temperatures T_{d5}, T_{d10}, and T_{d25} were measured at 5, 10, and 25% mass loss, respectively. Differential scanning calorimetry (DSC) was performed on a Perkin Elmer DSC 8000 to determine glass transition (T_g) and melting (T_m) temperatures, as applicable. Samples (5-8 mg) were heated from -10 to 200 °C at a rate of 10 °C/minand cooled to -10 °C at a rate of 10 °C/min. A minimum of two heating and cooling cycles were performed and T_g and T_m were measured from the second heating cycle. Pyris Manager was used to analyze the data.

Tert-butyl ester monomer synthesis. *p-Coumaroyl tert-butyl ester (**2a**)*. 4-hydroxybenzaldehyde (6.99 g, 57.3 mmol, 1 eq) was weighed and added to a round bottom flask along with tert-butyl malonate (11.01 g, 68.7 mmol, 1.2 eq). 30.0 mL of pyridine and 0.3 mL of piperidine were added to the reaction mixture and the reaction was heated to reflux overnight. After refluxing, the reaction was cooled to room temperature and concentrated under reduced pressure. The resulting residue was dissolved in diethyl ether (70 mL) and washed with saturated sodium bicarbonate (2×70 mL), 1 M HCl (2×40 mL), and deionized water (1×40 mL). The organic layer was dried over $MgSO_4$ and solvent was removed via rotary evaporation to yield the crude product. The compound was purified on silica gel via flash column chromatography using 3:2 hexanes:ethyl acetate as the elutant. Yield: 4.04 g, 32.1% ^{1}H NMR (300 MHz, d_6-DMSO): δH 7.67 (d, 2H, Ar-***H***), 7.62 (d, 1H, CC***H***=CHCOO(CH$_3$)$_3$), 7.20 (d, 2H, Ar-***H***), 6.54 (d, 1H, CCH=C***H***COO(CH$_3$)$_3$), 1.48 (s, 9H, COO(C***H***$_3$)$_3$).

*Feruloyl tert-butyl ester (**2b**)*. Yield: 6.49 g, 65.3% ^{1}H NMR (300 MHz, d_6-DMSO): δH 7.48 (d, 1H, CC***H***=CHCOO(CH$_3$)$_3$), 7.27 (s, 1H, Ar-***H***), 7.08 (d, 1H, Ar-***H***), 6.80 (d, 1H, Ar-***H***), 6.37 (d, 1H, CCH=C***H***COO(CH$_3$)$_3$), 3.81 (s, 3H, Ar-OC***H***$_3$), 1.47 (s, 9H, COO(C***H***$_3$)$_3$).

*Sinapoyl tert-butyl ester (**2c**)*. 3,5-dimethoxy-4-hydroxybenzaldehyde (3.17 g, 17.4 mmol, 1 eq) was weighed and added to a round bottom flask along with tert-butyl malonate (3.90 g, 24.4 mmol, 1.2 eq). 20.0 mL of pyridine and 0.2 mL of piperidine were added to the reaction mixture and the reaction was heated to reflux overnight. After refluxing, the reaction was cooled to room temperature and concentrated under reduced pressure. The resulting residue was dissolved in diethyl ether (50 mL) and washed with saturated sodium bicarbonate (2×50 mL), 1 M HCl (2×30 mL), and deionized water (1×30 mL). The organic layer was dried over MgSO$_4$ and solvent was removed via rotary evaporator to yield the product as a white solid. The compound was purified on silica gel via flash column chromatography using 3:2 hexanes:ethyl acetate as the elutant. Yield: 3.57 g, 73.1% ^{1}H NMR (300 MHz, d_6-DMSO): δH 8.89 (s, 1H, Ar-O***H***), 7.47 (d, 1H, CC***H***=CHCOO(CH$_3$)$_3$), 6.98 (s, 2H, Ar-***H***), 6.44 (d, 1H, CCH=C***H***COOtBu), 3.79 (s, 6H, Ar-OC***H***$_3$), 1.48 (s, 9H, COOC(C***H***$_3$)$_3$). ^{13}C NMR (500 MHz, d_6-DMSO): δC 166.46 (CCH=CH***C***OO(CH$_3$)$_3$), 148.46 (***C***-OCH$_3$), 144.87 (C***C***H=CHCOO(CH$_3$)$_3$), 138.50 (***C***-OH), 124.97 (***C***CH=CHCOO(CH$_3$)$_3$), 117.26 (CCH=***C***HCOO(CH$_3$)$_3$), 106.49 (Ar ***C***-H), 79.90 (***C***(CH$_3$)$_3$), 56.53 (O***C***H$_3$), 28.39 (C(***C***H$_3$)$_3$).

Tert-butyl ester dimer synthesis. *p*-Coumaroyl tert-butyl ester dimer (**3a**)[28] and feruloyl tert-butyl ester dimer (**3b**)[29] were synthesized as reported previously by Ouimet et al.

p-Coumaroyl tert-butyl ester dimer (**3a**). Yield: 2.33 g, 70.1% ^{1}H NMR (300 MHz, *d*$_6$-DMSO): δH 7.65 (d, 2H, Ar-***H***), 7.61 (d, 1H, CC***H***=CHCOOH), 7.21 (d, 2H, Ar-***H***), 6.56 (d, 1H, CCH=C***H***COOH), 2.69 (br s, 2H, -OC***H***$_2$CH$_2$), 1.77 (br s, 2H, -OCH$_2$C***H***$_2$), 1.49 (s, 9H,COO(C***H***$_3$)$_3$).

Feruloyl tert-butyl ester dimer (**3b**) Yield: 2.61 g, 74.4% ^{1}H NMR (300 MHz, *d*$_6$-DMSO): δH 7.50 (d, 1H, CC***H***=CHCOO(CH$_3$)$_3$), 7.31 (s, 1H, Ar-***H***), 7.20 (d, 1H, Ar-***H***), 6.99 (d, 1H, Ar-***H***), 6.46 (d, 1H, CCH=C***H***COO(CH$_3$)$_3$), 3.80 (s, 3H, Ar-OC***H***$_3$), 2.81 (br s, 2H, -OC***H***$_2$CH$_2$) 1.79 (br s, 2H, -OCH$_2$C***H***$_2$), 1.48 (s, 9H,COO(C***H***$_3$)$_3$)

*Sinapoyl tert-butyl ester dimer (**3c**)*. Sinapoyl tert-butyl ester (4.99 g, 17.8 mmol, 2 eq) was weighed and added to a two-necked round bottom flask along with 30 mL of *N,N*-dimethylformamide (DMF). The reaction mixture was cooled to 0 °C and sodium hydride (0.64 g, 26.7 mmol, 3 eq) was added portionwise. After 30 minutes, a solution of adipoyl chloride (1.3 mL, 8.9 mmol) in 5 mL DMF was added dropwise over 30 minutes via an addition funnel. The reaction was allowed to slowly warm to room temperature and stir for 5 hours. After 5 hours, the reaction was diluted with ethyl acetate (70 mL) and washed with deionized water (2×70 mL). The organic layer was separated, dried over MgSO$_4$, and volatiles were removed via rotary evaporator to yield the crude product as a white solid. The product was purified on silica gel via flash column chromatography using 3:2 hexanes:ethyl acetate as the elutant. Yield: 1.89 g, 31.7%^{1}H NMR (300 MHz, C$_6$D$_6$): δ 7.84 (d, 1H, CC***H***=CHCOO(CH$_3$)$_3$), 6.52 (d+s, 3H, Ar-H + CCH=C***H***COO(CH$_3$)$_3$), 3.23 (s, 6H, Ar-OC***H***$_3$), 2.44 (br s, 2H, OC***H***$_2$CH$_2$), 1.73 (br s, 2H, OCH$_2$C***H***$_2$), 1.52 (s, 9H, C(C***H***$_3$)$_3$).

^{13}C NMR (500 MHz, $\mathrm{C_6D_6}$): δ 170.49 ($\mathrm{COO\boldsymbol{C}CH_2CH_2}$), 166.04 ($\mathrm{CCH{=}CH\boldsymbol{C}OO(CH_3)_3}$), 153.19 ($\mathrm{\boldsymbol{C}OCH_3}$), 143.96 ($\mathrm{C\boldsymbol{C}H{=}CHCOO(CH_3)_3}$), 132.99 ($\mathrm{\boldsymbol{C}CH{=}CHCOO(CH_3)_3}$), 131.29 ($\mathrm{\boldsymbol{C}OOCCH_2CH_2}$), 120.69 ($\mathrm{CCH{=}\boldsymbol{C}HCOO(CH_3)_3}$), 104.74 (Ar), 80.16 ($\mathrm{\boldsymbol{C}(CH_3)_3}$), 55.58 ($\mathrm{CO\boldsymbol{C}H_3}$), 33.73 ($\mathrm{COOC\boldsymbol{C}H_2CH_2}$), 28.29 ($\mathrm{C(\boldsymbol{C}H_3)_3}$), 24.59 ($\mathrm{COOCCH_2\boldsymbol{C}H_2}$).

Diacid ester dimer synthesis. *p*-Coumaryl diacid dimer (**4a**)[28] and ferulyl diacid dimer (**4b**)[29] were synthesized as reported previously by Ouimet et al.

p-Coumaryl diacid dimer (**4a**) Yield: 1.08 g, 92.3% ^{1}H NMR (300 MHz, d_6-DMSO): 7.67 (d, 2H, Ar-$\boldsymbol{H}$), 7.62 (d, 1H, $\mathrm{CC\boldsymbol{H}{=}CHCOOH}$), 7.20 (d, 2H, Ar-$\boldsymbol{H}$), 6.54 (d, 1H, $\mathrm{CCH{=}C\boldsymbol{H}COOH}$), 2.67 (br s, 2H, $\mathrm{-OC\boldsymbol{H}_2CH_2}$), 1.75 (br s, 2H, $\mathrm{-OCH_2C\boldsymbol{H}_2}$).

Ferulyl diacid dimer (**4b**) Yield: 1.12 g, 94.8% ^{1}H NMR (300 MHz, d_6-DMSO): 7.51 (d, 1H, $\mathrm{CC\boldsymbol{H}{=}CHCOO(CH_3)_3}$), 7.29 (s, 1H, Ar-$\boldsymbol{H}$), 7.20 (d, 1H, Ar-$\boldsymbol{H}$), 6.98 (d, 1H, Ar-$\boldsymbol{H}$), 6.46 (d, 1H, $\mathrm{CCH{=}C\boldsymbol{H}COO(CH_3)_3}$), 3.82 (s, 3H, $\mathrm{Ar\text{-}OC\boldsymbol{H}_3}$), 2.82 (br s, 2H, $\mathrm{-OC\boldsymbol{H}_2CH_2}$) 1.78 (br s, 2H, $\mathrm{-OCH_2C\boldsymbol{H}_2}$)

Sinapyl diacid dimer (4c). Sinapoyl tert-butyl ester dimer (1.69 g, 2.5 mmol, 1 eq) was weighed and added to a round bottom flask along with trifluoroacetic acid (7.7 mL, 100.6 mmol, 40 eq). Reaction was stirred at room temperature for 4 hours. Volatiles were removed via rotary evaporation to yield the product as a white solid. Yield: 1.31 g, 93.1%^{1}H NMR (300 MHz, d_6-DMSO): δ 7.59 (d, 1H, $\mathrm{CC\boldsymbol{H}{=}CHCOOH}$), 7.09 (s, 2H, Ar-$\boldsymbol{H}$), 6.64 (d, 1H, $\mathrm{CCH{=}C\boldsymbol{H}COOH}$), 3.79 (s, 6H, $\mathrm{COC\boldsymbol{H}_3}$), 2.62 (br s, 2H, $\mathrm{OC\boldsymbol{H}_2CH_2}$), 1.77 (br s, 2H, $\mathrm{OCH_2C\boldsymbol{H}_2}$) ^{13}C NMR (500 MHz, d_6-DMSO): δ 170.54($\mathrm{\boldsymbol{C}OOCH_2CH_2}$), 167.63 ($\mathrm{CCH{=}CH\boldsymbol{C}OOH}$), 151.98 ($\mathrm{\boldsymbol{C}OCH_3}$), 143.82 ($\mathrm{C\boldsymbol{C}H{=}CHCOOH}$), 132.63 ($\mathrm{\boldsymbol{C}CH{=}CHCOOH}$), 129.43 ($\mathrm{\boldsymbol{C}OOCCH_2CH_2}$), 119.71 ($\mathrm{CCH{=}\boldsymbol{C}HCOOH}$), 105.18 (Ar), 56.14 ($\mathrm{CO\boldsymbol{C}H_3}$), 32.74 ($\mathrm{COOC\boldsymbol{C}H_2CH_2}$), 23.83 ($\mathrm{COOCCH_2\boldsymbol{C}H_2}$).

Poly(ester-amide) synthesis. *General polymerization procedure*. The desired diacid dimer (1 eq) was weighed and added to a round bottom flask. Thionyl chloride (20 eq) was added to the flask along with a drop of DMF, and the reaction was heated to reflux for 6 hours. Volatiles were removed under vacuum to yield the diacid chloride dimer. The desired diamine (3 eq) was weighed and added to a 100 mL beaker along with 15 mL of 0.5 M NaOH and a stir bar. The isolated diacid chloride dimer was dissolved in 15 mL of distilled dichloromethane and added quickly to the rapidly stirring diamine solution. A solid precipitate formed immediately and the resulting slurry was allowed to stir for two minutes. The slurry was transferred to an Eppendorf tube and centrifuged at 4.4×10^3 rpm for 20 minutes. The biphasic solution was decanted from the Eppendorf tube and the residual solid was washed with water (2×15 mL). After each washing, the slurry (water & polymer) was centrifuged at 4.4×10^3 rpm for 10 minutes. The resulting solid was dried under reduced pressure to yield the corresponding polymer as a pale yellow solid. The resulting polymers were insoluble to common solvents and sparingly soluble in DMF. Characterization data for each poly(ester-amide) can be found in Appendix A.

2.5 Appendix A

Figure S1: ^1H spectrum of **2c**

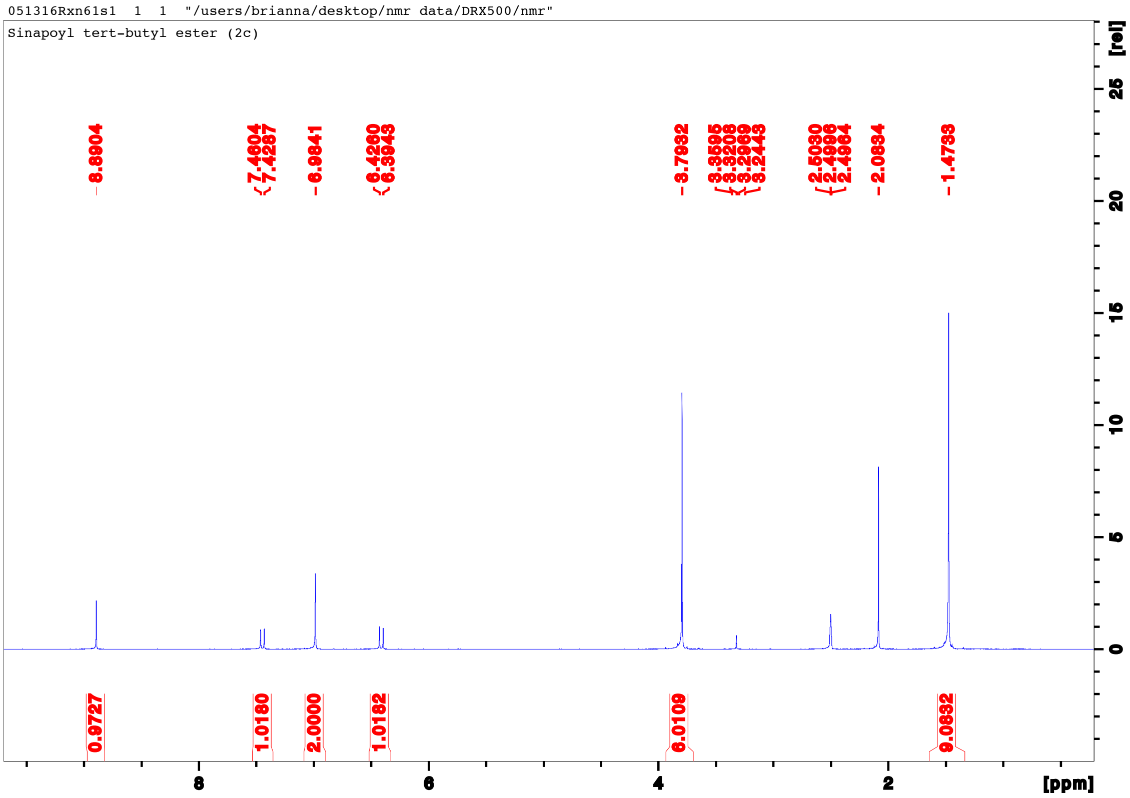

Figure S2: ^{13}C spectrum of **2c**

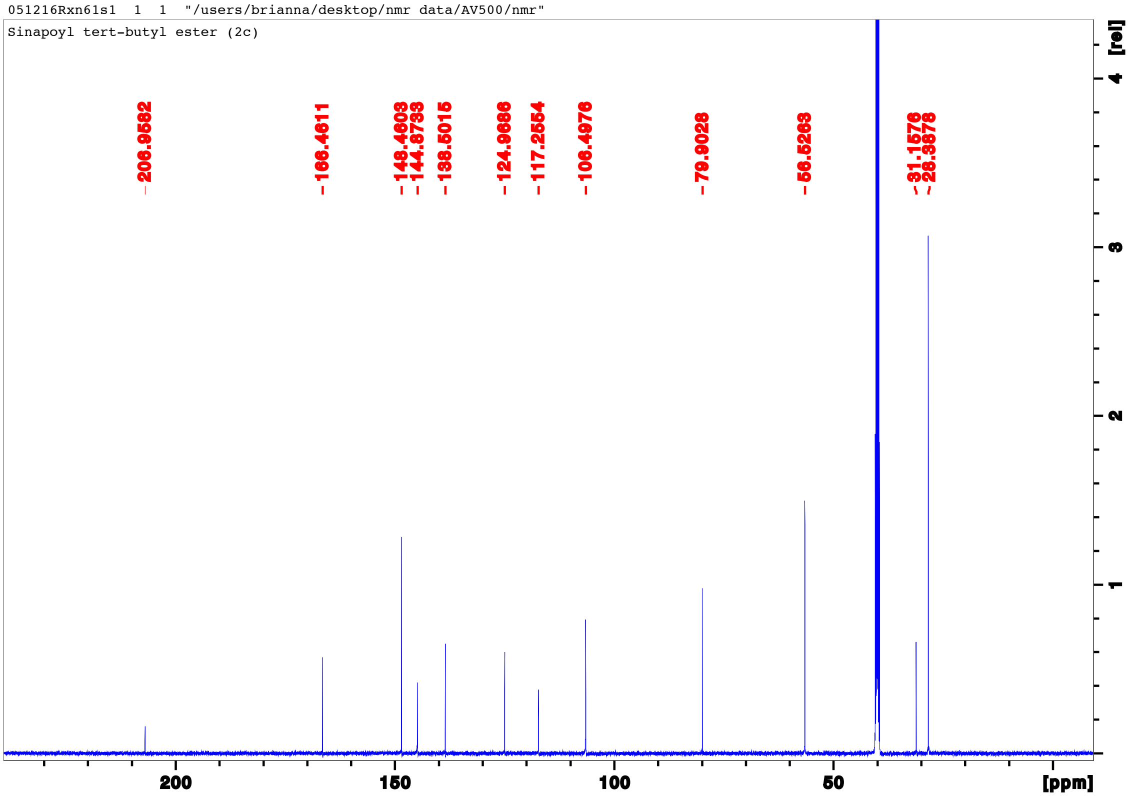

Figure S3: ^{1}H spectrum of **3c**

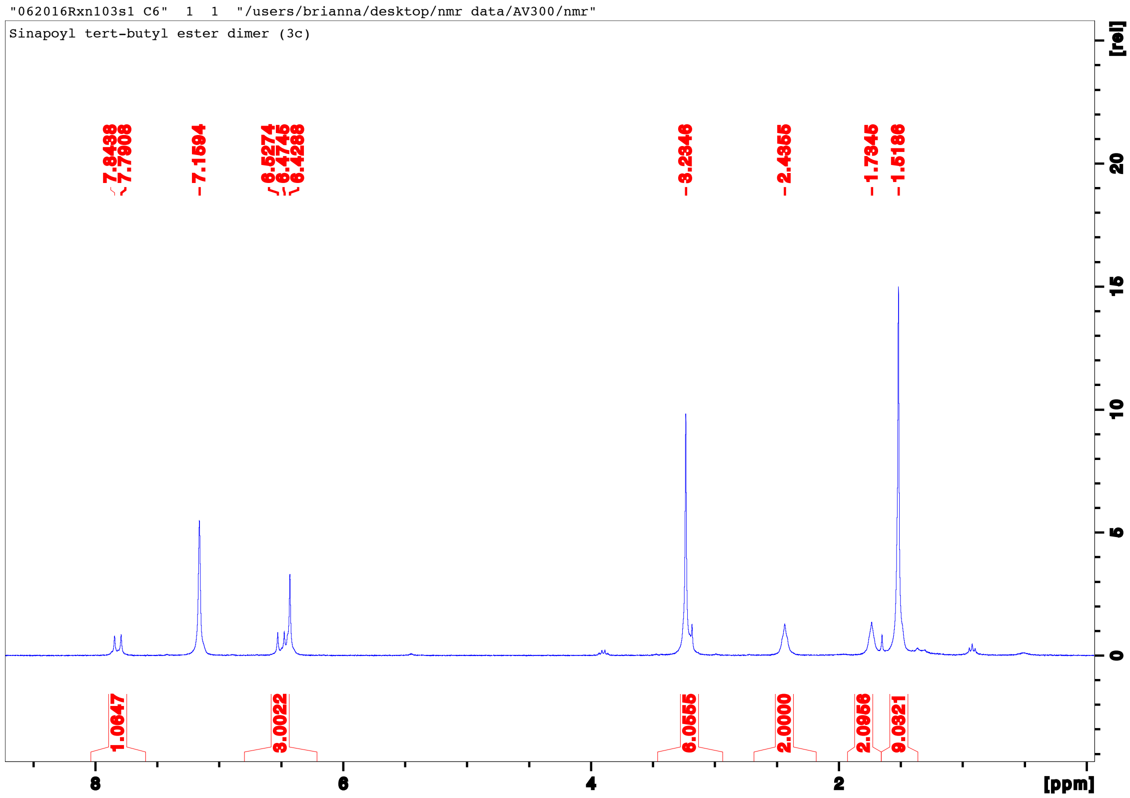

Figure S4: ^{13}C spectrum of **3c**

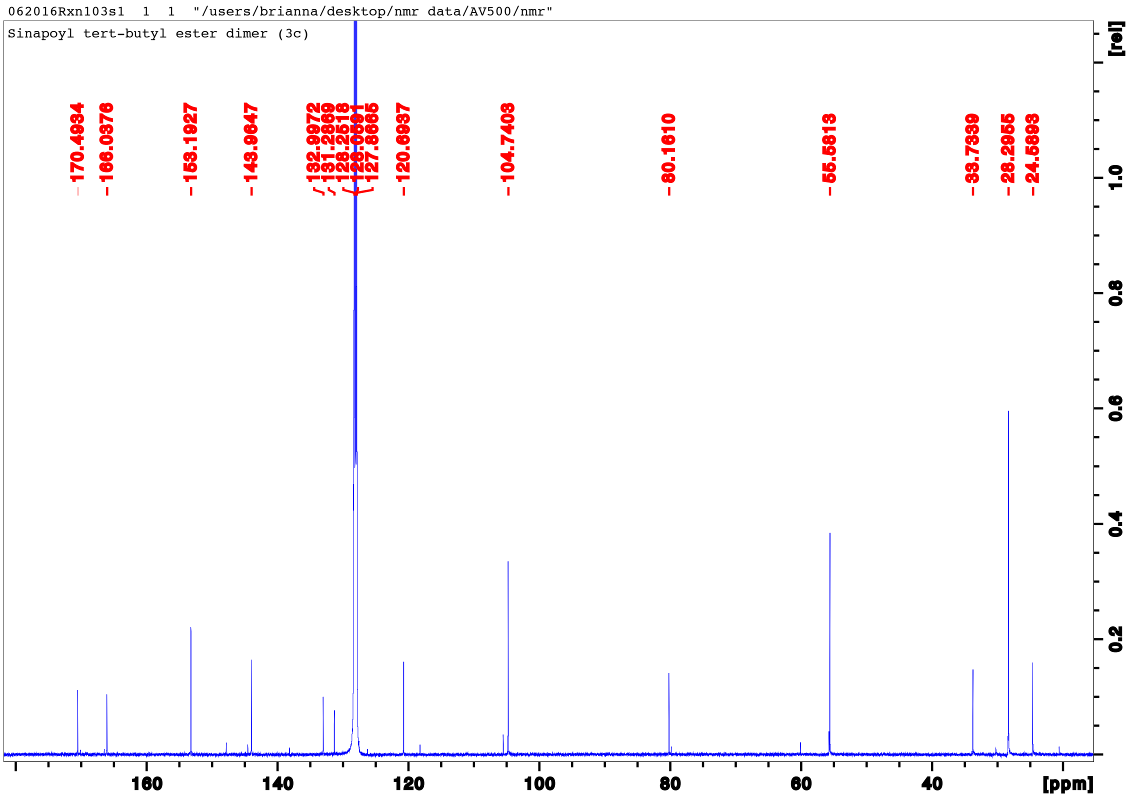

Figure S5: ^{1}H spectrum of **4c**

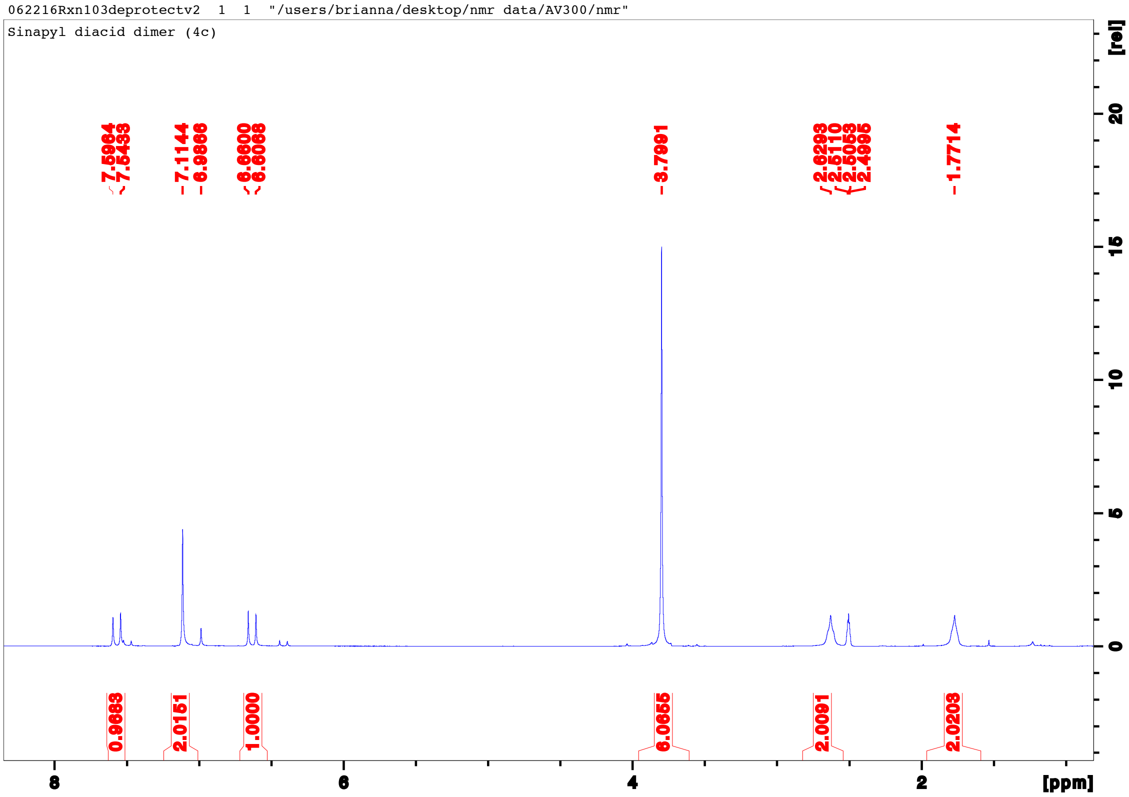

Figure S6: ^{13}C spectrum of **4c**

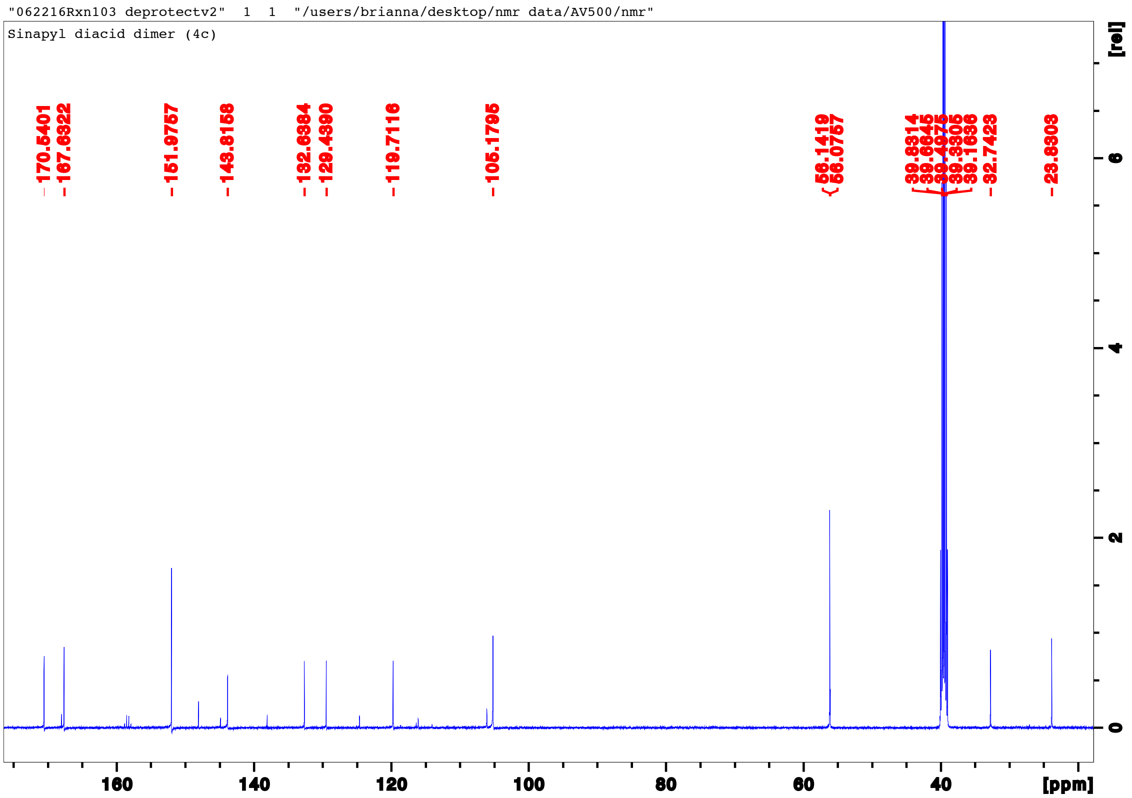

Polymer Characterization

p-Coumaryl diacid + ethylenediamine (**P1**). Yield 0.4002 g, 70.3%

p-Coumaryl diacid + 1,4-diaminobutane (**P2**). Yield 0.4773 g, 94.1%

p-Coumaryl diacid + 1,6-diaminohexane (**P3**). Yield 0.3493 g, 62.7%

p-Coumaryl diacid + 1,8-diaminooctane (**P4**). Yield 0.4023 g, 64.4%

p-Coumaryl diacid + 1,10-diaminodecane (**P5**). Yield 0.4614 g, 62.1%

p-Coumaryl diacid + *m*-phenylenediamine (**P6**). Yield 0.4384 g, 89.4%

p-Coumaryl diacid + *p*-phenylenediamine (**P7**). Yield 0.4564 g, 89.0%

Ferulic diacid + ethylenediamine (**P8**). Yield 0.4056 g, 83.6%

Ferulic diacid + 1,4-diaminobutane (**P9**). Yield 0.4298 g, 93.5%

Ferulic diacid + 1,6-diaminohexane (**P10**). Yield 0.3942 g, 87.1%

Ferulic diacid + 1,8-diaminooctane (**P11**). Yield 0.1054 g, 19.5%

Ferulic diacid + 1,10-diaminodecane (**P12**). Yield 0.2439 g, 55.8%

Ferulic diacid + *m*-phenylenediamine (**P13**). Yield 0.1056 g, 83.2%

Ferulic diacid + *p*-phenylenediamine (**P14**). Yield 0.4092 g, 59.7%

Sinapyl diacid + ethylenediamine (**P15**). Yield 0.3115 g, 67.0%

Sinapyl diacid + 1,4-diaminobutane (**P16**). Yield 0.3168 g, 66.9%

Sinapyl diacid + 1,6-diaminohexane (**P17**). Yield 0.4091 g, 56.1%

Sinapyl diacid + 1,8-diaminooctane (**P18**). Yield 0.5345 g, 85.0%

Sinapyl diacid + 1,10-diaminodecane (**P19**). Yield 0.1078 g, 98.8%

Sinapyl diacid + *m*-phenylenediamine (**P20**). Yield 0.4377 g, 70.9%

Sinapyl diacid + *p*-phenylenediamine (**P21**). Yield 0.5810 g, 83.9%

Infrared (IR) spectroscopy

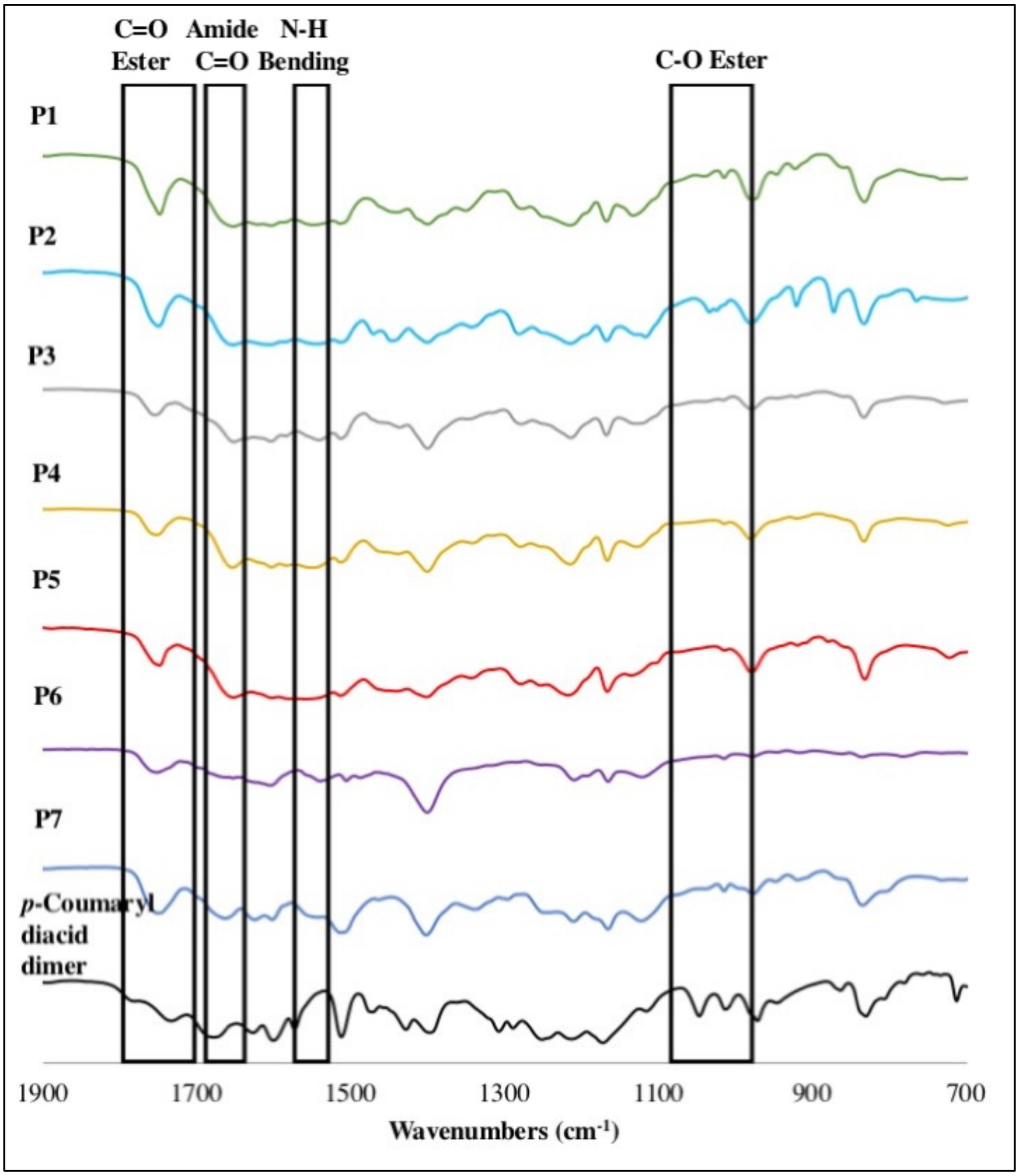

Figure S7: IR fingerprint region of *p*-Coumaryl-based poly(ester-amide)s (**P1-P7**)

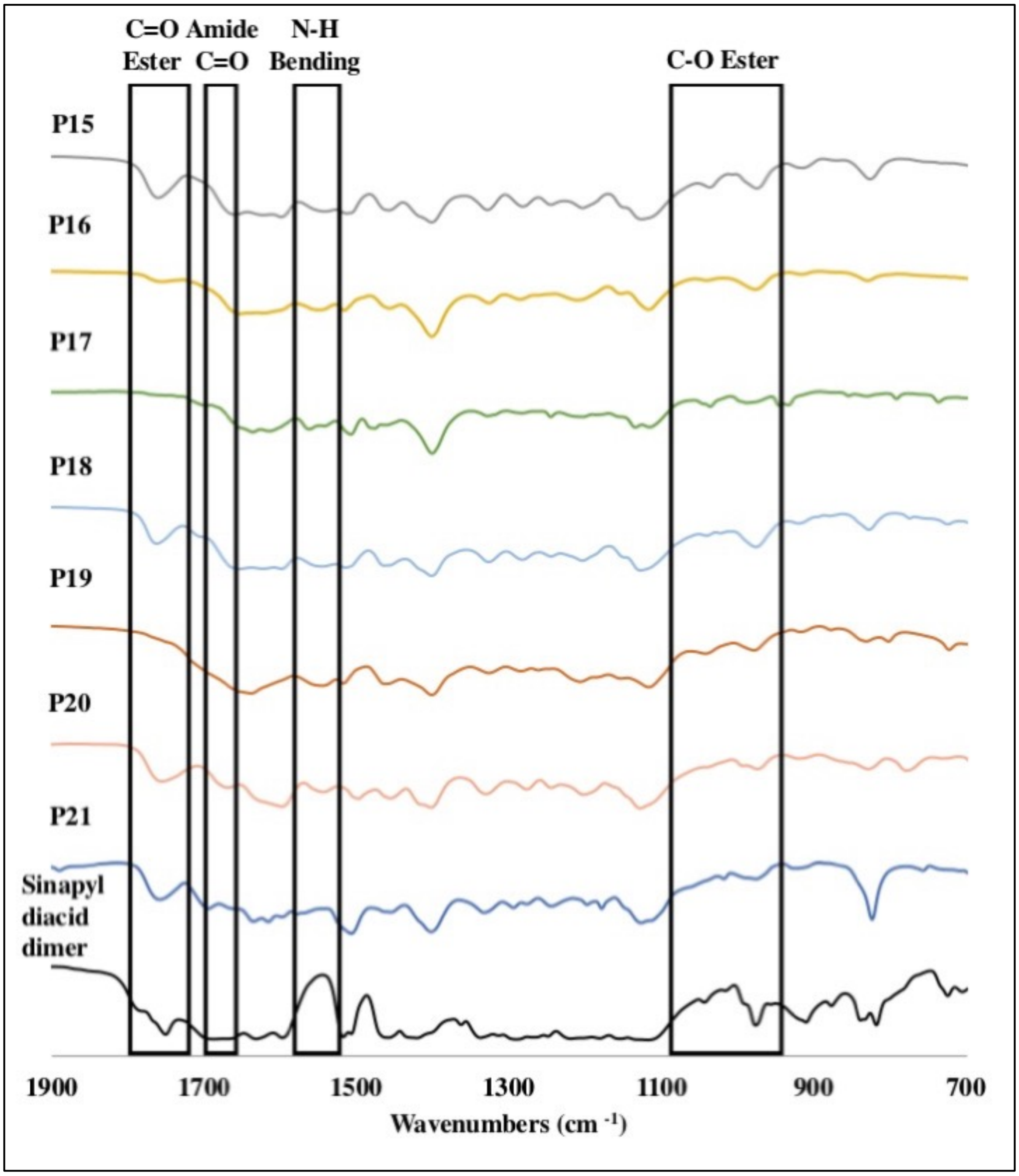

Figure S8: IR fingerprint region of Sinapyl-based poly(ester-amide)s (**P15-P21**)

Gel Permeation Chromatography (GPC)

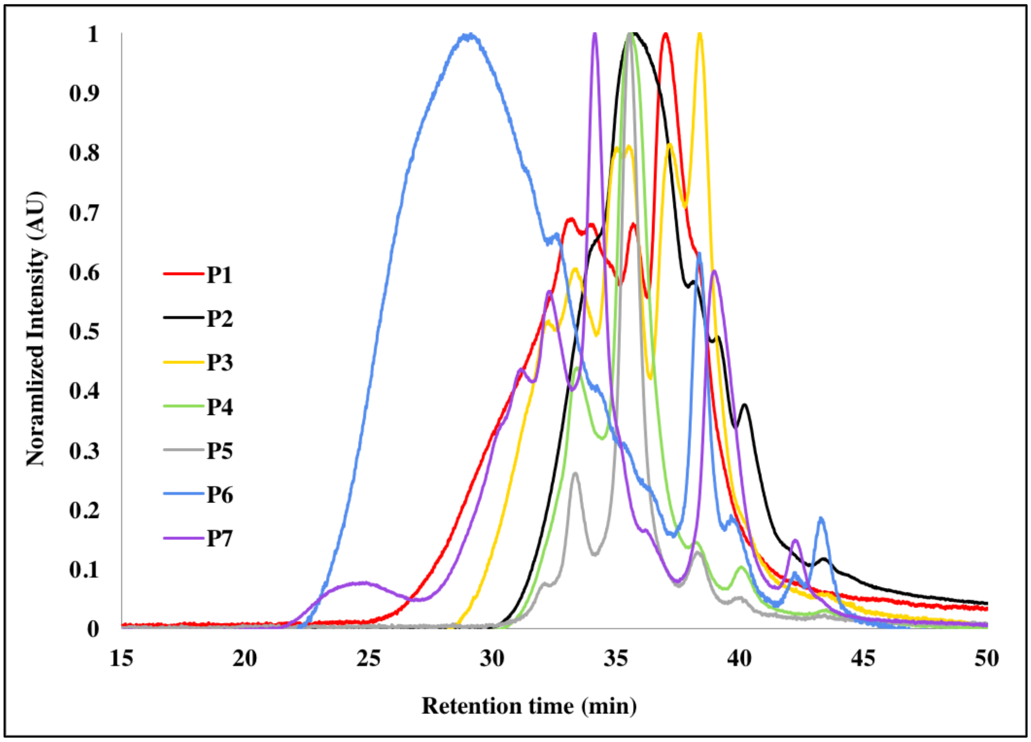

Figure S9: Stacked GPC traces of *p*-Coumaryl-based poly(ester-amide)s (**P1-P7**)

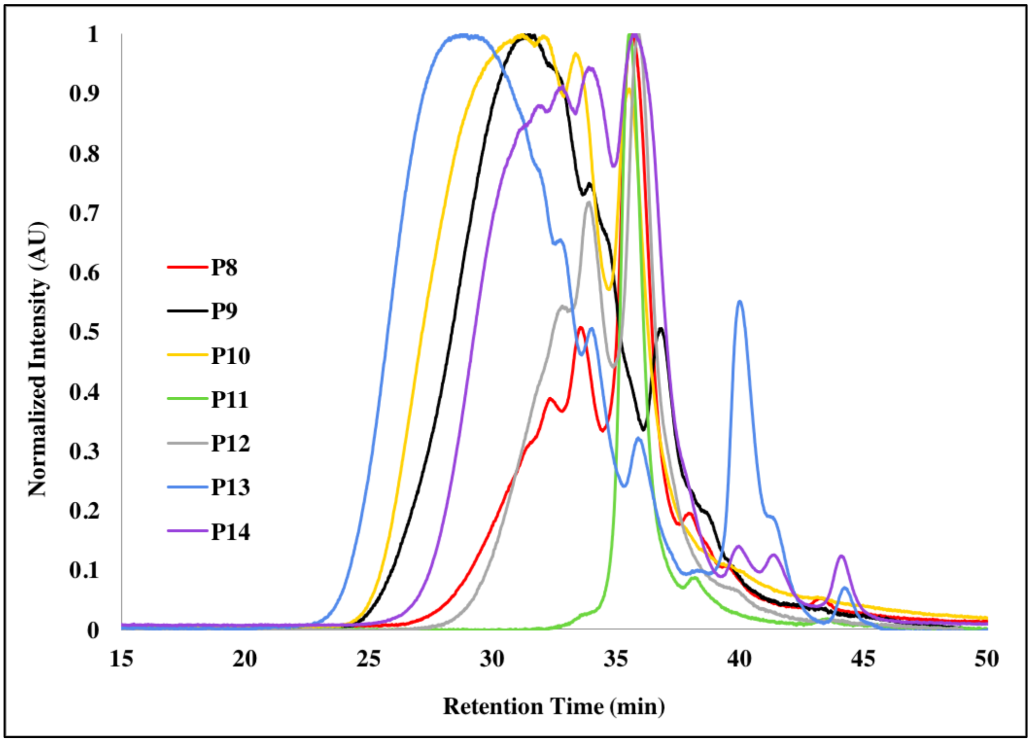

Figure S10: Stacked GPC traces of Ferulyl-based poly(ester-amide)s (**P8-P14**)

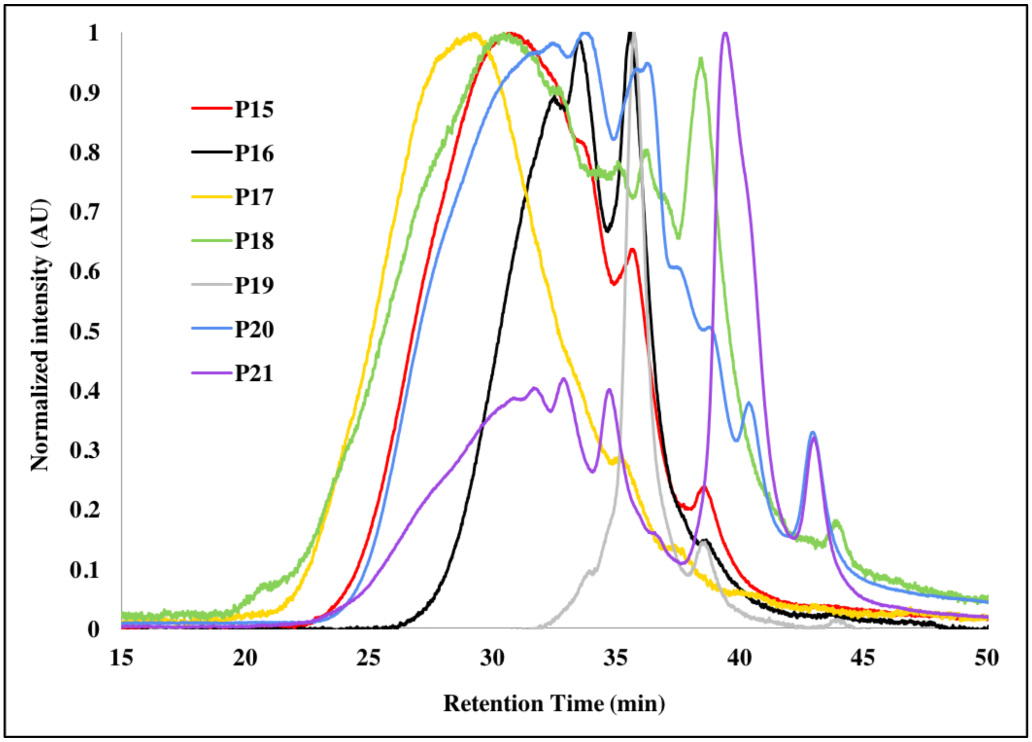

Figure S11: Stacked GPC traces of Sinapyl-based poly(ester-amide)s (**P15-P21**)

Differential Scanning Calorimetry (DSC)

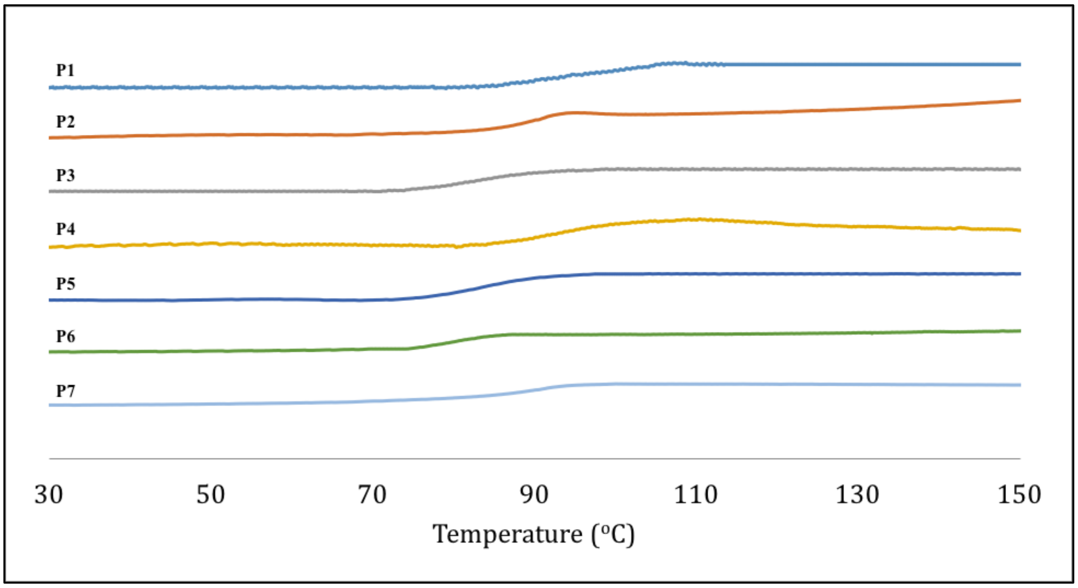

Figure S12: Stacked DSC traces of *p*-Coumaryl-based poly(ester-amide)s (**P1-P7**)

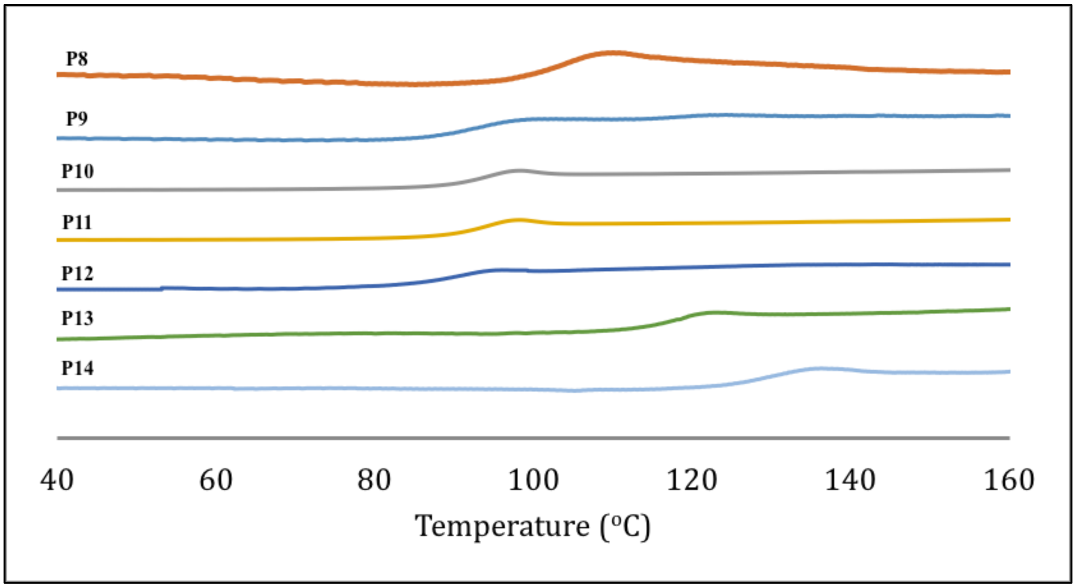

Figure S13: Stacked DSC traces of Ferulyl-based poly(ester-amide)s (**P8-P14**)

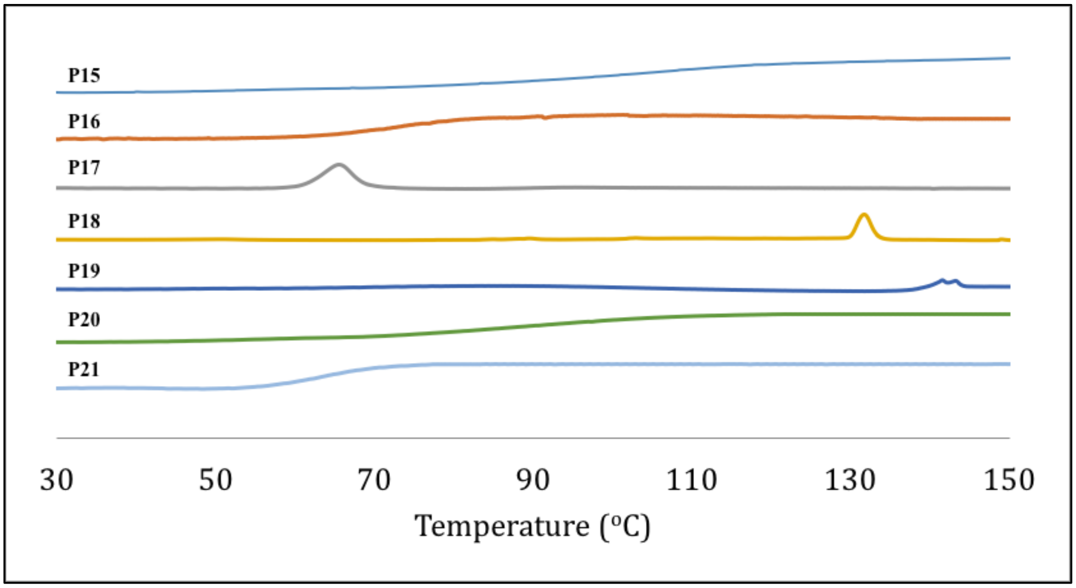

Figure S14: Stacked DSC traces of Sinapyl-based poly(ester-amide)s (**P15-P21**)

Thermogravimetric Analysis (TGA)

Figure S15: Stacked TGA traces of *p*-Coumaryl-based poly(ester-amide)s (**P1-P7**)

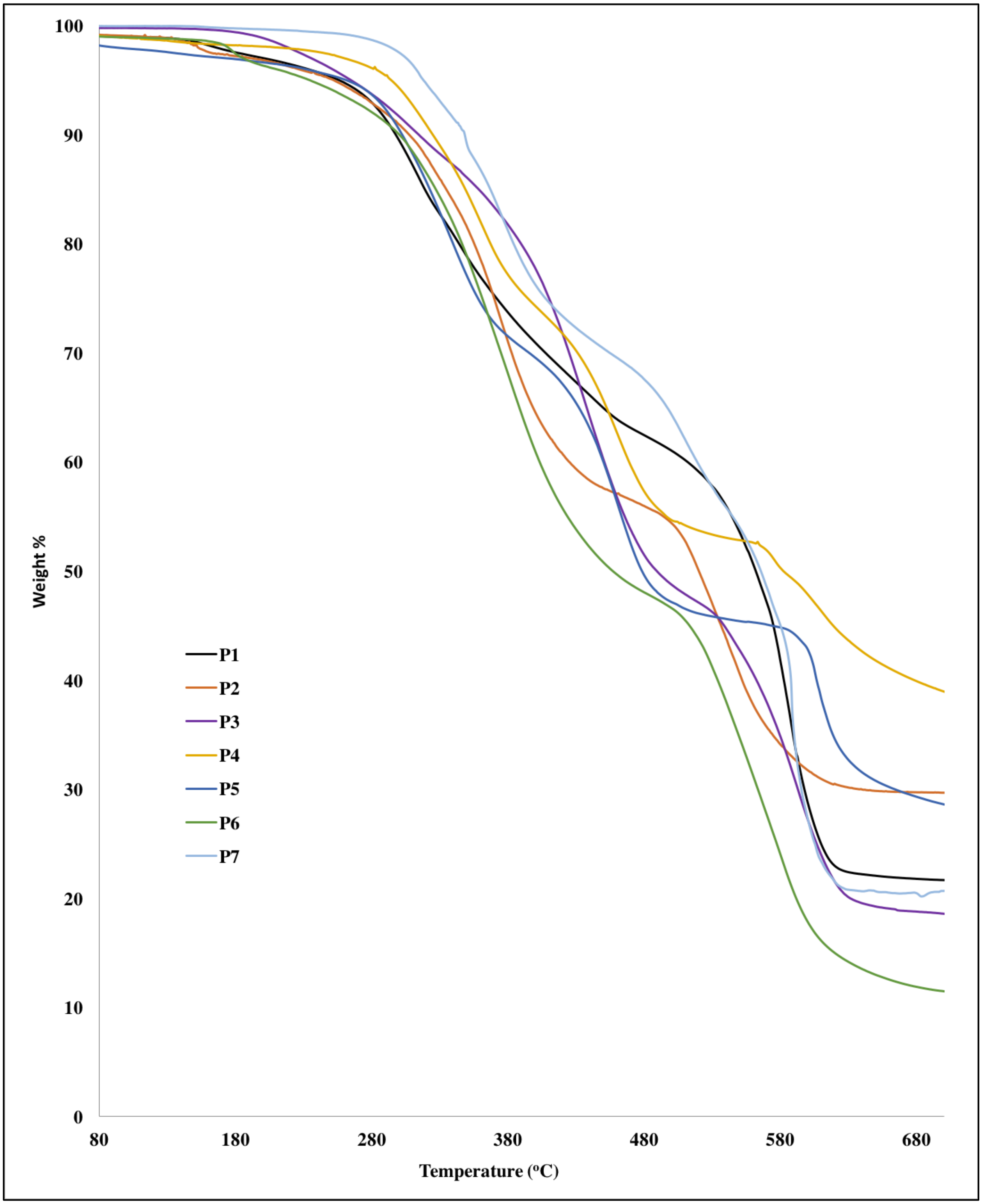

Figure S16: Stacked TGA traces of Ferulyl-based poly(ester-amide)s (**P8-P14**)

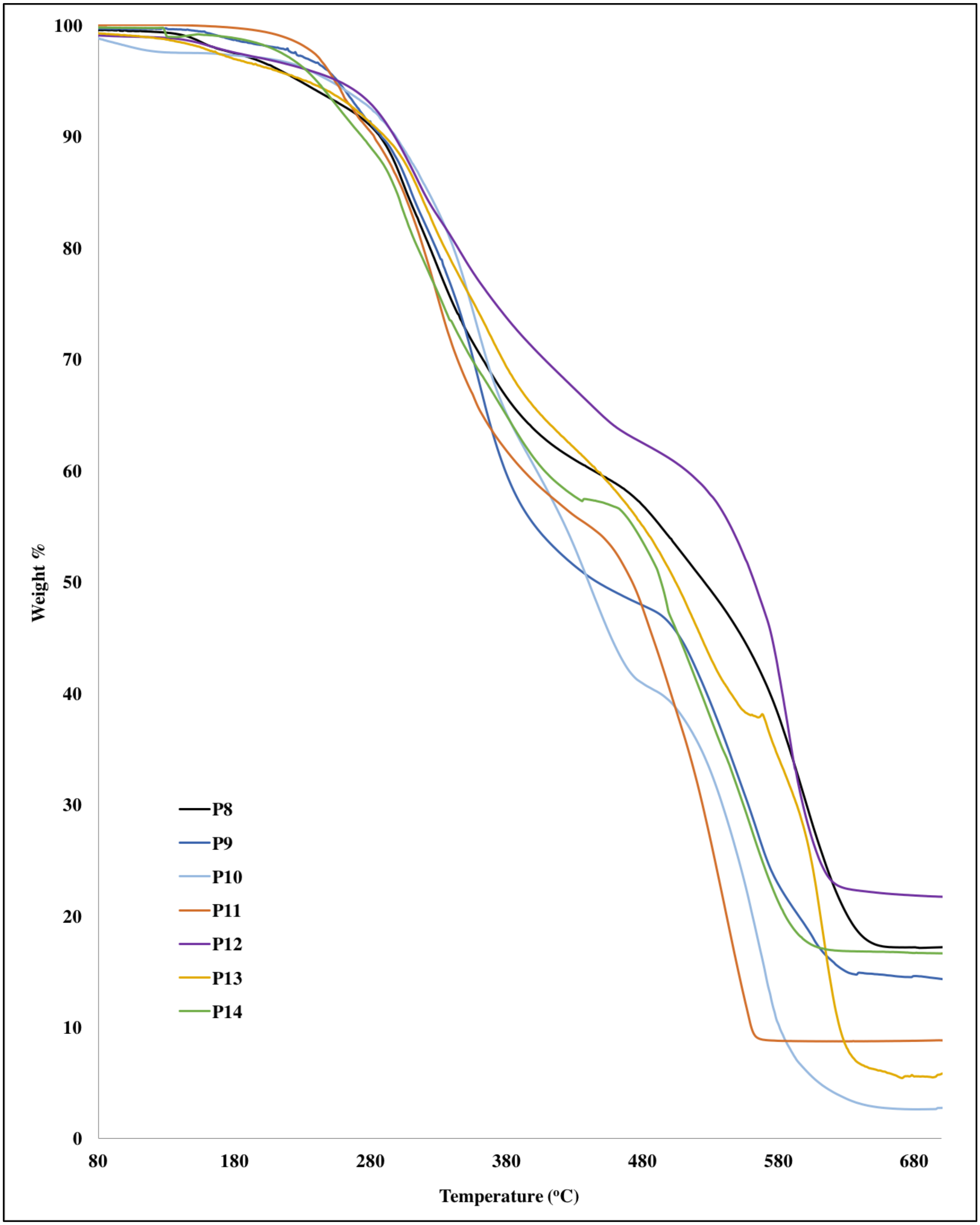

Figure S17: Stacked TGA traces of Sinapyl-based poly(ester-amide)s (**P15-P21**)

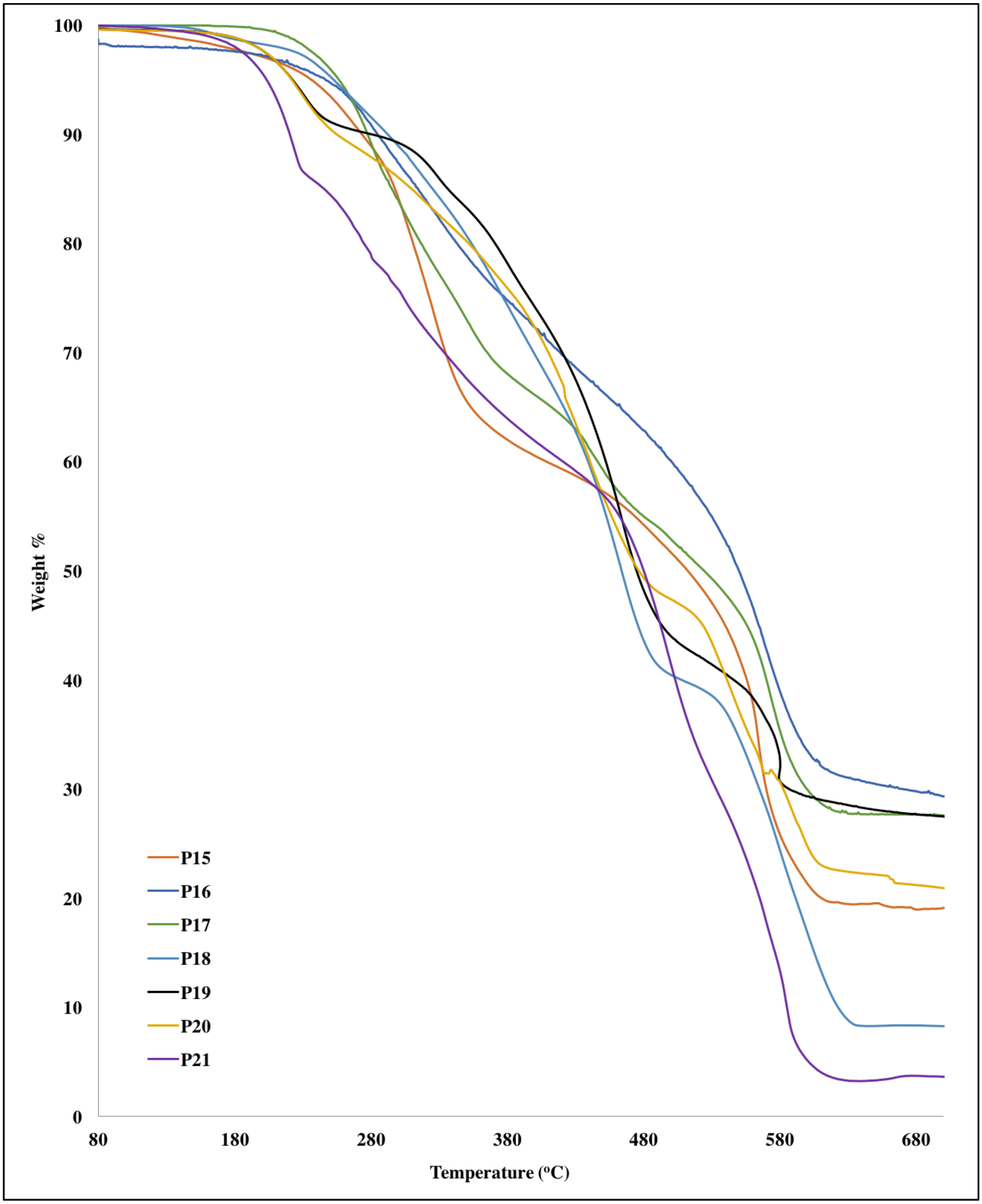

Decomposition Studies

Method

Polymer samples (10-20 mg) were weighed and added to 20 mL scintillation vials (two vials were prepared for each polymer sample). An aliquot of either pH 5.00 sodium acetate (0.5 M) buffer or pH 7.04 DI water was added to each vial (one solution of each for each polymer) to reach a concentration of 10 mg/mL. A small stir bar was added to each vial, the vials were capped, and the resulting suspensions were allowed to stir for 30 days. 0.1 mL aliquots of solution were taken on Day 7, 14, and 30 and stored in a -80 ^{o}C freezer until analysis via gel permeation chromatography (GPC). Samples were diluted to a final volume of 1.0 mL with 10 mM LiBr in *N,N*-dimethylformamide (DMF) and were passed through a 0.20 μm PTFE filter before injection. GPC for all polymers was conducted on a Jasco system equipped with a refractive index detector, a UV detector, a Waters Styragel guard column, and four Waters HR Styragel 5 μm columns (100-5K, 500-30K, 50-100K, 5-600 K) using 10 mM LiBr in *N,N*-dimethylformamide (DMF) at 40 °C and a flow rate of 1.0 mL min^{-1}. Calibration was performed using nine near-monodisperse polystyrene standards (M_n=1,250 to 549,000 Da)from Jordi Laboratories and chromatograms were analyzed using ChromNAV chromatography software. Due to the low sample concentration in each aliquot, raw GPC traces were smoothed using a median filter (n=15) and normalized in Microsoft Excel to minimize noise due to the absorptivity of DMF.

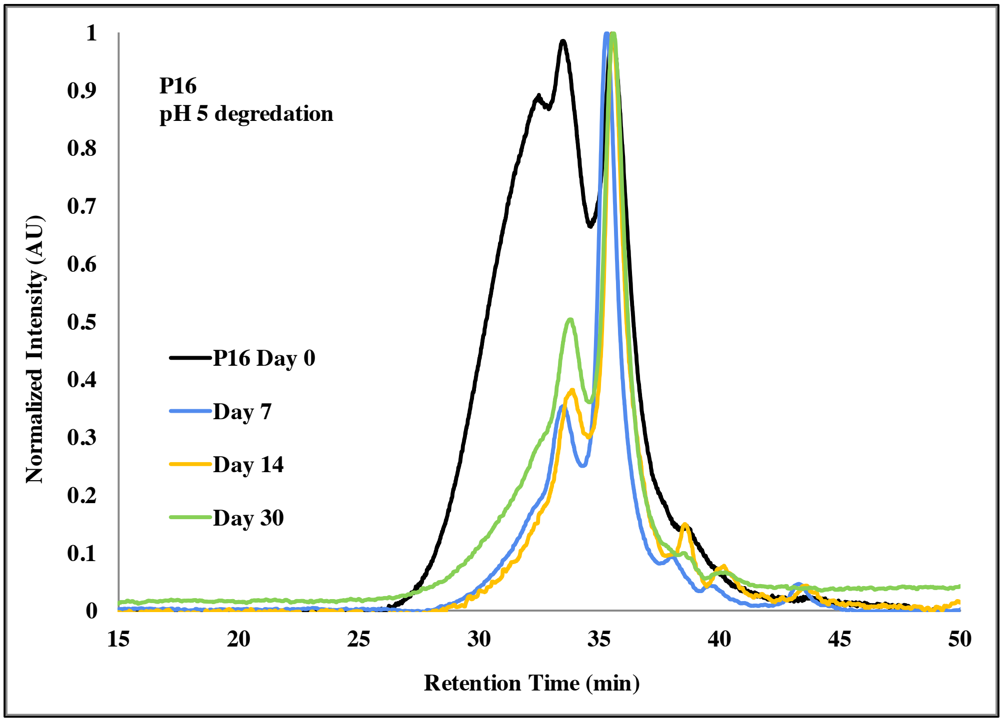

Figure S18: Stacked GPC traces of decomposition of P16 in pH 5.00 sodium acetate buffer

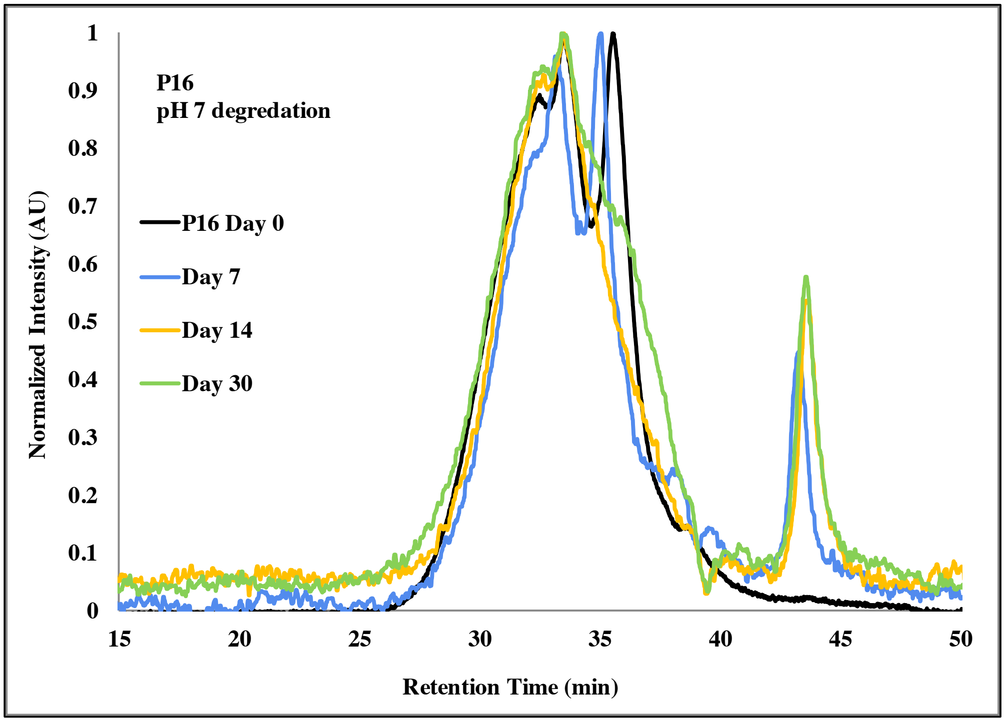

Figure S19: Stacked GPC traces of decomposition of P16 in pH 7.04 water

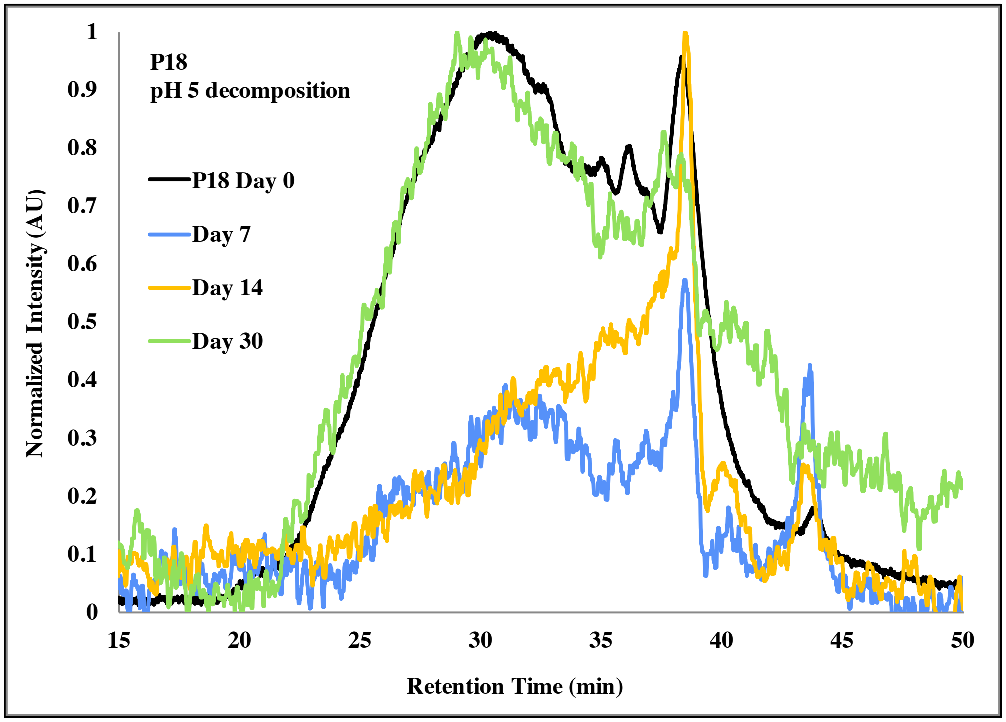

Figure S20: Stacked GPC traces of decomposition of P18 in pH 5.00 sodium acetate buffer

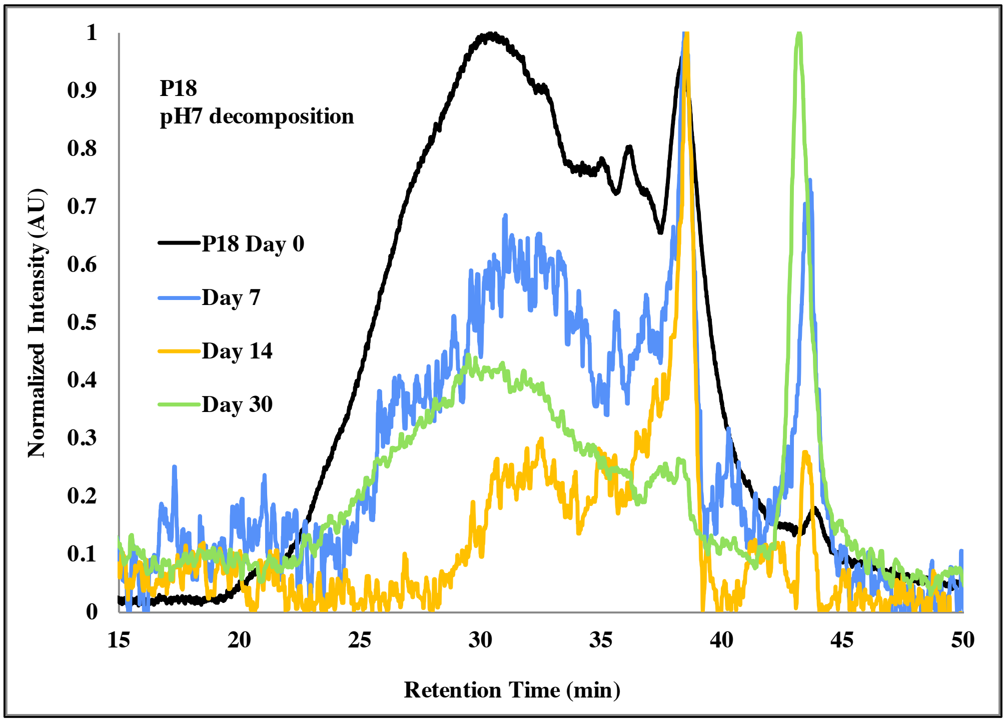

Figure S21: Stacked GPC traces of decomposition of P18 in pH 7.04 water

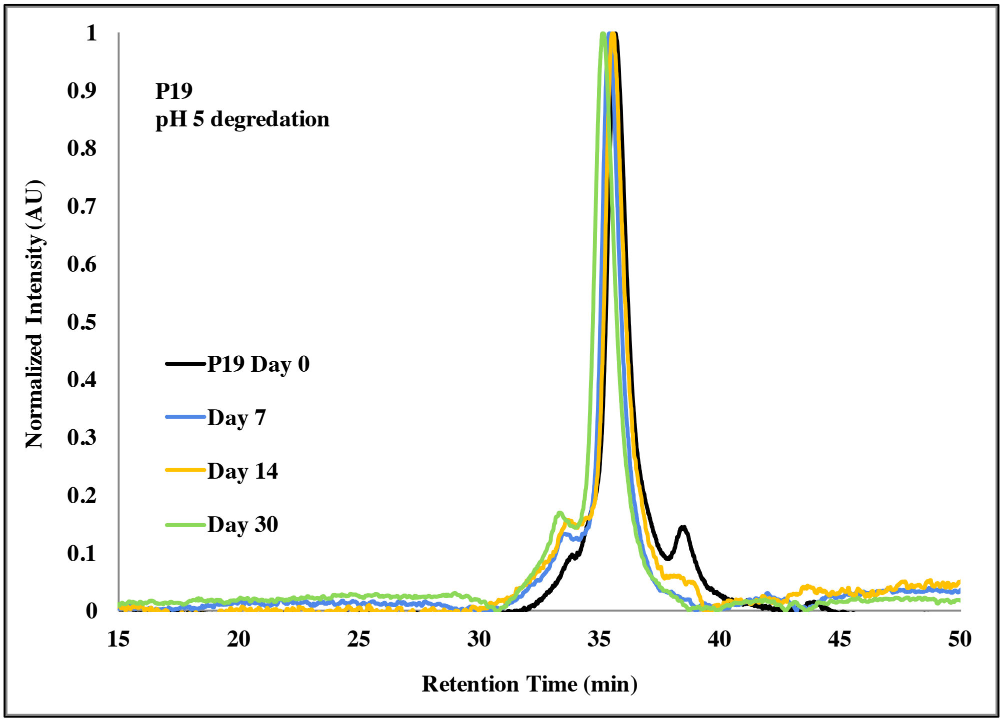

Figure S22: Stacked GPC traces of decomposition of P19 in pH 5.00 sodium acetate buffer

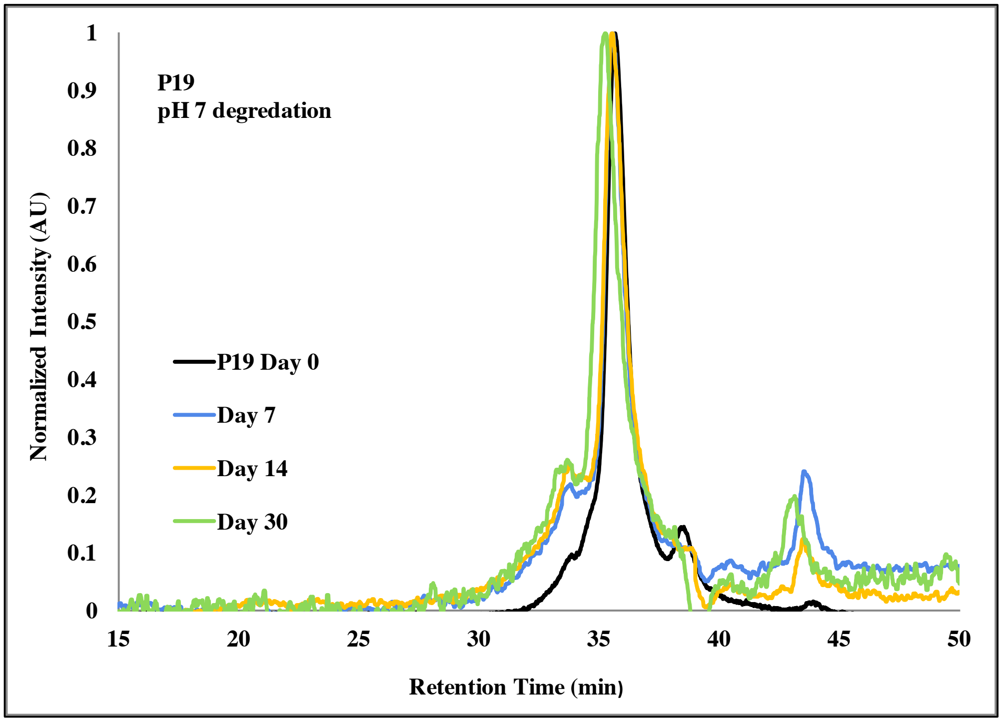

Figure S23: Stacked GPC traces of decomposition of P19 in pH 7.04 water

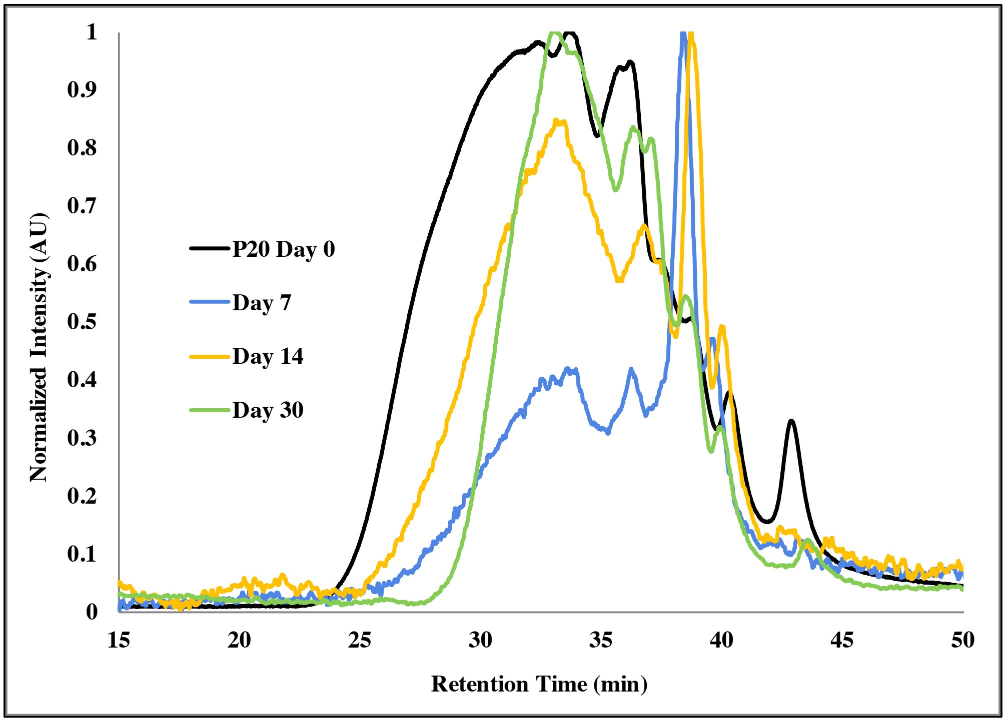

Figure S24: Stacked GPC traces of decomposition of P20 in pH 5.00 sodium acetate buffer

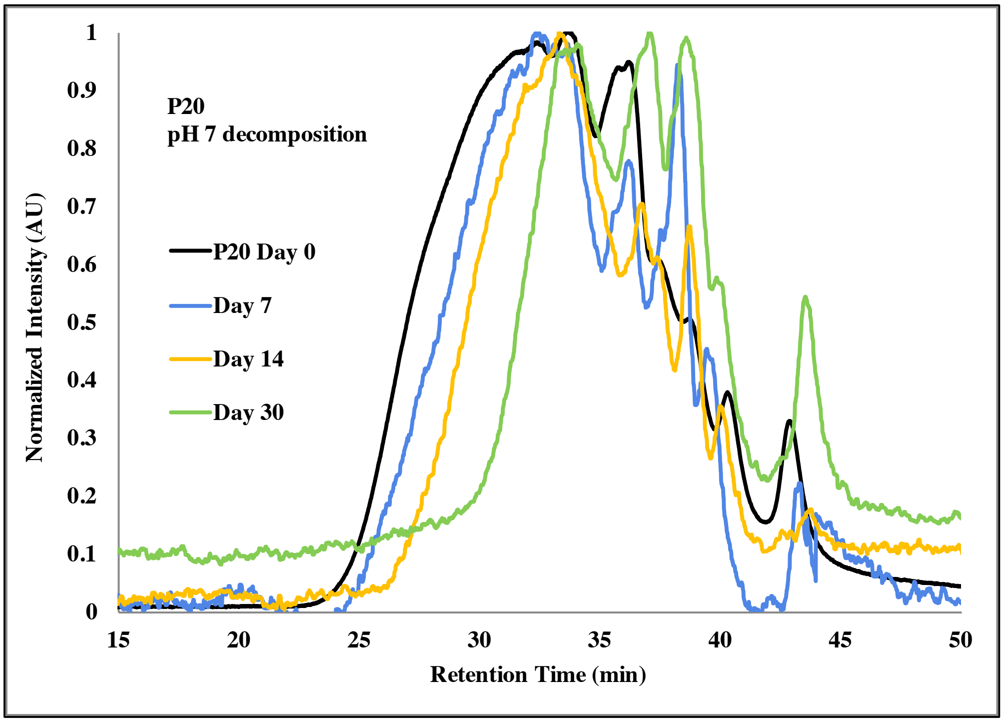

Figure S25: Stacked GPC traces of decomposition of P20 in pH 7.04 water

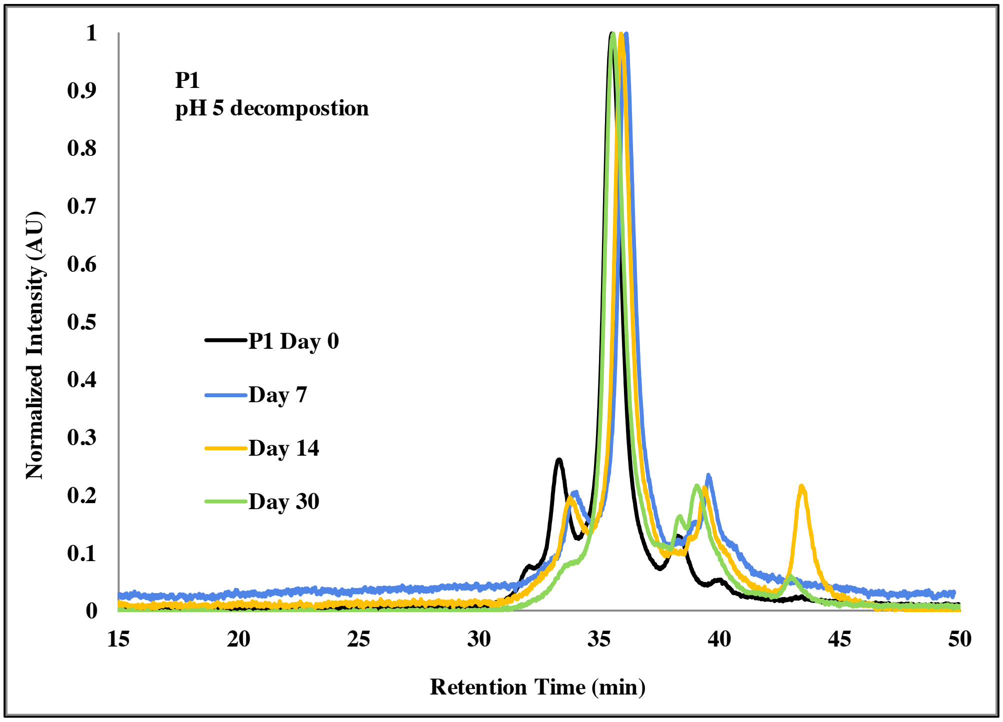

Figure S26: Stacked GPC traces of decomposition of P1 in pH 5.00 sodium acetate buffer

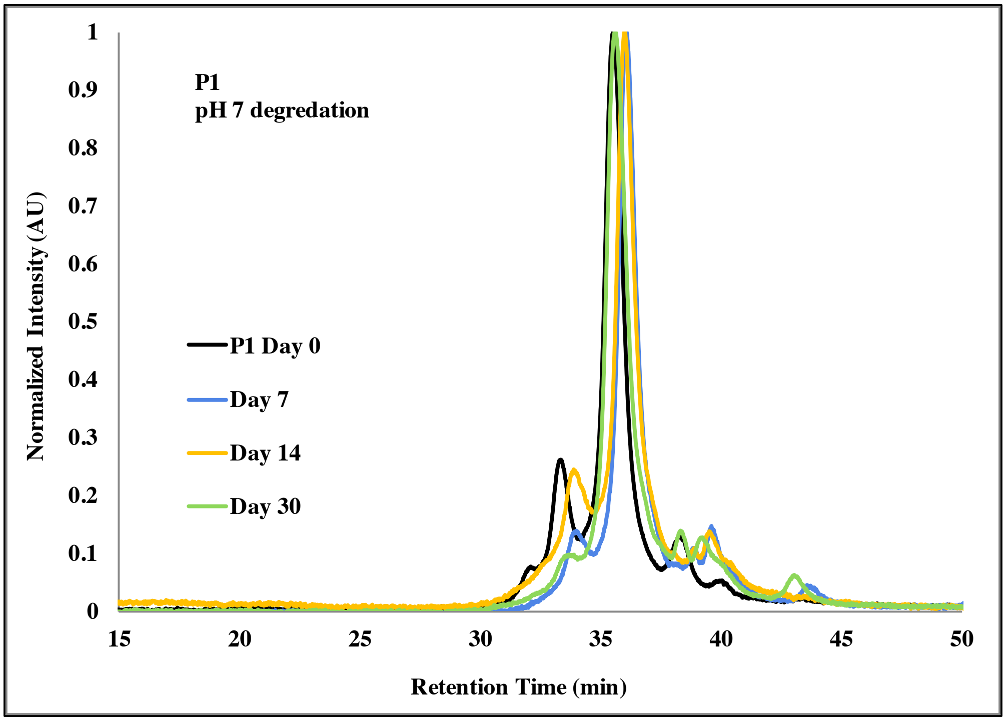

Figure S27: Stacked GPC traces of decomposition of P1 in pH 7.04 water

2.6 References

(1) Holladay, J. E.; White, J. F.; Bozell, J. J.; Johnson, D.; Energy, U. S. D. of. *Top Value-Added Chemicals from Biomass- Volume II—Results of Screening for Potential Candidates from Biorefinery Lignin*; Pacific Northwest National Laboratory: Richland, WA, 2007; Vol. 2.

(2) Kai, D.; Tan, M. J.; Chee, P. L.; Chua, Y. K.; Yap, Y. L.; Loh, X. J. *Green Chem.* **2016**, 1175.

(3) Lora, J. H.; Glasser, W. G. *J. Polym. Environ.* **2002**, *10* (1/2), 39.

(4) Thakur, V. K.; Thakur, M. K.; Raghavan, P.; Kessler, M. R. *ACS Sustain. Chem. Eng.* **2014**, *2*, 1072.

(5) Ten, E.; Vermerris, W. *J. Appl. Polym. Sci.* **2015**.

(6) Sen, S.; Patil, S.; Argyropoulos, D. S. *Green Chem.* **2015**.

(7) Lochab, B.; Shukla, S.; Varma, I. K. *RSC Adv.* **2014**, *4*, 21712.

(8) Farigrieve, S. *Degredation and Stabilization of Aromatic Polyesters*; iSmithers: Shropshire, United Kingdom, 2009.

(9) Müller, R.-J.; Kleeberg, I.; Deckwer, W.-D. *J. Biotechnol.* **2001**, *86* (2), 87.

(10) Fonseca, A. C.; Gil, M. H.; Simões, P. N. *Prog. Polym. Sci.* **2014**, *39* (7), 1291.

(11) Rodriguez-Galan, A.; Franco, L.; Puiggali, J. *Polymers (Basel).* **2010**, *3* (1), 65.

(12) Vert, M.; Feijen, J.; Albtersson, G.; Scott, G.; Chiellini, E. *Biodegradable polymers and*

plastics; The Royal Society of Chemistry: Whltshire, England, 1992.

(13) Murase, S. K.; Puiggali, J. In *Natural and Synthetic Biomedial Polymers*; Elsevier Inc., 2014; pp 145–166.

(14) Yonezawa, N.; Toda, F.; Hasegawa, M. *Die Makromol. Chemie, Rapid Commun.* **1985**, *6* (9), 607.

(15) Fey, T.; Keul, H.; Höcker, H. *Macromolecules* **2003**, *36* (11), 3882.

(16) Lebarbé, T.; Maisonneuve, L.; Nga Nguyen, T. H.; Gadenne, B.; Alfos, C.; Cramail, H. *Polym. Chem.* **2012**, *3* (10), 2842.

(17) Zuo, J.; Li, S.; Bouzidi, L.; Narine, S. S. *Polymer (Guildf).* **2011**, *52* (20), 4503.

(18) Triki, R.; Abid, M.; Tessier, M.; Abid, S.; El Gharbi, R.; Fradet, A. *Eur. Polym. J.* **2013**, *49* (7), 1852.

(19) Pinilla, I. M.; Martínez, M. B.; Galbis, J. A. *J. Polym. Sci. Part A Polym. Chem.* **2010**, *48* (21), 4711.

(20) Wang, R.; Ren, T.; Bai, Y.; Wang, Y.; Chen, J.; Zhang, L.; Zhao, X. *J. Appl. Polym. Sci.* **2016**, *133* (22), n/a.

(21) Isikgor, F. H.; Becer, C. R. *Polym. Chem.* **2015**, *6* (25), 4497.

(22) Tilley, T. G. *Ann. der Chemie und Pharm.* **1841**, *39* (2), 160.

(23) Brehmer, B. In *Bio-based plastics: Materials and applications*; Kabasci, S., Ed.; Wiley-

Interscience, 2013; pp 275–293.

(24) Mekonnen, T.; Mussone, P.; Khalil, H.; Bressler, D. *J. Mater. Chem. A* **2013**, *1* (43), 13379.

(25) Kuhire, S. S.; Avadhani, C. V.; Wadgaonkar, P. P. *Eur. Polym. J.* **2015**, *71*, 547.

(26) Pion, F.; Ducrot, P.-H.; Allais, F. *Macromol. Chem. Phys.* **2014**, *215*, 431.

(27) Oulame, M. Z.; Pion, F.; Allauddin, S.; Raju, K. V. S. N.; Ducrot, P.-H.; Allais, F. *Eur. Polym. J.* **2015**, *63*, 186.

(28) Ouimet, M. A.; Stebbins, N. D.; Uhrich, K. E. *Macromol. Rapid Commun.* **2013**, *34* (15), 1231.

(29) Ouimet, M. A.; Griffin, J.; Carbone-Howell, A. L.; Wu, W. H.; Stebbins, N. D.; Di, R.; Uhrich, K. E. *Biomacromolecules* **2013**, *14* (3), 854.

(30) Smith, A. M. R.; Rzepa, H. S.; White, A. J. P.; Billen, D.; Hii, K. K. *J. Org. Chem.* **2010**, *75* (9), 3085.

(31) Morgan, P. W.; Kwolek, S. L. *J. Chem. Educ.* **1959**, *36* (4), 182.

(32) Wittbecker, E. L.; Morgan, P. W. *J. Polym. Sci. Part A Polym. Chem.* **1996**, *34* (4), 521.

(33) Morgan, P. W. In *Condensation Polymers: By Interfacial and Solution Methods*; Interscience: New York, 1965; pp 65–115.

(34) Vera, M.; Almontassir, A.; Rodríguez-Galán, A.; Puiggalí, J. *Macromolecules* **2003**, *36*

(26), 9784.

(35) Vlachopoulos, J.; Strutt, D. *Mater. Sci. Technol.* **2003**, *19* (9), 1161.

(36) Wang, L.; Wang, Y.; Ren, L. *J. Appl. Polym. Sci.* **2008**, *109* (2), 1310.

(37) Chen, D.; Zachmann, H. G. *Polymer (Guildf).* **1991**, *32* (9), 1612.

(38) Rieger, J. *J. Therm. Anal.* **1996**, *46* (3-4), 965.

(39) Okada, M. *Prog. Polym. Sci.* **2002**, *27*, 87.

(40) Ouimet, M. A.; Faig, J. J.; Yu, W.; Uhrich, K. E. *Biomacromolecules* **2015**, *16* (9), 2911.

(41) Davidson, D.; Bernhard, S. A. *J. Am. Chem. Soc.* **1948**, *70* (10), 3426.

Chapter 3: Aromatic-aliphatic poly(ether-amides) from monolignol-based ether dimers

3.1 Introduction

The synthesis of bio-based polymers centers on the direct production of bio-polymers or bio-monomers from biological sources[1]. The demand for bio-based polymers has surged recently, due to declining petroleum reserves and an increased public awareness of the environmental issues surrounding the accumulation of petroleum-based plastic waste[2]. Commercial products produced from bio-based polymers are available, but generally feature weak thermo-mechanical properties in comparison to other commodity materials. Some bio-based materials exhibiting useful properties, similar to those of petroleum-based materials, have been produced but analogues of specialty polymers have yet to be developed. Specifically, few bio-based equivalents to commodity, aromatic polymers[3,4] have been produced, in stark contrast to the vast number of bio-based aliphatic polymeric materials available[5–7]. The difficulty in the production of these bio-based materials results from a lack of sources for biologically-derived aromatic monomers.

Lignin is the only naturally-occurring, aromatic polymer and is one of three components of lignocellulosic biomass. Unlike cellulose and hemicellulose, lignin is regularly isolated and discarded as a byproduct of several industrial processes. Polymerized in plant cell walls by the oxidative radical polymerization of *p*-hydroxycinnamyl alcohol monomers, lignin contains both ether and carbon-carbon linkages. Due to the uncontrolled polymerization method and functional groups present that are capable of chain transfer, the resulting polymeric structure is poorly defined and highly varying. In turn, the unpredictable polymeric structure makes utilizing lignin in polymers or composites difficult. However, as an aromatic polymer, lignin features commercially relevant properties, such as high strength and thermal stability[8–10]. While lignin itself is poorly defined, its monomers (monolignols) are well-defined, aromatic small molecules, making them ideal starting materials for polymer synthesis, without the difficulties associated with using lignin.

Modified monolignol-precursors have been used to synthesize polyesters[3,11,12], poly(ester-urethane)s[13,14], and poly(anhydride-ester)s.[15–17] Before incorporation, monolignols are commonly reduced to remove the unsaturation in their aliphatic side chain. A notable exception by Nguyen et al. features the comparison between polyesters with either modified or unmodified monolignols (Scheme 3.1)[18]. Copolymers from both monolignol variations were also synthesized. Retention of the double bond increased the glass transition temperature (T_g) of the resulting materials. T_g of polymers containing unsaturated monomers was higher due to the limited rotational freedom about the sp^2 carbon-carbon bonds. Additionally, when unmodified monolignols were incorporated into copolymers in desired ratios, the T_g could be tuned to match that of commodity materials.

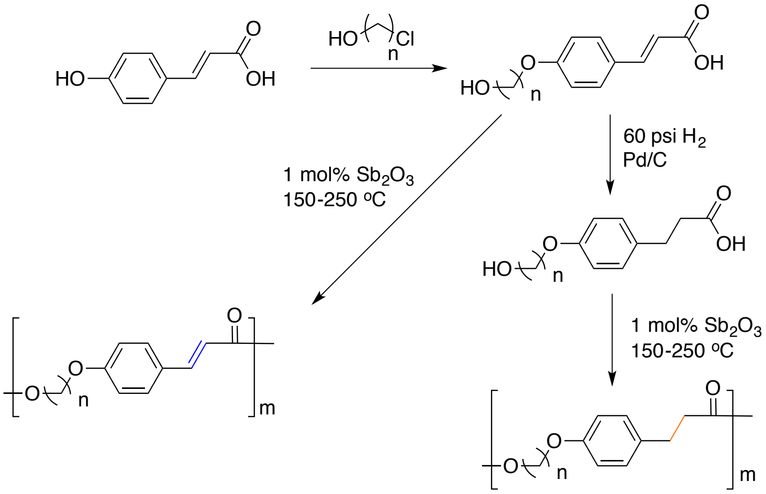

Scheme 3.1: Synthesis and characterization of polyesters containing modified and unmodified monolignols by Nguyen et al.[15]

Our group recently reported the synthesis and characterization of a series of monolignol-based poly(ester-amide)s as bio-based, biodegradable analogues to commodity aramids (**Figure 3.1**). The aromatic-aliphatic poly(ester-amide)s were insoluble in common

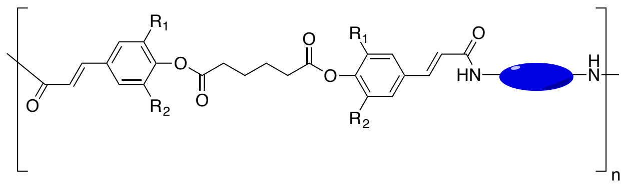

Figure 3.1: Previously synthesized and characterized monolignol-based poly(ester-amide)s

organic solvents, had moderate thermal stability, and were generally amorphous. Only three polymers in the series were crystalline, showing single melting temperatures on the second heating cycle in differential scanning calorimetry (DSC). The melting temperature of these polymers was between 70 and 140 °C , which is within temperatures typically used for thermal processing. When considered in addition to the thermal stability of these polymers, poly(ester-amide)s synthesized in that study offer promise for use in melt processing applications. While these polymers had useful physical properties, they were subject to degradation over an extended period of time, due to hydrolysis of the ester linkages. Depending on the targeted application, the degradation pathway could limit these materials to only short-term applications and create issues with shelf-life and/or storage. As an expansion of our previous work, we were interested in the synthesis and characterization of a series of poly(ether-amide)s from monolignols, replacing the ester linker in the dimer with an ether unit, to eliminate degradation, improve the observed thermal properties, and improve polymer solubility.

Poly(ether-amide)s are polymers that feature both ether and amide linkages in their backbone. The most common example of these types of polymers are block co-polymers featuring rigid polyamide segments and flexible polyether segments, yielding materials with highly tunable properties[19]. Depending on both the identity and equivalents of each segment used, the resulting material can be tailored for use in a diverse range of applications. Aliphatic-aromatic poly(ether-amide)s are of particular interest, as adding ether linkages, pendant groups, or flexible linkers are mechanisms frequently used to increase the solubility and lower the T_g of aromatic polyamides while maintaining their desirable thermal properties[20–24]. García et al. studied the thermal and physical properties of a series of aliphatic-aromatic poly(ether-amide)s by adding short polyethylene glycol (PEG) chains between aromatic diamines[25,26]. The resulting properties varied, but control over T_g and T_m was acheived by varying the length of the aliphatic spacer. Additionally, the use of different aromatic substitutions (para versus meta) was shown to affect both T_g and T_m. The use of meta-substituted linkers was shown to decrease the observed T_g due to reduced interchain interactions.

With this in mind, we synthesized a series of 21 poly(ether-amide)s from three monolignol-based carboxylic acid ether dimers and a series of seven aliphatic or aromatic diamines. While amide linkages are susceptible to hydrolysis over extended time scales, the degradation of these bonds is slow enough that amides are typically considered non-degradable in aqueous conditions. Additionally, the incorporation of an ether linkage into the monolignol dimer eliminates hydrolysis of the polymer backbone as a degradation mechanism, as ethers are only cleavable under harsh chemical conditions. β-O-4 ether linkages are the most common polymeric linkage found in native lignin (**Figure 3.2**). The high degree of incorporation of this chemically-resistant bond aids in the observed chemical and thermal robustness of lignin. We speculate that the incorporation of a structurally similar linkage into the poly(ether-amide) backbone, should impart additional durability to the isolated materials. We also hypothesized that the incorporation of an ether linkage would not only lower the T_g of

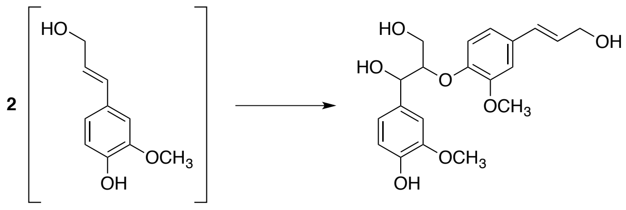

Figure 3.2: Dimerization of coniferyl alcohol leading to the formation of a β-O-4 linkage

the resulting materials with increased chain flexibility, but also improve polymer solubility by reducing interchain interactions.

3.2 Results and Discussion

Dimer synthesis. Based on our previous work synthesizing a series of monolignol-based poly(ester-amide)s, we sought to create a set of monolignol-based poly(ether-amide)s that would be resistant to hydrolysis, feature increased solubility in common organic solvents, and exhibit lower melting and glass transition temperatures while retaining thermal stability. Towards this goal, we envisioned the synthesis of a series of monolignol-based ether dimers and their polycondensation with a series of diamine linkers to yield the desired polymers. A series of three monolignol-based ether dimers were synthesized in three steps from the precursor aldehydes (1a, 1b, and 1c). As shown in **Scheme 3.2**, the tert-butyl protected esters (2a, 2b, and 2c) were synthesized in one step from a Doebner-modified Knoevenagel condensation with tert-butyl malonate and 4-hydroxybenzaldehyde, vanillin, or 3,5-dimethoxy-4-hydroxybenzaldehyde, respectively. While the yields for this condensation reaction were lower than expected, the yield increased with increasing methoxy substitution. While the electronic effects of aldehyde substitution are rarely

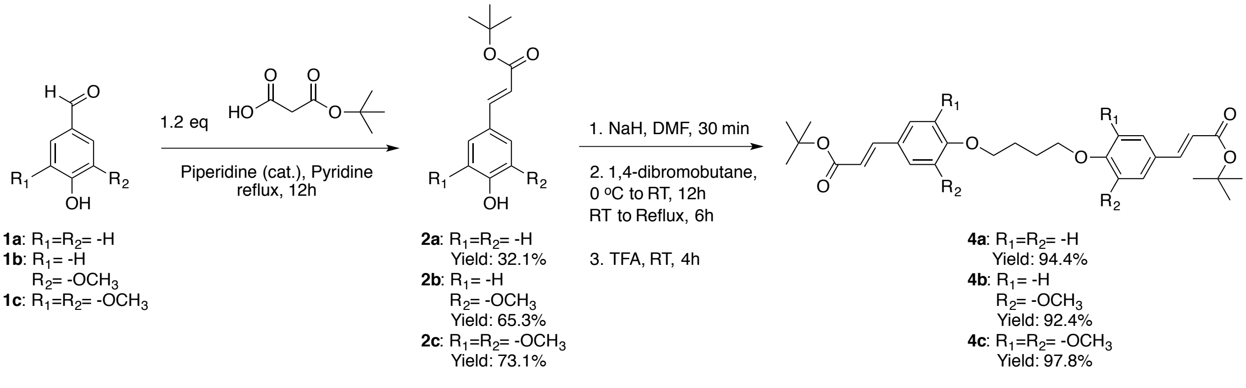

Scheme 3.2: Synthesis of monolignol-based ether dimers from precursor aldehydes 1a, 1b, and 1c

discussed for Knoevenagel condensation reactions, the inclusion of electron donating groups clearly affected the yield of the isolated enolates. The sodium salt of the protected ester monomers was synthesized with sodium hydride and then dimerized with 1,4-dibromobutane in *N,N*-dimethylformamide (DMF). The dimerization reaction did not proceed to completion at room temperature after 18 hours, so it was subsequently heated to reflux, in an attempt to increase conversion to the desired product. After heating to reflux for six hours, the reaction still did not reach full conversion, however increasing the reaction time led to the formation of undesired side products. Alternative methods (such as using a different base to deprotonate the protected ester monomers) were also attempted. These modifications increased the yield of side products (dimers with the addition of multiple ether linkers) rather than the desired ether dimer (**Scheme 3.3**). Despite the lack of full conversion, the desired ether dimers (3a, 3b, and 3c) were achieved in moderate yield (48.6% to 52.5%) after purification via column chromatography. Additionally, the unreacted tert-butyl ester monomers were also recovered via column chromatography, allowing their use in later reactions. The pure ether dimers were then deprotected using trifluroroacetic acid (TFA), to yield 4a, 4b, and 4c, in nearly quantitative yield. Similar to the previously synthesized ester analogues, a key structural property of these ether dimers is the retention of the degree of unsaturation in their aliphatic side chain. The retention of this functionality should increase the thermal

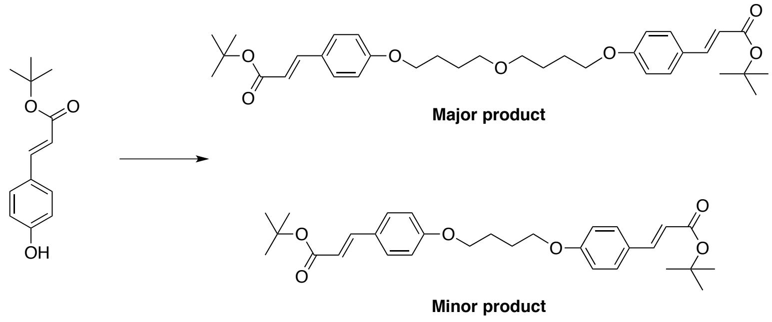

Scheme 3.3: Non-optimized reaction conditions led to the formation of side products over the desired ether dimer

stability and glass transition temperature of the resulting poly(ether-amide)s[18]. We hypothesize that the balance between the rigidity associated with carbon-carbon double bond and the flexibility associated with ether linkages should generate a series of materials with tunable physical properties.

Poly(ether-amide) synthesis. In the literature, poly(ether-amide)s are commonly aliphatic block co-polymers synthesized by condensation reactions of aliphatic polyether and polyamide segments. While aliphatic materials are useful, they typically feature low thermal stability and glass transition temperatures, due to high chain flexibility and minimal interchain interactions. In contrast to these materials, we were interested in isolating aromatic-aliphatic poly(ether-amide)s, as bio-based mimics to aramids, such as Kevlar or Nomex. We hypothesized utilizing monolignol-based dimers would yield polymers with physical strength similar to aramids, while utilizing aliphatic diamine linkers would increase the solubility and processability of the isolated polymers. Commercial aramids are typically produced via solution-phase methods, however due to difficulty identifying a common solvent, we utilized interfacial polymerization for poly(ether-amide) synthesis. Interfacial polymerization is an ideal polymerization technique as it does not require strict stoichiometric conditions, is less sensitive to impurities, requires short reaction times, and is commonly performed under mild reaction conditions[27]. Two immiscible monomer solutions, typically one aqueous and one non-aqueous, are prepared and carefully combined for polycondensation either by drawing a fiber from the interface, as utilized in the 'Nylon Rope Trick'[28], or as a precipitate from a vigorously stirring solution. Acid chloride hydrolysis is the largest limiting factor for this polymerization method, however due to the hydrophobic nature of the aromatic carboxylic acid ether dimer used, hydrolysis should be minimal. We initially attempted to draw fibers from the interface between the two solutions, but the poly(ether-amide)s produced were too brittle for isolation by this method. When polymers were allowed to form at the interface of the two solutions without stirring, the insolubility of the poly(ether-amide)s caused the resulting polymers to precipitate too rapidly to yield high molecular weight products. Due to these issues, we determined vigorous stirring was required during polycondensation to form high molecular weight poly(ether-amide)s[29], similar to what was required for synthesis of the poly(ester-amide)s presented in Chapter 2.

Three acid chloride ether dimers were generated *in situ* by refluxing the carboxylic acid ether dimer in thionyl chloride for six hours. After removal of excess thionyl chloride, the acid chloride dimers were then dissolved in distilled dichloromethane and added to a dilute sodium hydroxide solution containing the desired diamine (**Scheme 3.4**). The condensation polymerizations yielded twenty-one different aromatic-aliphatic poly(ether-amide)s. The resulting polymers were insoluble in most common organic solvents, but were

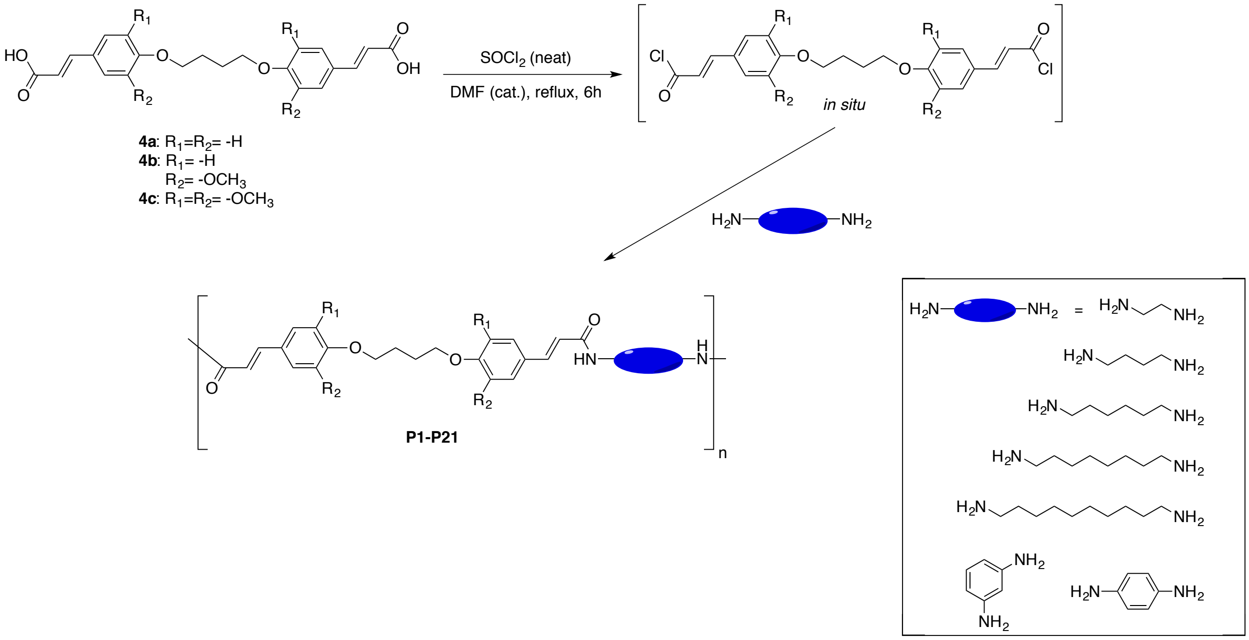

Scheme 3.4: Synthesis of poly(ether-amides) from monolignol-based ether dimers and diamine linkers via interfacial polymerization

sparingly soluble in DMF at room temperature. Poly(ether-amide)s from *p*-coumaryl acid and aliphatic diamines (P1-P5) featured exceedingly limited solubility in DMF, due to the lack of methoxy substitution. Even after soxhlet extraction in DMF for 24 hours, P1-P5 remained largely intractable. Due to poly(ether-amide) insolubility, polymerization was confirmed (P1-P21) using FT-IR spectroscopy. As seen in **Figure 3.3**, the C=O stretch in the ferulic acid carboxylic acid ether monomer shifted from ~1786 cm^{-1} to 1650-1660 cm^{-1} in P8-P14, confirming formation of the amide linkage. Additionally, N-H bending was seen from 1530-1560 cm^{-1} and C-O stretching was seen from 1033-968 cm^{-1}, confirming formation of amide bonds as well as the retention of the ether dimer throughout the polymerization reaction. Similar stretching frequencies can be seen in both the sinapyl and *p*-coumaryl-based polymers (Figures S1 & S2), confirming formation of the series of poly(ether-amide)s.

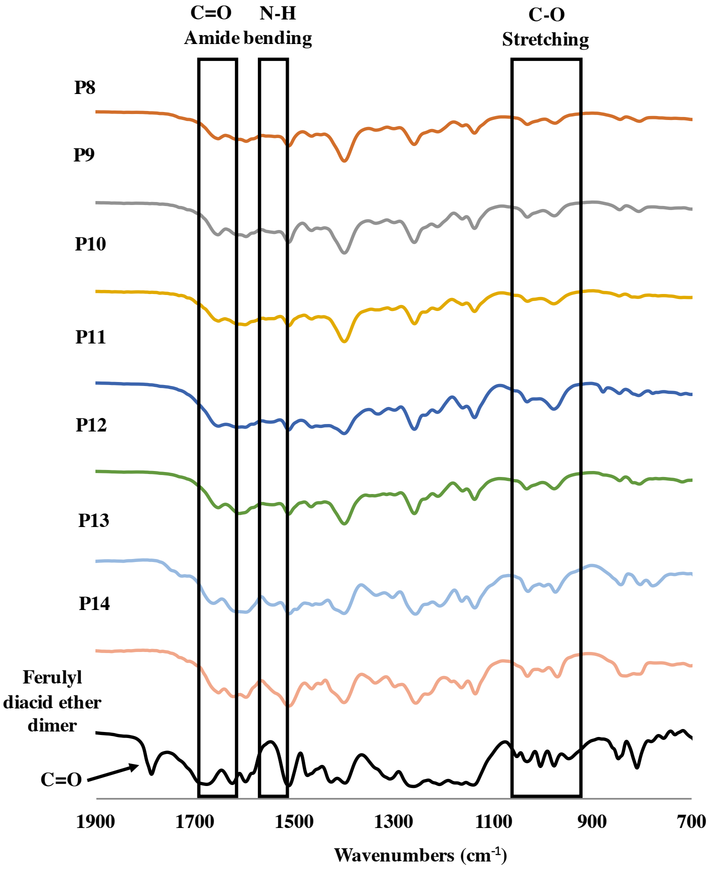

Figure 3.3: IR fingerprint region of P8-P14 and the corresponding ferulyl dimer starting material showing the formation of the amide linkage and presence of the ether linkage in the dimer.

Molecular weight characterization. The number and weight average molecular weights (M_n and M_w, respectively) of P1- P21 were determined using gel permeation

Table 3.1 Molecular weight characterization of poly(ether-amide)s by gel permeation chromatography

Polymer	Dimer	Diamine	M_n[a]	M_w[a]	Đ[b]
P1	*p*-Coumaryl	Ethylene diamine	3,700	5,060	1.37
			6,740[c]	11,020[c]	1.64[c]
P2		1,4-diaminobutane	3,950	5,680	1.44
			5,620[c]	15,780[c]	2.80[c]
P3		Hexamethylenediamine	6,330	9,240	1.46
			6,280[c]	16,500[c]	2.62[c]
P4		1,8-diaminooctane	6,410	9,130	1.42
			8,110[c]	38,360[c]	4.73[c]
P5		1,10-diaminodecane	3,650	4,380	1.20
			4,060[c]	5,130[c]	1.26[c]
P6		*m*-phenylenediamine	15,210	21,800	1.43
P7		*p*-phenylenediamine	7,690	9,460	1.23
P8	Ferulyl	Ethylene diamine	12,780	24,830	1.94
P9		1,4-diaminobutane	18,490	37,470	2.03
P10		Hexamethylenediamine	19,420	38,510	1.98
P11		1,8-diaminooctane	13,870	21,900	1.58
P12		1,10-diaminodecane	12,800	26,630	2.08
P13		*m*-phenylenediamine	12,920	20,080	1.55
P14		*p*-phenylenediamine	12,220	16,430	1.34
P15	Sinapyl	Ethylene diamine	26,640	47,560	1.79
P16		1,4-diaminobutane	28,270	51,060	1.81
P17		Hexamethylenediamine	28,630	49,050	1.71
P18		1,8-diaminooctane	12,160	26,300	2.16
P19		1,10-diaminodecane	7,550	10,600	1.40
P20		*m*-phenylenediamine	14,580	34,730	2.38
P21		*p*-phenylenediamine	8,430	19,290	2.29

[a]Determined by GPC, 1.0 mLmin^{-1}, 0.01 M LiBr in DMF; [b]D=M_w/M_n; [c]Molecular weight determined after soxhlet extraction, 24 h, with 0.01 M LiBr in DMF

chromatography (GPC) (**Table 3.1**). As mentioned previously, the isolated poly(ether-amide)s were sparingly soluble in DMF (**Table 3.2**), with a large fraction remaining intractable. This insolubility suggests that the molecular weights of the poly(ether-amide)s are higher than those determined by GPC, as GPC only characterizes the soluble fraction. This is clearly demonstrated in polymers P1-P5, which exhibited extremely low molecular weights by GPC (M_n: 3 to 6 kDa) when the polymers were added to DMF at room temperature. A similar effect was seen by Kwolek and Morgan, in the synthesis and

Table 3.2 Insolubility of poly(ether-amide)s in DMF after 24h[a]

	Polymer	Wt% insoluble[a]
p-coumaryl	P1	62.3
	P2	32.0
	P3	38.5
	P4	47.5
	P5	52.5
	P6	23.3
	P7	46.6
ferulyl	P8	49.7
	P9	67.4
	P10	18.5
	P11	74.3
	P12	57.3
	P13	25.4
	P14	26.7
sinapyl	P15	27.2
	P16	64.8
	P17	45.8
	P18	39.2
	P19	45.2
	P20	76.3
	P21	40.8

[a]1.0 mL of 10 mM LiBr in DMF was added to weighed polymer samples (10 mg) and allowed to sit at room temperature for 24 h. Solvent was decanted and the residual solid was dried in a vacuum oven overnight. Solid was weighed to determine wt% insoluble.

characterization of aromatic-aliphatic polyamides[30]. In their work, polyamides containing aliphatic linkers less than nine carbons in length or aromatic units without functional groups, were insoluble in all common organic solvents, even DMF. Suspensions of the aromatic-aliphatic *p*-coumaryl-based polymers were heated using several different methods to improve the solubility of high molecular weight components. Boiling DMF was added to each polymer sample and stirred until the suspension had cooled to room temperature. After filtration, GPC traces showed that the addition of heated DMF resulted in a slight increase in the solubility of higher molecular weight fractions (**Figure 3.4**). To determine if additional heating improved solubility, a 24-hour extraction with a soxhlet extractor was performed. Samples prepared via this method exhibited a significant increase in the observed molecular weight of P1-P4, as seen in Table 3.1. However, even after utilizing soxhlet extraction, molecular weights observed for P5 were still low. Limited molecular weights were also observed for ferulyl and sinapyl-based polymers synthesized with 1,10-diaminodecane, P12 and P19 respectively. Because P19 was the most soluble of the series, its overall molecular weight (soluble + insoluble) was likely lower than P5 or P12, which had larger insoluble fractions. One explanation for these lower molecular weights is the reduced solubility of 1,10-diaminodecane in the aqueous solution, as only lower molecular weight polymers were isolated for P5, P12, and P19. Similar results were seen in our previously studied poly(ester-amide) system.

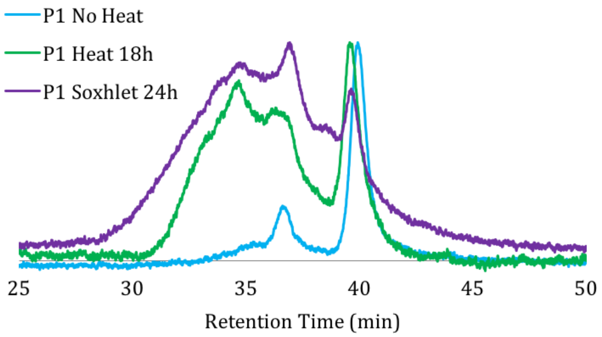

Figure 3.4: GPC traces of P1 using different extraction techniques to improve high molecular weight polymer solubility

Generally, the poly(ether-amide)s exhibited weight average molecular weights (M_w) between 20 and 40 kDa and dispersities between 1.5 and 2.2. The highest molecular weight polymers were produced from sinapyl acid-based ether dimers, likely due its increased solubility with the dimethoxy substitution pattern. The broad diversity of polymers obtained show the effectiveness of this polymerization method for the rapid generation of a series of polymers with tunable properties. Based on the polymerization method used, the dispersity of the resulting materials is not well controlled. However, values obtained are within acceptable values for commercial applications, suggesting that this polymerization method could be appropriate for use in an industrial setting.

Thermal properties. The thermal behavior of polymers P1-P21 were studied using both differential scanning calorimetry (DSC) and thermogravimetric analysis (TGA). Generally, aromatic polymers exhibit higher glass transition temperatures (T_g) than aliphatic polymers due to a lack of rotation about bonds between aromatic monomers, in comparison to aliphatic sp^3 bonds. This lack of rotational freedom causes reduced chain mobility and backbone flexibility. Additionally, with the inclusion of bulky side groups, T_g should also increase, as these modifications cause decreased chain mobility by limiting rotation about bond in the backbone. As the polymers in this study feature both aromatic and aliphatic

Table 3.3 Thermal characterization of poly(ether-amide)s by DSC and TGA

	Polymer	T_g(°C)[a]	T_{d5}(°C)[b,c]	T_{d10}(°C)[b,d]	T_{d25}(°C)[b,e]
p-coumaryl	P1	90.8	243.6	290.3	335.8
	P2	91.8	213.3	280.9	327.0
	P3	84.3	238.3	294.0	340.4
	P4	80.6	254.4	291.7	328.1
	P5	66.2	121.6	142.4	301.0
	P6	79.1	150.3	175.9	410.8
	P7	112.3	139.1	185.1	368.9
ferulyl	P8	103.1	143.9	276.7	344.5
	P9	92.4	123.5	251.9	353.9
	P10	98.1	170.9	241.6	317.9
	P11	110.1	194.2	264.8	310.8
	P12	82.3	123.3	157.6	307.5
	P13	108.3	216.5	317.9	404.3
	P14	124.7	233.7	310.9	386.5
sinapyl	P15	106.9	226.5	271.4	317.7
	P16	102.3	133.5	225.5	350.3
	P17	85.2	106.2	166.7	289.4
	P18	84.9	121.6	154.5	328.3
	P19	77.9	177.8	254.8	309.0
	P20	84.8	170.8	192.8	248.8
	P21	81.1	204.8	247.4	333.7

[a]Determined by DSC; [b]Determined by TGA; [c]T_{d5}= temperature at 5% mass loss; [d]T_{d10}= temperature at 10% mass loss; [e]T_{d25}= temperature at 25% mass loss

components, as well as varying degrees of methoxy substitution, structural effects on T_g are complex.

All of the poly(ether-amide)s were shown to be amorphous by DSC, as only a single glass transition temperature (T_g) was observed. Due to high backbone flexibility, polyethers typically exhibit extremely low T_g. In contrast, the poly(ether-amide)s synthesized featured moderately high T_g, as seen in **Table 3.3**. The glass transition temperature (T_g) should decrease as the length of the aliphatic spacer increases due to increased chain mobility and backbone flexibility, while the utilization of aromatic diamines as linkers should increase the observed T_g. While these trends are generally seen throughout the series of isolated

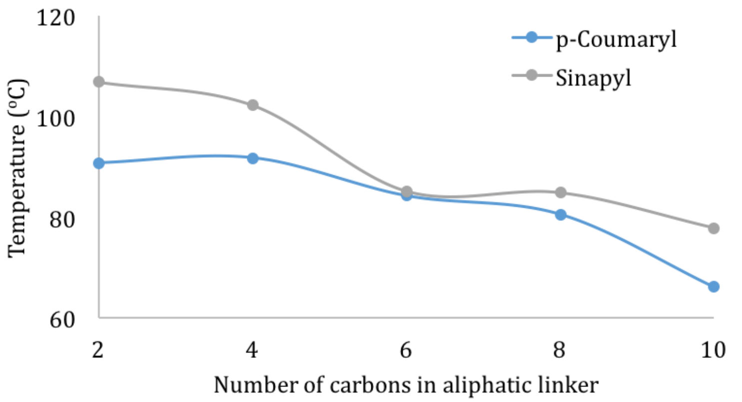

Figure 3.5 Glass transition temperature as a function of aliphatic linker length

poly(ether-amide)s, there are also several significant exceptions.

As seen in **Figure 3.5**, both the length of the aliphatic linker, as well as the identity of the monolignol dimer, have large effects on the observed T_g. The incorporation of substituted aromatic dimers (sinapyl-based dimers instead of *p*-coumaryl-based dimers), increases the observed T_g by limiting the rotational flexibility of the polymer chains. As expected, T_g generally increased with increasing degrees of methoxy substitution, as seen in the overall increase in T_g between P1-P7 and P15-P21. Similarly to our previous study, poly(ether-amide)s with long aliphatic linkers (such as hexamethylenediamine, 1,8-diaminooctane, 1,10-diaminodecane) exhibited T_g higher than expected, as seen in P10 and P11. These deviations in glass transition temperature likely occurred due increased chain interactions, which prevent polymer chain movement. Wang et al. saw a similar effect in the synthesis of poly(ether-amide)s with polyethylene glycol spacers[31]. As the length of the PEG spacer increased, the observed T_g also increased due to increased interchain interactions. In addition to effects seen by the incorporation of longer aliphatic spacers, the substitution pattern of aromatic diamines also significantly affected the observed glass transition temperature. The use of *m*-phenylenediamine instead of *p*-phenylenediamine showed a decrease in the observed T_g,, seen in a comparisons between P13 and P14. The meta-substitution pattern causes a non-linear structure, which will minimize π-π interactions and prevent the formation of strong hydrogen bonds between chains. In turn, the reduced interchain interactions cause a significant reduction in the observed T_g.

Molecular weight also played a significant role in the observed T_g of the poly(ether-amide)s. Polymer chain ends are less dense than interchain units, exhibiting greater free volume. A larger concentration of chain ends in a polymer sample (by the presence of smaller molecular weight polymers or a greater fraction of smaller molecular weight polymers) will lower the observed T_g, as free volume is inversely proportional to glass transition temperature. With this in mind, a large fraction of smaller molecular weight polymers in a non-monodisperse sample can have effects similar to that observed with the addition of plasticizers. As exemplified by their higher dispersity, P9 and P12 feature an increased fraction of smaller molecular weight polymers, which yields lower glass transition temperatures than would expected based on the length of their linker and T_g observed for other ferulyl-based polymers. As seen in Table 3.3, P11 featured a higher T_g than P18. While both polymers are synthesized with 1,8-diaminooctane, P11 is synthesized with the ferulyl-based dimer (single methoxy substitution) and should feature a lower glass transition temperature than P18. However, P11 exhibits a weight-average molecular weight more than 5 kDa greater than P18. This difference in molecular weight, and thus decreased number of chain ends present, is responsible for the observed increase in T_g. Additionally, P18 is more polydisperse with a dispersity of 2.16, in comparison to P11 which features a dispersity of 1.58. The higher dispersity of this sample causes broadening of the glass transition, which may play a role in the observed decreased T_g, as glass transition temperature is defined as the midpoint of the glass transition.

The thermal stability of the poly(ether-amides) was studied using thermogravimetric analysis (TGA). Polymer samples were heated from 30 to 800 °C under a nitrogen atmosphere (Figures S9-11). Most of the polymers in this series featured initial mass loss (T_{d5}) between 120 and 210 °C, lower temperatures than would be typically expected for these materials (Table 3.3). Despite efforts to remove water prior to the thermal decomposition studies, water loss was likely the cause of low initial decomposition temperatures. As these materials contain amide linkages, they are inherently hydroscopic and the retention of water is not surprising. The presence of water in the polymer samples can be further exemplified by the high temperatures required to reach 25% mass loss (T_{d25}). For example, P6 exhibits an initial decomposition temperature (T_{d5}) of 150.3 °C but requires the polymer sample to be heated to 410.8 °C to cause 25% mass loss. The length of the aliphatic diamine linker appeared to have no significant effect on the thermal stability of the poly(ether-amide)s. The incorporation of aromatic diamine linkers also did not have a substantial effect on thermal stability, regardless of the pattern of substitution. Overall, the polymers have mild thermal stability and potential for use in melt processing. Most commercial thermoplastics are processed between 100 and 250 °C, depending on their melting temperature[32]. Prior to large scale thermal processing, these poly(ether-amide)s should undergo more rigorous methods to remove residual water. After removal of the residual water, these materials will likely exhibit increased thermal stability in contrast to the data discussed here.

3.3 Conclusions

In this work, we have described the synthesis of a series of aromatic-aliphatic poly(ether-amide)s from monolignol-based ether dimers and various aliphatic and aromatic diamines. Aliphatic diamines were chosen as co-monomers to improve the solubility and processability of monolignol-based polymers. Additionally, the five aliphatic diamines used in this study are available from biological sources. While the isolated poly(ether-amide)s were insoluble in standard organic solvents (excluding DMF), the moderate glass transition temperatures and thermal stability observed offer promise for these materials in melt processing applications. Additionally, the modularity of this synthetic approach could be used to rapidly generate a series of diverse polymers with well-tuned properties. The versatility of this method increases the potential applications for this polymer system industrially.

In the future, our group will explore processing options with the series of poly(ether-amide)s generated, as well as utilizing these polymers as a framework for the creation of higher-order materials. With two grafting sites per monolignol-based ether dimer, these materials could easily be used in the preparation of densely grafted copolymers or three-dimensional polymer networks. Additionally, the distance between grafting sites could be well-controlled and tuned by altering either the length of the aliphatic spacer in the monolignol-based dimer or the length of the aliphatic diamine linker. In conclusion, this system allowed for the rapid preparation of a series of poly(ether-amide)s from biological-based components, which can easily be adapted and used for a variety of purposes. This targeted upgrading of underutilized bio-based materials has provided a unique set of functional materials, with the prospect of their use in the development of other novel materials.

3.4 Experimental Section

Materials. 4-hydroxybenzaldehyde (98%, TCI America), vanillin (99%, Alfa Aesar), 3,5-dimethoxy-4-hydroxybenzaldehyde (98%, Acros), malonic acid (99%, Alfa Aesar), tert-butanol (99%, Alfa Aesar), acetic anhydride (99.5%, Fisher), acetone (ACS Grade, Fisher), sulfuric acid (conc., ACS Grade, Fisher), piperidine (99%, Spectrum), trifluoroacetic acid (99.5%, Fisher) 1,4-diaminobutane (98+%, Alfa Aesar), 1,8-diaminooctane (98%, Acros), 1,10-diaminodecane (97%, Acros), *p*-phenylenediamine (99+%, Acros), *m*-phenylenediamine (99+%, Acros), sodium hydroxide (ACS Grade, Fisher), and N,N-dimethylformamide (HPLC grade, Alfa Aesar) were purchased and used as received. Pyridine (99%, Fisher) was distilled over KOH prior to use. Dichloromethane (ACS Grade, Fisher) was distilled from CaH_2 prior to use. Hexamethylene diamine (99.5%, Acros) was sublimed under reduced pressure prior to use. Ethylenediamine (98%, Acros) was distilled prior to use to remove discoloration. Meldrum's acid[33], tert-butyl malonate[34], and 1,4-dibromobutane[35] were synthesized according to published procedures. Silica gel 60 (230-400 mesh, Fisher) was used for column chromatography. Thin layer chromatography (TLC) was conducted with silica gel 60–F245 plates and visualized with a handheld UV lamp. NMR solvents d_6-DMSO, $CDCl_3$, and C_6D_6 were obtained from Cambridge Isotope Laboratories and used as received.

^{1}H, ^{13}C, and FTIR Spectroscopy. ^{1}H NMR spectra were recorded on Bruker AV-300 or Bruker DRX-500 spectrometers at room temperature in d_6-DMSO, unless either wise noted. Chemical shifts are reported with respect to internal solvent, 2.50 ppm (d_6-DMSO), 7.16 (C_6D_6), or 7.26 ($CDCl_3$) for ^{1}H NMR spectra. ^{13}C NMR spectra were recorded on a Bruker AV-

500 spectrometer with a dual cryoprobe (^{13}C, ^{1}H). Chemical shifts are reported with respect to internal solvent, 39.52 ppm (d_6-DMSO), 128.06 ppm (C_6D_6), or 77.16 ppm ($CDCl_3$) for ^{13}C NMR spectra. Infrared absorption spectra were collected using a Jasco 4210-FT/IR spectrometer from 4000 to 400 cm $^{-1}$ from KBr pellets. All samples were dried at 100 ^{o}C in a vacuum oven overnight (at least 12 h) prior to characterization.

Molecular Weight Characterization. Molecular weight (M_n and M_w) and dispersity ($Đ$=M_w/M_n) were determined using gel permeation chromatography (GPC). Samples were dissolved in 0.01 M LiBr in *N,N*-dimethylformamide (DMF) at a concentration of 2−5 mg/mL and were passed through a 0.20 μm PTFE filter before injection. GPC for all polymers was conducted on a Jasco system equipped with a refractive index detector, a UV detector, a Waters Styragel guard column, and four Waters HR Styragel 5 μm columns (100-5K, 500-30K, 50-100K, 5-600 K) using 0.01 M LiBr in *N,N*-dimethylformamide (DMF) at 40 °C and a flow rate of 1.0 mL/min. Calibration was performed using near-monodisperse polystyrene standards (M_n=1,250 to 549,000 Da) from Jordi Laboratories and chromatograms were analyzed using ChromNAV chromatography software.

Thermal Characterization. All samples were dried at 100 ^{o}C in a vacuum oven overnight (at least 12 h) prior to all thermal characterization. Thermogravimetric analysis (TGA) was conducted on a Perkin Elmer Pyris Diamond TG/DTA Thermogravimetric/Differential Thermal Analyzer. The TGA instrument was operated under an argon atmosphere, using platinum crucibles. Samples (6-12 mg) were heated from 25 °to 800 °C at a rate of 10 °C min/mL. Pyris Manager was used to analyze the data. Decomposition temperatures T_{d5}, T_{d10}, and T_{d25} were measured at 5, 10, and 25% mass loss, respectively. Differential scanning calorimetry (DSC) was performed on a Perkin Elmer DSC 8000 to determine glass transition temperature (T_g). Samples (5-8 mg) were heated from -30 to 200 ^oC at a rate of 10 °C/min and cooled to -30 ^oC at a rate of 10 °C/min. A minimum of two heating and cooling cycles were performed and T_g was measured from the second heating cycle. Pyris Manager was used to analyze the data.

Tert-butyl ester monomer synthesis. *p-Coumaroyl tert-butyl ester (**2a**)*. 4-hydroxybenzaldehyde (6.99 g, 57.3 mmol, 1 eq) was weighed and added to a round bottom flask along with tert-butyl malonate (11.01 g, 68.7 mmol, 1.2 eq). 30.0 mL of pyridine and 0.3 mL of piperidine were added to the reaction mixture and the reaction was heated to reflux overnight. After refluxing, the reaction was cooled to room temperature and concentrated under reduced pressure. The resulting residue was dissolved in diethyl ether (70 mL) and washed with saturated sodium bicarbonate (2×70 mL), 1 M HCl (2×40 mL), and deionized water (1×40 mL). The organic layer was dried over $MgSO_4$ and the solvent was removed via rotary evaporation to yield the crude product. The crude product was purified on silica gel via flash column chromatography using 3:2 hexanes:ethyl acetate as the elutant. Yield: 4.04 g, 32.1% ^1H NMR (300 MHz, d_6-DMSO): δH 7.67 (d, 2H, Ar-***H***), 7.62 (d, 1H, $CC\boldsymbol{H}=CHCOO(CH_3)_3$), 7.20 (d, 2H, Ar-***H***), 6.54 (d, 1H, $CCH=C\boldsymbol{H}COO(CH_3)_3$), 1.48 (s, 9H, $COO(C\boldsymbol{H}_3)_3$).

*Feruloyl tert-butyl ester (**2b**)*. Yield: 6.49 g, 65.3% ^1H NMR (300 MHz, d_6-DMSO): δH 7.48 (d, 1H, $CC\boldsymbol{H}=CHCOO(CH_3)_3$), 7.27 (s, 1H, Ar-***H***), 7.08 (d, 1H, Ar-***H***), 6.80 (d, 1H, Ar-***H***), 6.37 (d, 1H, $CCH=C\boldsymbol{H}COO(CH_3)_3$), 3.81 (s, 3H, $Ar\text{-}OC\boldsymbol{H}_3$), 1.47 (s, 9H, $COO(C\boldsymbol{H}_3)_3$).

*Sinapoyl tert-butyl ester (**2c**)*. 3,5-dimethoxy-4-hydroxybenzaldehyde (3.17 g, 17.4 mmol, 1 eq) was weighed and added to a round bottom flask along with tert-butyl malonate (3.90 g, 24.4 mmol, 1.2 eq). 20.0 mL of pyridine and 0.2 mL of piperidine were added to the reaction mixture and the reaction was heated to reflux overnight. After refluxing, the reaction was cooled to room temperature and concentrated under reduced pressure. The resulting residue was dissolved in diethyl ether (50 mL) and washed with saturated sodium bicarbonate (2×50 mL), 1 M HCl (2×30 mL), and deionized water (1×30 mL). The organic layer was dried over $MgSO_4$ and solvent was removed using a rotary evaporator to yield the product as a white solid. Yield: 3.57 g, 73.1% ^{1}H NMR (300 MHz, d_6-DMSO): δH 8.89 (s, 1H, Ar-O***H***), 7.47 (d, 1H, CC***H***=CHCOO$(CH_3)_3$), 6.98 (s, 2H, Ar-***H***), 6.44 (d, 1H, CCH=C***H***COOtBu), 3.79 (s, 6H, Ar-OC$\boldsymbol{H}_3$), 1.48 (s, 9H, COOC$(C\boldsymbol{H}_3)_3$). ^{13}C NMR (500 MHz, d_6-DMSO): δC 166.46 (CCH=CH***C***OO$(CH_3)_3$), 148.46 (***C***-OCH_3), 144.87 (C***C***H=CHCOO$(CH_3)_3$), 138.50 (***C***-OH), 124.97 (***C***CH=CHCOO$(CH_3)_3$), 117.26 (CCH=***C***HCOO$(CH_3)_3$), 106.49 (Ar ***C***-H), 79.90 (***C***$(CH_3)_3$), 56.53 (O***C***H_3), 28.39 (C(***C***$H_3)_3$).

Tert-butyl ether dimer synthesis. *p-Coumaroyl tert-butyl ether dimer* (**3a**). *p*-Coumaroyl tert-butyl ester (4.04 g, 18.4 mmol, 2.2 eq) was weighed and added to a two-necked round bottom flask along with 30 mL of *N,N*-dimethylformamide (DMF). The reaction mixture was cooled to 0 °C and sodium hydride (0.44 g, 18.4 mmol, 2.2 eq) was added portionwise. After 30 minutes, a solution of 1,4-dibromobutane (1.0 mL, 8.3 mmol, 1 eq)) in 5 mL DMF was added dropwise over 30 minutes via an addition funnel. The reaction was allowed to slowly warm to room temperature and stir overnight. After 12 hours at room temperature, the reaction was then heated to reflux for 6 hours. The reaction was then cooled to room temperature, diluted with ethyl acetate (70 mL), washed with deionized water (2×70 mL) and brine (1×50 mL). The organic layer was separated, dried over $MgSO_4$, and volatiles were removed via rotary evaporation to yield the crude product as an off-white crystalline solid. The crude product was purified on silica gel via flash column chromatography using a gradient of 7:3 to 3:2 hexanes:ethyl acetate as the elutant. Yield: 2.08 g, 50.4%^{1}H NMR (300 MHz, C_6D_6): δH 7.88 (d, 1H, CCH=C***H***COOtBu), 7.15 (d, 2H, Ar-***H***), 6.63 (d, 2H, Ar-***H***), 6.45 (d, 1H, CC***H***=CHCOOtBu), 3.49 (br s, 2H, -OC***H***$_2$CH$_2$), 1.60 (br s, 2H, -OCH$_2$C***H***$_2$), 1.51 (s, 9H, C(C***H***$_3$)$_3$). ^{13}C NMR (500 MHz, C_6D_6): δC 166.72 (***C***OOC(CH$_3$)$_3$), 161.18 (***C***OCH$_2$CH$_2$), 143.82 (***C***H=CHCOOtBu), 130.19 (Ar), 128.39 (***C***CH=CHCOOtBu, under C_6D_6), 118.75 (CH=***C***HCOOtBu), 115.32 (Ar), 80.04 (***C***(CH$_3$)$_3$), 67.66 (CO***C***H$_2$CH$_2$), 28.66 (C(***C***H$_3$)$_3$), 26.34 (COCH$_2$***C***H$_2$).

Feruloyl tert-butyl ether dimer (**3b**). Yield: 2.10 g, 52.5%^{1}H NMR (300 MHz, C_6D_6): δH 8.04 (d, 1H, CCH=C***H***COOtBu), 6.97 (d, 1H, Ar-***H***), 6.94 (s, 1H, Ar-***H***), 6.63 (d+d, 2H, Ar-***H*** and CC***H***=CHCOOtBu), 3.70 (br s, 2H, OC***H***$_2$CH$_2$), 3.38 (s, 3H, Ar-OC***H***$_3$), 1.84 (br s, 2H, OCH$_2$C***H***$_2$), 1.64 (s, 9H, C(C***H***$_3$)$_3$). ^{13}C NMR (500 MHz, C_6D_6): δC 166.75 (***C***OOtBu), 151.56 (***C***-OCH$_3$), 150.58 (***C***OCH$_2$CH$_2$), 144.43 (C***C***H=CHCOOtBu), 128.37 (***C***CH=CHCOOtBu), 122.69 (Ar), 118.61 (Ar), 113.10 (CCH=***C***HCOOtBu), 110.81 (Ar), 80.08 (O***C***(CH$_3$)$_3$), 68.65 (CO***C***H$_2$CH$_2$), 55.56 (C-O***C***H$_3$), 28.67 (OC(***C***H$_3$)$_3$), 26.60 (COCH$_2$***C***H$_2$).

*Sinapoyl tert-butyl ether dimer (**3c**)*. Yield: 1.98 g, 48.6%^{1}H NMR (300 MHz, C_6D_6): δH 7.88 (d, 1H, CCH=C***H***COOtBu), 6.54 (d+s, 3H, CC***H***=CHCOOtBu and Ar-***H***), 4.15 (br m, 2H, OC***H***$_2$CH$_2$), 3.27 (s, 6H, Ar-OC***H***$_3$), 2.09 (br m, 2H, OCH$_2$C***H***$_2$), 1.52 (s, 9H, C(C***H***$_3$)$_3$). ^{13}C NMR (500 MHz, C_6D_6): δC 166.26 (***C***OOtBu), 154.43 (***C***-OCH$_3$), 144.34 (C***C***H=CHCOOtBu), 140.56 (***C***OCH$_2$CH$_2$), 130.14 (***C***CH=CHCOOtBu), 119.52 (CCH=***C***HCOOtBu), 105.82 (Ar), 79.97 (O***C***(CH$_3$)$_3$), 73.14 (CO***C***H$_2$CH$_2$), 55.68 (C-O***C***H$_3$), 28.32 (OC(***C***H$_3$)$_3$), 27.35 (COCH$_2$***C***H$_2$).

Diacid ether dimer synthesis. *p-Coumaryl diacid ether dimer (**4a**)*. *p*-Coumaryl tert-butyl ether dimer (2.08 g, 4.2 mmol, 1 eq) was weighed and added to a round bottom flask along with trifluoroacetic acid (12.9 mL, 168.3 mmol, 40 eq). Reaction was stirred at room temperature for 4 hours. Volatiles were removed under vacuum to yield the product as a white solid. Yield: 1.52 g, 94.4%^{1}H NMR (300 MHz, *d*$_6$-DMSO, sparingly soluble): δH 7.64 (d, 2H, Ar-***H***), 7.56 (d, 1H, CH=C***H***COOH), 6.98 (d, 2H, Ar-***H***), 6.39 (d, 2H, C***H***=CHCOOH), 4.09 (br s, 2H, $\mathrm{OC}\boldsymbol{H}_2\mathrm{CH}_2$), 1.88 (br s, 2H, $\mathrm{OCH_2C}\boldsymbol{H}_2$). ^{13}C NMR (500 MHz, *d*$_6$-DMSO, sparingly soluble): δC 167.84 (***C***OOH), 160.33 ($\boldsymbol{C}\mathrm{OCH_2CH_2}$), 143.78 (***C***H=CHCOOH), 129.96 (Ar), 126.76 (***C***CH=CHCOOH), 116.44 (CH=***C***HCOOH), 114.83 (Ar), 67.30 ($\mathrm{O}\boldsymbol{C}\mathrm{H_2CH_2}$), 25.29 ($\mathrm{OCH_2}\boldsymbol{C}\mathrm{H_2}$).

*Ferulyl diacid ether dimer (**4b**)*. Yield: 1.5433 g, 92.4% ^{1}H NMR (300 MHz, *d*$_6$-DMSO): δH 7.55 (d, 1H, CH=C***H***COOH), 7.31 (s, 1H, Ar-***H***), 7.20 (d, 1H, Ar-***H***), 6.99 (d, 1H, Ar-***H***), 6.46 (d, 1H, C***H***=CHCOOH), 4.08 (br s, 2H, $\mathrm{OC}\boldsymbol{H}_2\mathrm{CH}_2$), 3.81 (s, 3H, $\mathrm{Ar{-}OC}\boldsymbol{H}_3$), 1.89 (br s, $\mathrm{OCH_2C}\boldsymbol{H}_2$). ^{13}C NMR (500 MHz, *d*$_6$-DMSO, sparingly soluble): δC 167.90 (***C***OOH), 150.12 ($\boldsymbol{C}\mathrm{OCH_3}$), 149.09 ($\boldsymbol{C}\mathrm{OCH_2CH_2}$), 144.19 (C***C***H=CHCOOH), 127.02 (***C***CH=CHCOOH), 122.64 (Ar), 116.65 (Ar), 112.48 (CCH=***C***HCOOH), 110.49 (Ar), 67.92 ($\mathrm{O}\boldsymbol{C}\mathrm{H_2CH_2}$), 55.67 ($\mathrm{CO}\boldsymbol{C}\mathrm{H_3}$), 25.44 ($\mathrm{OCH_2}\boldsymbol{C}\mathrm{H_2}$).

*Sinapyl diacid ether dimer (**4c**)*. Yield: 1.59 g, 97.8%^{1}H NMR (300 MHz, *d*$_6$-DMSO): δH 7.56 (d, 1H, CH=C***H***COOH), 7.02 (s, 2H, Ar-**H**), 6.56 (d, 1H, C***H***=CHCOOH), 3.93 (br s, 2H, $\mathrm{OC}\boldsymbol{H}_2\mathrm{CH}_2$), 3.79 (s, 6H, $\mathrm{Ar{-}OC}\boldsymbol{H_3}$), 1.78 (br s, 2H, $\mathrm{OCH_2C}\boldsymbol{H}_2$). ^{13}C NMR (500 MHz, *d*$_6$-DMSO): δC 167.76 (***C***OOH), 153.27 ($\boldsymbol{C}\mathrm{OCH_3}$), 144.25 (C***C***H=CHCOOH), 138.43 ($\boldsymbol{C}\mathrm{OCH_2CH_2}$), 129.67 (***C***CH=CHCOOH), 118.37 (CCH=***C***HCOOH), 105.78 (Ar), 72.16 ($\mathrm{CO}\boldsymbol{C}\mathrm{H_2CH_2}$), 56.01 ($\mathrm{CO}\boldsymbol{C}\mathrm{H_3}$), 26.18 ($\mathrm{COCH_2}\boldsymbol{C}\mathrm{H_2}$).

Poly(ether-amide) synthesis. *General polymerization procedure*. The desired diacid ether dimer (1 eq) was weighed and added to a round bottom flask. Thionyl chloride (20 eq) was added to the flask along with a drop of DMF, and the reaction was heated to reflux for 6 hours. Volatiles were removed under vacuum to yield the diacid chloride dimer. The desired diamine (3 eq) was weighed and added to a 100 mL beaker along with 15 mL of 0.5 M NaOH and a stir bar. The isolated diacid chloride dimer was dissolved in 15 mL of distilled dichloromethane and added quickly to the rapidly stirring diamine solution. A solid precipitate formed immediately and the resulting slurry was allowed to stir for two minutes. The slurry was transferred to an Eppendorf tube and centrifuged at 4.4×10^3 rpm for 20 minutes. The biphasic solution was decanted from the Eppendorf tube and the residual solid was washed with water (2x15 mL). After each washing, the slurry (water & polymer) was centrifuged at 4.4×10^3 rpm for 10 minutes. The resulting solid was dried under reduced pressure to yield the corresponding polymer as a yellow solid. Characterization data for each poly(ether-amide) can be found in Appendix B.

3.5 Appendix B

Figure S1: ^{1}H spectrum of **3a**

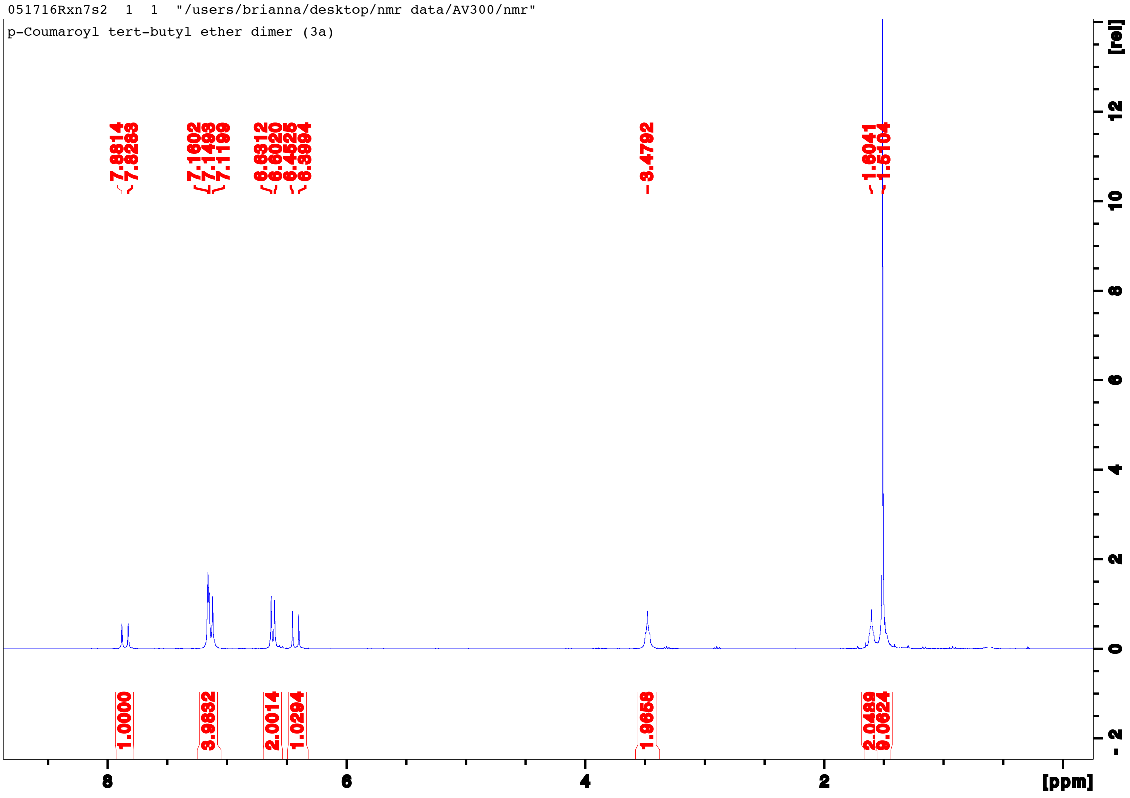

Figure S2: ^{13}C spectrum of **3a**

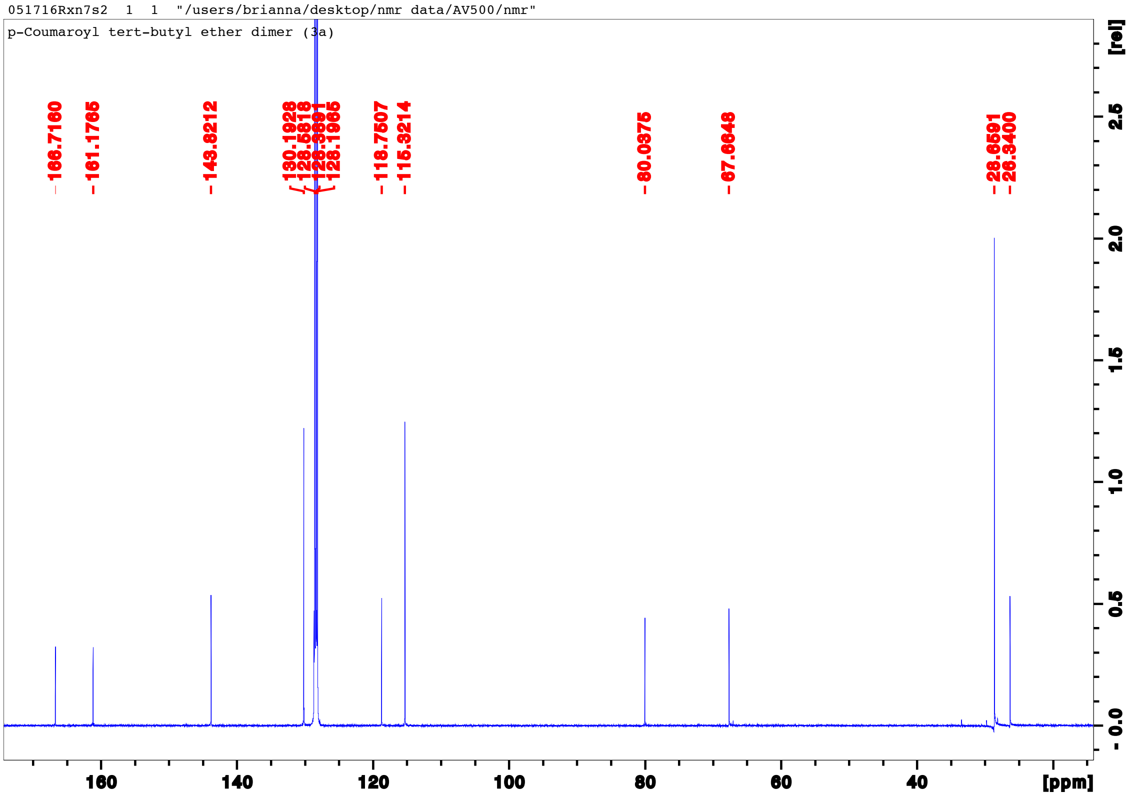

Figure S3: ^{1}H spectrum of **3b**

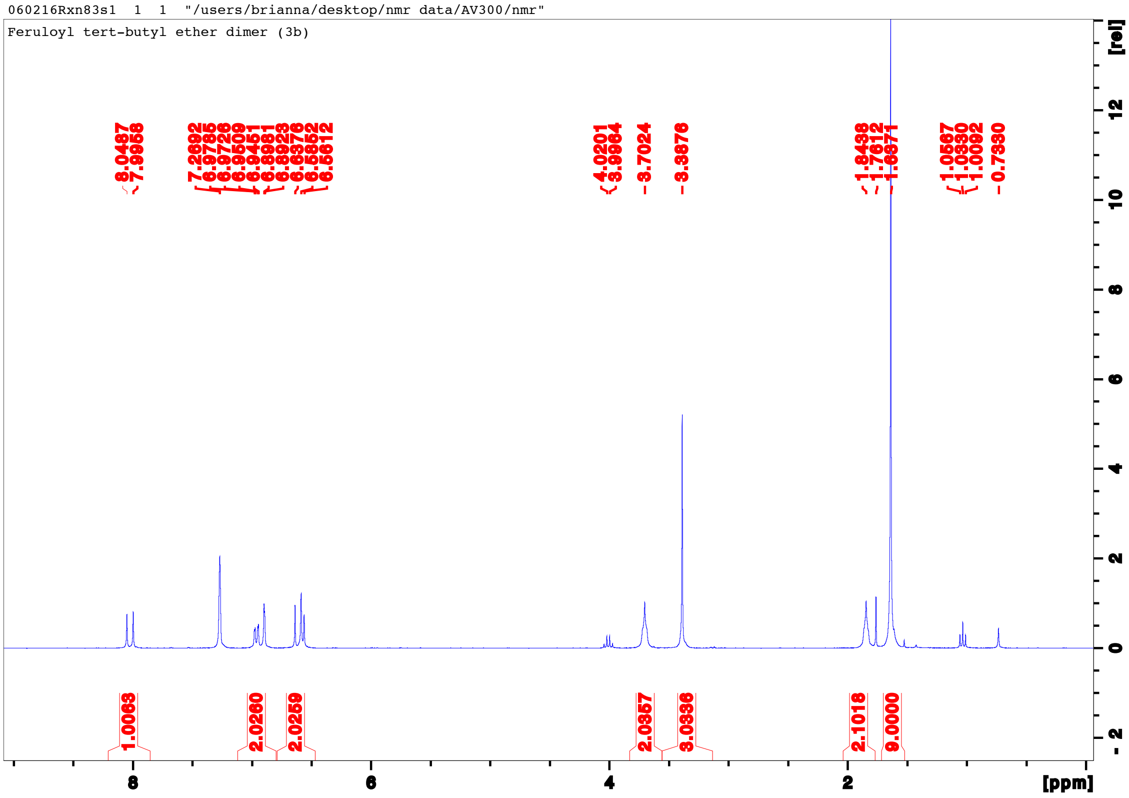

Figure S4: ^{13}C spectrum of **3b**

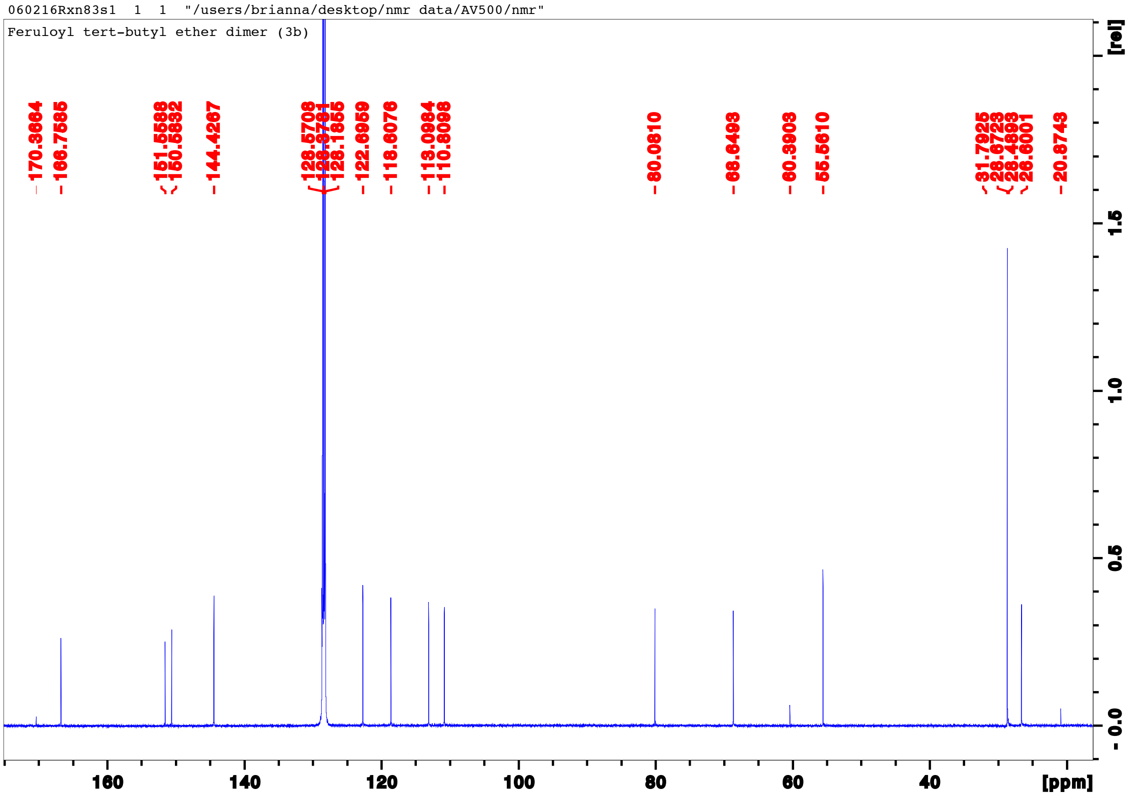

Figure S5: ^{1}H spectrum of **3c**

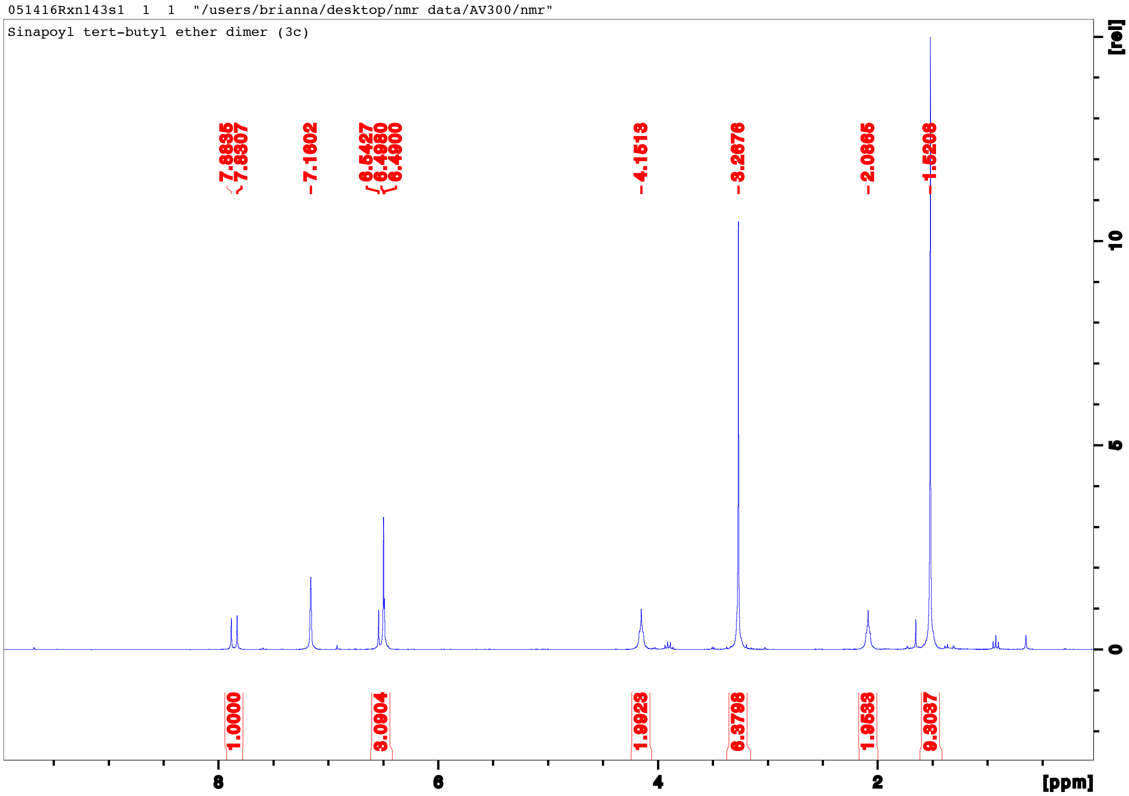

Figure S6: ^{13}C spectrum of **3c**

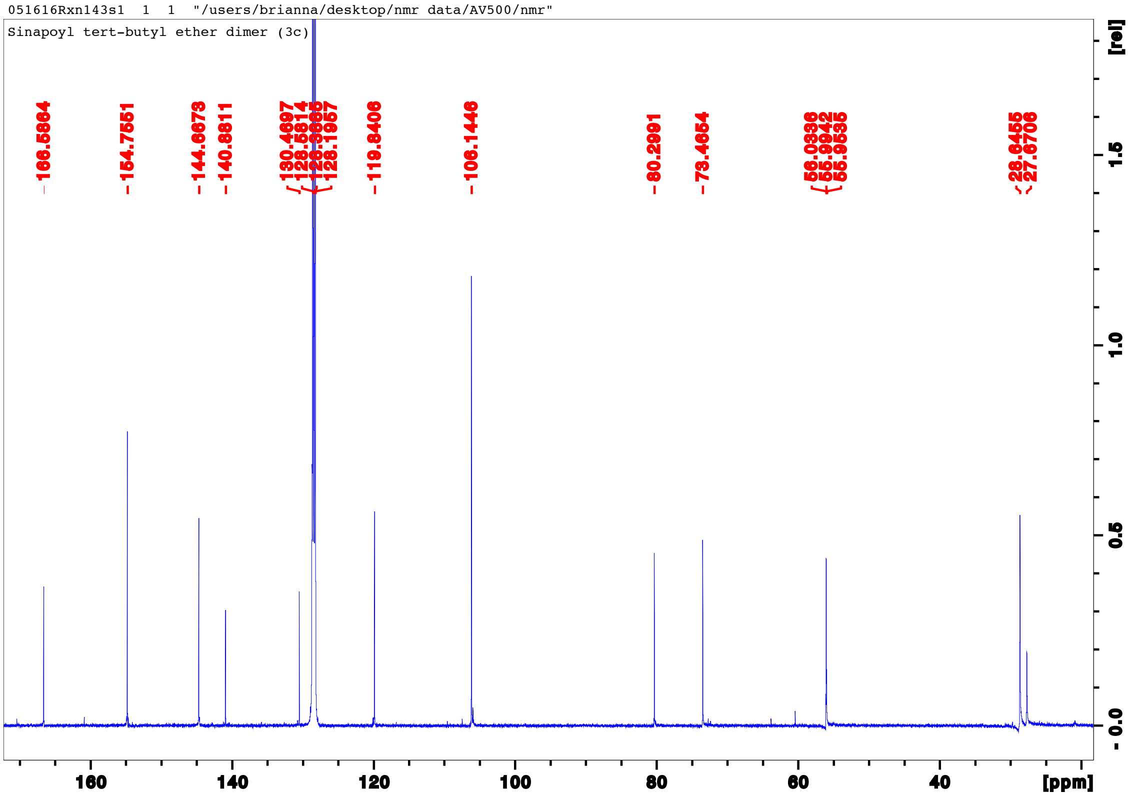

Figure S7: ^{1}H spectrum of **4a**

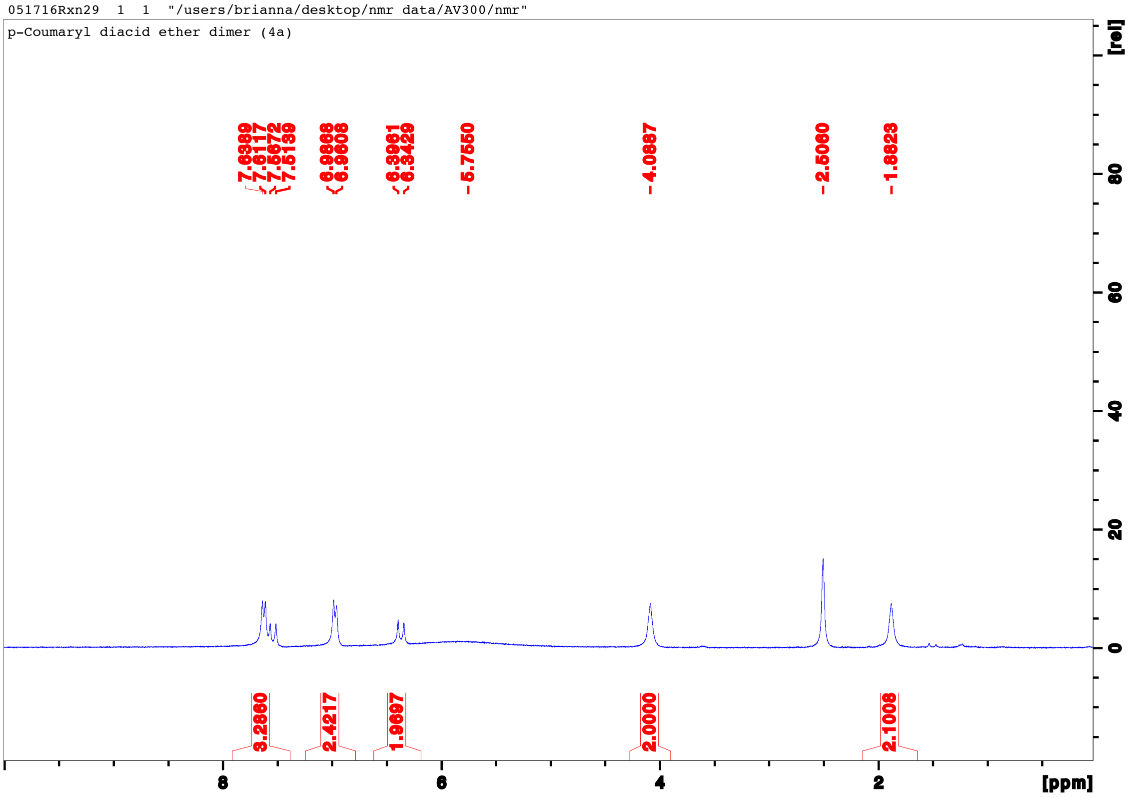

Figure S8: ^{13}C spectrum of **4a**

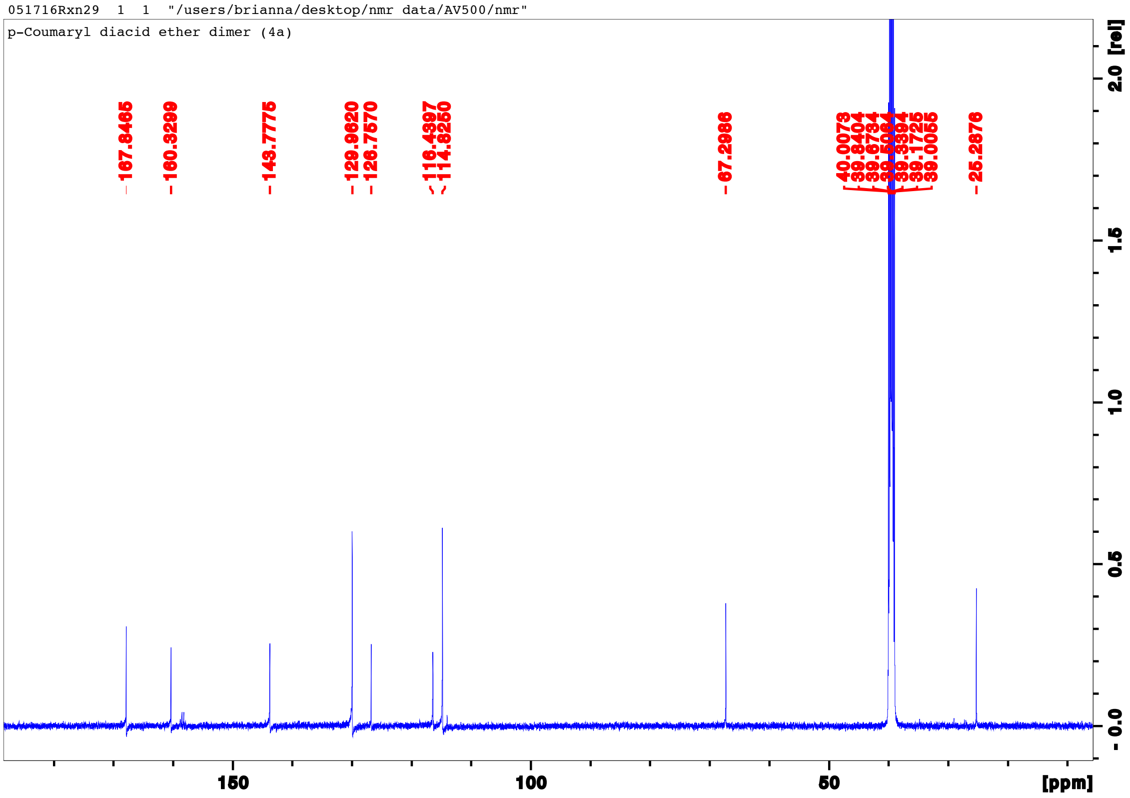

Figure S9: ^{1}H spectrum of **4b**

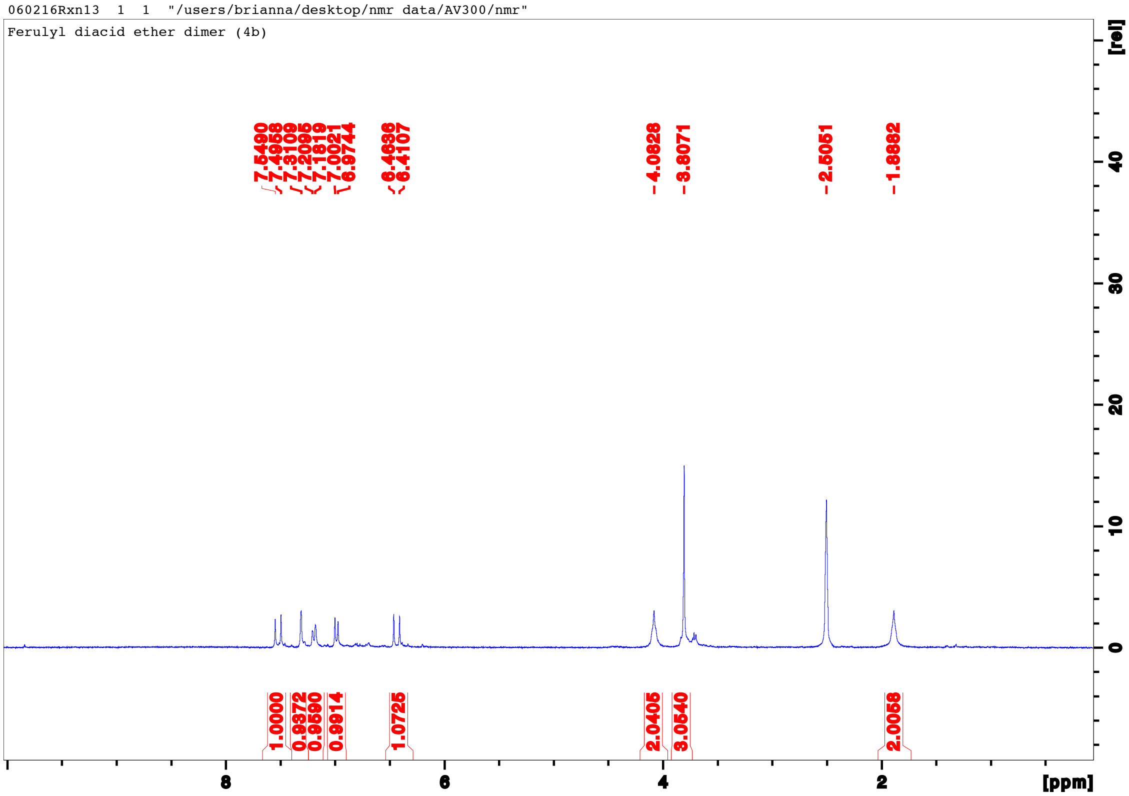

Figure S10: ^{13}C spectrum of **4b**

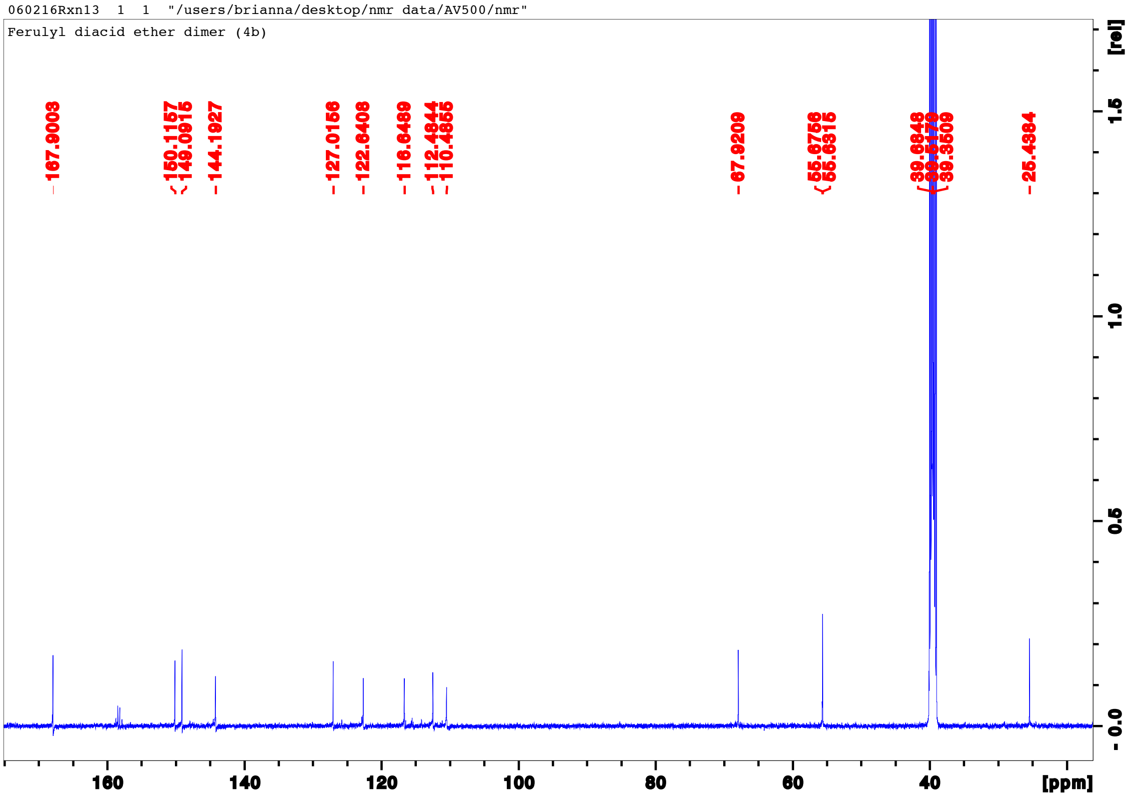

Figure S11: ^{1}H spectrum of **4c**

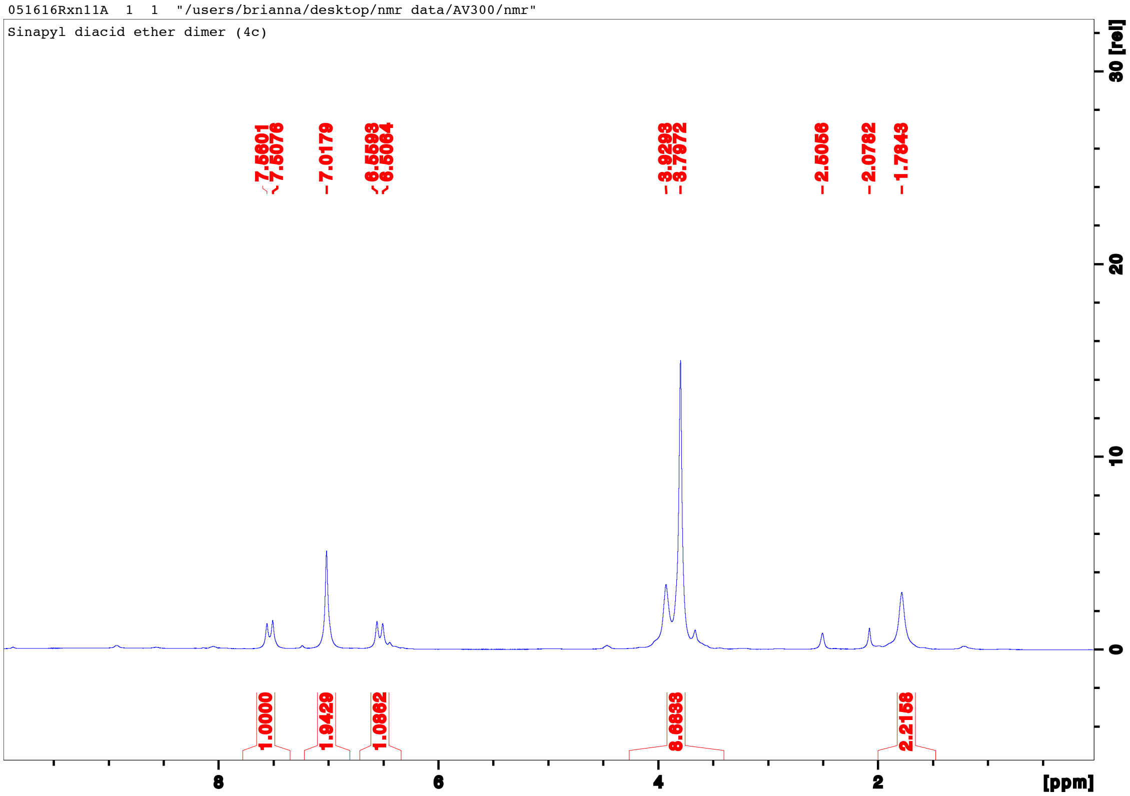

Figure S12: ^{13}C spectrum of **4c**

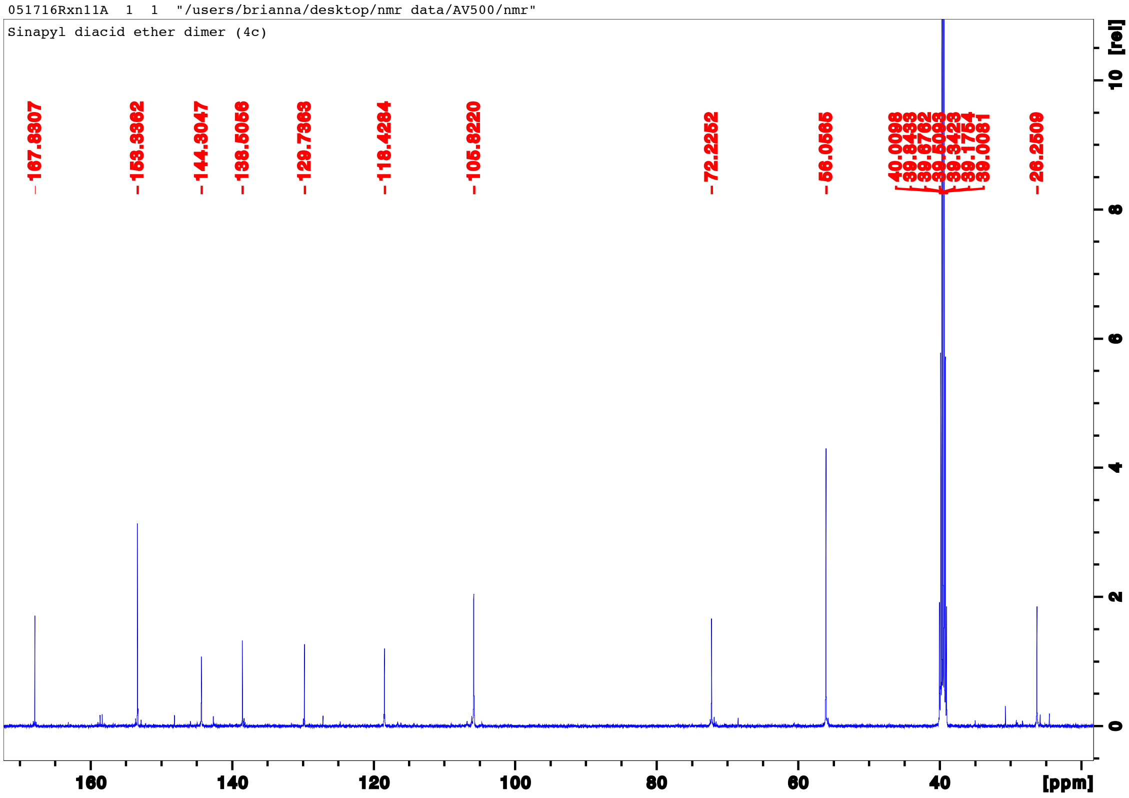

Polymer Characterization

p-Coumaryl diacid + ethylenediamine (**P1**). Yield 0.2321 g, 77.2%

p-Coumaryl diacid + 1,4-diaminobutane (**P2**). Yield 0.2346 g, 71.6%

p-Coumaryl diacid + 1,6-diaminohexane (**P3**). Yield 0.2486 g, 68.7%

p-Coumaryl diacid + 1,8-diaminooctane (**P4**). Yield 0.2161 g, 55.2%

p-Coumaryl diacid + 1,10-diaminodecane (**P5**). Yield 0.2622 g, 64.5%

p-Coumaryl diacid + *m*-phenylenediamine (**P6**). Yield 0.2604 g, 70.6%

p-Coumaryl diacid + *p*-phenylenediamine (**P7**). Yield 0.2994 g, 81.9%

Ferulic diacid + ethylenediamine (**P8**). Yield 0.1977 g, 56.3%

Ferulic diacid + 1,4-diaminobutane (**P9**). Yield 0.1789 g, 51.0%

Ferulic diacid + 1,6-diaminohexane (**P10**). Yield 0.2637 g, 70.6%

Ferulic diacid + 1,8-diaminooctane (**P11**). Yield 0.2529 g, 62.8%

Ferulic diacid + 1,10-diaminodecane (**P12**). Yield 0.3104 g, 73.9%

Ferulic diacid + *m*-phenylenediamine (**P13**). Yield 0.1892 g, 51.3%

Ferulic diacid + *p*-phenylenediamine (**P14**). Yield 0.2494 g, 68.4%

Sinapyl diacid *+* ethylenediamine (**P15**). Yield 0.2228 g, 65.1%

Sinapyl diacid *+* 1,4-diaminobutane (**P16**). Yield 0.2549 g, 68.6%

Sinapyl diacid *+* 1,6-diaminohexane (**P17**). Yield 0.2219 g, 56.5%

Sinapyl diacid *+* 1,8-diaminooctane (**P18**). Yield 0.4804 g, 87.9%

Sinapyl diacid *+* 1,10-diaminodecane (**P19**). Yield 0.4164 g, 74.4%

Sinapyl diacid *+ m*-phenylenediamine (**P20**). Yield 0.4564 g, 78.7%

Sinapyl diacid *+ p*-phenylenediamine (**P21**). Yield 0.3877 g, 78.8%

Infrared (IR) Spectroscopy

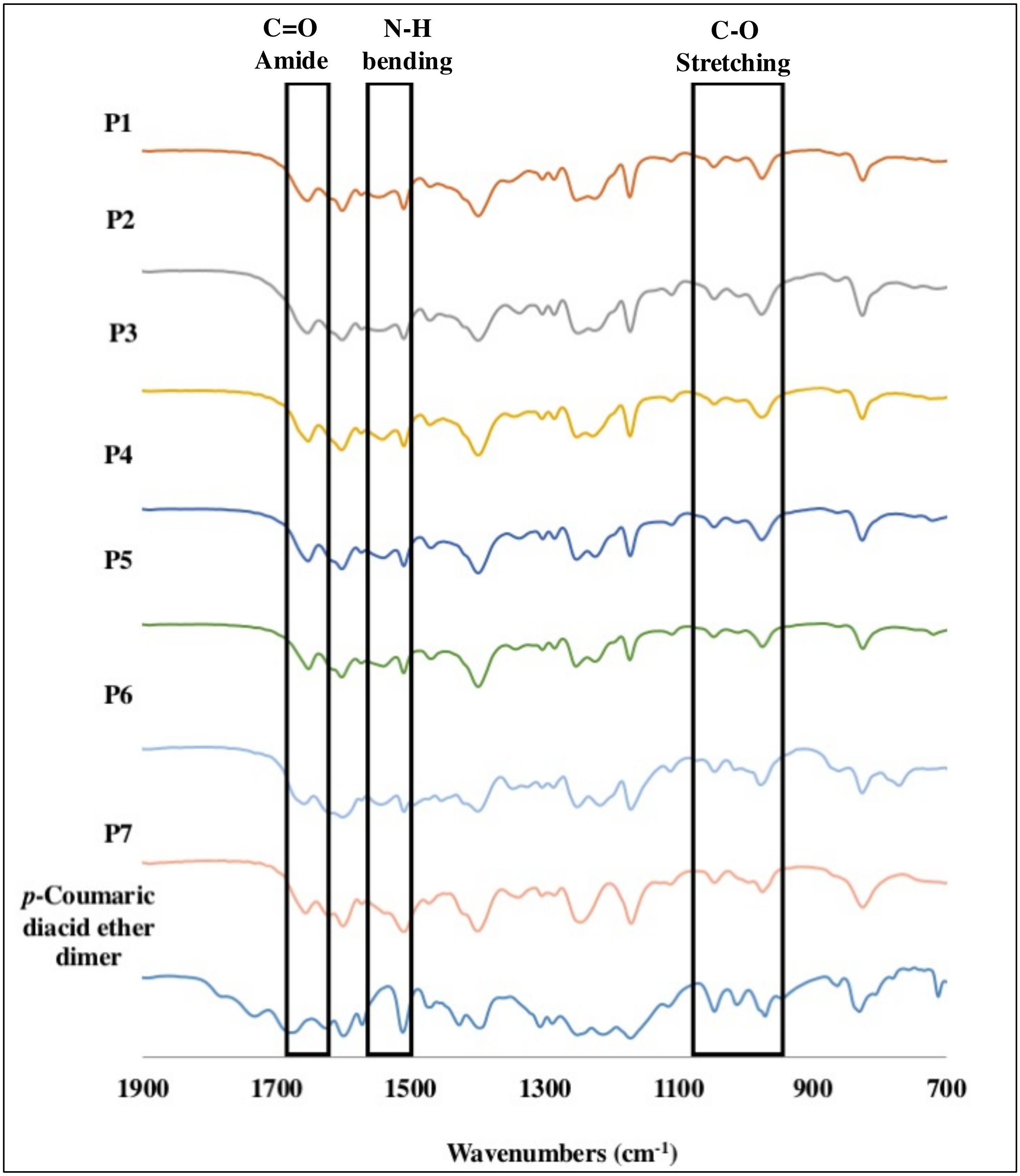

Figure S13: IR fingerprint region of *p*-Coumaryl-based poly(ether-amide)s (**P1-P7**)

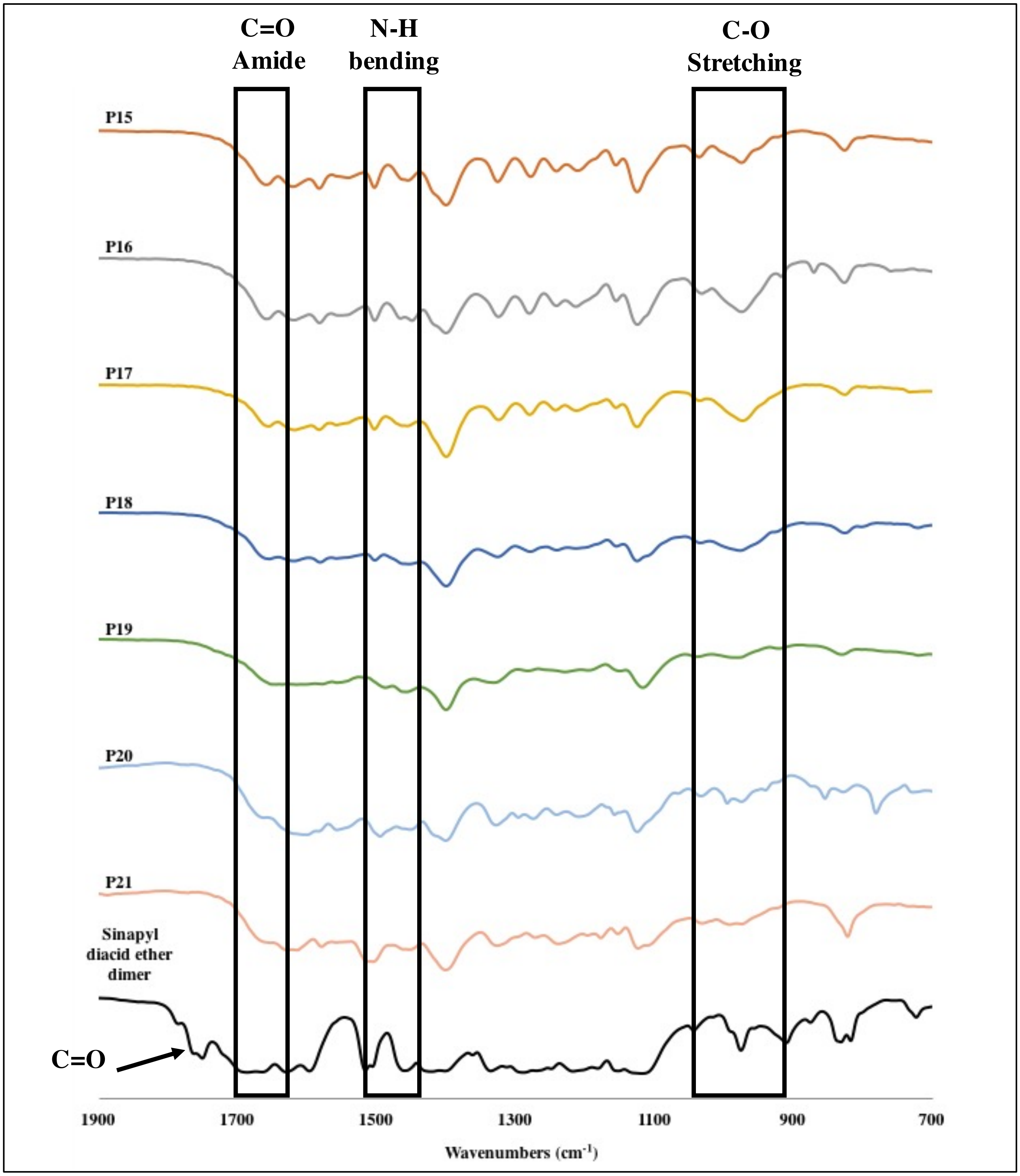

Figure S14: IR fingerprint region of Sinapyl-based poly(ether-amide)s (**P15-P21**)

Gel Permeation Chromatography (GPC)

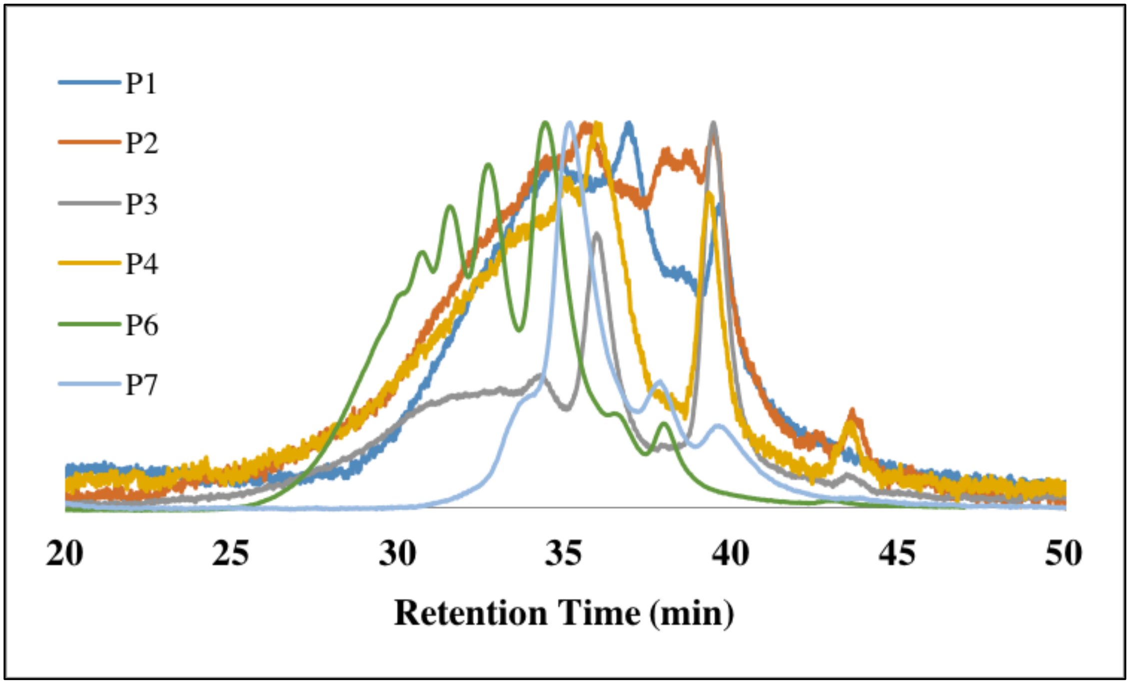

Figure S15: Stacked GPC traces of *p*-Coumaryl-based poly(ether-amide)s (**P1-P7**)

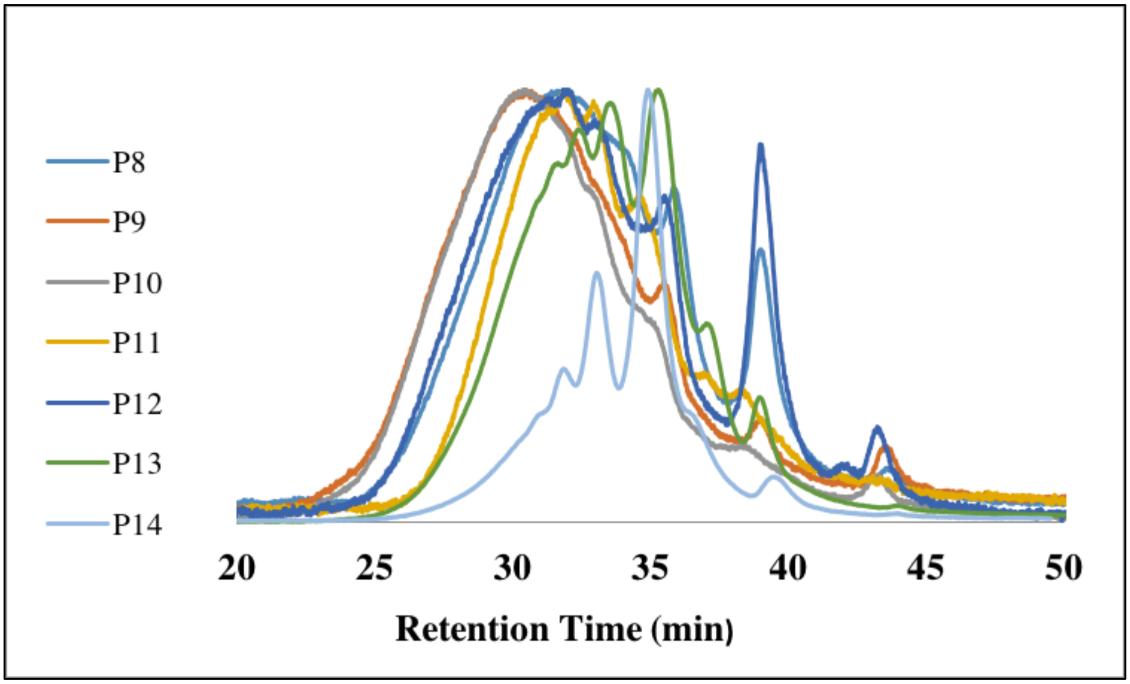

Figure S16: Stacked GPC traces of ferulyl-based poly(ether-amide)s (**P8-P14**)

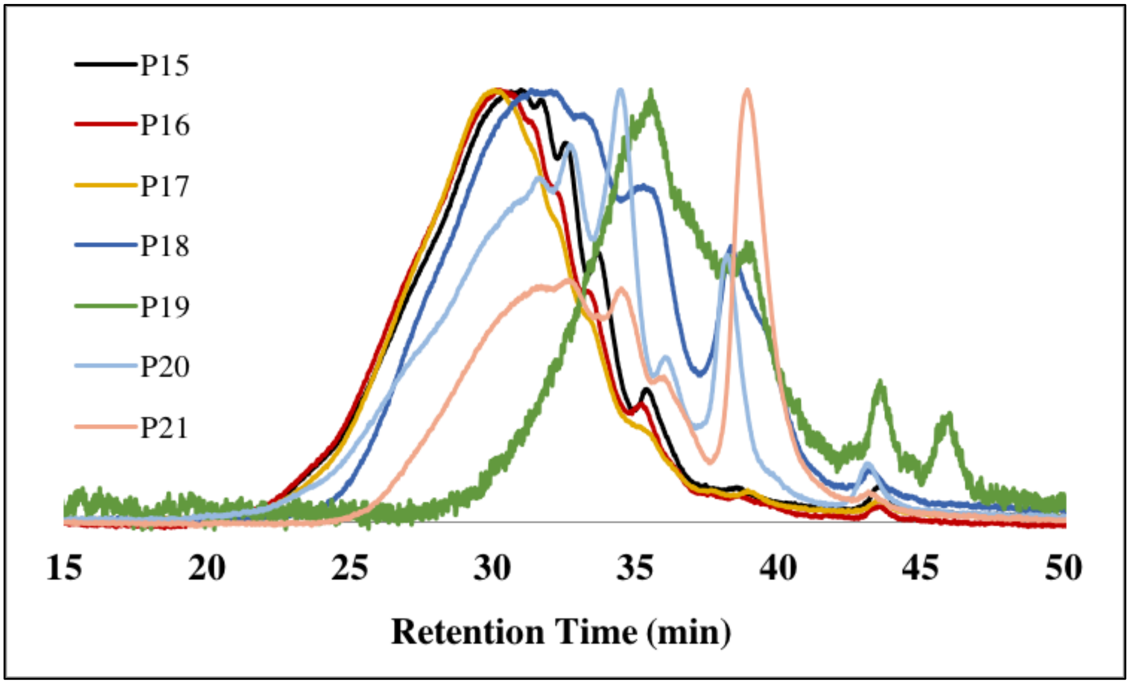

Figure S17: Stacked GPC traces of sinapyl-based poly(ether-amide)s (**P15-P21**)

Thermogravimetric Analysis (TGA)

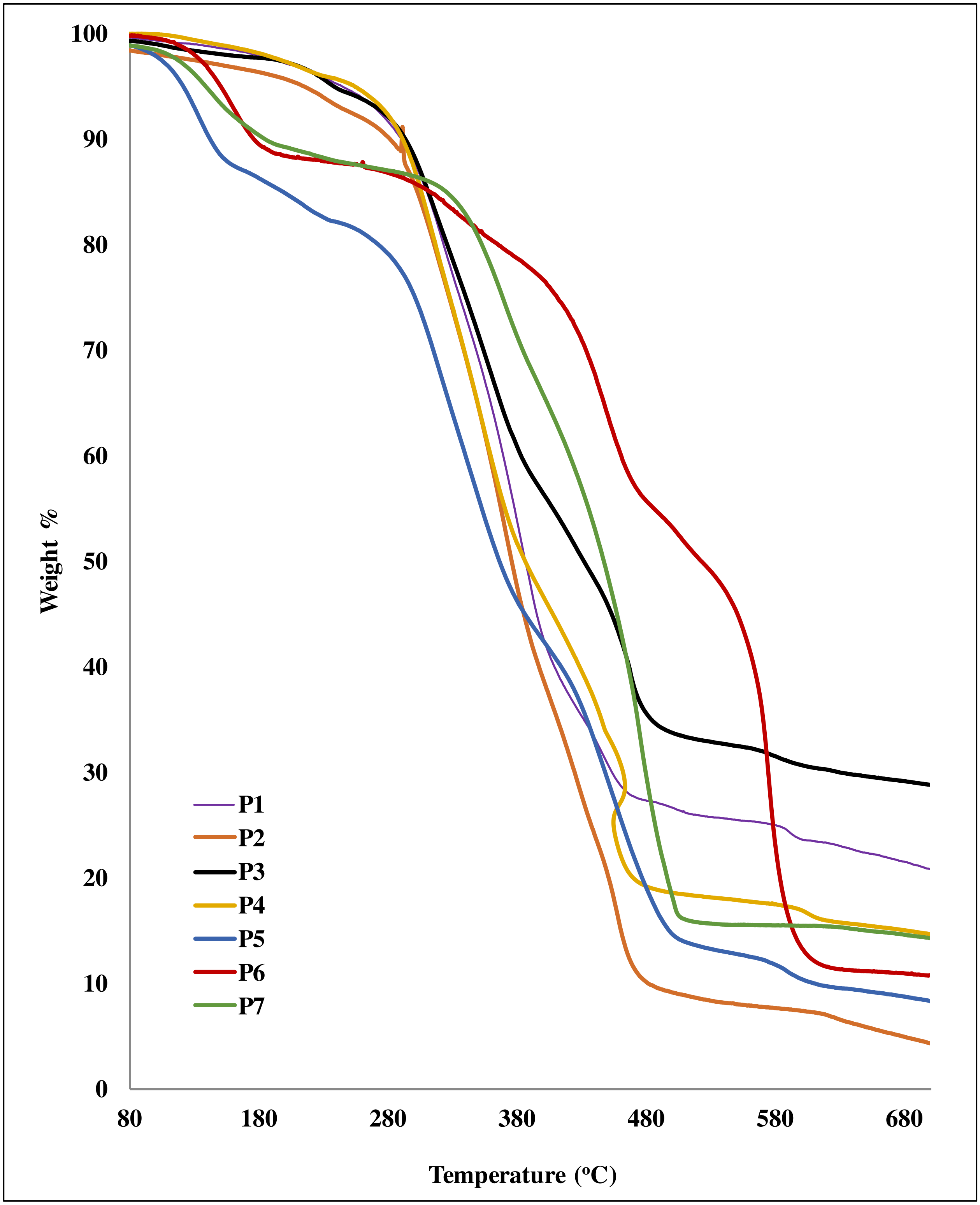

Figure S18: Stacked TGA traces of *p*-Coumaryl-based poly(ether-amide)s (**P1-P7**)

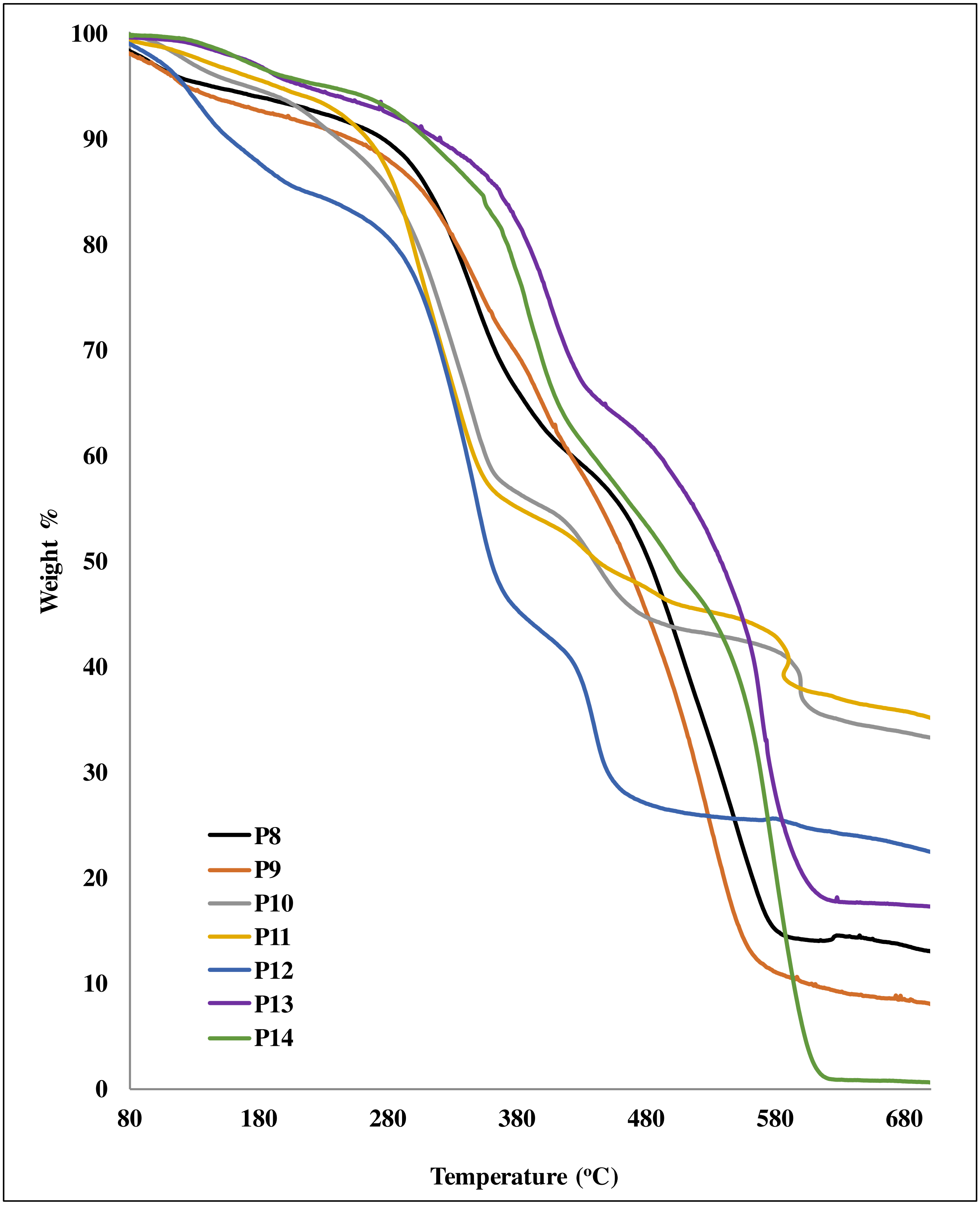

Figure S19: Stacked GPC traces of ferulyl-based poly(ether-amide)s (**P8-P14**)

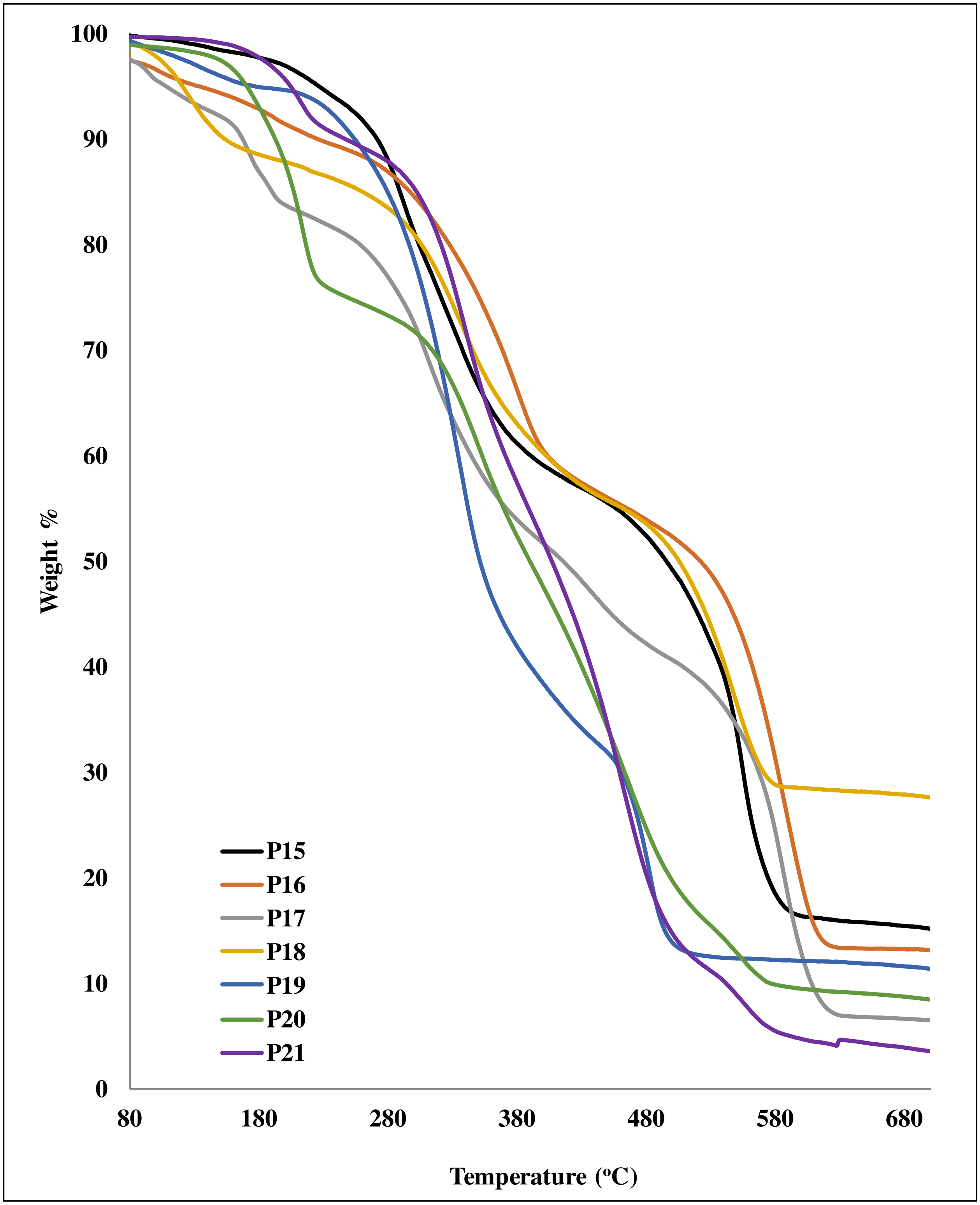

Figure S20: Stacked GPC traces of sinapyl-based poly(ether-amide)s (**P15-P21**)

Differential Scanning Calorimetry

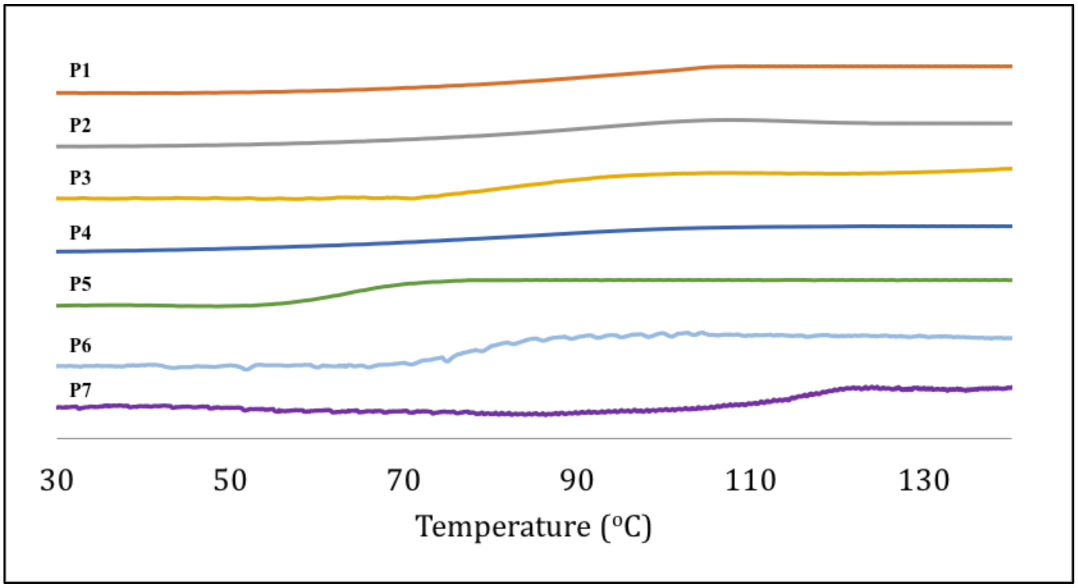

Figure S21: Stacked DSC traces of *p*-Coumaryl-based poly(ether-amide)s (**P1-P7**)

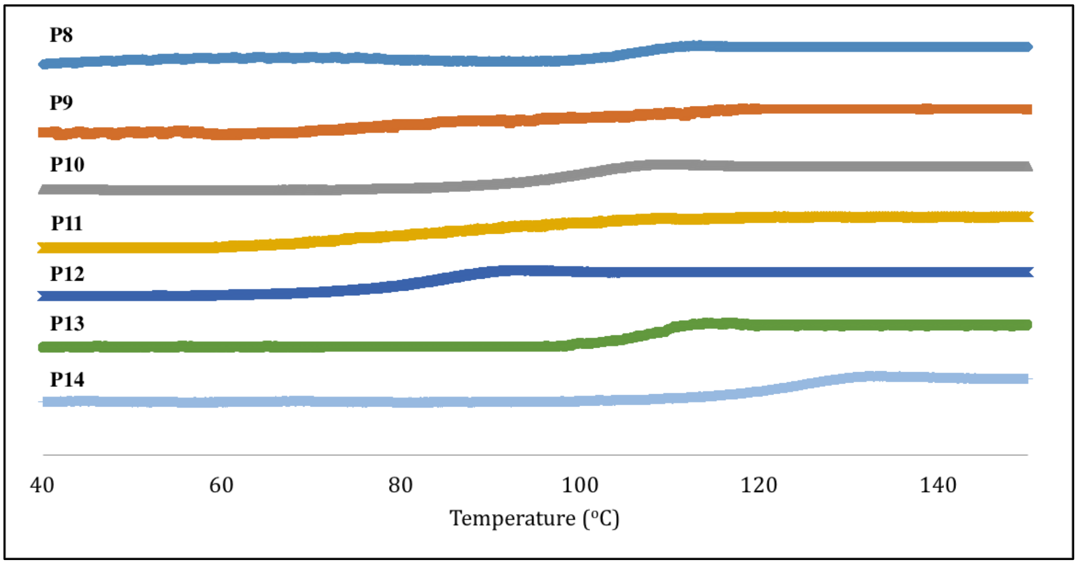

Figure S22: Stacked DSC traces of ferulyl-based poly(ether-amide)s (**P8-P14**)

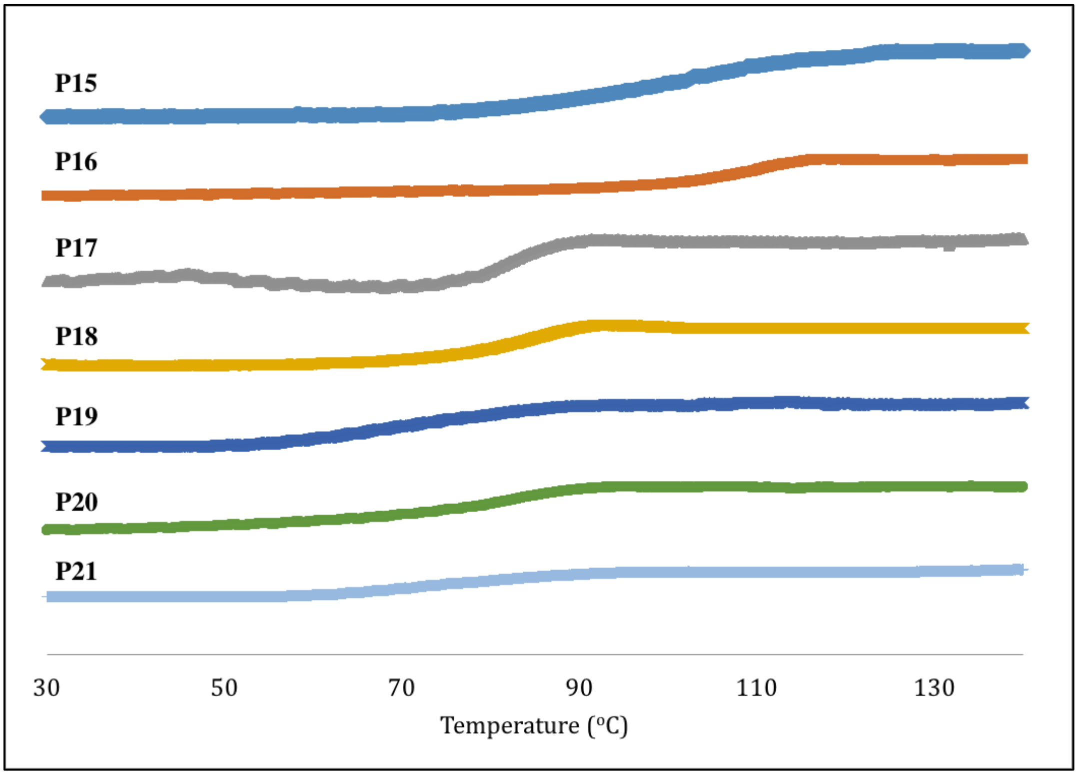

Figure S23: Stacked DSC traces of sinapyl-based poly(ether-amide)s (**P15-P21**)

3.6 References

(1) Berezina, N.; Martelli, S. M. In *Renewable Resources for Biorefineries*; 2014; pp 1–28.

(2) Jambeck, J. R.; Geyer, R.; Wilcox, C.; Siegler, T. R.; Perryman, M.; Andrady, A.; Narayan, R.; Law, K. L. *Science (80-.).* **2015**, *347* (6223), 768.

(3) Mialon, L.; Pemba, A. G.; Miller, S. A. *Green Chem.* **2010**, *12*, 1704.

(4) Mialon, L.; Vanderhenst, R.; Pemba, A. G.; Miller, S. A. *Macromol. Rapid Commun.* **2011**, *32*, 1386.

(5) Hillmyer, M. A.; Tolman, W. B. *Acc. Chem. Res.* **2014**, *47* (8), 2390.

(6) Díaz, A.; Katsarava, R.; Puiggalí, J. *Int. J. Mol. Sci.* **2014**, *15* (5), 7064.

(7) Gandini, A.; Lacerda, T. M.; Carvalho, A. J. F.; Trovatti, E. *Chem. Rev.* **2016**, *116* (3), 1637.

(8) Thakur, V. K.; Thakur, M. K.; Raghavan, P.; Kessler, M. R. *ACS Sustain. Chem. Eng.* **2014**, *2*, 1072.

(9) Ten, E.; Vermerris, W. *J. Appl. Polym. Sci.* **2015**.

(10) Sen, S.; Patil, S.; Argyropoulos, D. S. *Green Chem.* **2015**.

(11) Pion, F.; Ducrot, P.-H.; Allais, F. *Macromol. Chem. Phys.* **2014**, *215*, 431.

(12) Mialon, L.; Vanderhenst, R.; Pemba, A. G.; Miller, S. A. *Macromol. Rapid Commun.* **2011**, *32* (17), 1386.

(13) Oulame, M. Z.; Pion, F.; Allauddin, S.; Raju, K. V. S. N.; Ducrot, P.-H.; Allais, F. *Eur. Polym. J.* **2015**, *63*, 186.

(14) Kuhire, S. S.; Avadhani, C. V.; Wadgaonkar, P. P. *Eur. Polym. J.* **2015**, *71*, 547.

(15) Ouimet, M. A.; Griffin, J.; Carbone-Howell, A. L.; Wu, W. H.; Stebbins, N. D.; Di, R.; Uhrich, K. E. *Biomacromolecules* **2013**, *14* (3), 854.

(16) Ouimet, M. A.; Stebbins, N. D.; Uhrich, K. E. *Macromol. Rapid Commun.* **2013**, *34* (15), 1231.

(17) Ouimet, M. A.; Faig, J. J.; Yu, W.; Uhrich, K. E. *Biomacromolecules* **2015**, *16* (9), 2911.

(18) Nguyen, H. T. H.; Reis, M. H.; Qi, P.; Miller, S. A. *Green Chem.* **2015**, *17* (9), 4512.

(19) Hatfield, G. R.; Guo, Y.; Killinger, W. E.; Andrejak, R. A.; Roubicek, P. M. *Macromolecules* **1993**, *26* (24), 6350.

(20) Delaviz, Y.; Gungor, A.; McGrath, J. E.; Gibson, H. W. *Polymer (Guildf).* **1993**, *34* (1), 210.

(21) Gutch, P. K.; Banerjee, S.; Jaiswal, D. K. *J. Appl. Polym. Sci.* **2003**, *89* (3), 691.

(22) Hajibeygi, M.; Shabanian, M. *Des. Monomers Polym.* **2013**, *16* (3), 222.

(23) Onciu, M. *J. Appl. Polym. Sci.* **2007**, *103* (3), 2013.

(24) Hsiao, S.-H.; Lin, K.-H. *Polymer (Guildf).* **2004**, *45* (23), 7877.

(25) Garcia, J. M.; de la Campa, J. G.; de Abajo, J. *J. Polym. Sci. Part A Polym. Chem.* **1996**, *34*

(4), 659.

(26) Garcia, J. M.; Alvarez, J. C.; De La Campa, J. G.; De Abajo, J. *J. Appl. Polym. Sci.* **1998**, *67* (6), 975.

(27) Wittbecker, E. L.; Morgan, P. W. *J. Polym. Sci. Part A Polym. Chem.* **1996**, *34* (4), 521.

(28) Morgan, P. W.; Kwolek, S. L. *J. Chem. Educ.* **1959**, *36* (4), 182.

(29) Morgan, P. W. In *Condensation Polymers: By Interfacial and Solution Methods*; Interscience: New York, 1965; pp 65–115.

(30) Morgan, P. W.; Kwolek, S. L. *Macromolecules* **1975**, *8* (2), 104.

(31) Wang, L.; Wang, Y.; Ren, L. *J. Appl. Polym. Sci.* **2008**, *109* (2), 1310.

(32) Vlachopoulos, J.; Strutt, D. *Mater. Sci. Technol.* **2003**, *19* (9), 1161.

(33) Davidson, D.; Bernhard, S. A. *J. Am. Chem. Soc.* **1948**, *70* (10), 3426.

(34) Smith, A. M. R.; Rzepa, H. S.; White, A. J. P.; Billen, D.; Hii, K. K. *J. Org. Chem.* **2010**, *75* (9), 3085.

(35) Botkin, J. H.; Forsyth, D. A.; Sardellaib, D. J. *J. Am. Chem. Soc.* **1986**, *108* (11), 2797.

Chapter 4: Monolignol-based oligomers as plasticizers in polystyrene and poly(lactic acid) polymer blends

4.1 Introduction

Poly(styrene-co-maleic anhydride) (pSMA) is a nearly-perfect alternating copolymer of styrene and maleic anhydride. Maleic anhydride is unable to be homopolymerized, but when copolymerized with styrene, the copolymer is readily formed[1]. The exact mechanism for this polymerization is still debated, however the alternating copolymer is likely formed by one of two mechanisms[2]. The complex participation model relies the formation of charge-transfer complexes between electron-rich styrene and electron-poor maleic anhydride to describe the alternating behavior. The penultimate unit model states the identity of the penultimate unit controls radical reactivity to generate the alternating structure. pSMA is most commonly produced using uncontrolled free radical polymerization methods, however controlled radical polymerization methods, such as nitroxide-mediated polymerization (NMP)[3–5] or reversible addition-fragmentation chain transfer polymerization (RAFT)[6–10], have been studied. Both high and low molecular weight pSMA are commercially available; high molecular weight pSMA is typically used for engineering plastics while low molecular weight pSMA is used as a surfactant, as a papermaking additive, or in polymer-protein conjugates[2]. While these materials have a wide range of applications, both monomers used in this process are derived from petroleum[11]. With the decline of petroleum reserves[12] and an increase in environmental effects of petroleum-based plastic waste[13], both consumers and producers are seeking bio-based alternatives to traditional materials.

In addition to concerns regarding the environmental impact of polymeric materials, with the prevalence of additives increasing in everyday products and an increased chance of exposure due to polymer degradation or plasticizer leaching, the health effects and safety of certain polymeric materials have come into question. Most recently, there has been a large push to remove commonly utilized aromatic monomer and plasticizer additive bisphenol A (BPA) from polymeric products due to known health effects with significant exposure. Bisphenol A was first synthesized in the 1890s and later tested as a synthetic form of estrogen by Dodds in the 1930s.[14] BPA was found to be drastically less effective as a synthetic form of estrogen than other synthetic compounds, and instead was later utilized in the formation of plastics, such as polycarbonates, or as an antioxidant in plasticizers. Despite widespread commercial use, a BPA is a known endocrine disruptor and a significant body of literature has been published suggesting that BPA may adversely affect humans, even at low-dose exposures[15,16]. Therefore, consumer and scientific concerns have led to the search for alternative aromatic polymers with useful properties but without the associated adverse effects.

The only commercial non-petroleum source of aromatic chemicals is from the degradation of lignin. Found in the cell wall of plants, lignin is an aromatic polymer composed of three different cinnamaic acid monomers known as monolignols. While lignin features a poorly defined polymeric structure, monolignols are well-defined, aromatic small molecules, making them ideal for use in polymer synthesis. Moreover, monolignols can be described as β-substituted styrenes, as they feature a degree of unsaturation in their aliphatic side chain. Monolignols have yet to be isolated from lignin, however their precursor aldehydes are readily accessible, as exemplified by the commercial production of vanillin from lignin[17]. Beginning from the corresponding aldehyde, monolignols can be synthesized on large scales and in high yields in three steps[18]. While these pseudo-styrene monomers are typically polymerized using oxidative coupling methods, other polymerization methods could also be employed.

Itaconic acid is an aliphatic, dicarboxylic acid featuring an α,β-unsaturated double bond. With a worldwide production volume of 80,000 tons per year, itaconic acid is prepared industrially via the fermentation of carbohydrates with *Aspergillus terreus*[19]. In addition to its high production volume, the preparation of itaconic acid is relatively inexpensive, costing approximately $2 per kg (USD) to produce[20]. Citraconic anhydride is rapidly prepared from itaconic acid in a one-pot, two-step synthesis[21]. Citraconic anhydride has a complimentary structure to maleic anhydride, and thus is considered a bio-based mimic (**Figure 4.1**). With vigorous heating of itaconic acid, itaconic anhydride is rapidly formed by the elimination of water. Upon additional heating, itaconic anhydride undergoes a double bond rearrangement to form citraconic anhydride.

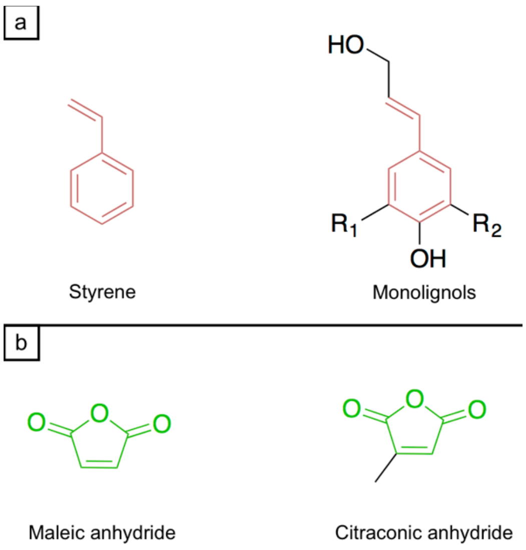

Figure 4.1 Structural similarities between a) styrene and monolignols and b) maleic anhydride and citraconic anhydride.

While monolignols and citraconic anhydride possess structural similarities to styrene and maleic anhydride, respectively, their polymerization and copolymerization is inherently more complicated. Monolignols feature two hydroxyl functional groups which could both serve as chain transfer sites during radical polymerizations, causing a reduced degree of polymerization, branching, or even inhibiting polymerization. In addition to the hydroxyl functional groups, monolignols are also pseudo-β-substituted styrenes, which typically feature reduced polymerization rates compared to unsubstituted styrenes, due to steric

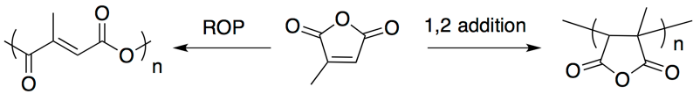

Figure 4.2 Polymerization of citraconic anhydride either via ring-opening polymerization (ROP) or 1,2-addition

hinderance[22,23]. Citraconic anhydride possesses an additional methyl group, which again could reduce the polymerization rate due to steric hindrance. Furthermore, citraconic anhydride is capable of undergoing polymerization either by ring-opening or by 1,2-addition, complicating possible reaction pathways or the resulting polymeric structures (**Figure 4.2**). With this in mind, we looked into the literature for previous work regarding the polymerization or copolymerization of similar monomers.

Synthetic lignin is typically prepared via a radical oxidative coupling process using horseradish peroxidase and hydrogen peroxide. However, as monolignols feature several sites capable of radical formation, the resulting polymer has a poorly defined final structure similar to that of native lignin. Due to the high degree of functional groups found in monolignols, simplified phenylpropanoid monomers such as isoeugenol, isosafrole, and anethole are typically chosen to represent monolignols instead. Satoh et al. reported the synthesis of linear lignin analogues by the cationic polymerization of anethole and isoeugenol initiated by boron trifluoride etherate (**Scheme 4.1**)[24]. With the addition of excess water and 4-methoxy-α-methylbenzyl alcohol, Satoh and coworkers were able to produce perfectly alternating co-polymers with molecular weights from 3.2 to 8.9 kDa and dispersity between 1.25 and 1.54. Nonoyama et al. studied the copolymerization

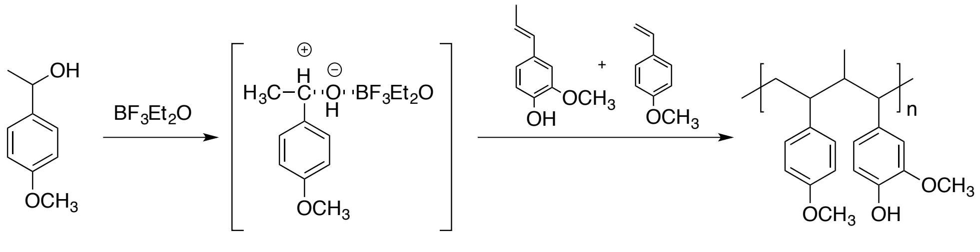

Scheme 4.1 Aqueous-controlled cationic copolymers from naturally occurring ß-methyl styrenes by Satoh et al[24].

of a series of naturally occurring β-methylstyrenes and acrylate monomers using either uncontrolled free radical polymerization or RAFT[25]. With the use of fluoroalcohols, such as 1,3-bis(2-hydroxyhexafluoroisopropyl)benzene, instead of toluene, they were able to increase molecular weight of the copolymers, as well as the incorporation of the β-methylstyrene monomer. The relative reactivity rate of the β-methylstyrene to the acrylate was shown to increase two to three times in fluorinated solvents. While the conversion and incorporation of the β-methylstyrene monomer was lower with RAFT in comparison to uncontrolled free radical polymerization, the resulting copolymers exhibited lower dispersity and higher glass transition temperatures, proving the utility of naturally occurring β-methylstyrenes as comonomers. In addition to work with β-methylstyrenes, Satoh and coworkers also synthesized a series of copolymers from naturally occurring terpenes and maleimide derivatives. Unlike the previously utilized, naturally-occurring β-methylstyrene monomers, terpenes are non-polar and do not feature any oxygenation. The use of these monomers could enable a higher degree of polymerization by mitigating potential side and chain transfer reactions. Matsuda et al. reported the selective 1:2 alternating copolymerization of a series of terpenes and electron-poor malemides via uncontrolled free radical polymerization in fluorinated solvents[26]. The copolymers obtained varied from 2.7 to 33.5 kDa and featured dispersities between 1.61 and 4.15. By varying quantities of both monomers, they determined both the steric bulk of the terpene monomer as well as hydrogen bonding between the fluorinated solvent and maleimide monomer units were crucial to the formation of the 1:2 alternating copolymer. The compilation of this and other work by Satoh and coworkers[27], provides inspiration that despite potential side reactions, monolignols could be utilized in the development of a bio-based poly(styrene-co-maleic anhydride) mimics.

With this in mind, we set out to develop a series of copolymers from monolignols and citraconic anhydride. Based on success in similar systems in the literature, we attempted to utilize both uncontrolled free radical and cationic polymerization to form the desired copolymer. However, despite several attempts and by modifying reaction conditions, we were unable to form the desired copolymer. Instead, utilizing cationic polymerization (with BF_3Et_2O), we were able to generate small oligomers of monolignols featuring an alternating pattern of intact and partially dehydroxylated monolignol monomers. There was no incorporation or conversion of citraconic anhydride, possibly due to an undesired ring-opening side reaction. These oligomers were then utilized as plasticizers in the preparation of polymer blends with either recycled polystyrene or poly(lactic acid). Little effect was seen in blends with polystyrene but, blends from PLA featured decreased glass transition temperatures, suggesting improvement to the brittle nature of poly(lactic acid). This chapter will focus on the synthesis of linear monolignol oligomers, the development of polymer blends from polystyrene and poly(lactic acid), and the study of the physical and thermal properties of the resulting polymer blends.

4.2 Results and Discussion

Synthesis of monolignols and citraconic anhydride. While many methods to degrade lignin exist, methods to specifically isolate monolignols from lignin have yet to be developed. Due to the promiscuous nature of the polymerization *in planta*, the double bond in the aliphatic chain is typically reacted into the polymeric structure via the formation of either ether or carbon-carbon bonds (**Figure 4.3**). Additionally, monolignol radicals favor

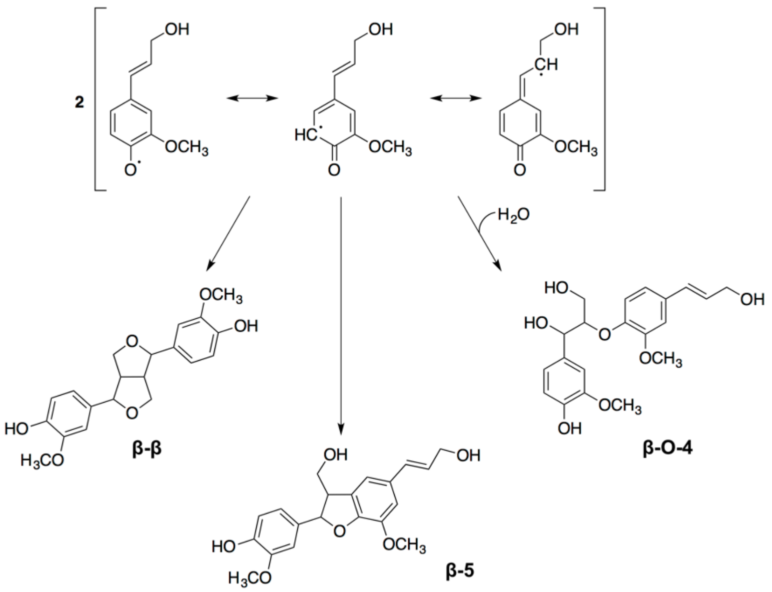

Figure 4.3 Most common linkages formed in lignification by radical coupling: β-O-4, β-5, and β-β

coupling at the β-position, resulting in primarily β-O-4, β-5, and β-β linkages in native lignin[28]. While ether bonds are cleavable under harsh chemical conditions, none of these methods are able to restore the α-β double bond. Instead, monolignols are produced in three steps from precursor aldehydes, 4-hydroxybenzaldehyde, vanillin, or 3,5-dimethoxy-4-hydroxybenzaldehyde, all of which are available from lignin (**Scheme 4.2**). The aliphatic side chain was added by a Doebner-modified Knoevenagel condensation with malonic acid, yielding *p*-coumaryl, ferulic, or sinapyl acid, respectively. The resulting carboxylic acid was converted to the corresponding methyl ester and then reduced to the primary alcohol using diisobutylaluminum hydride (DIBAL-H), yielding the desired monolignol as the final product. Citraconic anhydride was prepared in a one-pot, two-step reaction from itaconic acid (**Scheme 4.3**). Itaconic acid was rapidly heated to form itaconic anhydride through the elimination of water. Upon further heating, itaconic anhydride under goes a

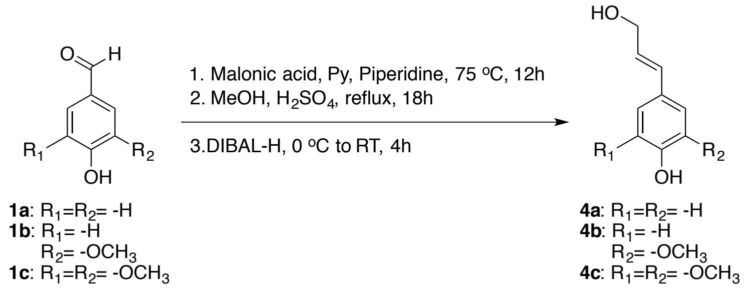

Scheme 4.2 Monolignol (4 a, b, and c) synthesis from precursor aldehydes (1a, b, and c) in three steps

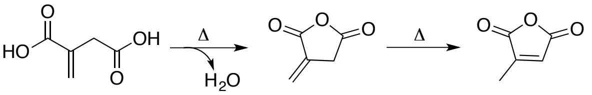

Scheme 4.3 Synthesis of citraconic anhydride from itaconic acid

double bond rearrangement to yield citraconic anhydride. The preparation of all four monomers was facile and generally high yielding. In the case of citraconic anhydride in particular, the synthesis is entirely green as it is run neat, without the addition of other chemicals, and the only byproduct is water. With these materials in hand, copolymerizations to produce bio-based poly(styrene-co-maleic anhydride) mimics were attempted.

Polymerization of monolignols and citraconic anhydride. While numerous components of previous work by Satoh and coworkers can be applied to our system, the polymerization of phenylpropanoids as a linear lignin mimics feature the most structural similarity to our targeted system. With this in mind, we first attempted the synthesis of poly(monolignol-co-citraconic anhydride) utilizing conditions similar to that as reported by Satoh et al. (**Scheme 4.4**)[24]. Equimolar quantities of the desired monolignol and citraconic anhydride were combined in an ampule, along with 4-methoxy-α-methylbenzyl alcohol (0.02 eq), water (0.005 eq), and a mixture of acetonitrile and dichloromethane (4:1). The solution was frozen in liquid nitrogen and a 10 mM solution of BF_3Et_2O in acetonitrile was added. Upon addition, the mixture was rapidly frozen to prevent the reaction from occurring and the ampule was sealed. The ampule was allowed to slowly warm to room temperature and stir for the desired length of time before the product was isolated via precipitation.

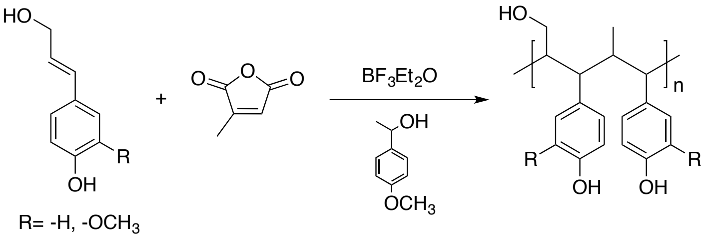

Scheme 4.4 Copolymerization of *p*-coumaryl or coniferyl alcohol and citraconic anhydride with boron trifluoride etherate and 4-methoxy-α-methylbenzyl alcohol.

Table 4.1 Molecular weight characterization of oligomers via gel permeation chromatography (GPC)

	Monolignol	**Catalyst**	**Catalyst loading**	**Reaction Time (h)**	**M_n**	**M_w**	**$Đ$**
O1	*p*-coumaryl	BF_3Et_2O	0.5 mol%	72 h	870	1490	1.72
O2				168 h	670	1360	2.01
O3				338 h	820	1690	2.09
O5				678 h	900	1570	1.73
O6		AIBN	1 mol%	48 h	1100	1660	1.51
O7			5 mol%	48 h	OR	OR	OR
O8			1 mol%	96 h	950	1280	1.35
O9			5 mol%	96 h	OR	OR	OR
O10	Coniferyl	BF_3Et_2O	0.5 mol%	72 h	1140	1820	1.60
O11				168 h	1490	2100	1.40
O12				338 h	830	1470	1.77
O14				678 h	2080	2680	1.29
O15		AIBN	1 mol%	48 h	990	1420	1.43
O16			5 mol%	48 h	OR	OR	OR
O17			1 mol%	96 h	1070	1470	1.38
O18			5 mol%	96 h	OR	OR	OR

GPC in THF (1.0 mL/min). OR= out of range. $Đ = M_w/M_n$

Initially, reactions were allowed to stir for 72 hours but low molecular weight products obtained (**Table 4.1**) suggested the polymerization was slower than what is typically observed in cationic polymerizations. Despite increasing the reaction time up to 678 hours, the molecular weight of the isolated oligomers did not increase beyond 2.1 kDa. Additionally, regardless of the reaction conditions, none of the products isolated featured any incorporation of the citraconic anhydride monomer. Homopolymerizations of citraconic anhydride showed no conversion even after the increased reaction time, which is not surprising given the similar behavior of maleic anhydride. Homopolymerizations of each monolignol generated similar oligomeric products, suggesting that citraconic anhydride served no role in monolignol oligomerization and was therefore eliminated from later reactions featuring BF_3EtO_2 as an initiator.

Citraconic anhydride is known to undergo ring-opening polymerization with Lewis acidic catalysts, such as magnesium diethoxide and aluminium triisopropoxide[29]. We speculate that citraconic anhydride was unable to be polymerized in this system via cationic polymerization due to an undesired ring-opening side reaction. As boron trifluoride etherate is a strong Lewis acid, we hypothesize that a stable, ring-opened citraconic anhydride intermediate is formed, preventing polymerization. However, attempts to isolate and characterize this proposed boron-based intermediate were unsuccessful. As removal of citraconic anhydride did not increase the molecular weight of the final oligomer, this side reaction is likely minimal and does not consume a large quantity of the polymerization catalyst. This supported by ^{11}B NMR (Figure S1), in which two products are seen upon reaction of BF_3Et_2O and citraconic anhydride. Two boron products are formed with citraconic anhydride only, the dominant of which appears to be different than that formed with either ferulic alcohol only or the mixture. This is suggestive that either the monomers feature staggeringly different reactivity ratios and citraconic anhydride is less reactive for cationic polymerization, or the stable intermediate is observable but formed in low quantities.

Despite the minimal side reactions, uncontrolled free radical polymerization with azobisisobutylnitrile (AIBN) was also attempted. Once again, both monomers were combined in a 1:1 ratio along with AIBN (either 1 or 5 mol%) and DMF. The solution was transferred to an ampule, degassed, and the ampule was sealed. The sealed ampules were heated to 70 ^{o}C for either 48 or 96 hours. Regardless of the monolignol, the product was unable to be precipitated from solution with a several non-solvents, possibly due to high product solubility in DMF. All polymerizations showed no incorporation of citraconic anhydride and required lower initiator concentration to yield oligomers. At higher initiator concentrations, the products isolated appeared to be monomers or small molecule byproducts by ^{1}H NMR due to lack of signal shifting and broadening. By GPC, observed oligomeric products were below the molecular weight of the lowest polystyrene standard used (M_n=682), confirming the low molecular weight products seen in ^{1}H NMR. Monolignol identity did affect oligomerization however, as oligomers were only obtained from reactions with either *p*-coumaryl alcohol or coniferyl alcohol.

As similar oligomers could also be isolated from free radical polymerization, the proposed cationic mechanism from Satoh utilizing BF_3Et_2O-activated 4-methoxy-α-methylbenzyl alcohol as an initiator complex is likely not the mechanism for this polymerization reaction. While the exact initiator species is currently unknown, we are working to elucidate the oligomerization mechanism and rationale for the observed alternating structure. We are also working to determine a rationale for the lack of polymerization or oligomerization with the dimethoxy-substituted monolignol, sinapyl alcohol. Finally, regardless of polymerization method, increasing the reaction time had no effect on incorporation of citraconic anhydride and minimal effect on the molecular weight of the oligomeric product obtained.

Molecular weight and structural characterization. Oligomers from the cationic and free radical polymerizations were characterized via ^{1}H NMR spectroscopy, gel permeation chromatography (GPC), and matrix-assisted laser-desorption/ionization (MALDI) spectrometry to determine both relative molecular weight and structure of the isolated oligomeric products. All oligomeric products obtained, regardless of polymerization method, were less than 2.1 kDa (**Table 4.1**), relative to polystyrene, and showed moderate dispersity. Lack of citraconic anhydride incorporation was seen by ^{1}H NMR and confirmed by MALDI. Most interestingly, the structure of oligomers produced via cationic polymerization with BF_3Et_2O appear to be alternating copolymers of intact and dehydroxylated monolignols (**Figure 4.4** and S2). Further structural characterization of these oligomers is currently being pursued by a collaborator using 2D mass spectrometry techniques.

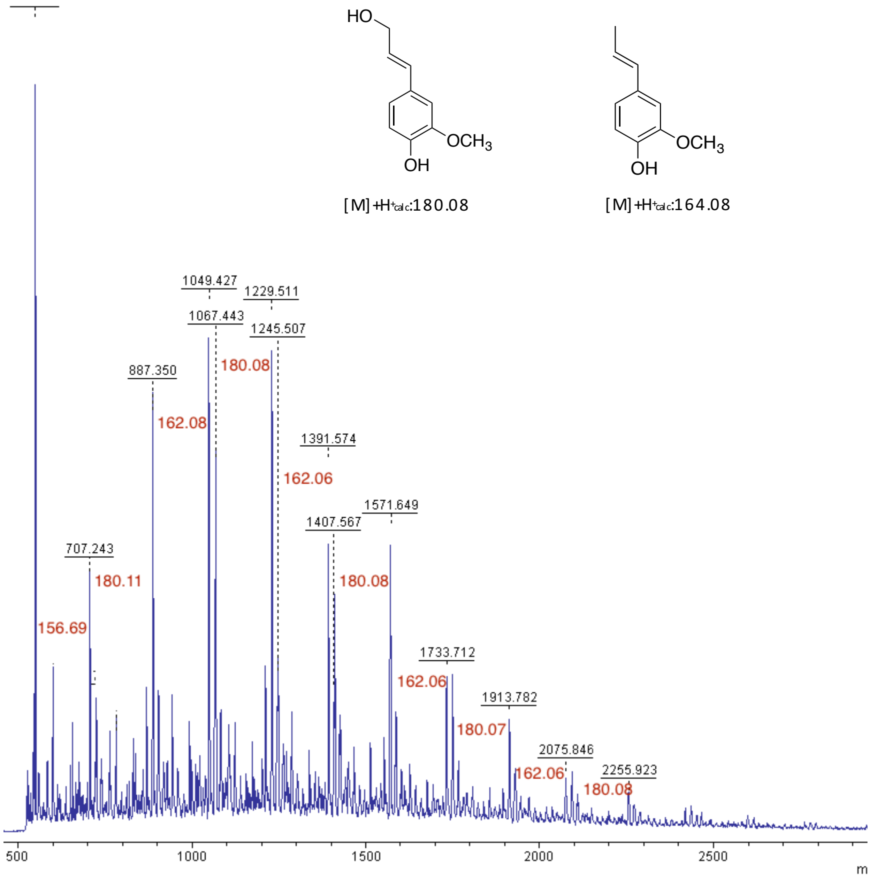

Figure 4.4 MALDI-TOF spectra of O11 showing alternating structure of intact and reacted monomer.

Synthesis of polymer blends. Bio-based polymers have the potential to eliminate both environmental and sustainability issues found with petroleum-based plastics. However, bioplastics are plagued with challenges such as high production cost, poor performance, and variability of properties with feedstock variability. Plasticizers are typically small, organic molecules added to polymers to improve processability, flexibility, and durability[30]. By reducing interchain interactions, the addition of plasticizers decreases structural rigidity, allowing deformation without failure. Ideal plasticizers for bio-based plastics are biodegradable, non-volatile, non-toxic, and significantly lower the material's glass transition temperature (T_g)[31].

Poly(lactic acid) (PLA) is a biodegradable, renewable, and biocompatible thermoplastic with potential biological, medical, and pharmaceutical applications. While poly(lactic acid) offers great potential as a replacement commodity material, it features poor impact strength, limited thermal processability, brittleness, hydrophobicity, and high cost; all of which impede its use commercially[32]. Due to its promise, significant effort has been put in identifying new plasticizers for different commercial uses of PLA[33]. In addition to small molecules, such as glycerol, or oligomers, such as oligomeric lactic acid, polymers have also

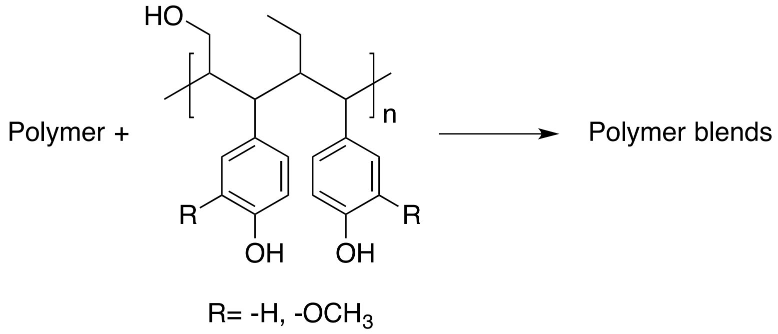

Table 4.2 Glass transition and melting temperatures for polymer blends from poly(lactic acid) and polystyrene

	Polymer	R	Oligomer %[a]	T_g[b]	T_m[c]
	Poly(lactic acid)	-	-	61.1	152.9
PB1		-H	5	57.4	149.9
PB2		-H	10	56.9	148.7
PB3		-H	20	52.6	-
PB4		-H	30	50.1	-
PB5		$-OCH_3$	5	60.8	150.8
PB6		$-OCH_3$	10	58.8	149.2
PB7		$-OCH_3$	20	50.4	147.1
PB8		$-OCH_3$	30	43.6	143.3
	Polystyrene	-	-	102.2	-
PB9		-H	5	101.4	-
PB10		-H	10	100.9	-
PB11		$-OCH_3$	5	101.6	-
PB12		$-OCH_3$	10	100.5	-

[a]Oligomer %= w/w%; [b] Determined by DSC; [c] Samples were not heated high enough to observe T_m for polystyrene

been utilized to lower T_g and improve mechanical properties[30]. Limitations of current plasticizers include lack of thermal stability, biocompatibility issues, cost, need for higher loading to offset PLA cost, and need for increased ductility and performance[30]. With this in mind, we set out to determine if the monolignol-based oligomers obtained by BF_3Et_2O-inititiated cationic polymerization could be used as plasticizers for poly(lactic acid) or polystyrene.

For these experiments, poly(lactic acid) was obtained from recycled PLA-based salad containers (Nature's PLAstic), as we were interested in using commercial materials and improving their physical and mechanical properties. The containers were finely divided, dissolved in chloroform, and precipitated from methanol to isolate PLA. Polymer blends were formed from a PLA dissolved in a mixture of dichloromethane and acetone, with varying amounts of oligomers from either coniferyl or *p*-coumaryl alcohol (PB1 and PB8). The volatile mixture of solvents was allowed to evaporate and once dried, the films were placed under vacuum overnight to ensure the removal of any volatile components. Concentrations as low as 5% and as high as 30% (w/w%) were produced and studied (**Table 4.2**). Polymer blends were also produced with polystyrene, which was also isolated from a recycled source, utilizing similar methods to those described above. For these blends, polystyrene was isolated by dissolving and precipitating a Styrofoam cooler lid. The resulting physical and mechanical properties of both the PLA and polystyrene blends were then studied.

Characterization of polymer blends. As mentioned previously, one of the key effects of a plasticizer is the reducing of polymer brittleness, as seen in a reduction of the glass transition temperature (T_g). In addition, to identifying improved physical properties,

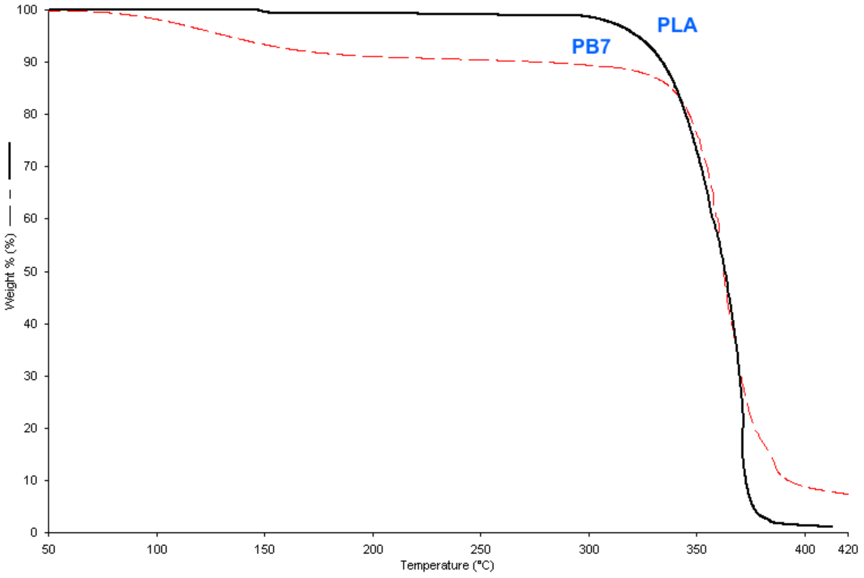

Figure 4.5 Comparison of thermal stability of PLA and PB7

T_g can also be used to identify if the polymer and plasticizer are miscible. Typically, if the two materials are miscible the T_g of the blended material will possess only one T_g, that occurs at a lower temperature than the non-blended starting material. If the materials are immiscible (and the plasticizer has a T_g), two glass transition temperatures will appear in the DSC trace, corresponding to each component. By visual inspections, all PLA and polystyrene blends appeared macroscopically miscible as pale orange, translucent films. In the case of the PLA blends produced, all blends appeared miscible by DSC, as only one glass transition temperature was observed. Significant lowering of T_g was not noted until at least 10% oligomer was added, however at high concentrations T_g and T_m were lowered significantly (Table 4.2). The high quantity of plasticizer required can be seen as a benefit in this case, as the plasticizer would also act as a filer to reduce the quantity of PLA needed ultimately lowering the cost of the final material. Additionally, the oligomers used are markedly larger than small molecules typically utilized as plasticizers. The increased size and non-volatility of these oligomers could minimize (or even eliminate) leeching from the material, a known issue that occurs commonly with plasticizers.

Polystyrene blends (PB9 to PB12) were also miscible, but less of an effect was seen by the addition of either oligomer. We believe this diminished effect may be due to the high similarity of the structures, as both oligomers are produced from the polymerization of β-substituted styrenes. With this negligible improvement in performance, only PLA blends were utilized in further physical and mechanical testing. PLA is known for poor thermal stability, so we were interested to determine if the addition of an aromatic-based plasticizer improved overall thermal stability. Unfortunately, the blends showed reduced initial thermal stability in comparison to pure PLA (**Figure 4.5**). However, the materials showed a higher char yield than pure PLA, due to the aromatic content of the plasticizer. Polystyrene blends showed no significant change in their thermal decomposition profile.

4.3 Conclusions

This chapter has focused on the synthesis of monolignol-based oligomers from *p*-coumaryl and coniferyl alcohol. While the obtained oligomers were not the initial synthetic targets, they proved to exhibit interesting structural and chemical properties. Regardless of the type of polymerization utilized (cationic or free-radical), we were unable to incorporate citraconic anhydride as a monomer. We speculate this difficulty arises from either a side reaction with the catalyst (in the case of BF_3Et_2O) or due to steric constraints, as the monomer features a pendant methyl group. Additionally, Satoh et al. reported no interaction of BF_3Et_2O and the hydroxyl functional group of isoeugenol, however by MALDI-TOF mass spectrometry, we determined that oligomers were formed between intact and dehydroxylated monolignols. While we speculate the pendant hydroxyl group reacted instead of the aromatic hydroxyl, we are still in the process of determining the exact oligomer structure. While the development of these materials was not intended, oligomers of *p*-coumaryl and coniferyl alcohol proved to be miscible, effective, bio-based plasticizers for

PLA. While the mechanical properties of these materials have yet to be tested, the significant improvement in the T_g of PLA is suggestive that the mechanical properties will also exhibit marked improvement compared to the initial material.

4.4 Experimental Section

Materials. 4-hydroxybenzaldehyde (98%, TCI America), vanillin (99%, Alfa Aesar), 3,5-dimethoxy-4-hydroxybenzaldehyde (98%, Acros), malonic acid (99%, Alfa Aesar), piperidine (99%, Spectrum), aniline (99%, Sigma Aldrich), methanol (ACS grade, Fisher), sulfuric acid (conc., ACS Grade, Fisher), 1.0 M DIBAL-H in hexanes (Acros), 4-methoxy-α-methylbenzyl alcohol (95%, Alfa Aesar), itaconic acid (99%, Alfa Aesar), acetonitrile (HPLC grade, Fisher), dichloromethane (ACS grade, Fisher) and N,N-dimethylformamide (HPLC grade, Alfa Aesar) were purchased and used as received. Pyridine (99%, Fisher) was distilled over KOH prior to use. Azobisisobutylnitrile (AIBN, 98%, Sigma Aldrich) was recrystallized twice from methanol and dried under vacuum prior to use. Thin layer chromatography (TLC) was conducted with silica gel 60–F245 plates and visualized with a handheld UV lamp. NMR solvents $CDCl_3$ and d_6-acetone were obtained from Cambridge Isotope Laboratories and used as received. Poly(lactic acid) was obtained from unused Nature's PLAstic salad boxes. The boxes were cut into ~1 in squares and dissolved in chloroform. Due to the high crystallinity of PLA, the viscous solution was stirred overnight to ensure the PLA was completely dissolved. The viscous solution was then poured into methanol, resulting in a white precipitate. The precipitate was collected on a coarse fritted filter and dried in a vacuum oven for 24 hours. PLA starting material was confirmed and characterized by ^{1}H NMR, GPC, DSC, and TGA. Polystyrene was obtained from a Styrofoam cooler lid (specific brand unknown, as box was not marked). The lid was broken into ~1 in cubes and dissolved in chloroform. The viscous solution was then poured into methanol, resulting in a white precipitate. The precipitate was collected on a coarse fritted filter and dried in a vacuum oven for 24 hours. Polystyrene starting material was confirmed and characterized by ^{1}H

NMR, GPC, and DSC.

^{1}H, ^{11}B, and ^{13}C Spectroscopy. ^{1}H and ^{11}B NMR spectra were recorded on Bruker AV-300 or Bruker DRX-500 spectrometers at room temperature in $CDCl_3$, unless either wise noted. Chemical shifts are reported with respect to internal solvent, 7.26 ($CDCl_3$), 2.50 (d_6-DMSO), or 2.05 (d_6-acetone) for ^{1}H NMR spectra. ^{13}C NMR spectra were recorded on a Bruker AV-500 spectrometer with a dual cryoprobe (^{13}C, ^{1}H). Chemical shifts are reported with respect to internal solvent, 77.16 ppm ($CDCl_3$) for ^{13}C NMR spectra.

Molecular Weight Characterization. Molecular weight (M_n and M_w) and dispersity ($Đ$=M_w/M_n) were determined using gel permeation chromatography (GPC). Samples were dissolved in tetrahydrofuran (THF) at a concentration of 2−5 mg mL^{-1} and were passed through a 0.20 μm PTFE filter before injection. GPC for all polymers was conducted on a Jasco system equipped with a refractive index detector, a UV detector, a Waters Styragel guard column, and four Waters HR Styragel 5 μm columns (100-5K, 500-30K, 50-100K, 5-600 K) using tetrahydrofuran (THF) at 30 °C and a flow rate of 1.0 mL min^{-1}. Calibration was performed using near-monodisperse polystyrene standards (M_n=684 to 549,000 Da) from Jordi Laboratories and chromatograms were analyzed using ChromNAV chromatography software.

Thermal Characterization. All samples were dried at 40 °C in a vacuum oven overnight (at least 12 h) prior to all thermal characterization. Differential scanning calorimetry (DSC) was performed on a Perkin Elmer DSC 8000 to determine glass transition (T_g) and melting (T_m) temperatures. Samples (7-15 mg) were heated from 0 to 160 °C at a rate of 10 °C min^{-1} and cooled to 0 °C at a rate of 10 °C min^{-1}. A minimum of three heating and two cooling cycles were performed and T_g was measured from the second heating cycle, unless otherwise noted. Pyris Manager was used to analyze the data. Thermogravimetric analysis (TGA) was conducted on a Perkin Elmer Pyris Diamond TG/DTA Thermogravimetric/Differential Thermal Analyzer. The TGA instrument was operated under air, using platinum crucibles. Samples (8-11 mg) were heated from 25 °to 500 °C at a rate of 10 °C min^{-1}. Pyris Manager was used to analyze the data.

Hydroxycinnemaic acid synthesis. *p-Coumaric acid*. 4-hydroxybenzaldehyde (7.0 g, 57.4 mmol) was weighed and added to a round bottom flask along with malonic acid (12.7 g, 122.3 mmol), pyridine (30 mL), and piperidine (300 μL). The reaction was heated to 60 °C overnight (18 h) and then cooled to room temperature. The reaction mixture was poured into a 600 mL beaker containing 200 mL of ice water. Concentrated HCl was added until the product precipitated from solution. The product was collected by filtration, washed with a small volume of cold water, and dried under vacuum to yield the product as an off-white solid. Yield: 8.28 g, 87.7% ^{1}H NMR (300 MHz, d_6-acetone) δ 12.23 (s, 1H, CCH=CHCOO***H***), 7.63 (d, 1H, CC***H***=CHCOOH), 7.55 (d, 2H, Ar-***H***), 6.91(d, 2H, Ar-***H***), 6.36 (d, 1H, CCH=C***H***COOH).

Ferulic acid. Vanillin (6.57 g, 43.2 mmol) was weighed and added to a round bottom flask along with malonic acid (9.59 g, 92.1 mmol), pyridine (30 mL), and piperidine (300 μL). The reaction was heated to 60 °C overnight (18 h) and then cooled to room temperature. The reaction mixture was poured into a 600 mL beaker containing 200 mL of ice water. Concentrated HCl was added until the product precipitated from solution. The product was collected by filtration, washed with a small volume of cold water, and dried under vacuum to yield the product as a yellow solid. Yield: 6.83 g, 81.9% ^{1}H NMR (300 MHz, d_6-acetone) δ 7.63 (d, 1H, CC***H***=CHCOOH), 7.08 (m, 2H, Ar-***H***), 6.94 (d, 1H, Ar-***H***), 6.31 (d, 1H, CCH=C***H***COOH), 3.80 (s, 3H, Ar-OC$\boldsymbol{H}_3$).

Sinapic acid. Synthesized as reported by Lancefield and Westwood.[34] 3,5-dimethoxy-4-hydroxybenzaldehyde (10.0 g, 54.9 mmol) was weighed and added to a round bottom flask along with malonic acid (12.6 g, 12.1 mmol), pyridine (27 mL), and aniline (658 μL). The reaction was heated to 60 °C overnight (18 h) and then cooled to room temperature. The reaction mixture was poured into a 600 mL beaker containing ice (55 g) and concentrated HCl (37%, 33 mL). The mixture was stirred once and left to crystallize for 30 minutes. The product was collected by filtration, washed with a small volume of cold water, and dried under vacuum to yield the product as a white crystalline solid. Yield: 10.31 g, 83.7% ^{1}H NMR (300 MHz, d$_6$-DMSO) δ 12.16 (s, 1H, CCH=CHCOO***H***), 7.50 (d, 1H, CC***H***=CHCOOH), 6.99 (s, 2H, Ar-H), 6.43 (d, 1H, CCH=C***H***COOH), 3.80 (s, 6H, Ar-OC***H***$_3$).

Methyl ester synthesis. *Methyl p-coumarate*. *p*-Coumaric acid (8.27 g, 50.4 mmol) was weighed and added to a round bottom flask along with 50 mL methanol and concentrated sulfuric acid (0.5 mL). The reaction mixture was heated to reflux overnight. The reaction was cooled to room temperature and diluted with dichloromethane (100 mL). The reaction mixture was washed with saturated sodium bicarbonate (3×30 mL). The organic layer was collected and dried over $MgSO_4$. Solution was filtered and volatiles were removed via rotary evaporation to yield the product as a viscous colorless oil. Yield: 7.49 g, 83.5% ^{1}H NMR (300 MHz, d$_6$-DMSO) δ 7.68 (d, 1H, CC***H***=CHCOOCH$_3$), 7.43 (d, 2H, Ar-**H**), 6.91 (d, 2H, Ar-**H**), 6.33 (d, 1H, CCH=C***H***COOCH$_3$), 3.81(s, 3H, d, 1H, CCH=CHCOOC***H***$_3$).

Methyl ferulate. Ferulic acid (6.83 g, 35.2 mmol) was weighed and added to a round bottom flask along with 60 mL methanol and concentrated sulfuric acid (0.6 mL). The reaction mixture was heated to reflux overnight. The reaction was cooled to room temperature and diluted with dichloromethane (100 mL). The reaction mixture was washed with saturated sodium bicarbonate (3×30 mL). The organic layer was collected and dried over $MgSO_4$. Solution was filtered and volatiles were removed via rotary evaporation to yield the product as a viscous pale yellow oil. Yield: 5.59 g, 76.3% ^1H NMR (300 MHz, d_6-acetone) δ 7.67 (d, 1H, $CC\boldsymbol{H}=CHCOOCH_3$), 7.10 (m, 2H, Ar-***H***), 6.95 (d, 1H, Ar-***H***), 6.34 (d, 1H, $CCH=C\boldsymbol{H}COOCH_3$), 3.93 (s, 3H, $CCH=CHCOOC\boldsymbol{H}_3$), 3.82 (s, 3H, $Ar\text{-}OC\boldsymbol{H}_3$).

Methyl sinapate. Synthesized as reported by Lancefield and Westwood.[34] 100 mL of methanol was added to a round bottom flask and cooled to 0 °C. Acetyl chloride (3.50 g, 44.6 mmol) was added dropwise and the mixture was allowed to stir for 15 minutes. Sinapic acid (10.0g, 44.6 mmol) was added and the mixture was heated to reflux for 1 hour. The reaction mixture was cooled to room temperature, causing crystallization of the product. The resulting slurry was then concentrated to remove residual methanol. The product was then collected by filtration and washed with a small amount of cold methanol to yield the product as a crystalline white solid. Yield: 9.97 g, 93.8% ^1H NMR (300 MHz, $CDCl_3$) δ 7.57 (d, 1H, $CC\boldsymbol{H}=CHCOOCH_3$), 6.73 (s, 2H, Ar-***H***), 6.28 (d, 1H, $CCH=C\boldsymbol{H}COOCH_3$), 3.88 (s, 6H, $Ar\text{-}OC\boldsymbol{H}_3$), 3.77 (s, 3H, $CCH=CHCOOC\boldsymbol{H}_3$).

Monolignol Synthesis. *p*-coumaryl, coniferyl, and sinapyl alcohol were synthesized as reported by Quideau and Ralph[18]*. p-Coumaryl alcohol.* Methyl *p*-coumarate (7.49 g, 42.0 mmol) was weighed and added to a round bottom flask along with 100 mL of toluene. The solution was cooled to 0 °C and 176.7 mL of 1 M DIBAL-H solution (in hexanes) was added over 45 minutes. After addition, the reaction was allowed to warm slowly to room temperature. Reaction progress was monitored via TLC. After complete (~4 h), the solution was cooled back down to 0 °C and 20 mL of ethanol was added slowly to quench unreacted DIBAL-H. The solution was then diluted with 300 mL of ethyl acetate and poured into 500 mL water. The biphasic solution was filtered using a coarse fritted filter to remove precipitated aluminum salts. The isolated salts were washed with additional ethyl acetate. The organic layers were separated, combined, and washed with DI water (2×50 mL) and brine (1×50 mL). The organic layer was dried over $MgSO_4$ and volatiles were removed under rotary evaporation to yield the product as a pale yellow solid. Yield: 3.31 g, 52.4%.^{1}H NMR (300 MHz, d_6-acetone) δ 7.29 (d, 2H, Ar-H), 6.81 (d, 2H, Ar-H), 6.54 (d, 1H, CC***H***=$CHCH_2OH$), 6.22 (dt, 1H, CCH=C***H***CH_2OH), 4.21 (m, 2H, CCH=CHC$\boldsymbol{H}_2$OH).

Coniferyl alcohol. Yield: 2.88 g, 42.2% ^{1}H NMR (300 MHz, d_6-acetone) δ 7.05 (s, 1H, Ar-***H***), 6.88 (m, 2H, Ar-***H***), 6.55 (d, 1H, CC***H***=$CHCH_2OH$), 6.28 (dt, 1H, CCH=C***H***CH_2OH), 4.24 (m, 2H, CCH=CHC$\boldsymbol{H}_2$OH).

Sinapyl alcohol. Yield: 1.43 g, 37.8% ^{1}H NMR (300 MHz, $CDCl_3$) δ 6.63 (s, 2H, Ar-***H***), 6.52 (d, 1H, CC***H***=$CHCH_2OH$), 6.24 (d, 1H, CCH=C***H***CH_2OH), 4.34 (br m, 2H, CCH=CHC$\boldsymbol{H}_2$OH), 3.90 (s, 6H, Ar-OC$\boldsymbol{H}_3$).

Citraconic Anhydride Synthesis. Synthesized as reported by Shriner et al.[21] Itaconic acid (65.0 g, 0.50 mol) was weighed and added to a round bottom flask along with a stir bar. A Vigreux column, Claisen adaptor, and cold-water condenser were added to the set up and the reaction was rapidly heated using a heating mantle. Water and other decomposition products were collected at temperatures below 200 °C. Once the temperature reached 200 °C, a new receiving flask was connected and the desired product was collected from 200-215 °C. The isolated crude product was distilled under vacuum (105 °C at 22 mmHg) to yield the final product as a colorless oil. Yield: 36.11g, 64.4% ^{1}H NMR (300 MHz, $CDCl_3$) δ 6.67 (s, 1H, CH_3C=C***H***), 2.17 (s, 3H, C$\boldsymbol{H}_3$C=CH).

Cationic Polymerizations. The desired monolignol (1 mmol) and citraconic anhydride (1 mmol) were weighed and combined in an ampule, along with 4-methoxy-α-methylbenzyl alcohol (0.02 mmol), water (0.005 mmol), and a mixture of 3.6 mL acetonitrile and 0.9 mL dichloromethane (4:1). The solution was frozen in liquid nitrogen and 0.5 mL of a 10 mM solution of BF_3Et_2O in acetonitrile was added. The solution was frozen again and the ampule was sealed under vacuum. Upon thawing, the solution became deep red. After stirring for ~24h solutions had become more orange in color. The reaction was allowed to stir for the desired amount of time before the ampule was broken open and 0.1 mL methanol was added. Volatiles were removed under rotary evaporation and oligomers were precipitated by adding hexanes or dichloromethane as a non-solvent. The precipitate was washed with DI water and hexanes before being dissolved in acetone. The acetone solution was dried over $MgSO_4$ and volatiles were removed via rotary evaporation.

Free Radical Polymerizations. Free radical polymerizations were conducted in a similar manner. The desired monolignol (1 mmol) and citraconic anhydride (1 mmol) were weighed and combined in an ampule. The desired amount of AIBN (1 or 5 mol%) was then added in the form of a stock solution in DMF. Then, DMF was added to the reaction mixture for a final total solution volume of 5 mL. The solution was degassed via the freeze-pump-thaw method. After degassing, the ampule was sealed and heated to 70 ^{o}C for the desired reaction time. After reaction time was complete, ampule was cracked open and diluted with ethyl acetate. Organic layer was washed with water (2×10 mL) and brine (1×10 mL), and dried over $MgSO_4$. Volatiles were removed using a rotary evaporator to yield the product.

4.5 Appendix C

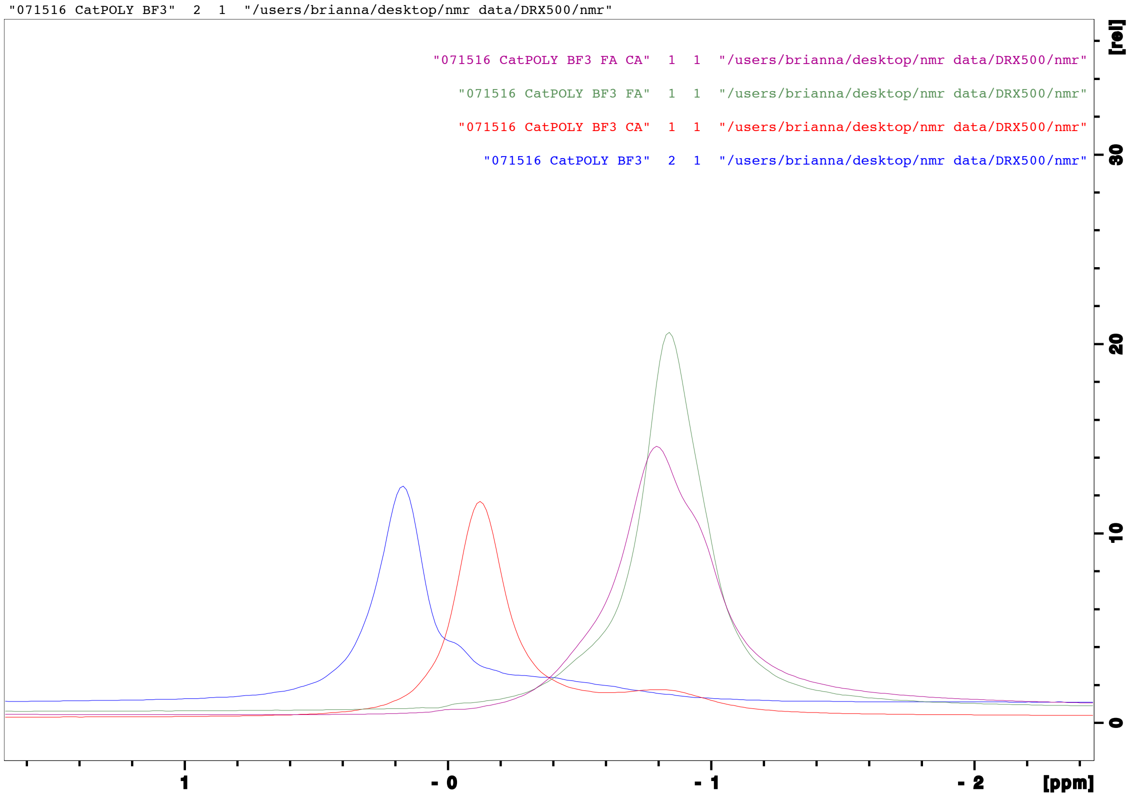

Figure S1: Stacked ^{11}B NMR spectra during *in situ* reaction. Blue: BF_3Et_2O starting material; Red: BF_3Et_2O + Citraconic anhydride; Green: BF_3Et_2O + Ferulic alcohol; Purple: BF_3Et_2O + Ferulic alcohol + Citraconic anhydride. Two boron products are formed with citraconic anhydride only, the dominant of which appears to be different than that formed with either ferulic alcohol only or the mixture. Suggestive that either is a competitive process and citraconic anhydride is less reactive for cationic polymerization, or the intermediate is the observed signal around 0 ppm but is formed in low quantities.

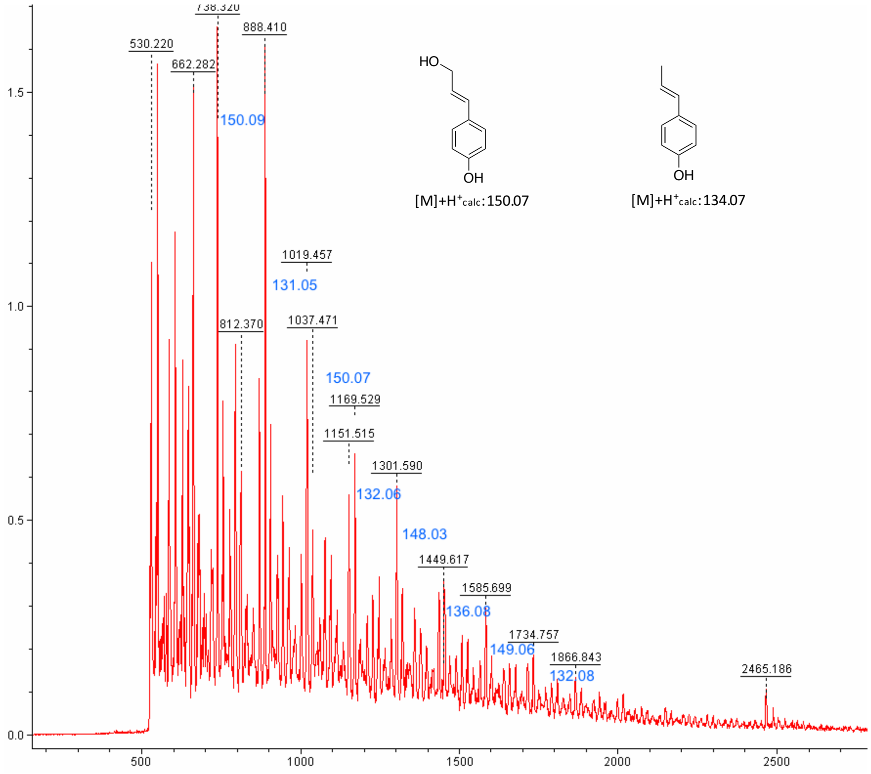

Figure S2: MALDI-TOF spectrum for O2 showing alternating copolymer. Signal at 2465 m/z is an artifact of the instrument.

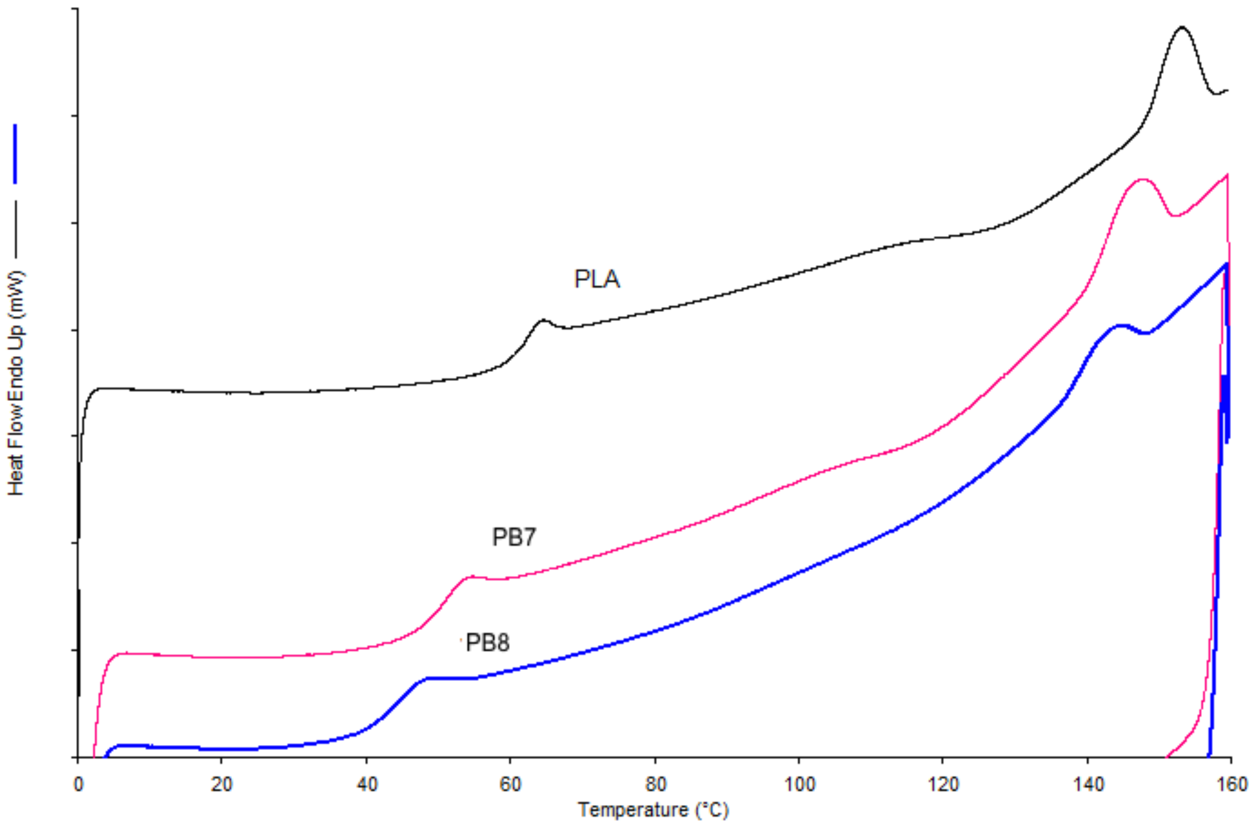

Figure S3: Second DSC heating scan for PB7 and PB8 in comparison to PLA.

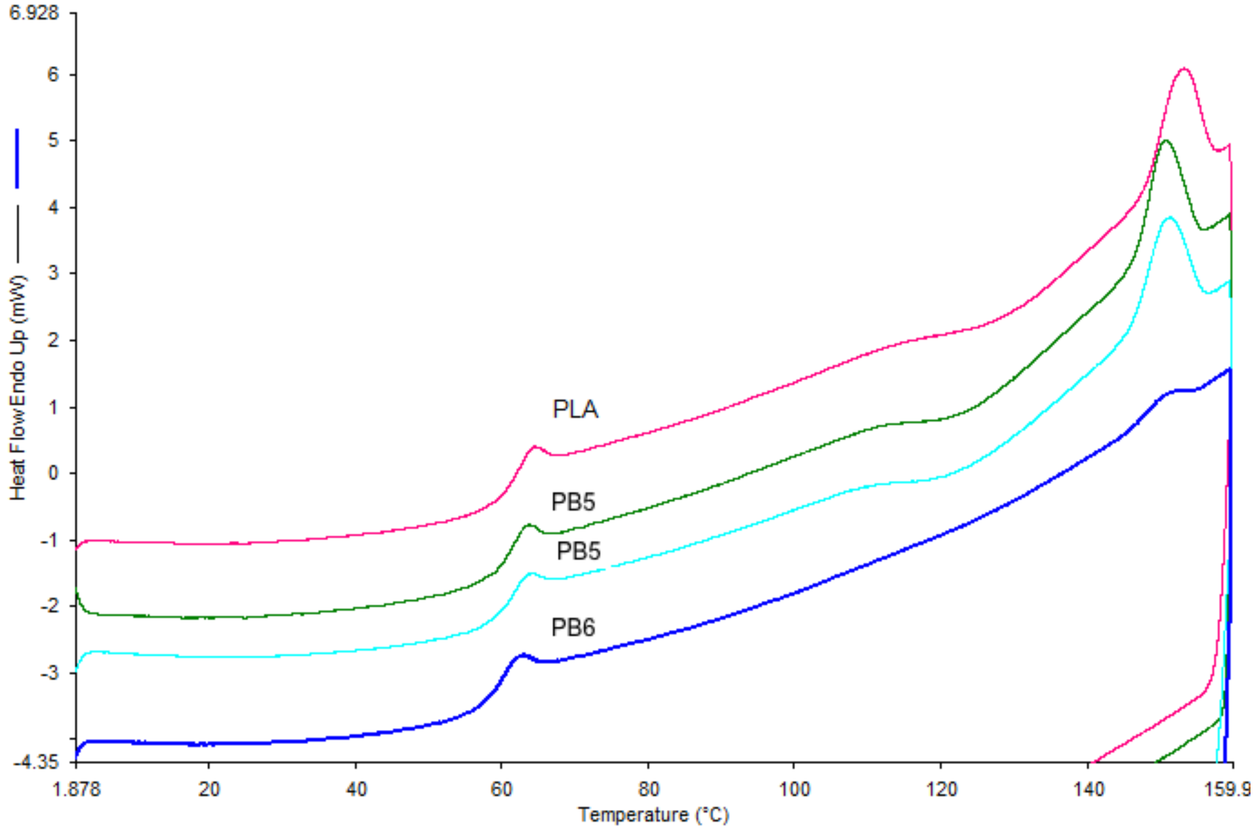

Figure S4: Second DSC heating scan for PB5 and PB6, in comparison to PLA

4.6 References

(1) Alfrey, T.; Lavin, E. *J. Am. Chem. Soc.* **1945**, *67* (11), 2044.

(2) Klumperman, B. *Polym. Chem.* **2010**, *1* (5), 558.

(3) Lessard, B.; Marić, M. *Macromolecules* **2010**, *43* (2), 879.

(4) Benoit, D.; Hawker, C. J.; Huang, E. E.; Lin, Z.; Russell, T. P. *Macromolecules* **2000**, *33* (5), 1505.

(5) Wang, Y.; Shen, Y.; Pei, X.; Zhang, S.; Liu, H.; Ren, J. *React. Funct. Polym.* **2008**, *68* (8), 1225.

(6) Chernikova, E.; Terpugova, P.; Bui, C.; Charleux, B. *Polymer (Guildf).* **2003**, *44* (15), 4101.

(7) van den Dungen, E. T. A.; Rinquest, J.; Pretorius, N. O.; McKenzie, J. M.; McLeary, J. B.; Sanderson, R. D.; Klumperman, B. *Aust. J. Chem.* **2006**, *59* (10), 742.

(8) McLeary, J. B.; Calitz, F. M.; McKenzie, J. M.; Tonge, M. P.; Sanderson, R. D.; Klumperman, B. *Macromolecules* **2004**, *37* (7), 2383.

(9) McLeary, J. B.; Calitz, F. M.; McKenzie, J. M.; Tonge, M. P.; Sanderson, R. D.; Klumperman, B. *Macromolecules* **2005**, *38* (8), 3151.

(10) Du, F.-S.; Zhu, M.-Q.; Guo, H.-Q.; Li, Z.-C.; Li, F.-M.; Kamachi, M.; Kajiwara, A. *Macromolecules* **2002**, *35* (17), 6739.

(11) Burnett, J. C.; Keppel, R. A.; Robinson, W. D. *Catal. Today* **1987**, *1* (5), 537.

(12) Miller, R. G.; Sorrell, S. R. *Philos. Trans. R. Soc. A Math. Phys. Eng. Sci.* **2013**, *372* (2006), 20130179.

(13) Jambeck, J. R.; Geyer, R.; Wilcox, C.; Siegler, T. R.; Perryman, M.; Andrady, A.; Narayan, R.; Law, K. L. *Science (80-.).* **2015**, *347* (6223), 768.

(14) DODDS, E. C.; LAWSON, W. *Nature* **1936**, *137* (3476), 996.

(15) Rochester, J. R. *Reprod. Toxicol.* **2013**, *42*, 132.

(16) Vogel, S. A. *Am. J. Public Health* **2009**, *99* (S3), S559.

(17) Holladay, J. E.; White, J. F.; Bozell, J. J.; Johnson, D.; Energy, U. S. D. of. *Top Value-Added Chemicals from Biomass- Volume II—Results of Screening for Potential Candidates from Biorefinery Lignin*; Pacific Northwest National Laboratory: Richland, WA, 2007; Vol. 2.

(18) Quideau, S.; Ralph, J. *J. Agric. Food Chem.* **1992**, *40* (7), 1108.

(19) Willke, T.; Vorlop, K.-D. *Appl. Microbiol. Biotechnol.* **2001**, *56* (3-4), 289.

(20) Okabe, M.; Lies, D.; Kanamasa, S.; Park, E. Y. *Appl. Microbiol. Biotechnol.* **2009**, *84* (4), 597.

(21) Shriner, R. L.; Ford, S. G.; Roll, L. J. *Org. Synth.* **1931**, *11*, 28.

(22) Murahashi, S.; Nozakura, S.; Emura, K.; Yasufuku, K. *Bull. Chem. Soc. Jpn.* **1965**, *38* (9), 1560.

(23) *Principles of Polymerization*, 4th Ed.; Odian, G., Ed.; Wiley-Interscience: Hoboken, NJ, 2004.

(24) Satoh, K.; Saitoh, S.; Kamigaito, M. *J. Am. Chem. Soc.* **2007**, *129* (31), 9586.

(25) Nonoyama, Y.; Satoh, K.; Kamigaito, M. *Polym. Chem.* **2014**, *5* (9), 3182.

(26) Matsuda, M.; Satoh, K.; Kamigaito, M. *J. Polym. Sci. Part A Polym. Chem.* **2013**, *51* (8), 1774.

(27) Satoh, K. *Polym. J.* **2015**, *47* (8), 527.

(28) Vanholme, R.; Demedts, B.; Morreel, K.; Ralph, J.; Boerjan, W. *Plant Physiol.* **2010**, *153* (3), 895.

(29) Takasu, A.; Ito, M.; Inai, Y.; Hirabayashi, T.; Nishimura, Y. *Polym. J.* **1999**, *31* (11_1), 961.

(30) Mekonnen, T.; Mussone, P.; Khalil, H.; Bressler, D. *J. Mater. Chem. A* **2013**, *1* (43), 13379.

(31) Vieira, M. G. A.; da Silva, M. A.; dos Santos, L. O.; Beppu, M. M. *Eur. Polym. J.* **2011**, *47* (3), 254.

(32) Garlotta, D. *J. Polym. Environ.* **2001**, *9* (2), 63.

(33) Zeng, J.-B.; Li, K.-A.; Du, A.-K. *RSC Adv.* **2015**, *5* (41), 32546.

(34) Lancefield, C. S.; Westwood, N. J. *Green Chem.* **2015**.

Chapter 5: Conclusions and future outlook

5.1 Conclusions

This doctoral work focused on the use of monolignols as alternative monomers for polymer synthesis. While monolignols are used as monomers *in planta*, the resulting polymer (lignin) is poor defined and highly variable. With this in mind, we set to create polymers featuring not only well-defined monomer units but also well-defined polymeric structures. In contrast to work by others, we wanted to work with monolignols to directly compare the observed properties of our synthetic systems to the properties observed in naturally occurring lignin. While monolignols are not currently a delignification product, as new techniques and methods are continually developed, we speculate that this chemical stream may soon become commercially available. Additionally, we were interested in the creation of bio-based mimics to well-known and well-studied petroleum-based aromatic polymers, such as Kevlar, Nomex, and poly(styrene-co-maleic anhydride). All of these materials have unique and beneficial properties, but are all produced from petroleum-based monomers. We wanted to determine if monolignols, as monomers from the only naturally-occurring aromatic polymer, could be utilized in the synthesis of mimics to commodity materials.

Chapter 2 focused on the synthesis of a series of 21 aromatic-aliphatic poly(ester-amide)s via interfacial polymerization from monolignol-based ester dimers and diamines. Although they are not yet biologically sourced, all aliphatic diamines utilized can be derived from plants. However, due to higher cost in comparison to petroleum-derived products, the biologically-derived diamines are not yet commercially available. As methods improve and with the push away from petroleum-based materials, we speculate that the bio-sourced versions will eventually become available. We were interested to determine the effects of aliphatic spacer length or aromatic spacer substitution patterns on the resulting physical and degradation properties. The majority of the polymers obtained were amorphous, shown by the lack of melting temperature (T_m), and showed moderate thermal stability (most T_d>230 ^{o}C). The largest drawback to this system was the lack of polymer solubility in common organic solvents. Poly(ester-amide)s are usually sought over polyamides due to their increased solubility, but due to the high aromatic content, degree of unsaturation found in the aliphatic monolignol side chain, and strong interchain hydrogen bonding, the isolated poly(ester-amide)s were only sparingly soluble in *N,N*-dimethylformamide (DMF). Based on the melting temperatures for P17-19 and the moderate thermal stability observed for all polymer, melt processing is a viable processing method for these materials. As these materials also contain hydrolysable ester linkages, we were interested in their degradation profile. Wholly aromatic poly(ester-amide)s are generally considered non-degradable due to their hydrophobicity, minimizing hydrolysis. However, as the polymers synthesized were aromatic-aliphatic poly(ester-amide)s, degradation was observed at both neutral (pH 7) and acidic (pH 5) conditions. Increasing the length of the aliphatic linker decreased degradation, while increasing the degree of methoxy-substitution (dependent on monolignol identity) increased the rate of degradation. However, the long term degradation (up to 30 days) of these materials was minimal, suggesting their usefulness in single use applications requiring good thermal properties and slow biodegradation. Overall, while these materials do not mimic the exact properties of well-known aramids, they feature robustness that can be directly attributed to similar properties seen in lignin. Additionally, the modular synthesis allows for the use of high-throughput techniques to rapidly generate a series of poly(ester-amide)s with tunable properties.

Chapter 3 focused on the synthesis of a series of 21 aromatic-aliphatic poly(ether-amide)s via interfacial polymerization from monolignol-based ether dimers and diamines. Based upon our work with poly(ester-amide)s from monolignols, we were interested in creating an analogous set of polymers that were incapable of degradation. We were also interested to see if replacing the ester linkage would improve solubility by reducing interchain interactions and increasing overall backbone flexibility. There are few examples of poly(ether-amide)s in the literature, but based on the strengths of polyamides and polyethers individually, we envisioned the combination of functional groups in the polymer backbone would yield useful materials. Unfortunately, the solubility of these polymers was significantly reduced in comparison to the analogous poly(ester-amide)s, especially those synthesized from *p*-coumaric acid. All polymers were only sparingly soluble in DMF, and *p*-coumaric acid variants were so insoluble they required soxhlet extraction for 24 hours to achieve a small degree of dissolution. Due to the decreased interchain interactions and increase backbone flexibility, the amorphous polymers also featured lower glass transition temperatures and reduced thermal stability. While these materials are less thermally stable, they are still good candidates for melt processing. Their insolubility in common organic solvents makes them ideal candidates for solvent-resistant applications. Additionally, as they are not susceptible to hydrolysis, they could also be utilized in applications with strong acids or bases.

Chapter 4 focused on the attempted synthesis of poly(styrene-co-maleic anhydride) mimics from monolignols and citraconic anhydride. This approach was attractive for several reasons, namely the use of naturally derived monomers rather than monomers derived from petroleum. Based on literature research regarding the polymerization of β-substituted styrenes, two different polymerization methods were chosen: cationic (with boron trifluoride etherate) and uncontrolled free radical (with azobisisobutyronitrile). Regardless of reaction conditions, citraconic anhydride was not incorporated into the isolated oligomer and oligomerization conversion of the monolignol was low. Even with increased reaction times (28 days), the molecular weight of the oligomers isolated did not exceed 2.1 kDa. Interestingly, oligomers isolated from cationic polymerizations showed an alternating structure between intact and dehydroxylated monolignol units. While this was not the targeted result, we utilized monolignol-based oligomers in polymer blends with recycled polystyrene and poly(lactic acid). Little effect was seen in polystyrene but, oligomers from coniferyl alcohol lowered the glass transition temperature of PLA by almost 20 °C, while maintaining the crystallinity. The blends also featured a lower melting temperature, suggesting these blends would be less likely to undergo degradation in melt processing, in comparison to unblended PLA. These bio-based, oligomeric plasticizers could also show improvement over other commercial plasticizers, by minimizing leaching and phase separation in final products.

5.2 Future outlook

While the work in this dissertation has established a foundation for the development of new polymeric materials from monolignols, significant work with these and other materials remains to be done. One of the most interesting characteristics of the poly(ester-amide) and poly(ether-amide) systems is the retention of the double bond found in the aliphatic side chain of monolignols during polymerization. As each dimer contains two double bonds in defined intervals, this system has endless possibilities in the formation of graft-co-polymers and polymer networks. For example, we envisioned this system could be used as a backbone for the preparation of graft-co-polymers with other bio-based monomers, such as itaconic acid and α-methylene-γ-butyrolactone. Due to their charged side chains, the resulting copolymer could then be used as flocculants for heavy metal sequestration. The double bond in the polymer backbone could also be used to form a three-dimensional network by alkene hydrothiolation (thiol-ene click) or Michael addition reactions. Through careful selection of the network linker, properties of the final network could be controlled relatively easily. While the limited solubility could be an issue in co-polymer or network formation, the modular synthesis of both poly(ester-amide)s and poly(ether-amide)s allows for tuning of the materials used to create polymers with specific properties, i.e. improved solubility. Based on the system design, the polymer systems reported in the first two dissertation chapters serve only as a framework, from which significant progress and material development are yet to come.

In addition to the polymers discussed in Chapters 2 and 3, the monolignol-based oligomers synthesized in Chapter 4 also provide several interesting directions to be explored. The cationic polymerizations of both coniferyl and *p*-coumaric alcohol, generated oligomers with an alternating structure of intact and dehydroxylated monolignols. This is particularly interesting, as the alternating structure is similar to what is known for poly(styrene-co-maleic anhydride), but does not have the electronic or structural monomer differences to explain selectivity during polymerization. Further mass spectrometry studies to confirm the exact oligomeric structure, in addition to mechanistic studies may in turn answer questions regarding which copolymerization model (penultimate or complex participation) describes not only this system, but potentially other copolymerization reactions. The success of these materials as plasticizers for PLA and polystyrene also offers great potential in their use in other commodity materials. A systematic study of blends with other commercial polymers should also be undertaken to determine if they are effective, comprehensive polymer additives. While the methods used in this system were unable to generate oligomers of sinapyl alcohol, future efforts also should be placed on the synthesis of sinapyl-base oligomers to study the effects of additional methoxy-substitution.

While a foundation for the implementation of monolignols as monomers in the synthesis of commodity polymers has been outlined here, the potential growth and future directions for this project are limitless. As social demand for bio-sourced materials grows with an increasing awareness of diminishing petroleum resources and the environment impacts of petroleum extraction, scientists must continue to develop materials that meet the needs of both producers and consumers. While the work found in this dissertation is a significant contribution to this goal, further strides must be made to yield suitable bio-based materials for everyday life.